the work of the
Rutherford Laboratory
1975

Printed by Swindon Press Limited, Swindon, Wiltshire

The Work of the Rutherford Laboratory 1975

Edited and designed by Gordon Fraser

Compiled by the Laboratory Information Panel
Published by the Scientific Administration Group

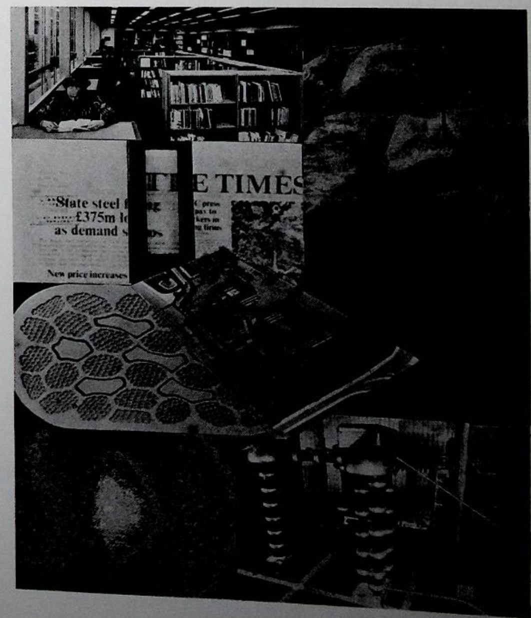

Science Research Council
Rutherford Laboratory
Chilton, Didcot
Oxfordshire OX11 0QX
May 1976

Director's Introduction

Established specifically as a research centre for nuclear science, the Rutherford Laboratory has over the years found itself increasingly involved in many different areas of science and technology required to support a comprehensive research programme in High Energy Physics. High Energy Physics research constantly requires new and sophisticated apparatus, and this in turn demands a wide range of technical and engineering expertise. Thus a major proportion of the Laboratory's resources, both in terms of manpower and hardware, has been geared to the design, development and production of special apparatus. We are now finding that our broadly-based activities are in increasing demand in areas of research outside the field of High Energy Physics. A particular example of this is our work on superconductivity and superconductor technology, which has been in progress for many years as part of the High Energy Physics development programme, but it is now meeting a need over a wide field of university science.

The widening scope of the Laboratory's activities is also reflected in its increasing involvement with the various boards of the Science Research Council. For the Science Board, the Neutron Beam Research Unit at the Laboratory supports the work being done by university scientists at research reactors both in the UK and abroad. The Unit has constructed several specialised instruments for use at the Institut Laue-Langevin in Grenoble as well as apparatus such as guide tubes, collimators and detectors; work which in part has benefitted from techniques developed initially for use in High Energy Physics.

The Atlas Computer Laboratory has traditionally supplied computer services across a whole spectrum of university research. A particularly important development during the year was its incorporation into the Rutherford Laboratory where, as the Atlas Computing Division, it still caters for the specialised needs of a large body of university computer users. Another Science Board activity which recently has been approved is the High Power Laser Centre. This centre will serve university research scientists in an important and rapidly developing field.

The provision of interactive graphics facilities for engineers has been identified by the Engineering Board as a new requirement and this will bring the Laboratory into close contact with another community of university research workers. The superconductivity and interactive graphics work could well form the nucleus of a developing involvement between the Laboratory and the SRC's Engineering Board. Already the Engineering Board is funding the continuing work on the filamentary niobium-tin high-performance superconductors developed through the Laboratory.

This diversification of activities within the Laboratory is a trend which will undoubtedly grow still further as new areas of expertise in the Laboratory develop through the cross-fertilisation of ideas possible in a multi-disciplined research laboratory.

A large proportion of the Laboratory's resources will always be devoted to High Energy Physics, and as a result of the SRC's decision to discontinue the High Energy Physics programme at its Daresbury Laboratory, the Rutherford Laboratory will soon become the sole SRC centre responsible for supporting the work done by university scientists in this area. This means that the Laboratory will have an increasingly important part to play in assisting the UK research effort in High Energy Physics both at home and abroad, at a time when exciting new developments are taking place. The Laboratory expects to participate in the exploitation of the new electron-positron storage facility, PETRA, at the DESY Laboratory in Hamburg. The initial groundwork carried out for the proposed EPIC facility at the Rutherford Laboratory, now regrettably defunct, will therefore not be wasted.

G H Stafford
Director

Contents

The Role of the Rutherford Laboratory in University Research

The Rutherford Laboratory aims to foster University research and development work by designing, building and operating equipment which by its scale, cost or level of complexity is beyond the resources of individual universities. This role is a simple extension of the motivation behind its establishment in 1957 as the first Laboratory of the National Institute for Research in Nuclear Science to provide university scientists with equipment for nuclear physics research which was beyond the means of individual universities. In 1965 the Laboratory became part of the Science Research Council, retaining this principal function.

Since then, the continual accumulation of skills and resources which has been achieved has meant that the Laboratory has become involved in an ever-widening range of University science and technology, and this diversification is reflected in the titles of the Sections of this Annual Report: Particle Physics, Neutron Beam Research, Laser Research, Forward Technology, Computing, Accelerator Operations and Development, Design and Construction of Buildings and General Resources.

Although the Laboratory now works closely with a number of different and largely independent scientific and technological communities, its internal activities are very much interrelated.

A closer look at the contents of the Report reveals this: the Particle Physics Section includes the Instrumentation and Data Handling Technology required to support Particle Physics experiments; the Forward Technology Section includes the work on Polarised Targets for special Particle Physics experiments; the Nuclear Physics experiments described in the Particle Physics Section use many of the reactor resources used in Neutron Beam Research; the Accelerator Developments are very much geared to the demands of a number of Particle Physics and Neutron Beam Research groups; nearly all groups have some requirement for Computing.

The picture which emerges is of a smoothly integrated scheme of interrelated research, development and support effort, the aim of which is to encourage, participate in and complement the work being done by British scientists and technologists in universities and research centres in the UK and abroad.

Laboratory Organisation, December 1975

Director:
G. H. Stafford

Deputy Director:
G. Manning

Administration Division
Personnel, finance, general and scientific administration.
Division Head and Laboratory Secretary: J. M. Valentine

Applied Physics Division
Applications of superconductivity; magnet design; development of polarised targets; rapid cycling bubble chamber studies.
Division Head: D. B. Thomas

Atlas Computing Division
Computing services and research and development work using an ICL 1906A and special equipment as well as the Laboratory's main IBM 360/195 computer.
Acting Division Head: G. Manning

Computing and Automation Division
Operation and development of the Laboratory's central IBM 360/195 computer and associated remote system; computer applications for bubble chamber and spark chamber film analysis; interactive computing and network development.
Division Head: W. Walkinshaw

Engineering Division
Design and manufacture of experimental apparatus; mechanical, electrical and building services; chemical technology; safety and radiation protection services.
Division Head and Chief Engineer: P. J. Bowles

General Studies Division
Investigation and design of new accelerators.
Division Head: D. A. Gray

High Energy Physics Division
Experiments in particle physics and nuclear physics in collaboration with university groups; nuclear electronics.
Division Head: J. J. Thresher

Laser Centre
Establishment of a national centre for university research in the interaction of laser radiation with matter and in laser technology.
Acting Division Head: L. C. W. Hobbis

Neutron Beam Research Unit
Supporting research by universities using UK reactors and the reactor at the Institut Laue-Langevin, Grenoble; development of new instruments and techniques; study of new neutron sources; participation in experiments.
Head of Unit: L. C. W. Hobbis

Nimrod Division
Operation and development of Nimrod 8 GeV proton synchrotron accelerator; accelerator design; experimental area management; development of beam line components and cryogenic targets.
Division Head: G. N. Venn

Theory Division
Studies in theoretical physics
Division Head: R. J. N. Phillips

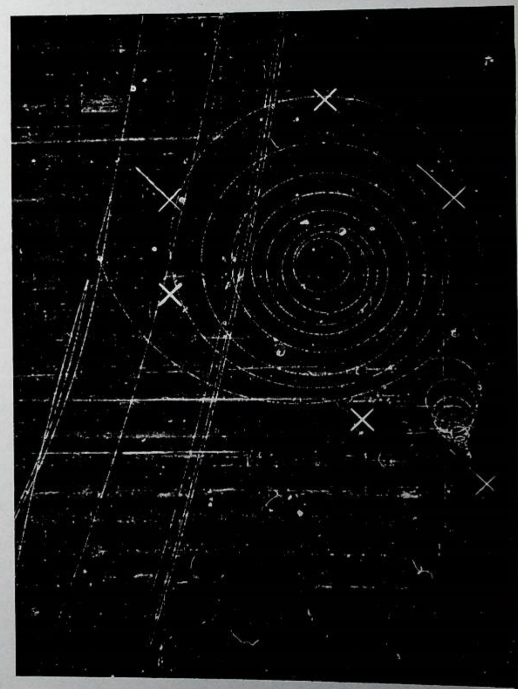

1. Particle Physics

1. Particle Physics

Particle Physics at the Rutherford Laboratory is centered on High Energy Physics with work also being done in the fields of Nuclear Physics and Radiobiology.

1975 has been a truly remarkable year for High Energy Physics – the study of elementary particles. The subject has been characterised by a few periods of vital discovery. Following these discoveries have been long periods of careful work leading up to an enormous expansion of our understanding. An example of a period of great discovery was 1947, which marked the observation of the pi-meson. This gave substance to the first attempts to understand the origin and nature of the strong nuclear force. It is clear that the discoveries of 1974/75 place us in another era of great promise, which may well prove to be the greatest ever for High Energy Physics.

For any discipline to be a science it is necessary that though theory proposes, experiment disposes. It is however a characteristic feature of High Energy Physics that many experimental discoveries have been at most only vaguely expected on theoretical grounds. This is because as we go into a domain where both quantum mechanics and relativity are important, we are taken far beyond the realm of direct observational experience. There, even the skill and intuition of great minds are inadequate to solve the mysteries of nature, unless illuminated by the results of experiment.

There is, however, a key theoretical idea which, since its presentation in 1964, has explained many diverse phenomena. This is the notion that there are 'quarks' which are the basic building blocks of strongly interacting matter. This concept – with only three varieties of quark – was able to offer a good representation of the spectrum of observed sub-nuclear particles and many of their properties. In particular it was a crucial ingredient of the understanding of how the proton and neutron behaved when probed with electromagnetic radiation. Until this year there was no experimental evidence that any more than three varieties of quark would be required.

What then are some of the great discoveries of 1975?

The recent intensive study of the annihilations of electrons and positrons has revealed many new particles. They are associated with the ψ (or J) and ψ' particles discovered in 1974, the most significant features of which are that they are massive and long lived. Compared to typical light particles with lifetimes characteristic of the strong nuclear interaction they are 4 to 5 times more massive yet live 500 to 2000 times longer. If the ψs were made from the same variety of quarks as their lighter cousins, one would expect such massive states to be much shorter lived. It is therefore suggested that these states are made from at least one new variety of quark, more massive than the 'old' quarks.

If the above explanation for the ψs were correct, it might be possible for other comparatively long lived states, with masses less than the ψ' to exist. Such states have now been discovered.

The rate at which electrons and positrons annihilate each other and produce strongly interacting particles has been measured at high energy. The dependence on energy was found to be consistent with extensions of the quark concept – but the magnitude is too large to be explained by the three 'old' quarks. This is believed to be the effect of one or more new quarks.

Anomalous events have been found in the interaction of neutrinos with matter. The understanding of these events is far from complete, but an interpretation in terms of the new quarks is possible. Neutrinos have only weak interactions, and weak interactions can turn one of the three 'old' quarks into a different member of the triplet. No other interaction can do this. It may therefore be that weak interactions change one of the old quarks into a new heavy quark, which then changes back into a light quark by a weak interaction, causing the anomalous events.

A remarkable signal has been found in the mutual annihilation of electrons and positrons in addition to the new particles. A significant number of events have been seen where the annihilation products consist of an electron, a muon and missing energy. Once again, the interpretation is so far uncertain. However the explanation which is currently most favoured is that the signal is due to the production of a new heavy member of the lepton family and its antiparticle. The lepton family (the electron, muon, electron neutrino and muon neutrino) does not have strong interactions. It might therefore seem that a new lepton will have no connection with the increased richness of the strongly interacting quarks. There are, however, theoretical requirements that the number of leptons should increase if the variety of quarks increases.

Further experiment will tell if the explanations given for the new discoveries have any validity. However, it is characteristic of these discoveries that no trivial extension of our present ideas can give a satisfactory explanation.

The discoveries of the past year have had a direct bearing on the programme of experiments supported by the Rutherford Laboratory. Two searches were initiated for 'charm'- a property of particles which contain one of the new types of quark. The discovery of 'charmed' particles would indicate the existence of a fourth quark in a dramatic way.

Furthermore, theoretical ideas which explain the new experimental results will imply features in the scattering of particles by the strong nuclear force, particularly in high energy "head on" collisions, and in the study of the characteristics of the well known particles and their higher energy excited states (resonances). This laboratory is playing a large part in these two fields. In the latter, meticulous work has pointed the way for theories concerned with the grouping together of apparently dissimilar particles into clusters whose composition and symmetry directly reflect the nature of the more fundamental building blocks of the particles.

Since experiments, to a large extent, have paved the way for progress in High Energy Physics, further progress requires better experiments either using the new generation of accelerators or more sophisticated apparatus at older accelerators. Thus the rate at which advances are made in High Energy Physics depends directly on the quality of the technical support it receives. Institutions such as the Rutherford Laboratory, with its integrated technological expertise, are essential to High Energy Physics. The technological demands made by this field in turn stimulate and push to the limit the technology of the day.

Information on particle properties is also obtained from research in Nuclear Physics, in which the low energy interactions of particles with nuclei are studied. A better understanding of particle properties improves the understanding of nuclei and some properties of nuclei can shed light on the structure of particles.

In addition to research into the fundamental aspects of Particle Physics, the practical application of particle beams to the field of radiobiology is being studied. The use of particle beams in radiobiology is mainly directed towards the treatment of cancer. Compared to γ- or X-rays, beams of charged particles are more easily controlled and have a greater potential for destroying a tumour and leaving healthy tissue viable.

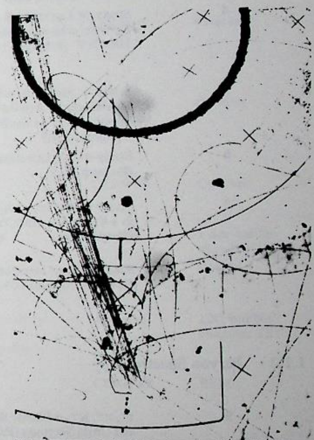

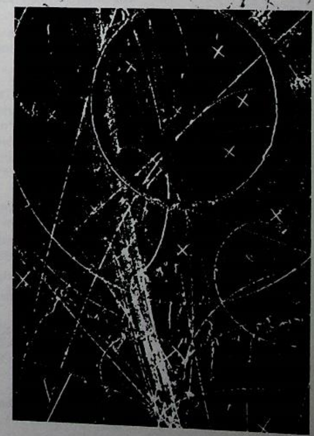

Particle Physics Experiments

1.1 High Energy Physics

1.1.1 Meson Spectroscopy

Section	Experiment Number	Title	Collaboration	Accelerator or Location	Technique
1.1.1	1	Study of Neutral Bosons using a Time of Flight Trigger (Proposal 88)	Birmingham University Tel Aviv University Westfield College, London Rutherford Laboratory	CERN PS	Counter
	2	Polarisation Measurements for $p\bar{p}$ Annihilations into $\pi^-\pi^+$ (Proposal 103)	Queen Mary College, London Daresbury Laboratory Rutherford Laboratory	CERN PS	Counter
	3	Meson Production Very Close to Threshold (Proposals 99, 128)	Imperial College, London Southampton University	Nimrod	Counter
	4	Study of Exclusive Reactions in πp and Kp Interactions in the Energy Range up to 100 GeV (Proposal 145)	CERN Max Planck Institute, Munich Amsterdam University Oxford University Rutherford Laboratory	CERN SPS	Counter
	5	Study of Meson Resonances Decaying into Strange Particles in the Omega Spectrometer at the SPS (Proposal 158)	Birmingham University	CERN SPS	Counter
	6	Study of $\pi^+ d$ Interactions at 4 GeV/c (Proposal 36)	Birmingham University Durham University Rutherford Laboratory	CERN PS	2m bubble chamber
	7	Study of $\pi^+ p$ Interactions at 4 GeV/c in a Track Sensitive Target (Proposal 91)	CERN Lawrence Berkeley Laboratory Rutherford Laboratory Turin University	Nimrod	1·5m bubble chamber
	8γ	Study of K^-p Interactions at 14·3 GeV/c (Proposal 109)	Ecole Polytechnique, Paris CEN, Saclay Rutherford Laboratory	CERN PS	2m bubble chamber

1.1.2 Baryon Spectroscopy

Section	Experiment Number	Title	Collaboration	Accelerator or Location	Technique
1.1.2	9	π^+, π^-, K^-–p Elastic Scattering Differential Cross Sections (Proposals 83, 105 120)	Bristol University Southampton University Rutherford Laboratory	Nimrod	Counter
	10	Coherent Production of $I = \frac{1}{2}$ Baryon States on Helium (Proposal 95)	CERN University College, London Uppsala University Rutherford Laboratory	CERN PS	Counter
	11	Measurement of the Differential Cross Section and Polarisation of the Reactions $\pi^-p \rightarrow \pi^0 n$, $\pi^-p \rightarrow \eta^0 n$ (Proposals 81, 101)	Rutherford Laboratory	Nimrod	Counter
	12	Differential Cross Sections and Polarisation in the Reaction $\pi^-p \rightarrow K^0\Lambda^0$ (Proposals 87, 114)	Cambridge University Bristol University Rutherford Laboratory	Nimrod	Counter
	13	Polarisation Measurements in K^+N Interactions (Proposal 136)	Queen Mary College, London Rutherford Laboratory	Nimrod	Counter
	14	Study of K^-p Interactions in the 1 GeV/c Region (Proposals 108, 159)	Imperial College, London Rutherford Laboratory	CERN PS	2m bubble chamber
	15	Study of π^+p Interactions in the 1 GeV/c Region (Proposals 39, 86)	Cambridge University Imperial College, London Westfield College, London	Nimrod	1·5m and 80cm bubble chambers
	16	Study of the K^0_L and of $K^0_L p$ Interactions in the range 300 to 800 MeV/c (Proposal 89)	Bologna University Edinburgh University Glasgow University Pisa University Rutherford Laboratory	CERN PS	2m bubble chamber
	17	K^+d Interactions in the 2 to 3 GeV/c Region (Proposal 56)	Imperial College, London Westfield College, London	Nimrod	1·5m bubble chamber

Section	Experiment Number	Title	Collaboration	Accelerator or Location	Technique
	18	Interactions of Slow and Stopped K^- Mesons (Proposal 117)	University College, London Birmingham University Free University of Brussels Durham University	Nimrod	1·5m bubble chamber TST
	19	High Strangeness Baryon Resonance Studies Using the Rapid Cycling Bubble Chamber (Proposal 119)	Oxford University Rome University CEN Saclay College de France Paris Rutherford Laboratory	Nimrod	Hybrid

1.1.3 Intermediate Energy Production Mechanisms

Section	Experiment Number	Title	Collaboration	Accelerator or Location	Technique
1.1.3	20	Study of Exchange Mechanisms in Quasi Two Body Final States using the RMS Spectrometer (Proposals 126, 150)	Edinburgh University Westfield College, London Rutherford Laboratory	Nimrod	Counter
	21	Differential Cross Sections and Polarisations in Hypercharge Exchange Reactions (Proposal 100)	Birmingham University Genova University Stockholm University CERN Rutherford Laboratory	CERN PS	Counter
	22	Spin Rotation Parameters in $\pi^-p \rightarrow K^0\Lambda$ (Proposal 124)	Imperial College, London Southampton University ETH Zurich CERN Helsinki University	CERN PS	Counter
	23	Spin Dependence of Inclusive Reactions and Low Cross Section pp Elastic Scattering (Proposal 112)	CERN Paris-Sud University Oxford University	CERN PS	Counter
	24	Study of $p\bar{p}$ Annihilations at 2 GeV/c (Proposal 115)	Tata Institute, Bombay Melbourne University	Nimrod	1·5m bubble chamber TST
	25	Y^* Production in π^+p and K^-p Interactions (Proposal 147)	Imperial College, London SLAC Purdue University	SLAC	Hybrid
	26	$p\bar{p}$ Interactions in the Range 2·6 - 5·7 GeV/c (Proposal 162)	Argonne National Laboratory Melbourne University Carnegie-Mellon University Rutherford Laboratory	Argonne	12ft bubble chamber TST
	27	π^-p Interactions at 22 GeV/c (Proposal 134)	Oxford University Pisa University Pavia University Rutherford Laboratory	CERN PS	BEBC
	28	Hyperon-Proton Interactions up to 24 GeV/c (Proposals 49, 82)	Cambridge University	CERN PS	2m bubble chamber

1.1.4 Higher Energy Experiments

Section	Experiment Number	Title	Collaboration	Accelerator or Location	Technique
1.1.4	29	Exclusive Hadronic Processes at Large Transverse Momentum (Proposal 151)	CERN University College, London Genova University Oslo University Paris-Sud University	CERN SPS	Counter
	30	High Transverse Momentum Behaviour at the ISR (Proposal 129)	Liverpool University Daresbury Laboratory Rutherford Laboratory	CERN ISR	Counter
	31	Study of High Transverse Momentum Phenomena in the Split Field Magnet (Proposal 130)	Liverpool University Orsay Laboratory Rutherford Laboratory Scandinavian Universities	CERN ISR	Counter
	32	Inclusive Particle Production at Low Transverse Momenta and Large Angles at the CERN Intersecting Storage Rings (Proposal 131)	CERN University College, London Bristol University Massachusetts Inst. of Tech.	CERN ISR	Counter
	33	ISR Solenoid Experiment to Study Electron Production (Proposal 146)	CERN Oxford University Columbia University Rockefeller University	CERN ISR	Counter

Section	Experiment Number	Title	Collaboration	Accelerator or Location	Technique
	34	Σ^-p Interactions at 50 and 100 GeV/c and meson-proton interactions at 50 and 200 GeV/c (Proposals 122, 127)	Cambridge University	Fermilab	15ft bubble chamber
	35	K^-p Interactions at 45 and 65 GeV/c (Proposal 161)	Glasgow University CEN Saclay Rutherford Laboratory	CERN SPS	BEBC
	36	Internal Targets at the Fermilab (Proposal 143)	Imperial College, London Rochester University Rutgers University	Fermilab	Counter
	37	$p\bar{p}$ Interactions at 100 GeV/c	Fermilab Cambridge University Michigan State University	Fermilab	30in bubble chamber
1.1.5	**Weak and Electromagnetic Interactions**				
	38	Muon-Nucleon Scattering (Proposal 96)	Chicago University Harvard University Illinois University Oxford University	Fermilab	Counter
	39	Experiments with High Energy Charged Hyperons (Proposal 140)	Bristol University Geneva University Heidelberg University Lausanne University Orsay Laboratory Rutherford Laboratory CRN Strasbourg-Cronenbourg	CERN SPS	Counter
	40	Study of Neutrino and Antineutrino Reactions (Proposal 160)	Brussels University University College, London Bari University Rutherford Laboratory	CERN SPS	BEBC TST
	41	CP in a High Magnetic Field (Proposal 168)	Imperial College, London Rutherford Laboratory	Nimrod	Counter
1.1.6	**Searches for New Particles**				
	42	Heavy Particle Search (Proposal 144)	University College, London AWRE Aldermaston Rutherford Laboratory	Cosmic Rays	Mass spectrometer & counter
	43	Search for Short-Lived Particles Produced in Neutrino Interactions (Proposal 163)	Brussels University University College, Dublin Fermilab University College, London Rome University Strasbourg University	Fermilab	Counter
	44	Charm Search at Omega (Proposal 164)	Bari University Birmingham University Bonn University CERN Daresbury Laboratory DESY Ecole Polytechnique Paris ETH Zurich Freiburg University Glasgow University Liverpool University Milan University Orsay Laboratory Rutherford Laboratory CEN Saclay Westfield College, London	CERN PS	Counter

Section	Experiment Number	Title	Collaboration	Accelerator or Location	Technique
1.2	Nuclear Physics				
	45	Parity and Time Reversal Symmetry Tests	Sussex University Glasgow University Harvard University ILL	ILL	
	46	Search for an Electric Dipole Moment of the Neutron	Sussex University Rutherford Laboratory Oxford University Harvard University Oak Ridge Laboratory Technical University Munich CEN Grenoble ILL	ILL	
	47	A Measurement of the Neutron Lifetime	Sussex University Rutherford Laboratory ILL	ILL	
	48	Measurement of Triple Scattering Polarisation Parameters in Nucleon-Nucleon Scattering at 500 MeV	Bedford College, London AERE, Harwell Surrey University Queen Mary College, London British Columbia University Victoria University	TRIUMF	
	49	Experiments with K^-–Mesic Atoms	Birmingham University Surrey University Rutherford Laboratory	Nimrod	
	50	Measurements of the Decay Rate $\pi^0 \rightarrow e^+e^-$ with the Omicron Spectrometer	Birmingham University Oxford University Daresbury Laboratory University College, London	CERN	
	51	Coulomb/Nuclear Interference in Alpha Particle Scattering	Kings College, London	AERE	
	52	Scattering of Polarised ^{3}He Beams	Kings College, London Birmingham University	AERE	
	53	Helium-3 Elastic and Inelastic Scattering and the (h,α) Reaction	Kings College, London	AERE	
	54	Elastic and Inelastic Scattering of 53 MeV ^{3}He from the Samarium Isotopes	Kings College, London Oak Ridge Laboratory	AERE	
1.5	Radiological Experiments				
	55	Chromosome Aberrations in White Blood Cells	National Radiological Protection Board Rutherford Laboratory	Nimrod	
	56	Irradiation of Frozen Cancer Cells	Glasgow Inst of Radio-therapeutics Rutherford Laboratory	Nimrod	
	57	Irradiation of Cancer Cells at Room Temperature	Medical College of St Barthol-omews Hospital, London	Nimrod	
	58	π^- Irradiation of the Testis in Mice	Medical College of St Barthol-omews Hospital, London	Nimrod	
	59	Study of the Physical Nature of π^- Induced Radiation	Medical College of St Barthol-omews Hospital, London Rutherford Laboratory Leeds University	Nimrod	

1.1 High Energy Physics

The experimental High Energy Physics programme supported by the Rutherford Laboratory is based principally on the proton accelerators at the European Centre for Nuclear Research (CERN) in Geneva and the Rutherford Laboratory. The two high energy machines currently operating at CERN are the 28 GeV Proton Synchrotron (PS) and the Intersecting Storage Rings (ISR).

The ISR provides European physicists with the opportunity of studying particle interactions at the highest energy available in any laboratory in the world. Two proton beams with energies of up to 31 GeV are made to collide almost head on. The centre of mass energy is equal to that which would be obtained if a beam from a 2000 GeV conventional accelerator were directed onto protons in a liquid hydrogen target.

The experimental facilities at CERN will be further enhanced when the 400 GeV Super Proton Synchrotron (SPS) comes into operation towards the end of 1976. Time scales in High Energy Physics research are such that construction of apparatus at the Rutherford Laboratory is almost complete for some of the first experiments which will use the SPS.

Nimrod, the 8 GeV proton synchrotron at the Rutherford Laboratory provides facilities complementary to those available at the higher energy CERN machines. The continuing interest and importance of physics at the low energy end of the High Energy domain is clearly illustrated by the current intense experimental activity around Nimrod.

The Rutherford Laboratory is also involved in experiments at the Stanford Linear Accelerator Centre (SLAC), the Fermi National Accelerator Laboratory (FNAL) and the Argonne National Laboratory (ANL) in the United States.

During the past year a total of 44 experiments, at all stages of development from design to data analysis, have been supported by this Laboratory. Of these, 26 use electronic detectors and 16 are based on the analysis of bubble chamber film. Two experiments attempt to combine the major advantages of the bubble chamber technique – good spatial resolution and isotropic detection efficiency – with the selectivity of counter experiments, using hybrid systems.

The experiments are listed in the table according to the physics topic studied, although the classification of bubble chamber experiments is rather arbitrary since a wide range of information may be obtained in one film exposure.

The emphasis on the study of resonances (unstable particle states) at Nimrod is in the tradition of the Laboratory since it has made major contributions to this field in the past. The new experiments are much more sophisticated than their predecessors. In particular, experiments 12 and 13 which use new types of polarised target and the hybrid experiment, 19, will provide entirely new information on baryon resonances. Experiments 7 and 18, studying meson and baryon resonances respectively, are noteworthy since they were the first to employ the revolutionary new bubble chamber technique of the track sensitive target (TST) developed at the Rutherford Laboratory. The urgent need for a complete understanding of baryon and meson spectroscopy has recently been underlined by the theoretical attempts to explain the new long-lived states which have been discovered during the past year.

The dynamics of the strong interactions are most conveniently studied in measurements of two body and quasi two body production at medium energies. This is the result of a compromise between using the highest possible energy, where it is simplest to interpret data in terms of Regge exchange models, and lower energies where the cross sections for exclusive channels are higher.

Progress in the understanding of these processes can only come from a direct determination of the scattering amplitudes. This requires a complete set of measurements for each reaction including, if possible, studies made with a polarised proton target. Experiments 20 and 22 are perfect examples of the adoption of this approach and will provide unique new data on exchange mechanisms.

There are two important reasons for studying particle interactions at high energy. Firstly, many of the assumptions made in formulating current models of hadronic interactions only apply at infinite energy. Thus, inclusive reactions whose cross sections remain large are best studied at the highest possible energy in order to simplify the interpretation of the data, and experiments 32 and 37 are motivated by this consideration. The second reason concerns the small fraction of events in which particles are emitted from high energy collisions with large momentum transverse to the incident particle direction. Because of the uncertainty principle, these high transverse momentum particles yield information on the behaviour of the strong interaction at small distances.

Experiments 30 and 31 at the CERN ISR are probing the inner structure of protons through the measurement of high transverse momentum events. Results from other experiments are consistent with the hypothesis that strongly interacting particles or hadrons are composed of point-like constituents called partons, and there are indications that these objects may be identified with the quarks first postulated to explain the spectrum of resonances observed in low energy experiments. Thus a single aesthetically attractive explanation for a wide range of phenomena observed in High Energy Physics may be close.

Weak and electromagnetic phenomena are studied for their intrinsic interest and also for the information they can provide on the properties of hadrons. The point-like nature of leptons (electrons, muons and neutrinos) makes them ideal projectiles in scattering experiments designed to study the detailed structure of the target nucleons.

The recent progress made with gauge theories, which describe both the weak and electromagnetic interactions in a unified way, is a first step towards the ultimate goal of constructing a single unified theory for all the types of interaction between elementary particles.

Experiments 38 and 40 will provide information on the sub-structure of hadrons and on the relationship between the weak and electromagnetic interactions. Comparisons of the weak decay properties of the so-called stable particles, such as those made in experiment 39, provide additional indirect data for both these fields of study. These two types of experiment, high energy scattering and particle decay, are related in a similar way to high energy, high transverse momentum studies and low energy resonance experiments on hadronic interactions.

1.1.1 Meson Spectroscopy

EXPERIMENT 1

A Study of Neutral Bosons Using a Time of Flight Trigger

Birmingham University; Tel Aviv University; Westfield College, London; Rutherford Laboratory

This experiment is designed to study the reaction

$$\pi^- p \rightarrow n + X^\circ$$

using the Omega spectrometer at CERN. The neutron is detected in an array of neutron counters and the decay products of X° in the Omega spark chamber system. Events are selected by requiring neutrons in the energy range 10 - 400 MeV using a time of flight technique. The experiment has been run with incident pion momenta of 8, 12 and 15 GeV/c, corresponding to an X° mass in the range of 600 - 1700, 600 - 2300, and 600 - 2600 GeV/c^2 respectively.

Reactions of the type

$$\pi^- p \rightarrow \pi^+\pi^- n \qquad 1$$

$$\pi^- p \rightarrow \pi^+\pi^\circ\pi^- n \qquad 2$$

$$\pi^- p \rightarrow \pi^+\pi^-\pi^+\pi^- n \qquad 3$$

are being extracted from the data tapes. Reactions 1 and 2 have been fully investigated at 8 GeV/c. Magnetic tapes containing fully fitted events exist for Reactions 1 and 2 at 12 GeV/c, and physics analysis is proceeding. The problems of efficiently extracting events of Reaction 3 at 12 GeV/c are being investigated. Reactions 1 and 2 at 15 GeV/c have been looked at and processing of the complete data sample is about to commence.

25,000 events of Reaction 1 at 12 GeV/c have been obtained and the angular distribution of the $\pi^+\pi^-$ in its centre of mass has been analysed in terms of spherical harmonic functions. A full partial wave analysis of the $\pi\pi$ system is currently being performed.

23,000 events of Reaction 2 at 12 GeV/c and 2700 at 8 GeV/c have been obtained. Both data samples contain a clear signal for the reaction $\pi^- p \rightarrow \omega n$, and assuming an ω width of 10 MeV, a Breit-Wigner fit gives a mass resolution of 15 MeV at 8 GeV/c and 21 MeV at 12 GeV/c.

The ω differential cross section at 8 and 12 GeV/c has been calculated and density matrix elements evaluated as a function of t, the four momentum transfer squared, between the proton and neutron. Using these quantities the contribution from natural and unnatural parity exchange in the process $\pi^- p \rightarrow \omega n$ can be calculated. These contributions have been studied as a function of incident pion momentum, using results at 8 and 12 GeV/c and other published data.

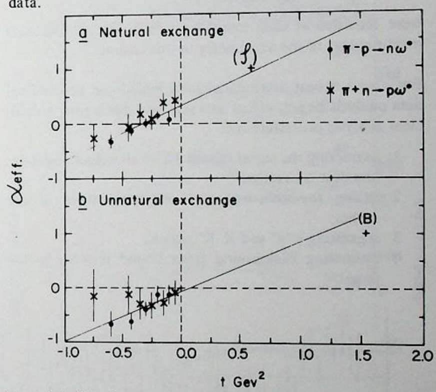

Figure 1.1 Effective trajectories for natural and unnatural parity exchanges. The points for $\pi^+ n \rightarrow \omega^\circ p$ are from published data. (Experiment 1)

Interpretation of the data in terms of a simple Regge exchange model allows the effective trajectory to be extracted as a function of t. The trajectories obtained are shown in Figure 1.1, where they can be seen to pass close to the ρ and B poles.

For final normalisation of the results the efficiency of the neutron counter as a function of neutron energy is required, and the data-taking stage of an experiment to measure this has been completed at CERN. In this experiment, 600 MeV neutrons were elastically scattered off a hydrogen target, the recoiling protons were detected in an array of wire chambers and scintillation counters, and the neutron counter was positioned to intercept the scattered neutrons. 30 million triggers have been taken of which one million are fully measured neutron-proton elastic scatters and a further one million are neutron-proton elastic events where only the proton was detected.

EXPERIMENT 2

Polarisation Measurements for $\bar{p}p$ Annihilations into $\pi^-\pi^+$

Queen Mary College, London; Daresbury Laboratory; Rutherford Laboratory

This experiment aims to measure the angular distribution of the asymmetry parameter in the reaction

$$\bar{p}p \rightarrow \pi^-\pi^+$$

using a polarised proton target made of propanediol. The measurements were made in the m11 beam line at CERN, and several thousand events were recorded at each of 11 momenta, in the range 1·0 to 2·2 GeV/c. (Previous world data on the asymmetry consisted of 350 events at one momentum). In addition, several hundred events of the reaction

$$\bar{p}p \rightarrow K^-K^+$$

were recorded at each momentum, allowing a crude first measurement of the asymmetry in this channel.

For about a year after data-taking ended and before final data analysis began, effort was put into developing an efficient analysis procedure for:

1 extracting the signal (about 1% of all triggers) without loss of $\pi^-\pi^+$ events,
2 fitting the centre-of-mass scattering angle of the events,
3 separating $\pi^-\pi^+$ and K^-K^+ signals,
4 estimating background from bound protons in the target.

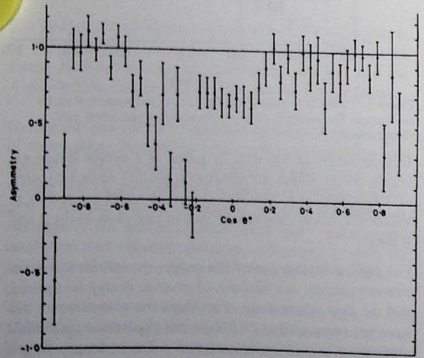

Figure 1.2 Asymmetry parameter for $\bar{p}p \rightarrow \pi^-\pi^+$ at 1·6 GeV/c. (Experiment 2)

Figure 1.2 shows the measured asymmetry parameter at 1·6 GeV/c, and agreement between measured differential cross section and the previous results of the group using a liquid hydrogen target is excellent.

The next step is to combine the asymmetry results with these previous measurements of the differential cross section to do a form of Barrelet zero amplitude analysis in order to establish the existence and quantum numbers of any direct channel resonances which are present.

EXPERIMENT 3

Meson Production Very Close to Threshold

Imperial College, London; Southampton University

While much attention in particle physics is directed towards the behaviour of matter at very high energies, there are still many questions to be settled in the study of resonant states at the lower energies available with Nimrod at the Rutherford Laboratory. The production of narrow-width mesons close to the reaction threshold is an example of this: The advantages of such experiments stem from the simplicity of the possible final states, the high resolution available, particularly in missing mass, and from the possibility of studying the effect of the threshold on the other channels, particularly for elastic scattering.

Earlier π^-p experiments have included a precision measurement of the mass and width of the ω, an upper limit to the η' width of 0·8 MeV, an explanation of a curious effect seen at the threshold for K^+K^- production in terms of the production and decay of the S* meson, and the discovery of anomalies in the production cross sections for the ω and particularly the η' meson. In this last case the matrix element is found to rise rapidly as threshold is approached from above.

A new experiment has been performed with apparatus of improved resolution. All the data has been collected and analysis is in progress. As an example of the use of the new data, it should be possible to study the anomaly in the η' cross section down to a kinetic energy in the centre of mass of only 200 keV, an order of magnitude nearer the threshold than achieved in the earlier data. This should be valuable in elucidating the effect, particularly when used in conjunction with the data now available in the same region from the elastic π^-p channel.

EXPERIMENT 4

Study of Exclusive Reactions in πp and Kp Interactions in the Energy Range up to 100 GeV

CERN; Max Planck Institute, Munich; Amsterdam University; Oxford University; Rutherford Laboratory

This experiment is being prepared for running at the CERN SPS and will enable the study of inelastic exclusive reactions, especially pion production, to be extended to higher energies.

EXPERIMENT 5

Study of Meson Resonances Decaying into Strange Particles in the Omega Spectrometer at the SPS

Birmingham University

Mesons made of strange quark-antiquark pairs are produced much more copiously by incident kaons than by pions since the kaon itself contains a strange quark. Apart from the ϕ-meson, only one other, the f′ (1514), is known to be in this class. Several more are expected and will be searched for using the Omega spectrometer and the RF separated beam at the SPS.

EXPERIMENT 6

Study of π^+d Interactions at 4 GeV/c

Birmingham University; Durham University; Rutherford Laboratory

In this experiment 735,000 pictures were taken in the CERN 2m Bubble Chamber in two separate runs in 1970 and 1972. With the exception of one or two topics, which are still being studied, the physics analysis is now complete.

In the last few years there has been considerable interest in the phenomenology of "quasi two-body reactions" and the availability of high statistics data from this experiment has allowed a significant contribution to be made to this aspect of strong interaction physics.

The four reactions $\pi^+n \rightarrow \rho^\circ p$, $\pi^+n \rightarrow f^\circ p$, $\pi^+n \rightarrow \omega^\circ p$, $\pi^+n \rightarrow A_2^\circ p$, form a quartet of quasi two-body reactions whose production mechanisms may be related to one another (and to other two-body processes), using the predictions of current theories. The study of the first two of these reactions has now been supplemented by detailed analyses of ω° and A_2° production. It has been confirmed that the ideas of Regge phenomenology and of SU(3) do indeed give a satisfactory simultaneous description of these and other processes. For example, SU(3) predicts that the differential cross-sections for ρ° and ω° production should be related to analogous data for K* production. Using ρ° and ω° data from this experiment with other K* data, this is generally found to be the case in the range $0 < |t| < 0{\cdot}6\ (\mathrm{GeV/c})^2$.

Although many meson resonances have now been known for some years, there are others, predicted for instance by the quark model, which have so far not been detected. In particular, resonances with spin-parity $J^P = 1^+$ are proving very difficult to find. Using a powerful technique developed at Illinois University, different spin-parity components have been extracted from the $\pi^+\pi^-\pi^\circ$ system in the reaction

$$\pi^+n \rightarrow \pi^+\pi^-\pi^\circ p$$

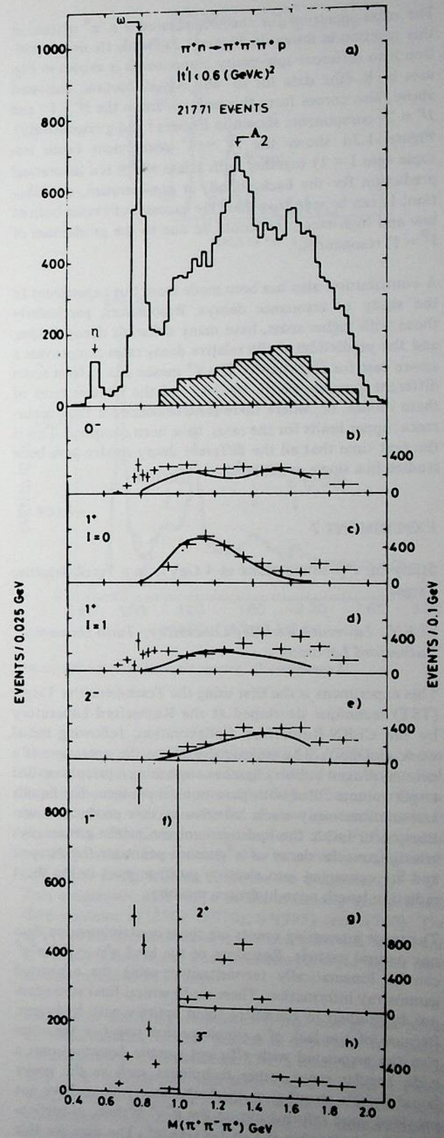

Figure 1.3 Effective mass (a) and decomposition of $\pi^+\pi^-\pi^\circ$ into different spin-parity components. The shaded area is the contribution to Δ production. (Experiment 6)

The mass spectrum for the unseparated $\pi^+\pi^-\pi^0$ system in this reaction is shown in Figure 1.3a, while its decomposition into different spin-parity components is shown in Figures b - h; (the data for ω^0 and A_2^0 production, discussed above, also comes from this reaction and is the $J^P = 1^-$ and $J^P = 2^+$ components shown in Figures f and g respectively). Figure 1.3d shows the $J^P = 1^+$ component (with isotopic spin I = 1) together with a line which is a theoretical prediction for the background, or non-resonant, contribution. It can be seen that there are excesses of events both at low and high mass; this could be due to the production of $J^P = 1^+$ resonances.

A contribution also has been made from this experiment to the study of resonance decays. Resonances, particularly those with higher mass, have many different decay modes, and the prediction of the relative decay rates can provide a severe test for any theory. The f^0 meson has at least seven different possible decay modes, and the relative rates of these modes, or, where there is no evidence for their occurrence, upper limits for the rates, have been compiled. This is the first time that all the different decay modes have been studied in a single experiment.

EXPERIMENT 7

Study of π^+p Interactions at 4 GeV/c in a Track-Sensitive Target

CERN; Lawrence Berkeley Laboratory; Turin University; Rutherford Laboratory

This experiment is the first using the Track-Sensitive Target (TST) technique developed at the Rutherford Laboratory by the CERN-Rutherford Collaboration, following initial work at DESY. The technique involves the operation of a neon-hydrogen bubble chamber containing a perspex-walled target volume filled with pure liquid hydrogen. The liquids are simultaneously track sensitive so that production vertices occur inside the hydrogen volume, whilst gamma rays arising from the decay of π^0-mesons penetrate the perspex and are converted into electron positron pairs in the short radiation length neon-hydrogen mixture.

The most interesting events are those containing more than one neutral particle. Reactions of the kind $\pi^+p \rightarrow p\pi^+\pi^0\pi^0$ can be kinematically reconstructed using the converted gamma ray information. These multineutral final states cannot be studied in chambers filled entirely with hydrogen. Because of the lack of a simple proton target or the complexities associated with efficient gamma detection over a wide angular range, other techniques such as the heavy liquid bubble chamber or spark chamber systems have not provided good information on the $\pi^0\pi^0$ system, in particular in the mass range 0·3 to 1·5 GeV/c². The data for this experiment consists of over 600,000 pictures in a steel-framed TST and over 500,000 pictures with an all-perspex TST. The all-perspex TST film has been fully scanned and measured, and remeasurements will be completed early in 1976.

The TST system represents a major development of the bubble chamber technique and because of the additional information content of the pictures poses a number of new problems associated with optical reconstruction, kinematical fitting and event selection. Fortunately these problems have essentially been solved and future TST experiments, even with large volume chambers, should benefit considerably from the groundwork which has now been done.

The status of the analysis is such that detailed physics information is just appearing. As an example of this analysis the reaction $\pi^+p \rightarrow \Delta^{++}\pi^0\pi^0$ is particularly interesting and is at present under study. Figure 1.4 shows a preliminary $\pi^0\pi^0$ mass spectrum based on ~ 30% of the sample of events from the perspex TST. The f^0 peak is quite clear together with a broad distribution of low $\pi^0\pi^0$ masses. Although this analysis is still at an early stage, it is already clear that clean information with reasonable statistical significance will be obtained on the s-wave $\pi\pi$ interaction. Also plotted in Figure 1.4 is the π^0 detection probability as a function of the $\pi^0\pi^0$ mass. This shows that there is no bias against detecting events with a high $\pi^0\pi^0$ mass.

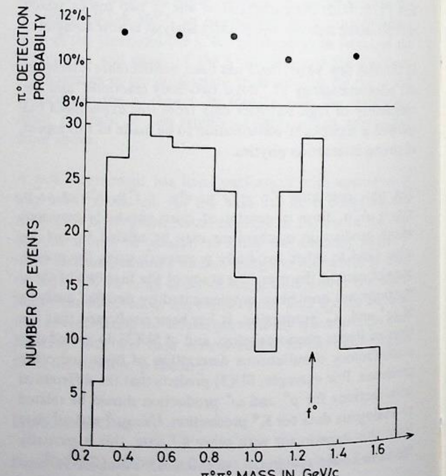

Figure 1.4 $\pi^0\pi^0$ mass distribution and detection probability from the reaction $\pi^+p \rightarrow \Delta^{++}\pi^0\pi^0$. (Experiment 7)

An interesting sideline to the main experiment has been the observation of the relativistic rise in bubble density for tracks in the neon-hydrogen mixture surrounding the TST. Figure 1.5 shows the expected rise on the basis of the data. It was found that relativistic particles have 28 ± 2% more bubbles per unit length than minimum ionising particles. This observation could provide a useful method for distinguishing $\pi^\pm$ mesons, $K^\pm$ mesons and protons at momenta in the 5-20 GeV/c range in future experiments using TSTs at the high energy machines.

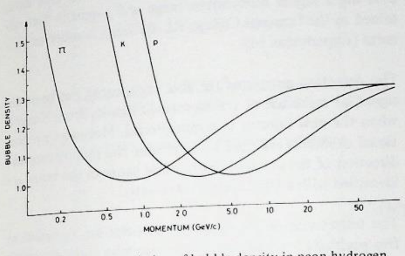

Figure 1.5 Expected variation of bubble density in neon-hydrogen. (Experiment 7)

EXPERIMENT 8

Study of K^-p Interactions at 14·3 GeV/c

CEN, Saclay; Ecole Polytechnique, Paris; Rutherford Laboratory

This profitable experiment, based on the 2m hydrogen-filled bubble chamber at CERN, was aimed at obtaining information on the general features of K^-p interactions with a K^- beam energy of 14·3 GeV/c, together with detailed information on strange meson states and various production mechanisms. All these aims have been achieved after six years of effort, and analysis is concluding after 28 papers already have been published.

In particular, the year saw the continued analysis of the final data sample which consists of half a million events. Studies have been made of both exclusive reactions in which all produced particles are identified and measured, and inclusive reactions, in which only a small number of produced particles are identified and measured for each event, and the recoiling system can contain any number of particles, e.g. $K^-p \rightarrow \Lambda$ + (anything).

Exclusive Reactions. The first observation of the recently discovered high mass strange $K\pi^-$ resonance, K*(1780), being produced in a reaction where no charge is exchanged was made in the data on the reaction $K^-p \rightarrow (\bar{K}^0\pi^-)p$, and the $\bar{K}^0\pi^-$ mass spectrum for this reaction is shown in Figure 1.6. An analysis of the decay angular distributions favours a spin 3 and negative parity assignment. This classifies the particle as the strange doublet in the SU(3) nonet of particles consisting of K*(1780), g(1680), ω(1675) and an as yet unseen non-strange meson with properties similar to the φ(1019).

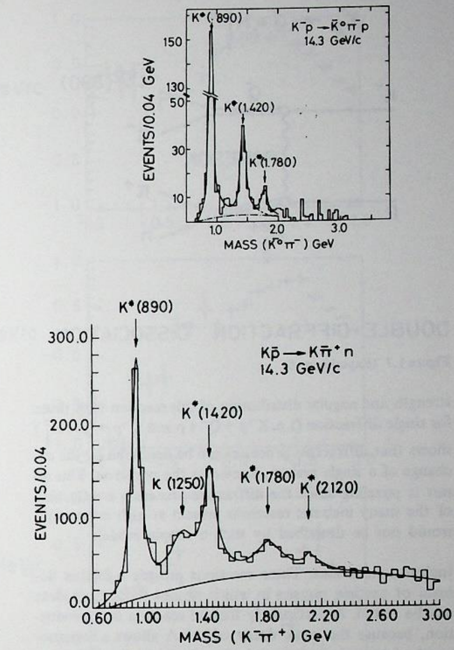

Figure 1.6 $K\pi$ effective mass spectra. (Experiment 8)

The reaction, $K^-p \rightarrow (K^-\pi^+)n$, in which $K\pi$ resonances can be produced by a charge exchange process was also studied. It was found to contain a wealth of spectroscopic information, as can be seen from the $K^-\pi^+$ mass spectrum shown in Figure 1.6. The $K\pi$ resonance seen at 1·2 GeV, designated κ(1250), is seen more clearly than in previous experiments and a spin parity analysis confirms the assignment $J^P = 0^+$. This assignment puts the κ in the symmetry group which then contains κ(1250), δ(970), S*(993) and ε(700). The K*(1780) is also seen besides the well known K*(890) and K*(1420). There is also weak evidence for a yet higher mass strange meson at 2120 MeV.

Diffraction scattering dominates at high energy and hence an understanding of this process is important for understanding how particles interact. Thus a study of the reaction $K^-p \rightarrow K^{*0}(890)\pi^-n\pi^+$ was made and a sample of events which may be produced by a mechanism known as Double Diffraction Dissociation was isolated. For this reaction it corresponds to a meson system, Q, and a baryon system, $N^*_{\frac{1}{2}}$, being produced simultaneously by a diffractive process, i.e. $K^-p \rightarrow Q^- + N^{*+}_{\frac{1}{2}}$ (see Figure 1.7). A comparison of the

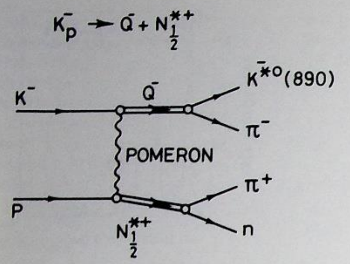

DOUBLE DIFFRACTION DISSOCIATION

Figure 1.7 (Experiment 8)

strength and angular distribution of this reaction with those for single diffraction (i.e. $K^-p \rightarrow Q^- + p$ and $K^-p \rightarrow K^- + N^*_{\frac{1}{2}}$) shows that diffractive processes can be described by the exchange of a single system, known as the pomeron. This result is puzzling since the diffractive process is a reflection of the many inelastic reactions present at high energy and would not be described by such a simple model.

Inclusive Reactions. These reactions provide a further domain of particle physics in which various theoretical ideas can be tested. A particularly fruitful reaction is Λ production, because the weak decay of the Λ allows a measurement of its polarisation and gives further information on the amplitudes describing the reaction. The final data consists of 36,000 events which is a threefold increase on the sample used in a previous analysis. A new analysis of the polarisation of the high momentum Λs shows that a simple peripheral model (Triple Regge) with the exchange of a single baryon can reproduce the dominant features of the polarisation data. The implication of this result is that this reaction can be useful to probe the process of baryon exchange which occurs very weakly in other reactions at high energy.

1.1.2 Baryon Spectroscopy

EXPERIMENT 9

π^+, π^-, K^- -p Elastic Scattering Differential Cross-Sections

Bristol University; Southampton University; Rutherford Laboratory

This experiment on K^- mesons is one of a series carried out by this collaboration, designed to study meson-proton scattering with high statistical accuracy and good normalisation.

Final results of measurements on π^+, π^-p scattering are in preparation and will be released soon.

The K^-p system in the momentum range 600 MeV/c to 2500 MeV/c shows a large number of resonant states, and the aim of this experiment is to measure approximately 50,000 K^-p elastic scattering events per momenta in the momentum range 1200 MeV/c to 2500 MeV/c. This data, covering a higher momentum range will augment that obtained in the Imperial College/RL Bubble Chamber experiment (Experiment 14).

The detection apparatus for this experiment has been designed to make use of the increased intensity from Nimrod when the new injector is commissioned. Multiwire proportional chambers are used to determine the momentum and direction of the incident beam, while kaons in the beam are identified with a DISC Cerenkov counter.

The trajectories of the scattered particles are recorded at five positions by modules of large area wire spark chambers with capacitive readout, and this system, containing 80,000 wires and capable of being read into an on-line computer in 3 msec, is now working. Multiwire proportional chambers are used to detect scattered particles close to the beam where the high flux of beam particles may confuse the interpretation of the scattered event.

The off-line analysis programs are being prepared for the main 360/195 computer and it will be possible to analyse data soon after it is collected by the on-line PDP 11/45 computer.

EXPERIMENT 10

Coherent Production of I = ½ Baryon States on Helium

CERN; University College, London; Uppsala University; Rutherford Laboratory

This experiment, designed to study the elastic and inelastic scattering of high-energy protons on helium nuclei when the α-particle recoils coherently, has been completed, and final data analysis is well under way.

EXPERIMENT 11

Measurement of the Differential Cross Section and Polarisation of the Reactions $\pi p \rightarrow \pi^\circ n$ and $\pi p \rightarrow \eta^\circ n$

Rutherford Laboratory

In a high precision study of the pion-nucleon system at the Rutherford Laboratory, measurements have been made of the $\pi^\circ n$ and $\eta^\circ n$ differential cross-sections and polarisation parameters.

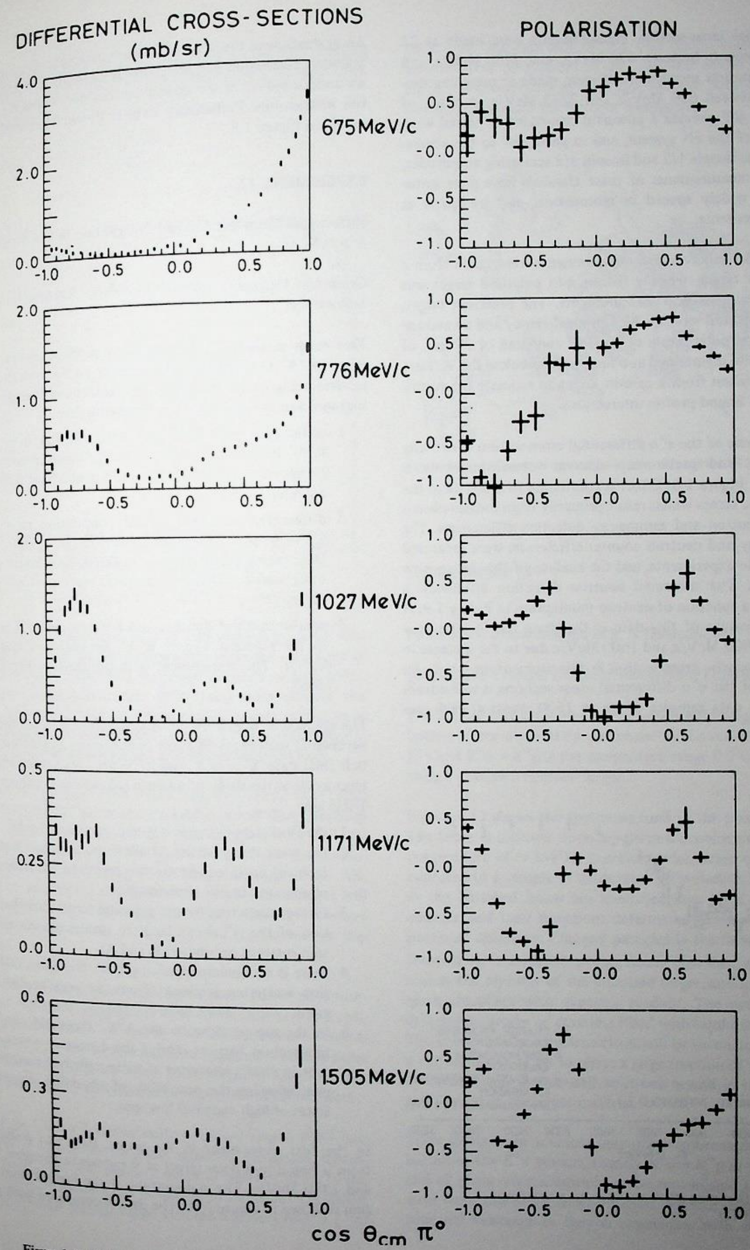

Figure 1.8 Differential cross-sections and polarisations in the reaction $\pi^-p \rightarrow \pi^\circ n$. (Experiment 11)

Differential cross-section measurements were made at 23 beam momenta between 620 MeV/c and 2730 MeV/c, and 22 polarisation measurements were made at matching momenta between 620 MeV/c and 2270 MeV/c. A study of this data will provide a powerful constraint to partial wave analyses of the πN system, and in particular to the separation of the isospin 1/2 and isospin 3/2 scattering amplitudes. Existing measurements of these channels have poor statistics, are widely spaced in momentum, and are sparse at higher momenta.

Differential cross-section measurements were taken from a hydrogen target, while a frozen spin polarised target was used for polarisation measurements. The polarised target, which operated with an 85% user-efficiency and an average free-proton polarisation of $\sim$ 70%, consisted of 20 cm^3 of propanediol maintained at a temperature below 0·5°K. Data was also taken from a carbon target to estimate the contribution of bound proton interactions.

The analysis of the $\pi^0 n$ differential cross-section is virtually complete, and preliminary data at several momenta is shown in Figure 1.8. Effort is continuing to understand the systematic errors which result primarily from measurements of the neutron and gamma-ray detection efficiencies. The gamma-ray and neutron counter efficiencies were measured in separate experiments, and the analysis of this data is now complete. The measured neutron detection efficiency is shown as a function of neutron momentum in Figure 1.9. A notable feature of this data is the sharp rise in efficiency between 800 MeV/c and 1600 MeV/c due to the increase in the np inelastic cross-section in this momentum range. An analysis of the $\eta^0 n$ differential cross sections is well advanced, with data samples of up to 1500 events at each momentum.

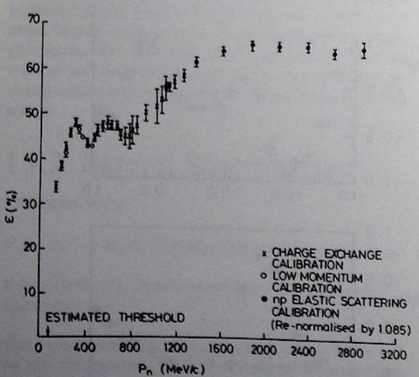

Figure 1.9 Detection efficiency of neutron counters. (Experiment 11)

An evaluation of the $\pi^0 n$ polarisation parameter is progressing well. The major analysis effort is now concentrated on an understanding of the contamination due to bound proton interactions. Preliminary data is shown at several momenta in Figure 1.8.

EXPERIMENT 12

Differential Cross-sections and Polarisation in the Reaction $\pi^- p \to K^0 \Lambda^0$

Cambridge University; Bristol University; Rutherford Laboratory

This team is studying the associated production reaction $\pi^- p \to K^0 \Lambda^0$ in a series of experiments on Nimrod, the objectives being to study nucleon resonances and their groupings into supermultiplets. The experiments are:

1 differential cross-section and polarisation in $\pi^- p \to K^0 \Lambda^0$ between 0·9 and 1·4 GeV/c beam momentum (Proposal 87). This experiment is in the final stages of analysis.

2 differential cross-section and polarisation in $\pi^- p \to K^0 \Lambda^0$ between 1·4 and 2·4 GeV/c. (Proposal 114). Data taking has just been completed, and should yield more statistics than any previous work in this energy range.

3 measurement of the spin rotation parameters R and A in the reaction $\pi^- p \to K^0 \Lambda^0$ between 1·0 and 2·4 GeV/c. This experiment is in preparation (Proposal 166).

The reaction $\pi^- p \to K^0 \Lambda^0$, although suffering from the experimental drawbacks of a low cross-section and a four particle final state, $K^0 \to \pi^+ \pi^-$ and $\Lambda^0 \to p\pi^-$, has several advantages as far as the study of nucleon resonances is concerned. These are:

1 the final state is a pure isotopic spin state, $I = \frac{1}{2}$;
2 the weak decay of the Λ^0 allows polarisation and differential cross-section measurements to be made simultaneously in one experiment;
3 further scattering from a polarised target and observation of the Λ^0 decay leads to measurements of the spin rotation parameters R and A;
4 there is no Pomeron exchange and, therefore, diffraction scattering is absent from the angular distributions;
5 in the region close to the $\Lambda^0 K^0$ threshold, angular momentum barriers inhibit the dominant waves present in elastic scattering at these centre-of-mass energies, allowing the possibility of observing 'daughter' states of high mass but low spin.

In the first experiment in the series, data was collected from a liquid hydrogen target at 9 momenta between 930 and 1340 MeV/c. The polarisation at the highest momentum is shown in Figure 1.10. The data is compared with predictions from the three solutions in the partial wave analysis by Wagner and Lovelace which did not use the data from this experiment.

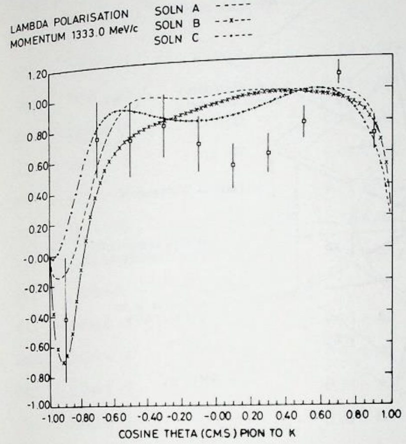

Figure 1.10 Λ polarisation in $\pi^- p \to K^0 \Lambda^0$. (Experiment 12)

This data and all other data in this channel has been subjected to a new partial wave analysis using the technique of Barrelet zeros. Since this technique depends on both polarisation measurements and differential cross-sections, the new data is essential in obtaining continuous partial wave solutions in the momentum interval 1170 to 1500 MeV/c where polarisations were not well measured previously.

The need for $S_{11}(1700)$, $P_{11}(1780)$, $P_{13}(1810)$, $D_{13}(1700)$ and $D_{15}(2100)$ resonances is established and their couplings have been compared to the predictions of the $SU(6)_W$ model. Not seen were the $D_{15}(1670)$ and $F_{15}(1638)$ resonances, which, according to $SU(6)_W$, decouple from ΛK. Data at the higher energies of the current experiment will be invaluable in elucidating the higher mass region, where resonances in the S_{11}, F_{17}, G_{17} and H_{19} waves are suggested.

The current experiment uses scintillation counters, proportional chambers, magnetostrictive spark chambers and optical spark chambers viewed by four on-line vidicon cameras (Figure 1.11). The system has been triggered 6 million times and data recorded on some 1200 magnetic tapes. As yet, only preliminary analysis has been performed on this data.

Early in 1976 a longitudinally polarised target, PT55 (see Section 4.1) is to be installed, replacing the present hydrogen target, and will enable a series of measurements of the spin rotation parameters R and A to be made. The initial centre-of-mass energy range covered will be 1700 to 2400 MeV, and this data will be the first measurements of the spin rotation parameters of any reaction in the resonance region. Measurements of such spin rotation parameters substantially eliminate the Barrelet ambiguities.

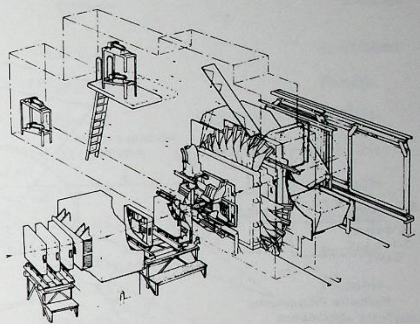

Figure 1.11 Diagram of apparatus used in Experiment 12.

EXPERIMENT 13

Polarisation measurements in K^+N Interactions

Queen Mary College, London; Rutherford Laboratory

The aim of this experiment is to measure the angular distribution of the asymmetry parameter in the reactions $K^+n \to K^+n$ and $K^+n \to K^0p$ in the momentum range 0·7 - 1·4 GeV/c using a polarised neutron target.

Figure 1.12 shows the apparatus used in the measurement. The beam is incident upon a polarised deuteron target; at a temperature of $\sim$ 0·4°K, deuteron polarisation of $\sim$ ·28 is expected in a sample of deuterated propanediol. The kaons in the enriched beam are identified in a DISC Cerenkov counter, and their directions determined from a set of proportional chambers. Charged particles in the final states are detected in a J-shaped proportional chamber which surrounds the cryostat of the polarised target, and in arrays of spark chambers with capacity readout. The neutrons are detected in arrays of counters filled with liquid scintillator. The energy of the struck nucleon will be reconstructed and a cut applied in order to reject a large fraction of the events occurring from unpolarised neutrons bound in the carbon and oxygen of the target material.

There exists at the moment only one measurement of polarisation in the K^+n system, namely $K^+n \to K^0p$ at 0·6 GeV/c, and all phase shift solutions for the zero isospin KN system stem from this single determination. Various solutions propose the existence of baryon resonances with strangeness

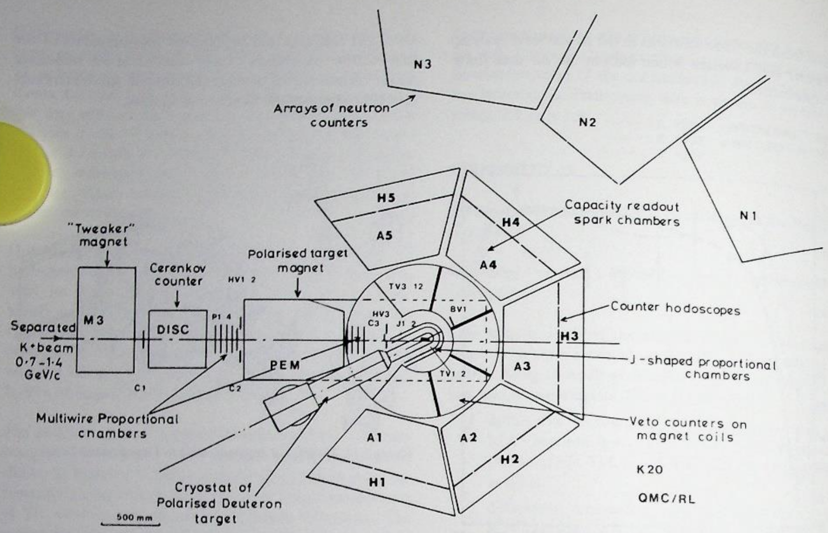

Figure 1.12 Layout of apparatus for Experiment 13.

equal to +1 (Z*), the most popular being a P_{01} state at 1740 MeV(P_{lab} = 0·9 GeV/c) and a D_{03} state at 1830 (P_{lab} = 1.1 GeV/c). These resonances, if real, are undesirable in the context of the quark model. Perhaps more important, recent theoretical work has attempted to predict the KN amplitudes from the known πN amplitudes, but progress is currently hampered by a rather poor knowledge of the zero isospin KN amplitude. This experiment should provide a good definitive comparison.

In the course of setting up the experiment, polarisation data will be collected in the experimentally simpler reactions of π^-p and K^-p elastic scattering. This information should help to resolve experimental conflicts in the π^-p system and add significantly to the partial wave analysis in the K^-N system.

EXPERIMENT 14

Study of K^-p Interactions in the 1 GeV/c Region

Imperial College, London; Rutherford Laboratory

This experiment is a high statistics study of K^-p interactions in the momentum range 0·96 to 1·40 GeV/c using some 415,000 pictures from CERN 2m hydrogen bubble chamber. The data, averaging about 1·4 events/μb at each of 11 incident beam momenta doubles the available data in this region.

For the two body reactions

$K^-p \to K^-p$	(167,034 events)
$K^-p \to \bar{K}^0n$	(12,928 events)
$K^-p \to \Sigma^+\pi^-$	(7,634 events)
$K^-p \to \Sigma^-\pi^+$	(9,842 events)
$K^-p \to \Lambda^0\pi^0$	(18,454 events)

final cross-sections, angular distributions and polarisation distributions (where appropriate) have been published. These include the remaining 42% of the two-prong topology events that were not measured in the original experiment. As an example of the quality of data from this type of experiment the K^-p elastic differential cross-sections are shown in Figure 1.13.

The main objective of this experiment is to study the formation of Y* resonances. To achieve this, an extensive partial wave analysis has been performed on the three two-body channels $\bar{K}N \to \bar{K}N$, Σπ, and Λπ using the new data in the energy range 1775 to 1960 MeV combined with all available recent data over the wide energy range 1480 to 2170 MeV. In particular the data included preliminary results from Lawrence Berkeley Laboratory in the lowest energy region, the latest K^-N total cross-section data from Brookhaven National Laboratory, and the new type of data for the channel $K_L{}^0p \to \Sigma^0\pi^+$ from the Rutherford Laboratory experiment (Experiment 16).

Preliminary results from this work were presented at the London Conference (1974) and the Palermo Conference (1975). Since then this analysis, which represents the most comprehensive study ever performed of Y* formation ex-

Resonance Parameters obtained from the $\bar{K}N$, Σπ and Λπ channel partial wave analysis

Wave	Mass (MeV)	Width (MeV)	Amplitude at Resonance $t_{\bar{K}N}$	$t_{\Sigma\pi}$	$t_{\Lambda\pi}$	Comment
S01	1670 ± 5	45 ± 10	0.20 ± .03	-0.31 ± .03		Established
S01	1825 ± 20	230 ± 20	0.37 ± .05	-0.08 ± .05		Possible
S11	1770 ± 15	60 ± 10	0.15 ± .03	-0.09 ± .05	0.04 ± .03	Probable
S11	1955 ± 15	170 ± 40	0.44 ± .05	0.20 ± .04	(±)0.08 ± .03	Probable
P01	1573 ± 25	147 ± 50	0.24 ± .04	-0.16 ± .04		Probable
P01	1853 ± 20	166 ± 20	0.21 ± .04	-0.24 ± .04		Probable
P11	1738 ± 10	72 ± 10	0.14 ± .04	–	–	Possible
P11	1676 ± 15	120 ± 20	–	-0.16 ± .03	–	Probable
P03	1900 ± 5	72 ± 10	0.18 ± .02	-0.09 ± .03		Now established
D03	1519 ± 1	15 ± 0.5	0.47 ± .01	0.46 ± .01		Established
D03	1690 ± 5	60 ± 5	0.24 ± .03	-0.25 ± .03		Established
D13	1670 ± 5	50 ± 5	0.08 ± .03	0.21 ± .02	0.10 ± .02	Established
D13	1920 ± 50	300 ± 80	–	-0.08 ± .04	-0.06 ± .03	Possible
D05	1825 ± 10	94 ± 10	0.04 ± .03	-0.17 ± .03		Established
D15	1774 ± 5	130 ± 10	0.41 ± .03	0.13 ± .02	-0.28 ± .03	Established
F05	1822 ± 2	81 ± 5	0.57 ± .02	-0.28 ± .03		Established
F05	2100 ± 50	200 ± 50	0.07 ± .03	0.10 ± .03		Possible
F15	1920 ± 10	130 ± 10	0.05 ± .03	-0.19 ± .03	-0.09 ± .03	Established
F17	2040 ± 5	190 ± 10	0.24 ± .02	-0.15 ± .03	0.18 ± .02	Established
G07	2110 ± 10	250 ± 30	0.30 ± .03	0.12 ± .04		Established
G09	1808 ± 5	27 ± 5	0.04 ± .01	–		Possible

A dash (–) indicates no contribution detected.

periments, has been completed. The final values of the Y* resonance parameters are given in the Table. By studying the three channels in parallel, reliable and consistent values for the parameters of the established resonances have been obtained. In addition, there is good evidence for the existence of many other states, some of which have been reported in earlier analysis, but others which have been seen for the first time in this work.

For example the P03 (1900) resonance is now established since there is clear evidence for this state in the $\bar{K}N$ data from this experiment and it is also found in the Σπ channel. Evidence is also found for a new state at 1808 MeV with a spin of 9/2 and negative parity in the $\bar{K}N$ channel. Such a state is not predicted by usual quark models and hence is of considerable interest.

Further tests of the quark model and $SU(6)_W$ predictions are provided by the decays of Y*s into the quasi two-body final states such as Λ(1520)π, K(890)N, and Σ(1385)π. The data for these reactions from the three body channels of this experiment has been obtained and the analysis work is proceeding. From the two-body analyses of available data it was clear that better data was required in certain energy regions, and to provide this data two extensions of the experiment are in progress. The first comprises 310,000 bubble chamber pictures of 4 incident K^- momenta between 0·92 and 1·04 GeV/c including one very high statistics point at 1·00 GeV/c. This data is now processed and ready for analysis.

The second extension covers the momentum region 450 to 900 MeV/c. This data, comprising 5 x 10^5 pictures, should

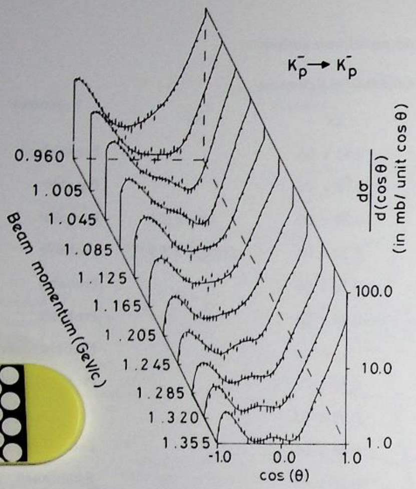

Figure 1.13 K^-p elastic differential cross-sections. (Experiment 14)

be taken at CERN early in 1976 and together with some existing film from the Heidelberg-Munich Collaboration which is being measured, should increase the statistics by about a factor of 10 over the present data.

When this experiment is complete, it means there will be high statistics K^-p data over the energy range 450 MeV/c to 1800 MeV/c coming from just two collaborations, CERN-Heidelberg-Munich and Imperial College-Rutherford. With this data many of the uncertainties and problems in the present $\bar{K}N$ partial wave solutions may be solved.

EXPERIMENT 15

Study of π^+p Interactions in the 1 GeV/c Region

Cambridge University; Imperial College, London; Westfield College, London

The Imperial College isobar-model partial-wave analysis of the dominant inelastic channels $p\pi^+\pi^0$ and $n\pi^+\pi^+$ has been extended in the past year to six energies in the centre-of-mass energy range 1540-1700 MeV, and by a number of refinements to the four-variable maximum likelihood fitting programme. Good continuity has been found between the energy-independent solutions and some interesting results are emerging. The general features of the theoretically favoured SLAC-Berkeley solution B, now confirmed by the SLAC-Berkeley-Imperial College-Westfield College Collaboration, are well reproduced. However, the higher π^+p statistics available from this experiment enable some additional features to be observed. In the centre of the energy range, the P_{31} wave appears strong and there is also evidence of the D_{35} wave which the SLAC-Berkeley analysis did not require at any energy. Further interpretation of these new waves awaits the conclusion of detailed studies of the phase variations by K-matrix and other techniques.

In addition the solution shows clear evidence for the decay of the $S_{31}(1650)$ into $N^*(1470)\pi$. This is the first observation of the decay of a $(70,1^-)$ resonance into a $(56,0^+)$ radial excitation in a $[SU(6),L^P]$ classification. This result was presented at the Palermo International Conference and has been used to predict rates for further S-wave decays to the radially excited $(56,0^+)$.

The technical improvements to the analysis include a thorough analysis of the errors on the fitted parameters and the addition of one-pion-exchange isospin 2 $\pi^*\pi$ scattering contribution. Evidence for the presence of the latter effect comes in particular from fits to the $n\pi^+\pi^+$ channel which previous analyses have not attempted to fit.

Recently there has been much theoretical speculation about the importance of such corrections, which are expected to be present by consideration of the constraints of two-body unitarity. It is expected that by testing the consistency of fits on the two halves of the Dalitz plot, limits on the magnitude of such effects can be obtained.

EXPERIMENT 16

Study of the K^0_L Interactions in the Range 300 to 800 MeV/c

Bologna University; Edinburgh University; Glasgow University; Pisa University; Rutherford Laboratory

The experiment consists of two separate exposures in the CERN 2 metre hydrogen bubble chamber. The 520,000 pictures taken in October 1972 have been scanned and measured and results of analyses of this data has been obtained. The second exposure, using a new monoenergetic K^0_L beam designed by the Rutherford Laboratory group, to the same chamber, yielded over 500,000 pictures. A double scan and first measure of the Rutherford share of this film (30%) is virtually complete and data is available on data summary tape. Events for remeasurement are being identified.

The main purpose of the experiment is to examine the strong interaction channels:–

$K^0_Lp \rightarrow K^0_Sp$	1
$\Sigma^0\pi^+$	2
$\Lambda^0\pi^+$	3
$\Lambda^0\pi^+\pi^0$	4

An analysis of Reaction 1 has been performed using published amplitudes, and an ability to distinguish a preference for some of the classes of strangeness +1, isospin 0 solutions, found from other data, has been noted, yielding valuable information relating to the strangeness +1 baryon resonance (Z^*) question. Sensitivity to the strangeness −1, isospin 1 amplitude is also evident, although this has so far been taken as fixed in fitting this new data with only the strangeness +1 amplitudes being allowed to vary.

Differential cross-sections and polarisation measurements from Reaction 2 have been included in an analysis of $\bar{K}N \rightarrow \Sigma\pi$ final states. Being a pure isospin 1 state, this channel has proved a useful addition to the mixed isospin data from $K^-p \rightarrow \Sigma^\pm\pi^\mp$ especially with regard to the D_3 (1660) and a possible P_1 (1700) resonance.

Reaction 3 data has proved consistent with that from the isospin-related reaction $K^-p \rightarrow \Lambda\pi^0$, and has been utilised for normalisation of cross-sections. The second exposure includes data in fine energy intervals in the region of 1580 MeV centre-of-mass energy where evidence for a narrow resonance in this latter data has been reported.

An analysis of the weak decays $K^0_L \rightarrow \pi e\nu, \pi\mu\nu$ and $\pi^+\pi^-\pi^0$ is in progress, the τ decay mode already having been studied as a check on the flux normalisation.

EXPERIMENT 17

K^+d Interactions in the 2 to 3 GeV/c Region

Imperial College, London; Westfield College, London

Using data from the Rutherford Laboratory 1·5 metre deuterium-filled bubble chamber at Nimrod, analyses of some features of the single and double pion production channels have been completed.

Further investigations into possible strangeness +1 Z^* baryon resonances have also been carried out. Simple quark models of elementary particles predict that no baryon resonances with positive strangeness should exist. The data for this experiment covers a range of beam momenta in which the total K^+-nucleon cross-sections show a small, wide peak, often a sign of s-channel resonances when π or K^- mesons are incident.

When the angular distributions of the mixed isospin K^+n charge exchange are analysed as a function of centre-of-mass energy, there may be some hint of structure at an incident meson energy corresponding to 2·4 GeV/c.

However, it seems likely that any Z^* would not be strongly coupled to the elastic channel, so a first attempt is being made at a partial wave analysis of the K^* nucleon final states, which have cross sections of a few millibarns.

The K^+p initial state is pure isospin 1 while the K^+n is mixed isospin, but having both K^{*+} and K^{*0} final states it is possible to separate the isospin 0 and isospin 1 contributions. The spread of the K^+-nucleon centre-of-mass energy due to the Fermi motion inside the deuteron and the three different K^+ momenta covers the range 2·2 to 2·6 GeV.

An attempt has been made to fit the two body K^+-nucleon production and K^* decay data with amplitudes freely parametrised in such a form that they can assume resonance-like behaviour if the data demands it. The available data allows only the general features of the amplitudes to be deduced. For isospin 1 the DD3 wave seems to require to be large, with a significant phase variation with respect to the other waves. The main features of all waves seem to be consistent between different solutions.

For the isospin 0 amplitudes, higher partial waves are required. Two classes of solution seem to exist, differing by the extent of the phase change of the large SS1 with respect to SD1. However several other waves also seem to require both to be large and to have a significant phase variation, although the present data does not constrain the fits sufficiently well. It is hoped to be able to improve these analyses.

EXPERIMENT 18

Interactions of Slow and Stopped K^- Mesons

Birmingham University; Durham University; Free University of Brussels; University College, London

The major aim of the experiment is to analyse the $\Lambda\pi^0$ and $\Sigma^0\pi^0$ channels from K^-p collisions in a momentum region where they have previously been badly separated, and where the data is unevenly distributed. All collaborating laboratories are now primarily concerned with the measurement and reconstruction of events. Over 10,000 events have been measured, and these are being used to establish unbiassed reconstruction procedures before information is extracted.

A subsidiary experiment is under way involving a small sample scan of the stopped K^- film. It is anticipated that this will give a considerable improvement in the value of the ratio of Σ^+ to Σ^- production by stopped K^-, as well as resolving a long-standing disagreement between two previous measurements.

The group of Prof. A. Zakrzewski, from the University of Warsaw, has been accepted as a new member of the collaboration, and four members of this group are at present working in one or another of the collaborating laboratories. Film is to be analysed in Warsaw during 1976.

EXPERIMENT 19

High Strangeness Baryon Resonance Studies using the Rapid Cycling Bubble Chamber

CEN Saclay; College de France, Paris; Oxford University; Rutherford Laboratory.

The Rapid Cycling Vertex Detector bubble chamber (RCVD) used to detect short-lived baryon resonances is designed to cycle at 60 Hertz compared with the conventional bubble chamber rate of one or two cycles per second. This high cycling rate will allow experiments to be performed with a cross section sensitivity up to 1000 events per microbarn, subject to triggering efficiencies. The essential advantages of the bubble chamber technique – detailed vertex resolution, precision, isotropy and multitrack efficiency, are retained. To avoid using very large quantities of film, picture-taking is triggered using external counters, and these can also be used to provide measurement information to compensate for the short tracks in the small chamber or to give supplementary information such as particle identification.

The current experiment is designed to study the $S = -2$ resonances in the mass region just below 2·0 GeV/c^2, which is a relatively unexplored region of resonance physics. Only the $\Xi(1530)$ and more recently the $\Xi(1820)$ are firmly established out of a large number of SU(3) predicted states. A high statistics study giving both production and decay information for J^P assignments is highly desirable and cannot be provided by conventional means because of the microbarn cross sections involved. Because of the high strangeness of the final states, the bubble chamber technique is clearly required to resolve the many close vertices.

The formation of such resonances is characterised by many-particle final states and a multiplicity $\geqslant 5$ trigger has therefore been adopted. The trigger information is provided in two stages – a series of four cylindrical spark chambers surround the vacuum tank of the bubble chamber and these in turn are surrounded by a set of scintillation counters. A feature of the bubble chamber is the long memory ($\sim$1–2 msec) associated with the growth of the bubbles to photographable size. This allows the complete read-out of the spark chambers, a hardware multiplicity determination for each chamber and a software decision to be made in the PDP11/40 computer.

The beam momentum is chosen to be 2·8 GeV/c to allow the Ξ^* mass range up to $\sim$ 2·0 GeV/c^2 to be studied in detail and to maintain the feasibility of the multiplicity trigger, and such a beam is well matched to Nimrod.

During the year, much progress has been made towards the realisation of this experiment. The bubble chamber itself, designed and built in the Applied Physics Division (Section 4.2), is essentially complete and will be cooled down early in 1976. The capacity read-out spark chambers have been designed and constructed by the Nuclear Physics Apparatus Group using the film wire technique (Section 1.4). The CAMAC logic following the read-out, together with the PDP11/40 computer system, has been provided by the Rome group. These systems are being tested and developed by the Rome physicists together with the Saclay and Rutherford groups and then will be moved to their final position near the RCVD. The Saclay College de France groups have provided the pre-trigger scintillators and their associated fast logic all of which has been successfully set up and tested and is ready for final assembly. The experimental beam line, designed by the Oxford group, has been commissioned and is currently being tuned. The experiment has planned for 5 cycles of data taking at Nimrod and should yield $\sim$ 20,000 events in about 10^8 chamber expansions.

1.1.3 Intermediate Energy Production Mechanisms

EXPERIMENT 20

Study of Exchange Mechanisms in Quasi Two Body Final States, Using the RMS Spectrometer

Edinburgh University; Westfield College, London; Rutherford Laboratory

The current phenomenological approach towards an understanding of hadronic reactions is based on Reggeised exchange models for the amplitudes involved. Thus it is towards the problem of extracting amplitudes from experimental data that attention is increasingly being given. In the case of quasi two body reactions, information on the structure of the production amplitudes can be deduced from the angular distributions and joint decay correlations of the final state particles.

This collaboration using the Rutherford Multiparticle Spectrometer facility (RMS) at Nimrod, proposes a programme of studies of such reactions, initially using a hydrogen target then with a frozen spin polarized proton target, since a full model independent amplitude analysis is only possible with a polarized target (and then not in all cases).

The initial experiment scheduled for RMS is a study of π^+ induced reactions involving either a $\Delta(1236)$ or $\Sigma(1385)$ in the final state, e.g. $\pi^+p \rightarrow \omega\Delta^{++}$, $\pi^+p \rightarrow K^+\Sigma(1385)$, and data taking will be completed before the polarized target is installed late in 1977.

During 1977 the 70 MeV injector for Nimrod will become operational, with considerably increased beam intensities. RMS should then be equipped with a separated beam, allowing both π and K induced reactions to be studied.

A successful programme of testing was completed during the year, and RMS will be assembled during the first few months of 1976, with setting up starting early in the summer.

The RMS magnet is a conventional 'H' type magnet with a pole gap of 1·35m and pole faces of 2·58m x 1·3m. An aperture of 1·9m x 1·95m in the downstream side yoke and minimum size pillars give maximum access. With a 1·2MW power supply the maximum field should be just over 1 Tesla.

To map the field of this magnet, a large automatic field mapping machine has been built, with three dimensional motorised movement over a 3m x 3m x 1·6m (high) volume.

EXPERIMENT 21

Differential Cross-Sections and Polarisations in Hypercharge Exchange Reactions

Birmingham University; Genova University; Stockholm University; CERN; Rutherford Laboratory

The running of this experiment at CERN was completed in August 1974. Final analysis will give measurements of the differential cross-sections and polarisations in the pairs of line reversed hypercharge exchange reactions

$$\pi^+p \rightarrow K^+\Sigma^+ \qquad \text{I}$$
$$K^-p \rightarrow \pi^-\Sigma^+$$

and

$$\pi^+p \rightarrow K^+\Sigma^+(1385) \qquad \text{II}$$
$$K^-p \rightarrow \pi^-\Sigma^+(1385)$$

Measurements were made at 7 and 10 GeV/c incident momentum, and cover a range of (four-momentum transfer)^2, t, from 0 to about -4 (GeV/c)^2.

To date the low t differential cross-sections at 10 GeV/c have been obtained. These results are very interesting in that they show only modest breaking of the exchange degeneracy (EXD) prediction of equal differential cross-sections, in contrast to the strong EXD breaking which had been suspected on the basis of earlier experiments. This experiment, in which both reactions were studied with the same apparatus, has far smaller uncertainty in normalisation than previous experiments.

Results are shown in Figure 1.14 for reactions I and in Figure 1.15 for reactions II.

There also exists recent data on the SU(3) related KN charge exchange reactions $K^+n \rightarrow K^\circ p$ and $K^-p \rightarrow \bar{K}^\circ n$; $K^+p \rightarrow K^\circ\Delta^{++}$ and $K^-p \rightarrow \bar{K}^\circ\Delta^\circ$, from an experiment at the Argonne National Laboratory which also studied both line reversed partners in the same equipment. This has also produced a surprise compared with the indications of earlier experiments. The new experiment finds modest EXD breaking in these reactions also, whereas the earlier work suggested equal cross-sections.

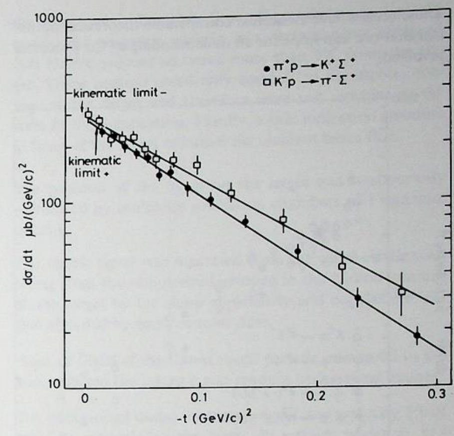

Figure 1.14 Differential cross-sections for $\pi^+p \rightarrow K^+\Sigma^+$ and $K^-p \rightarrow \pi^-\Sigma^+$. (Experiment 21)

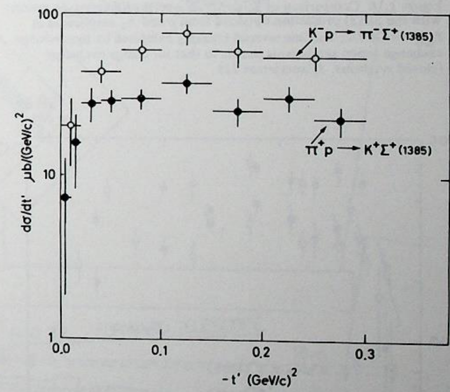

Figure 1.15 Differential cross-sections for $\pi^+p \rightarrow K^+\Sigma^+(1385)$ and $K^-p \rightarrow \pi^-\Sigma^+(1385)$. (Experiment 21)

Thus the apparent discrepancy between charge exchange and hypercharge exchange reactions has disappeared. Both show a similar amount of EXD breaking and in fact the SU(3) relations work remarkably well. Figure 1.16 shows this for reactions I with their charge exchange partners, and Figure 1.17 shows this for reactions II with their charge exchange partners.

These results have awakened considerable theoretical optimism that one can hope for an understanding of the processes involved.

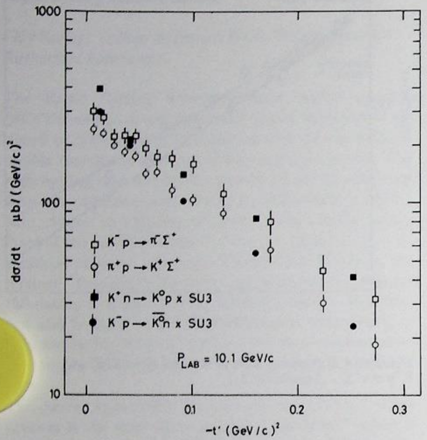

Figure 1.16 Comparison of $K^-p \to \pi^-\Sigma^+$ and the line reversed process with the SU(3) prediction obtained from ρ and A_2 amplitudes at P_{lab} = 4 GeV/c. The line reversal breaking exhibited by hypercharge exchange (open symbols) is similar to that for charge exchange (closed symbols). (Experiment 21)

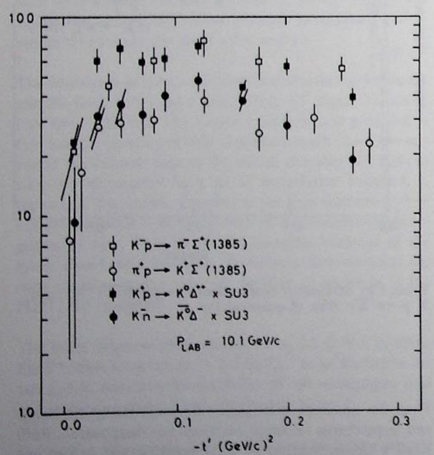

Figure 1.17 Comparison of $K^-p \to \pi^-\Sigma^+(1385)$ and the line reversed process with the SU(3) prediction obtained from data on $K^+p \to K^0\Delta^{++}$ and $K^-n \to \bar{K}^0\Delta^-$ at P_{lab} 6 GeV/c. The line reversal breaking exhibited by hypercharge exchange (open symbols) is similar to that for charge exchange (closed symbols). (Experiment 21)

EXPERIMENT 22

Spin Rotation Parameters in $\pi^-p \to K^\circ\Lambda$

Imperial College, London; Southampton University; ETH, Zurich; CERN; Helsinki University

This experiment is designed to measure polarisation and spin rotation parameters in the reaction $\pi^-p \to K^\circ\Lambda$ using a 5 GeV/c π^- beam at CERN. The decay products of the K° and Λ are revealed by spark chambers mounted in the CERN-ETH 1 Tesla magnet, which are viewed by seven T.V. cameras. Stereoscopic images are obtained by three pairs of cameras mounted above the magnet; the critical region around the target is also seen via a side mirror from a camera mounted downstream.

To provide a large solid angle for the slow Λ decays the (CERN-Helsinki) frozen spin target is used. This propanediol target is polarised daily in a local 2·5 Tesla field provided by special pole pieces mounted at one corner of the magnet and is then moved into position inside the spark chambers.

The target is surrounded by a scintillator/tungsten sandwich of anti-coincidence counters so that charged particles and gamma-rays are excluded as secondary products in the selected events.

About 5 million pictures have been obtained with this trigger. Of these, about 40% show single V° decays, about 7% show two V° decays and about half of these appear to be $K^\circ\Lambda$. Some 5 million pictures have also been taken without the gamma-ray anti-coincidence in the trigger; and with these the reaction $\pi^-p \to K^\circ\Sigma^\circ$ can be obtained.

EXPERIMENT 23

Spin Dependence of Inclusive Reactions and Low Cross-Section pp Elastic Scattering.

CERN; Paris-Sud University; Oxford University

In 1974, the CERN-IPN Orsay-Oxford Collaboration completed an experiment at the Rutherford Laboratory which measured spin effects in pp elastic scattering and pp inclusive scattering at 7·9 GeV/c. The collaboration is continuing its study of spin effects in pp interactions with a measurement of the polarization parameter P_o in elastic scattering in the 24 GeV/c C_9 beam at the CERN PS.

It is known that at energies above 7 GeV, structure develops in the proton-proton differential cross-section at about a (four momentum transfer)^2 $t = -1{\cdot}5(\text{GeV/c})^2$ and that this is coupled with a large polarization parameter, P_o, at the same momentum transfer, which persists up to the largest energy measured of 17·5 GeV. At the same time, the height of the first peak in P_o below $|t| = 0{\cdot}6(\text{GeV/c})^2$ appears to decrease as $\frac{1}{s}$, where s is the square of the centre-of-mass energy. Recent measurements from Serpukhov at 45 GeV out to $|t| = 1(\text{GeV/c})^2$ indicate that at high energy the minimum in P_o near $|t| = 1(\text{Gev/c})^2$ may become negative.

The proton beam with an intensity of 5×10^8 protons per pulse was incident on a standard CERN polarized proton target using propanediol. This gave an initial polarization of 85% which gradually reduced due to radiation damage. After about 10^{14} protons had passed through the target and the polarization had fallen to about 60%, the propanediol sample was changed.

The normal fine focus of the extracted proton beam (2mm x 2mm) was defocussed in order to spread the radiation damage of the polarized target over a region 6mm x 6mm. Two NMR coils of differing areas allowed the localized radiation damage to be studied and a correction to the data was found.

Three independent beam monitoring systems were used to afford adequate cross-checks for the measurement of asymmetries of less than 1%. A pair of three-counter telescopes was directed towards the target in the plane of the target polarization so that the telescopes would be insensitive to the polarization direction. Secondly, a three-counter telescope with magnetic analysis in a vertical plane accepted 300 MeV/c protons scattered more than 90° from the target. These protons could only come from the carbon content of the target and therefore were not sensitive to the state of the polarization. Thirdly, a thin ionization chamber in front of the target recorded the incident beam flux.

The position of the beam on the target was continuously monitored by multiwire ionization chambers of 1 mm wire spacing.

The elastic signal was separated from the quasi-elastic scattering from the unpolarized protons in the carbon content of the target by the sharp coplanarity and angular correlation afforded by small counter sizes.

Time of flight of the slower recoil particle, measured to 0·5 nsec, rejected the inelastic and random background counts.

The background under the elastic signal was typically 5% of the data, except for the larger $|t|$ settings where at $|t| = 1(\text{GeV/c})^2$ it reached 50%.

Preliminary results (Figure 1.19) for the polarization parameter P_o at 24 GeV show that up to $|t| \sim {\cdot}4(\text{GeV/c})^2$, P_o is constant at $\sim +3\%$ then falls to zero at $|t| \sim {\cdot}8$ reaching a value of $\sim -3\%$ at $|t| = 1{\cdot}0(\text{GeV/c})^2$.

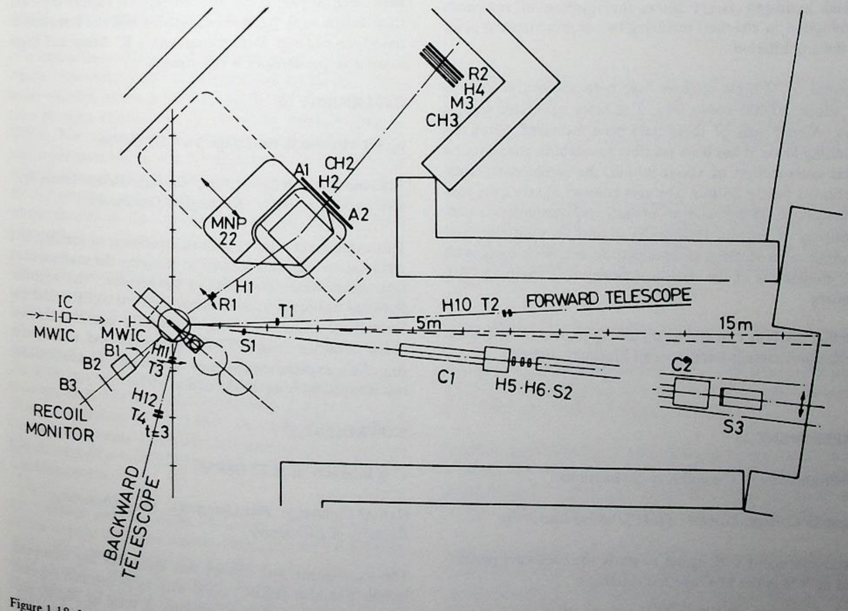

Figure 1.18 Layout of apparatus (Experiment 23)

The experiment is continuing to take data to extend the measurements up to $|t| \sim 5{\cdot}0(\text{GeV/c})^2$.

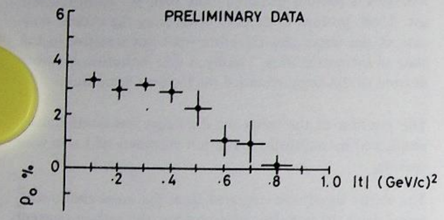

Figure 1.19 Polarisation in pp scattering at 24 GeV/c. (Experiment 23)

EXPERIMENT 24

Study of $\bar{p}p$ annihilations at 2 GeV/c

Tata Institute, Bombay; Melbourne University

This experiment at Nimrod uses the Track-Sensitive Target (TST) technique to study multipion production in $\bar{p}p$ annihilation reactions. The high conversion efficiency (35 - 39%) in the liquid neon and hydrogen mixture outside the liquid hydrogen target allows investigation of resonance production in channels involving two or more neutral pions in the annihilation.

A total of 110,000 pictures have been scanned yielding in about 20,000 events with 2 or more associated gamma rays. Almost half of these have been measured. From the scanning alone it has been possible to establish that out of a total cross-section of about 90 mb, the annihilation cross-section is nearly 36 mb. The rest consists of an elastic contribution of 28 mb and an inelastic non-annihilation contribution of 26 mb. Preliminary results on multipion production cross-sections in annihilation reactions agree with the predictions of the statistical model of Orfandis and Rittenberg.

Further analysis and results on multipion and two-body annihilation channels have to await kinematic fitting.

EXPERIMENT 25

Y* Production in π^+p and K$^-$p Interactions

Imperial College, London; SLAC; Purdue University

This experiment is designed to study the backward production of Y*s in the line reversed reactions:

$$\pi^+ p \rightarrow K^+ Y^{*+} \qquad 1$$
$$K^- p \rightarrow \pi^+ Y^{*-} \qquad 2$$

With the successful commissioning of the large multicell Cerenkov downstream from the 40" hydrogen bubble chamber, the beam-defining proportional wire chambers and Cerenkov counters and two of the three planned large downstream proportional wire chambers, the hybrid facility at SLAC is almost complete. With positive pions in the beam, the information from the large downstream multicell Cerenkov allows the logic to discriminate against the high momentum outgoing positive particle being a pion.

Film taking during the various test runs has enabled modifications to the apparatus to be tested, and optical constants for the 40" chamber have been obtained. These test runs also proved the feasibility of using the information from the beam planes to guide the scanners to the events that triggered the system.

For Reaction 1 film equivalent to approximately 5 events/μb has been taken and the preliminary scanning has proved to be encouraging.

Progress has also been made on the second phase of the experiment. With an RF separator in the beam a flux of 10-12 kaons per pulse is achieved at the chamber. The contamination at 6·9 GeV/c was estimated to be only 10%. The trigger system for this part of the experiment requires a muon veto detector and funds for the construction of this detector have been approved by the Rutherford Laboratory. The final design work has been completed and the components have been ordered. Data taking with a K$^-$ beam will begin as soon as this detector is constructed.

EXPERIMENT 26

$\bar{p}p$ Interactions in the Range 2·6 – 5·7 GeV/c

Argonne National Laboratory; Carnegie-Mellon University; Melbourne University; Rutherford Laboratory

This experiment aims at a clean separation of inelastic and annihilation channels as well as studying the multi-neutral final states which dominate in annihilation. The Argonne National Laboratory, in collaboration with CERN and the Rutherford Laboratory, has successfully operated its new Track Sensitive Target (TST) equipment, and a short test run of the experiment has been carried out. The data-taking run is expected towards the end of 1976.

EXPERIMENT 27

π^- p Interactions at 22 GeV/c

Oxford University; Pisa University; Pavia University; Rutherford Laboratory

The experiment was carried out using the Big European Bubble Chamber (BEBC) filled with hydrogen and exposed to a beam of 22 GeV/c π^- mesons. A total of 50,000 pictures were taken. The purpose of the experiment is to study inclusive differential cross-sections of K°s, Λ°s, γs and π°s and to look at the π° multiplicity distribution. The bubble chamber BEBC is particularly good for this task due to its large size and hence large conversion length for neutral particles.

The highest possible momentum that could be obtained in the West Hall at CERN PS was chosen for the experiment. This enabled the experiment to approximate best to possible future work planned for BEBC at SPS energies and so give a good understanding of possible problems that may arise in an experiment planned for the future.

The preliminary analysis of the experiment is well under way, a large part of the scanning having been completed and a conventional measuring chain has been set up. The film has also been measured on an HPD.

EXPERIMENT 28

Hyperon-Proton Interactions up to 24 GeV/c

Cambridge University

This experiment has now been completed at CERN. In all, about 20,000 neutral-induced events involving strange particle production were measured on some 150,000 frames. From these, results on Λ°p scattering have been obtained together with exclusive and inclusive strange particle production in np interactions up to 24 GeV/c.

Λ°p Interactions. Fits to the reactions $\Lambda p \rightarrow \Lambda p$ and $\Lambda p \rightarrow \Lambda p \pi^+ \pi^-$ have been made, these being the first results on the latter reaction above 5 GeV/c, and having better statistics than previous experiments on the elastic process above 5 GeV/c. The substantial proportion of high energy events was made possible by the Λ° enrichment of the primary neutral beam. Only 3-C fits have been made for these events, whether induced by beam Λ°s, or induced Λ°s whose sources in the chamber have been identified and measured.

The elastic cross-section (see Figure 1.20) was found to be consistent with existing low energy Λ°p data, and had fallen to 6·0 ± 1·5 mb at $\sim$ 16 GeV/c. The Λ°p elastic cross-section lies systematically below pp values. The |t| behaviour of the elastic events is consistent with pp data, and the intercept at |t| = 0 is in agreement with the optical theorem limit. The inelastic channel $\Lambda^\circ p \rightarrow \Lambda^\circ p \pi^+ \pi^-$ shows strong production of $\Sigma^-(1385)$ and $\Delta^{++}(1236)$ below 8 GeV/c, while above 8 GeV/c it is dominated by the diffractive process $\Lambda^\circ p \rightarrow (\Lambda^\circ \pi^+ \pi^-)p$, with no indications of proton dissociation.

np → strange particles above 10 GeV/c. Efforts in this part of the experiment have mainly been directed towards the study of exclusive processes, a subject which has received little attention hitherto above $\sim$ 10 GeV/c. Fits were attempted at 29 exclusive channels with statistics of $\sim$ 8 events/μb. The main findings are:

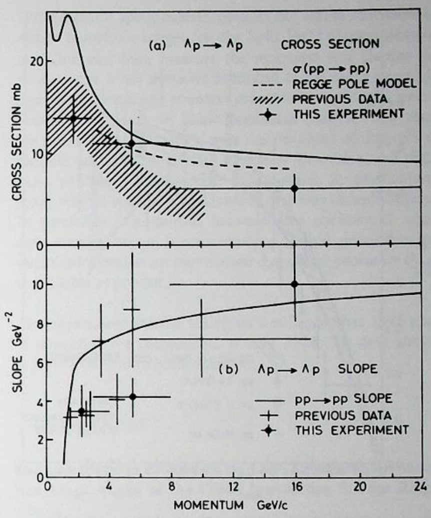

Figure 1.20 Cross-section and exponential slope in |t| as a function of momentum for $\Lambda^\circ p \rightarrow \Lambda^\circ p$. (Experiment 28)

(i) Hyperon production is roughly constant with multiplicity in lower multiplicity channels ($\lesssim$ 5) between 6 and 20 GeV/c while in higher multiplicities it has increased rapidly. In contrast kaon pair production has increased in all multiplicities.

(ii) Cross-sections in the three-body final states (ΛK)N and (ΣK)N show a slow fall with energy from 6 GeV/c, and an isospin analysis has identified this decrease with isovector exchange, while the isoscalar component has remained constant.

(iii) In four-body final states, $\Lambda K N \pi$ or $\Sigma K N \pi$, the baryons are strongly correlated one with each initial nucleon, while the kaon is generally associated with the hyperon. The pion tends to be associated with that vertex which will allow zero quantum number exchange if possible.

(iv) Strong production of $\Sigma^*(1385)$, $\Delta(1236)$ and $K^*(890)$ resonances is seen. In particular, very substantial contributions from $\Sigma^-(1385)$ and $\Delta^{++}(1236)$ are observed in the $\Lambda^\circ K^+ p \pi^-$ and $\Sigma^- K^\circ p \pi^+$ channels, right up to 24 GeV/c.

Data has also been obtained on the inclusive reactions np → strange particles. The rapidity distribution for the fragmentation process $n \rightarrow \Lambda^\circ$ is in good agreement with $p \rightarrow \Lambda^\circ$. Estimates of inclusive Ξ^-, $\Sigma^\pm(1385)$ and $K^\pm(890)$ cross-sections have also been made. A search was made for the

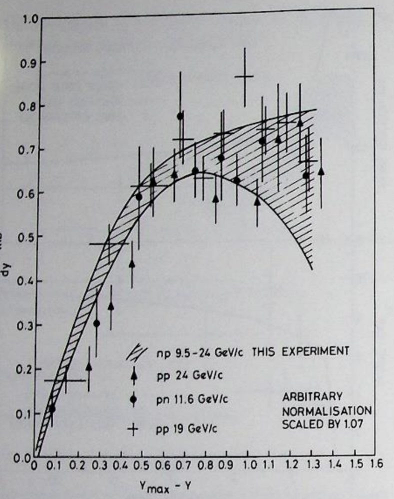

Figure 1.21 Distribution of the rapidity variable for $np \to \Delta^{\circ}X$, compared with pp and lower energy pn data. (Experiment 28)

inclusive production of "charmed" particles decaying into strange particles, without success.

1.1.4 Higher Energy Experiments

EXPERIMENT 29

Exclusive Hadronic Processes at Large Transverse Momentum

CERN; University College, London; Genova University; Oslo University; Paris-Sud University

This experiment, which is currently in preparation, is designed to study two-body exclusive reactions at large centre-of-mass angles, at a range of incident energies from 20 to 100 GeV/c. In particular, measurements will be made of large-angle elastic scattering in the $\pi^{\pm}p$, $K^{+}p$, pp and $\bar{p}p$ systems, and of $\bar{p}p$ annihilations into $\pi^{+}\pi^{-}$ and $K^{+}K^{-}$. Working near 90° in the centre-of-mass ensures that there will be large transfers of transverse momentum in these reactions and the results are then sensitive to models of the inner structure of the hadrons. Different constituent models give varying predictions for the ratios of the cross-sections for these processes as well as their angular and energy dependencies.

The secondary beam used in this experiment is expected to have an intensity of up to 10^8 particles per burst and will be incident on a 1 m liquid hydrogen target which is partly inside a large-aperture magnet. The particles are sorted by a set of three high-pressure gas differential Cerenkov counters designed at CERN. Two spectrometer arms are envisaged, one for the 'recoil' particle and one for the 'fast' particle. For both particles, the angle and momentum are measured and where possible both particles are identified in pairs of atmospheric pressure gas threshold Cerenkov counters in each arm. Correlations between the scattered particles are established in the trigger by using pulses for arrays of scintillation counters to make decisions by means of fast coincidence matrices. The particle trajectories are studied with multi-wire proportional chambers which will be read out into hardware processors. These will then decide if the information should be written onto magnetic tape, via a NORD-10 computer.

Most of the equipment for this experiment is now being manufactured, and many prototypes of chambers, hodoscopes read-out systems etc, have been tested in beams at CERN. The whole experiment is scheduled to be mounted on the floor of the West Area of the SPS towards the end of the summer in 1976.

EXPERIMENT 30

High Transverse Momentum Behaviour at the ISR

Liverpool University; Daresbury Laboratory; Rutherford Laboratory

As an extension to the investigation of inclusive single-particle production phenomena at the CERN ISR, this experiment was designed to measure the multiplicity distribution, the pseudo-rapidity distribution and the azimuth distribution of charged particles produced in association with charged triggers of high transverse momenta.

The Wide-Angle Spectrometer (WAS), previously utilised by the British-Scandinavian Collaboration, was used to trigger and completely identify charged pions, kaons, and protons in the momentum range 500 MeV/c to 5 GeV/c, except for the momentum range 1·3 GeV/c to 1·8 GeV/c where only partial particle identification was possible.

A multiplicity detector constructed in collaboration with the CERN-Holland-Lancaster-Manchester group (CHLM) was installed around a 12 intersection bicone. It is an assembly of 80 scintillation counters, arranged in eight 'octants' of longitudinal strips and lateral hoops. These counters provide information on the polar and azimuth distributions of associated particles. Additional counters supplement the angular acceptance of the detector, and large spark chambers improve the directional resolution of some tracks.

Data was taken at all five ISR energies from 23 GeV to 63 GeV and at spectrometer angles of 90°, 62·5°, and 45° to the bisector of the intersecting beams. The bulk analysis of data has been completed, and physics questions now being studied include:—

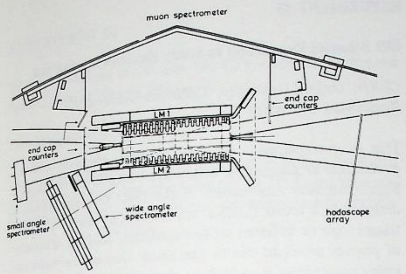

Figure 1.22 Multiplicity detector (Experiment 30)

(a) The dependence of the associated multiplicity on the energy, transverse momentum, quantum numbers, and centre-of-mass scattering angle of the trigger particle
(b) The behaviour of the pseudo-rapidity distributions
(c) The two-particle correlations between secondary tracks, and an evaluation of the rapidity gap distribution between associated secondaries
(d) An evaluation with increased statistics of single particle distributions measured by the British-Scandinavian Collaboration
(e) An evaluation of the cross section for $\phi \to K^{+}K^{-}$ production, at momenta above 3 GeV/c
(f) Correlation measurements with the wide angle spectrometer (WAS), and the small angle spectrometer (SAS) of the CHLM Collaboration in coincidence.

This experiment has the unique ability to identify the momentum and quantum numbers of the high transverse momentum particles.

EXPERIMENT 31

Study of High Transverse Momentum Phenomena in the Split Field Magnet

Liverpool University; Orsay Laboratory; Scandinavian Universities; Rutherford Laboratory

This experiment is studying particle correlations associated with high transverse momentum secondaries at the Split Field Magnet facility at the ISR. The experiment is an extension of previous investigations using the Wide Angle Spectrometer (experiment 30) in which the unexpectedly high cross-section for single charged hadron production at high transverse momenta was established, and in which the angular distribution of the associated charged particles was measured. Theoretical explanations for the observed phenomena invoke either small distance effects, for example in the parton model involving point-like hadron constituents, or the production of new objects with relatively large masses.

The magnetic spectrometer used in the earlier ISR experiments provides a trigger for the Split Field Magnet detectors. One can then measure the momenta and charges of most of the other particles produced in the same event. A system of hodoscope counters provides time-of-flight measurements of many of these associated particles and thus identifies them. Effective mass distributions of identified particle pairs will be studied to search for evidence of high mass particles. The particle distributions in momentum space will be studied to search for evidence of hadron jets. In particular, correlations between two particles of non-zero strangeness or baryon number should provide more direct information on the internal dynamical processes than is available at present.

The experiment started taking data in September 1975 and is scheduled for completion in July 1976. To date about 2 x 10^6 events have been recorded.

EXPERIMENT 32

Inclusive Particle Production at Low Transverse Momenta and Large Angles at the CERN Intersecting Storage Rings

CERN; University College, London; Bristol University; Massachusetts Institute of Technology; Niels Bohr Institute; Lund University

Data taking for this experiment was completed at the beginning of the year. Single particle inclusive spectra from proton-proton interactions have been measured for $\pi^{\pm}$, π°. $K^{\pm}$, $p^{\pm}$ and $d^{\pm}$ at 90° in the centre of mass, down to very low values of transverse momentum, extending to 50 MeV/c for the pion spectra. This data extends the measurements of the British-Scandinavian collaboration in the "central region" to a region which contains a significant fraction of the inelastic cross section. This is of particular interest as it is now known that the total inelastic cross-section increases with energy over the ISR energy range. Data has been obtained at all five standard ISR energies, using the total cross-section experiment of the Pisa-Stonybrook collaboration as a luminosity monitor to obtain accurate normalisation.

Data was taken in collaboration with the Pisa-Stonybrook experiment to study correlated event topologies with an identified charged particle at 90° in the centre of mass. These results were obtained for both low and high values of transverse momenta.

The analysis of the low momentum correlation data is essentially complete and work is currently in progress on the high momentum correlations. In the analysis of the inclusive spectra, the initial emphasis has been placed on the charged pions. The inclusive pion cross section in the central region is predicted to become independent of energy according to the Feynman scaling hypothesis. Early data from previous ISR experiments did not indicate any appreciable deviation from this prediction, within rather large errors. More accurate preliminary data from this experiment shows that there

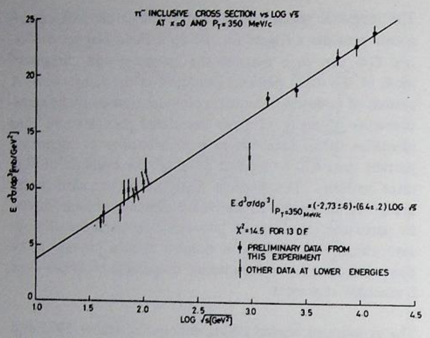

Figure 1.23 Inclusive π^- invariant cross-section as a function of $\log\sqrt{s}$, showing energy dependence. (Experiment 32)

is a very significant energy dependence implying a breakdown to Feynman scaling in the ISR energy range. (Figure 1.23).

In many models the approach to scaling is expected to be of the form $A + Bs^{-\alpha}$, where s is the square of the centre-of-mass energy, popular values of α being $\frac{1}{2}$ or $\frac{1}{4}$. An $s^{-\frac{1}{2}}$ dependence is ruled out by this data. Figure 1.24 shows the inclusive pion cross section as a function of $s^{-\frac{1}{4}}$, an approach of this form is not excluded by the preliminary data from this experiment, but it is clear that it is difficult to fit such a form to include the low energy data.

The analysis of the transverse momentum dependence of the pion data is almost complete, and work is in progress on the analysis of the other charged particle spectra.

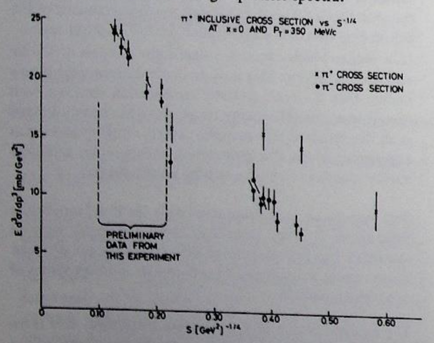

Figure 1.24 Pion inclusive cross-sections. (Experiment 32)

EXPERIMENT 33

ISR Solenoid Experiment to Study Electron Production

CERN; Oxford University; Columbia University; Rockefeller University

This is an experiment designed to study electron and π^0 production in association with other charged particles, at a high luminosity intersection of the ISR. The apparatus is designed in a rather flexible way, so that by using different trigger logic or different off-line computer analysis, a variety of physics problems can be examined. One of the most exciting possibilities is to look at electron pairs, alone or with associated gammas, measuring the cross-sections for production of the new family of ψ particles and searching for similar particles of higher mass.

Another possibility is to look at single electrons. It is known that the yield of single electrons is anomalously high, about 10^{-4} of pion yields, but as yet the source of these electrons is unknown. The theoretical models proposed to account for the phenomena – charmed particles, heavy leptons, quark bremsstrahlung or vector mesons are the main candidates – all have difficulties in accommodating existing data. A large solid angle allows this experiment to detect particles produced in association with the single electrons, and should enable the source of these electrons to be identified. Once the source is known, additional particle identification could be incorporated for muons or kaons for example, to study the properties of any new kinds of particle.

The superconducting solenoidal coil of the apparatus produces a field of 1·5 Tesla around the intersection region. In the region, there are four double-gapped magnetic field compensated drift chambers which provide 8 azimuthal and 8 longitudinal (by delay line) coordinates for each charged track. Particles pass through the drift chambers, through the superconducting coil, are seen in scintillation counter hodoscopes and are finally absorbed in an array of lead-glass counters. Identification of electrons depends on pulse-height measurements in the three counter hodoscopes, and on a comparison of measured particle momentum with total shower energy seen in the lead glass.

The inner ring of counters – constructed at the Rutherford Laboratory – has 64 light pipes, connected to photomultipliers mounted outside the iron yoke of the magnet. A hodoscope has also been constructed at the Rutherford Laboratory. Test running of the apparatus is scheduled to start without magnet in the Spring, with magnet in the Autumn 1976.

EXPERIMENT 34

Σ^-p Interactions at 50 and 100 GeV/c and Meson-Proton Interactions at 50 and 200 GeV/c

Cambridge University

These experiments, using equipment developed at the Rutherford Laboratory, are scheduled for the US Fermi National Laboratory. The meson-proton experiments will include π^+p and $K^\pm$p reactions.

EXPERIMENT 35

K^-p Interactions at 45 and 65 GeV/c

Glasgow University; CEN Saclay; Rutherford Laboratory

This experiment, designed to be run at the CERN SPS using the Big European Bubble Chamber, (BEBC) is at the proposal stage (Proposal 161).

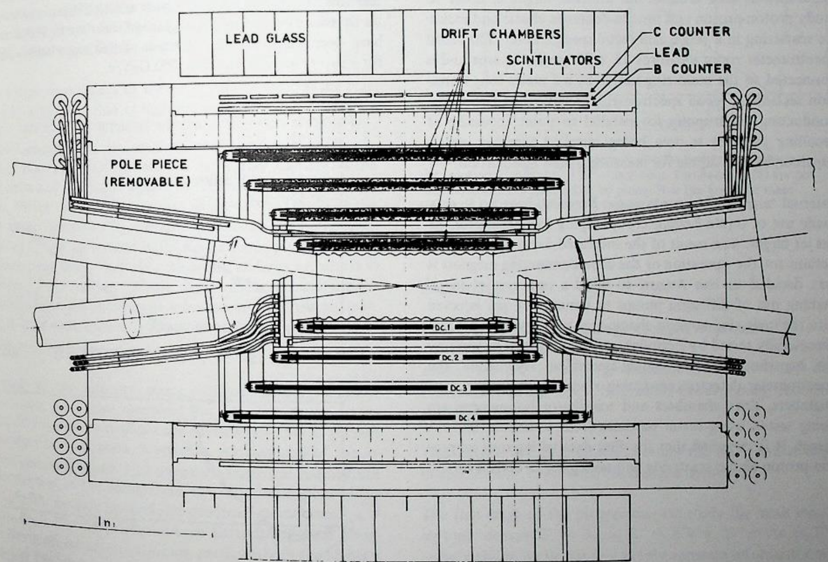

Figure 1.25 Horizontal section through the apparatus for Experiment 33, showing scintillation counter hodoscopes, the lead glass counters and the solenoid coils.

EXPERIMENT 36

Internal Targets at the US Fermi National Laboratory

Imperial College, London; Rochester University; Rutgers University

During the past three years this group has conducted experiments on pp and pd inclusive reactions within the confines of the main ring tunnel enclosure of Fermilab's 400 GeV/c accelerator. The principal advantage of such experiments using internal targets is the very wide range of incident energy, between injection of 8 GeV/c and extraction at 400 GeV/c, over which reactions of interest can be studied. Up to now however the kinematic range over which final state particles could be studied was severely restricted by space limitation imposed by the 4 metre wide tunnel section.

In 1974 the group put forward a proposal to build a new experimental area around the internal target in order to study proton-proton and proton-deuteron elastic and inelastic scattering in a single arm recoil spectrometer. The recoil spectrometer room measures 15 x 20 metres in area and is connected to the main ring tunnel by a 5 metre long transition section. A recoil spectrometer consisting of two superconducting quadrupoles for parallel to point focussing of recoiling particles is now being installed together with a superconducting dipole for measuring their momentum.

Internal target experiments at the Fermilab have up to now made use of liquid helium cryopumping techniques for the gas jet target. As a result of the increased demands on liquid helium for the operation of the superconducting magnets it was decided in late August to build a new gas jet target making use of diffusion pumps to remove the gas injected into the main ring vacuum chamber. A prototype target was successfully tested by Fermilab and the target to be used by the experiment is now being assembled. Meanwhile, the spectrometer detectors consisting of multiwire proportional chambers, drift chambers and scintillator hodoscopes are being tested using recoil particles from a carbon filament target. It is expected that the first data taking runs on proton-proton elastic scattering will take place in early 1976.

EXPERIMENT 37

$\bar{p}p$ Interactions at 100 GeV/c

Fermi National Laboratory; Cambridge University; Michigan State University

The experimental programme at Fermilab has made a successful start this year with a 100,000-picture exposure at the 30" hydrogen bubble chamber using a tagged beam of $\bar{p}$ and π^- at 100 GeV/c. Approximately 50% of the interactions are induced by identified $\bar{p}$'s. Analysis of this experiment is well advanced, and already interesting results have emerged, particularly in connection with the "annihilation" component of $\bar{p}p$ interactions. The annihilation contributions may be estimated from the differences between $\bar{p}p$ and pp cross-sections, and show markedly different properties from the "non-annihilation" part. For example the mean charged multiplicity for $\bar{p}p$ annihilations is 9·06 ± 0·56, compared to 6·32 ± 0·07 for pp interactions at this energy. Figure 1.26 shows the mean number of negatives $<n_->$ as a function of energy, and the correlation parameter, f_2^{--}, as a function of $<n_->$ for annihilations. The linear dependence of f_2^{--} on $<n_->$ at low energies, explicable in terms of the breaking of a single cluster or fireball, seems to be no longer followed at 100 GeV/c, suggesting multiple cluster formation may be taking place.

Inclusive production of π^+, π^-, π^0, K_S^0 and $\Lambda^0/\bar{\Lambda}^0$ in $\bar{p}p$ interactions has also been examined. In all cases they are produced more copiously than in pp interactions, and the differences are associated with higher multiplicities, and tend to be concentrated in the region y* near to 0. Proposals have been made for an extension of this experiment, and for a survey experiment at ∼ 200 GeV/c.

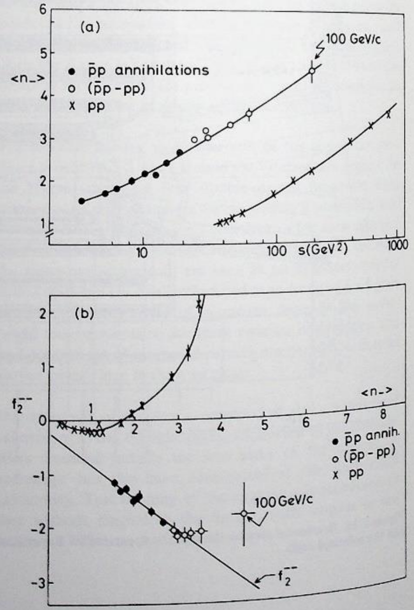

Figure 1.26 Mean number of negatives, $\langle n_- \rangle$, as a function of s and correlation parameter f_2^{--} as a function of $\langle n_- \rangle$. (Experiment 37)

1.1.5 Weak and Electro-Magnetic Interactions

EXPERIMENT 38

Muon-Nucleon Scattering

Chicago University; Harvard University; Illinois University; Oxford University

The purpose of this experiment is to probe the internal structure of the nucleon by using the electromagnetic interaction involved in the inelastic scattering of high energy muons by protons and neutrons.

Extensive running of the experiment took place in 1974 and early in 1975 in the muon beam at the Fermilab at incident energies of 100 and 150 GeV/c. The data analysis is well under way and some results are now available.

One important aspect of the experiment is to test the scaling hypothesis – that at high values of the scaling variable $\omega = 2My/Q^2$, the nucleon structure functions W_1 and W_2, which in principle are functions of Q^2 and ν, depend only upon the ratio ν/Q^2, where ν is the energy transfer to the nucleon and Q^2 is the square of the four-momentum transfer. Within the statistical errors of approximately 20%, the structure function νW_2 at fixed ω is found to be independent of Q^2, in agreement with the scaling hypothesis. These results also show that νW_2 decreases at large ω, which in terms of the parton picture means that the scattering is mainly from the three basic valence quarks of the nucleon, with little contribution from quark-antiquark pairs.

Details of the hadronic states produced in deep inelastic scattering were also measured. In principle these results should tell even more about the substructure, but at present no clear interpretation is possible. As examples of the results obtained, Figure 1.27 shows the transverse momentum distribution of the hadrons for two different regions of the Feynman variable (scaled longitudinal momentum) x = $2P_{11}^*/\sqrt{s}$. These distributions are flatter than those observed in hadron-hadron collisions, particularly in the higher x region. The average transverse momentum of the hadrons is approximately 0·4 GeV/c at x = 0 rising to 0·6 GeV/c near x = 1. This is substantially different to hadron-hadron collisions where the average value of the transverse momentum is less than 0·4 GeV/c and decreases near x = 1.

Running of the experiment will continue at a higher energy in 1976 with several improvements and additions including a large gas Cerenkov hodoscope for identifying the individual hadrons.

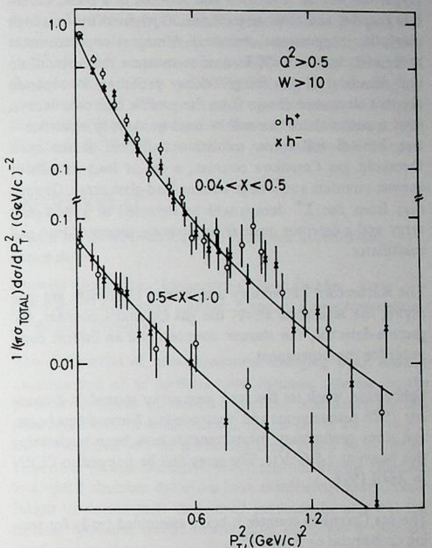

Figure 1.27 Transverse momentum distributions of hadrons from the reaction $\mu^+ + N \rightarrow \mu^+ + h^{\pm}$ + anything. The hadrons (h) are not identified but are assumed to be pions. W is the invariant mass (GeV) of the total hadronic system. (Experiment 38)

EXPERIMENT 39

Experiments with High Energy Charged Hyperons

Bristol; Geneva; Heidelberg; Lausanne Universities; Lab. de l'Acc. Lin., Orsay; CRN, Strasbourg-Cronenbourg; Rutherford Laboratory

This experiment is designed to study the weak and strong interactions of 75–150 GeV/c charged hyperons.

The first stage of the programme will study the weak semi-leptonic decays; $\Xi^- \rightarrow \Lambda e^- \bar{\nu}$, $\Xi^- \rightarrow \Sigma^0 e^- \bar{\nu}$, $\Sigma^- \rightarrow \Lambda e^- \bar{\nu}$, $\Sigma^+ \rightarrow \Lambda e^+ \nu$ and in particular will supply accurate information to check the validity of the Cabibbo theory which gives a relationship between the various hyperon decays.

Previous hyperon decay data has been severely limited by the low fluxes of hyperons obtainable from low momentum beams. A specially designed short beam channel using superconducting quadrupoles is being built to maximise the hyperon fluxes. This, together with the large acceptance of decay products and long hyperon lifetime which follow from the use of high momentum hyperons, should ensure order of magnitude improvements in the estimates of the decay parameters.

Hyperons will be identified and selected in a DISC Cerenkov counter and their trajectories determined by four high resolution proportional chambers. A magnetic spectrometer with drift chambers will be used to measure the momentum and direction of the charged decay products. To separate the rare electronic decays from the prolific hadronic decays, four types of detectors will be used to identify electrons – two lithium foil-xenon transition radiation detectors, a threshold gas Cerenkov counter, a set of lead-scintillator shower counters and a large volume lead-glass array. Gamma rays from the Σ^o decays will be detected in a lead-glass array and a detector made from alternate sheets of lead and scintillator.

The Rutherford Laboratory and Bristol University are supplying the lead glass array, the gas Cerenkov counter, the gamma-detector, the shower counters and an on-line computer for the experiment.

Calibration work on the lead glass array started in December 1975 using muons and electrons in a Nimrod test beam, and some preliminary measurements have been made using this beam at 2·5 GeV/c. The array will be shipped to CERN in April 1976.

The gas Cerenkov counter is being assembled ready for testing on Nimrod early in 1976.

The data collection system is based on software written at the Rutherford Laboratory for the Honeywell DDP516 computer. The computer will be used to write data transmitted via a number of CAMAC modules to magnetic tape.

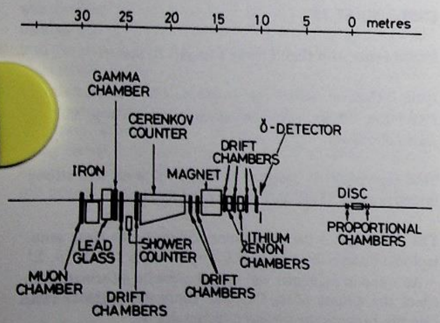

Figure 1.28 Layout of apparatus in the West Area at CERN. (Experiment 39)

It will also produce histogram information for monitoring purposes. To increase the data handling capacity of the system, a NORD 10 computer and a CAMAC mini-processor will be coupled to the DDP516. Data will be passed through a preliminary filtering process using these intermediate devices to improve the quality of the event sample at the on-line stage.

All the equipment will be installed in the West Area at CERN beginning in April 1976 and it is expected that about six months of setting up time will be required before the first data can be taken.

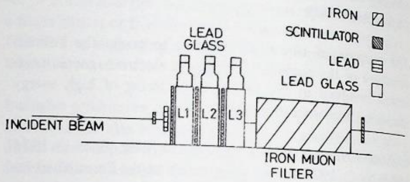

Figure 1.29 Experimental set-up in the Nimrod beam area for preliminary tests on lead glass counters. (Experiment 39)

EXPERIMENT 40

Study of Neutrino and Antineutrino Reactions

Brussels University; University College, London; Bari University; Rutherford Laboratory

This experiment scheduled for the CERN SPS is designed to use the track sensitive target (TST) technique to look for previously undetectable reactions with neutral pions in the final state. The recently-found anomalous dilepton events and charmed particles will also be investigated.

EXPERIMENT 41

CP in a High Magnetic Field

Imperial College, London; Rutherford Laboratory

The idea that several of the apparently fundamental interactions of matter are not independent and that the differences between them arise from a spontaneous breaking of a symmetry has been exploited with considerable success by Salam and Weinberg in their unified theory of weak and electromagnetic interactions. A likely consequence of such theories is that the masses of the gauge bosons mediating the interactions are dependent on the local environment and in particular could go to zero in a sufficiently high magnetic field. In this case the differences between the related reactions would disappear. Salam and Strathdee have suggested that while the critical field needed is probably well outside our reach, such an effect might be seen in the CP violating decay $K_L^o \rightarrow \pi^+ + \pi^-$ for magnetic fields attainable in the laboratory.

It is proposed to perform an experiment at Nimrod to look for such an effect using a beam of K_L^o mesons in a pulsed magnetic field. Any effect will show as a regeneration of a small amplitude of K_S^o mesons with subsequent interference. It is hoped to use a field between 30 and 40 Tesla.

1.1.6 Searches for New Particles

EXPERIMENT 42

Heavy Particle Search

University College, London; AWRE Aldermaston; Rutherford Laboratory

This experiment is designed to detect new stable or very long lived particles with charge +e and in the mass range 5 to 300 GeV. Any such particles would be produced at a very small but nevertheless finite rate by cosmic ray interactions (e.g. by pair production) and this would, during the lifetime of the earth, result in a small accumulated concentration (typically $\sim 10^{-26}$ – 10^{-20}) in ordinary matter. In particular particles of charge +e would form heavy hydrogen-like atoms and (like natural tritium) become a constituent of terrestrial water. By using known separation techniques for hydrogen isotopes this concentration can be increased to a level capable of detection by sensitive mass spectrometry techniques, or in the case of particles of finite lifetime, by observation of the decay products.

The majority of the enrichment is being achieved by the electrolysis of heavy water (itself manufactured by enrichment of natural water) and 6000 litres D_2O are being processed, in collaboration with AEE Winfrith and AERE Harwell, to produce sample volumes in the region 1 to 10^{-3} mℓ in which the concentration of any heavy particles will have been increased by a factor of 10^{11} to 10^{13} relative to ordinary water. Enrichment by a further factor 10^3 can then be achieved by conversion to D_2 gas and using thermal diffusion or laser techniques. By the end of 1975 this work reached the half way stage, the 6000 litres D_2O having been progressively electrolysed to produce enriched volumes in the region 0·1 to 1 litre. A corresponding progressive increase in the natural tritium concentration provided confirmation of the theoretically-expected enrichment factors at each stage.

A detector array for finite lifetime particles was completed and background runs were carried out in preparation for running with an enriched sample during 1976. Some preliminary mass spectrometer comparisons were made between partially enriched D_2O samples (converted to D_2 gas) and unenriched samples. These set an upper limit of about 10^{-17}, for the concentration in H_2O, of new particles in the mass range 5 GeV to 300 GeV. Using samples of higher enrichment and improved mass spectrometry techniques this limit will be progressively lowered, eventually reaching the levels ($<10^{-26}$) expected for pair-produced heavy particles.

EXPERIMENT 43

Search for Short-lived Particles Produced in Neutrino Interactions

Brussels University; University College Dublin; Fermi Laboratory; University College, London; Rome University; Strasbourg University

The discoveries of non-strangeness changing weak neutral currents and of ψ particles have focussed interest on the possible existence of charmed particles and heavy leptons that could well have lifetimes in the range 3 x 10^{-15} to 3 x 10^{-12} sec. One way of producing these could be in the interactions of fast neutrinos with nucleons. Bubble chamber and spark chamber detectors have insufficient spatial resolution to detect such short-lived particles directly but the nuclear emulsion should enable their detection if they are produced in this way. To scan a large emulsion stack for neutrino interactions without any other aid would be practically impossible. By using a hybrid arrangement in which secondaries from such interactions are located in associated spark chambers and then followed back through the emulsion to their origin, such neutrino interactions in emulsion have been located. It is proposed to use a similar technique in an exposure of nuclear emulsion to the neutrino beam at the Fermilab. The neutrino interaction is either located by track following as previously or by area scanning of the region of the emulsion where the origin of the interaction is predicted from a reconstruction of the secondary tracks observed in the spark chamber.

The present proposal envisages a search for neutrino interactions in an emulsion stack of volume 20 litres, the secondaries being located by wide gap chambers down-beam from the stack. These chambers would be triggered by a scintillation counter system coincidence signal indicating a neutrino interaction in the emulsion stack. The arrangement will be triggered for interactions in which either one of the secondary particles is a muon or electron of energy greater than some specified value. A spark-chamber scintillation counter arrangement, constituting a shower detector, will be used to estimate fast secondary electron energies. Additional information about the hadronic and muonic contents of the events may be obtained from some of the detectors of the experiment downstream (Fermilab proposal 310).

For an exposure of 2 x 10^{18} protons on target approximately 500 neutrino interactions would be expected in the emulsion stack. With the scanning and analysis strength available to the collaboration it is anticipated that the work of locating and analysing these would take approximately one year.

Figure 1.30 shows the experimental set-up employed. The wide gap chambers are triggered by a signal which would be produced by a muon emerging from a neutrino interaction in the emulsion. Alternatively they can be triggered by the signal representing a fast electron of energy E ($> E_0$) emerging from a neutrino interaction in the emulsion.

Preliminary tests of backgrounds have been made and the whole apparatus consisting of counter, wide gap chambers and shower detector have been shipped to Fermilab after previous testing at CERN, and has now been set up in the neutrino beam at Fermilab. The main run is expected to commence in January 1976 and to continue for several months.

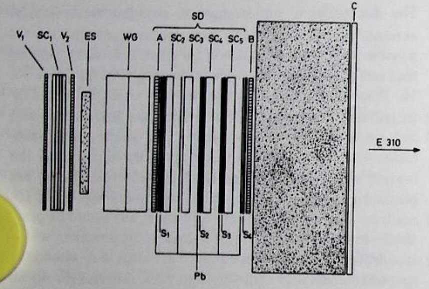

Figure 1.30 Set-up for Experiment 43. The veto counters V_1 and V_2 and narrow gap spark chamber SC_1 are placed on the up-beam side of the emulsion stacks ES. The wide gap chambers WG are followed by a scintillation counter A and a shower detector SD containing scintillation counters S_{1-4}, spark chambers SC_{2-5} and five lead sheets. A concrete block about 1 metre long behind SD is followed by another scintillation counter.

EXPERIMENT 44

Charm Search at Omega

Bari University; Birmingham University; Bonn University; CERN; Daresbury Laboratory, DESY; Ecole Polytechnique (Paris); ETH (Zurich); Freiburg University; Glasgow University; Liverpool University; Milan University; Orsay; CEN Saclay; Westfield College; Rutherford Laboratory

The unexpectedly narrow widths of the newly discovered ψ (3100) and ψ'(3700) indicate that their strong decay is severely inhibited. One attractive interpretation has been to suppose that the ψ and ψ' were the first examples of mesons made from a charmed quark carrying charm +1 and an anti-quark carrying charm −1. Then if charm (like strangeness) is conserved in strong interactions, the Zweig rule would inhibit decay of the ψ(3100) or ψ'(3700) into hadrons made from any of the 3 conventional quarks which carry charm 0.

Beside the mesons with hidden charm (zero net charm) there should exist hadrons with explicit charm (non-zero net charm). Such are the D-meson and C-baryon. Charmed hadrons should have to be relatively massive because the ψ and ψ' would otherwise decay into, for example, a $D\bar{D}$ pair via the strong interaction and hence have short lives. The D-meson mass is thus above 1·85 GeV/c^2. The lowest mass charmed hadrons can only decay weakly to the available non-charmed states of even lower mass. Their decays in the charm model would obey the rule Δ(charm) = $\Delta S = \Delta Q$ so that many strange particles might be expected among their products.

The present experiment using the Omega multiparticle spectrometer at CERN to look for the production of charmed hadrons was proposed in January 1975 following the early observations of the ψ. The experiment was designed to search for the associated production of charmed hadrons in the exclusive channels

$$\pi^- p \rightarrow K^- K^+ \pi^- p \qquad 1$$

and $$\pi^- p \rightarrow K^- K^+ \pi^+ \pi^- \pi^- p \qquad 2$$

at a beam momentum of 19 GeV/c.

The objectives of the trigger arrangement were twofold: first, to be sensitive to the multiparticle final states containing charged K-mesons which result from the decay of charmed hadrons. Second, to filter out the processes in which the K-mesons result from the decay of low mass non-charmed K*s and Y*s.

The experimental trigger requires firstly a fast forward K^- (or $\bar{p}$) as identified by a down-stream low pressure Cerenkov. The Cerenkov can distinguish π^- from K^- or $\bar{p}$ between 3 and 10 GeV/c. Secondly the triggering particle should have a high transverse momentum so that it cannot come from the decay of a low mass object. This requirement is set by a hardware coincidence between proportional chambers which restrict p_t to be above 500 MeV/c. Thirdly the measured multiplicity is required to be 3 or more.

In the 15 days of production running in March, 3·2 million triggers were recorded. So far, only the kinematic fitting of 4-constraint hypotheses has been carried out. 4500 fits to the Reaction 1 and 3000 fits to the Reaction 2 were obtained. Separation from alternative hypotheses with the K^+K^- pair replaced by $p\bar{p}$ is excellent.

Searches were performed on this exclusive channel data for any narrow peaks in the effective mass distributions which could be evidence for the production of pairs of charmed hadrons. The effective interval of good acceptance was 1·5 to 2·5 GeV/c^2 for the D-mesons and 2·0 to 3·5 GeV/c^2 for the C-baryons. No convincing accumulation of events has been seen in any channel and the table shows the upper limits for the production cross-section multiplied by the decay branching fractions of the charmed hadrons. These limits are an order of magnitude improvement over the limits from previous experiments.

During June there was a second experimental run to examine a different region of phase space for a charm signal. In particular it was designed to study a small but suggestive fluctuation seen in Reaction 2, perhaps evidence for the process $C^0 \rightarrow K^- p$ and $\bar{D}^0 \rightarrow K^+\pi^+\pi^-\pi^-$. Two million triggers were recorded in June. Kinematic analysis yielded a further 6000 fits to Reaction 2. No charm signal is apparent in this data; we thus conclude there is no evidence in the exclusive 4-constraint data for the production of new particles.

Analysis is continuing with the aim of examining the channels with a single neutral in the final state, where one of the charmed particles can decay hadronically and the other leptonically.

1.2 Nuclear Physics

Nuclear Physics, in the context of experimental work supported by the Rutherford Laboratory, means the study of the static properties of elementary particles and the symmetries of their behaviour at low energies as well as their interactions with themselves and with complex nuclei in the so-called intermediate energy range 50 to 500 MeV. Facilities for such experiments are provided on the Variable Energy Cyclotron at the Atomic Energy Research Establishment (AERE), Harwell; the 8 GeV proton accelerator Nimrod at the Rutherford Laboratory; the High Flux Beam Reactor at the Institut Laue-Langevin (ILL) at Grenoble, France; the 600 MeV proton Synchrocyclotron (CERN S.C.) at CERN, Geneva, and the 500 MeV H^- cyclotron (TRIUMF) at Vancouver, Canada. This work on the nuclear physics of elementary particles extends and complements the study of nuclear structure physics at low energy (tens of MeV) which is widely carried out at Van de Graaff machines throughout the country and for which the new 30 MV Nuclear Structure Facility (NSF) is being built at the SRC's Daresbury Laboratory.

The Institut Laue-Langevin at Grenoble, France, is an international laboratory supported by the British, French and German governments for use by their own physicists and based on a 50 Megawatt nuclear reactor with a core flux of 10^{15} neutrons/cm^2/sec. Such a neutron source provides facilities for studying the structural properties of matter and is supported through the Neutron Beam Research Unit of the Rutherford Laboratory. In addition, the high neutron flux provides facilities, unique in the western world, for nuclear physicists to investigate the static properties of neutrons and their low energy interactions. Four such experiments, supported through the Rutherford Laboratory, are in the course of preparation for running at the ILL reactor: neutron scattering from polarized and then unpolarized nucleons to test the invariance of time reversal and of spatial symmetry in the strong and electromagnetic interactions, a continuation of the programme of experiments to increase the sensitivity of measurements on a possible electric dipole moment of the neutron, which in turn implies a breakdown of both space and time reversal invariances, and a new experiment to measure the lifetime of the neutron. This latter experiment uses a new technique, which was recently tested successfully at the AERE LIDO reactor by the University of Sussex group, of trapping the protons from neutron decay in an electro-magnetic bottle for subsequent release and observation in solid state detectors. These four experiments are described in more detail later.

The 8 GeV proton accelerator at the Rutherford Laboratory continues to be used as a source of stopped K^- mesons for studies of both interaction effects and nuclear properties. With a continuous flux in excess of 10^7 stopped K^- mesons per day for most of the year, this beam is superior to any in the world. This resource has been exploited over the past year by a collaborative effort of American visitors, Rutherford Laboratory staff and British University visitors and a detailed report of their work is given in Experiment 49.

The past year has seen the commissioning of three new high current, intermediate energy machines, so-called 'pion factories'; SIN at Zurich Switzerland; LAMPF at Los Alamos, USA; and TRIUMF at Vancouver, Canada. In addition the CERN Synchrocyclotron, a machine of similar energy, has been re-vitalised by amendments to its acceleration system designed to give an accelerated proton current of 10 μA. These high current machines provide the opportunity for increasing the precision of measurement on low cross section processes and of rare decay modes. In addition, the provision of polarized beams used in conjunction with polarized targets enables the spin structure of scattering amplitudes to be evaluated. Two British collaborative efforts, supported by the Rutherford Laboratory, are involved in this programme of intermediate energy physics. One, the so-called BASQUE collaboration, uses the TRIUMF accelerator in Vancouver to investigate the spin structure of nucleon nucleon scattering at 500 MeV and a preliminary report on their work is given in Experiment 48. The other, a collaboration between the Daresbury Laboratory and the Universities of Oxford, London and Birmingham, has designed and is building a large volume spectrometer magnet to exploit the possibilities of observing rare pion decay modes which the uprating of the CERN Synchrocyclotron has presented. A brief report of their progress and plans is given in Experiment 50.

The four Experiments 51–54, by the Kings College London group represent their work and progress over the past year on experiments using the various accelerators at AERE Harwell. This work, which in part involves low energy nuclear structure investigations and is a continuation of a long research programme, is still supported by the Rutherford Laboratory for historical reasons. At AERE Harwell, the Tandem Van de Graaff, the Synchrocyclotron and the Variable Energy Cyclotron provide facilities for nuclear structure research which are not available at the University. Beams of He^3 ions and of α particles have been used in these experiments and the results analysed in terms of optical model potentials, a view of the scattering process which extends from the highest to the lowest energies.

EXPERIMENT 45

Parity and Time Reversal Symmetry Tests

Sussex University; Glasgow University; Harvard University; ILL

The extent to which the fundamental interactions, strong, weak and electromagnetic are invariant under the different symmetry operations is of fundamental significance. Parity violation in the weak interaction appears to be complete while the decay of K^o_L indicates that CP is violated and this in turn may imply T violation. More recently evidence of P violation in electromagnetic transitions has been accumulating although the source is not yet identified. Of the latter experiments the most significant result is that obtained by Lobashov et al for the circular polarization of the 2·2 MeV γ-ray emitted following neutron capture by a proton. Their value, $P\gamma = (1{\cdot}6 \pm 0{\cdot}4)\times10^{-6}$ is almost two orders of magnitude greater than theoretical estimates. It is felt that the estimates are as complete as current theory can provide and it is thus very important to establish this result.

There has been a continuing programme of experiments to test T-violation in weak and electromagnetic interactions. So far these experiments have achieved a relatively poor accuracy, the present limit for the amplitude of a T-violating component being $\sim 10^{-3}$. T-violation experiments are in general difficult since a P-conserving but T-violating process requires a term similar to J. $(k_1 \times k_2)$ to be determined rather than a simple pseudoscalar such as J.k for a P-violating process.

At the moment experiments are being prepared for ILL to carry out further symmetry tests.

P-violation: The n+p→d+γ measurement will be repeated since this is a crucial experiment. The limit of accuracy obtained by Lobashov et al will be matched from a statistical point of view but when measurements of such high accuracy are attempted many small and previously unexpected systematic errors can arise.

A target will be located at the centre of a tube which runs through the reactor to within 50 cm from the centre of the core. At this region the neutron flux is 10^{15} n cm^{-2} sec^{-1} and the circular polarization of the radiation will be measured using transmission magnets. The magnetization will be periodically reversed and a search will be made for a small change in the detector current. Measurements will be made simultaneously on each side of the target so that a comparison can be made between two simultaneous measurements rather than between results forming a sequence of measurements.

The great problem in such an experiment is shielding the analyser detector from circularly polarized bremsstrahlung arising from β-decay of fission products in the core. The in pile section is at present being designed.

T-violation: Ensembles of polarized nuclei may be conveniently created following the capture of polarized neutrons. By measuring a γ-γ directional correlation from such an ensemble it is possible to search for a term such as J.$(k_1 \times k_2)$.

A multi-detector configuration with correlation angles of $\theta = 45°$ and 135° is particularly convenient since the asymmetry term in the correlation function is proportion to sin 2θ. An asymmetry may be identified by comparing the results from different detector pairs (correlation angles) or from the same detector pair when the nuclear spin (neutron spin) is reversed.

A high degree of symmetry is an essential feature of the instrumentation and careful attention is paid to possible inherent asymmetries due to electronic modules behaving differently for the various detector outputs. A GEC 4080 computer will be used to store and process the data and to carry out the many statistical tests.

Initial measurements will begin early in 1976 and because of the high flux of polarized neutrons 5×10^8 n sec^{-1} on 0·5 cm by 3·0 cm, large effective source strengths may be created and it will be possible to match the statistical accuracy of past measurements in a much shorter time. Improved statistical precision could allow some limiting features to be assessed, e.g., the precision with which the source must be centered and the correlation angle known.

A cryogenic polarized source will become available later in 1976 and preparations are being made to test T-violation in the weak interaction by measuring a β-γ directional correlation. The main features of this experiment are the same as those of the γ-γ correlation.

EXPERIMENT 46

Search for an Electric Dipole Moment of the Neutron

Sussex University; Oxford University; Harvard University; Oak Ridge National Laboratory; Technical University Munich; Centre d'Etudes Nucleaire Grenoble; ILL; Rutherford Laboratory

Apparatus is being built with the aim of making a more sensitive search for a possible electric dipole moment in the neutron. The quantity $(\mu_e \cdot \mu_m)$ thought of as an operator is odd under the time reversal operation T which reverses the direction of the magnetic dipole moment μ_m but not the electric dipole moment μ_e, and is odd under the parity operation P which reverses the direction of μ_e but not μ_m. This means that the observation of a non-zero expectation value for the quantity $(\mu_m \cdot \mu_e)$ would be direct evidence for the violation of T and P symmetries. The possibility of observing T violation is the chief incentive for the experiment. Such an observation would be the first known case of T violation outside the K meson system and would help to determine which interaction is responsible for these effects.

Predictions of various magnitudes for a neutron electric dipole moment are appearing regularly in the literature generally using a variety of models to relate the magnitude of the neutron electric dipole moment to the observed CP and T violating properties of the K° mesons. A recent prediction is that (μ_e/e) would be $\leqslant 10^{-24}$ cm depending on the mass of the Higgs boson as M^{-2}. The most recent experiment by Dress et al has produced the result $(\mu_e/e) < 3 \times 10^{-24}$ cm. It is expected that the experiment now being prepared could achieve a further increase of sensitivity of about two orders of magnitude.

The method uses recently developed techniques for very slow ultra-cold neutrons which can be bottled in evacuated chambers for tens of seconds. To produce ultra-cold neutrons in sufficient numbers a special source is being constructed by ILL engineers in collaboration with the Neutron Beam Research Unit of the Rutherford Laboratory. This source is due to be installed in the High Flux Reactor at ILL at the end of 1976 or in 1977. Inside the pile there will be an electro-polished stainless steel neutron guide terminating close to the core in a thin zircaloy end window. Outside the pile there will be several metres of curved nickel-coated glass guide designed to pass neutrons with velocities less than 50 ms^{-1} whilst removing unwanted radiations. Ultra cold neutrons are generated in a thin layer of water close to and on the outside of the zircaloy window and will pass through the window into the evacuated guide.

Polarized neutrons will be periodically bottled in an evacuated chamber of a few litres capacity. The rest of the apparatus is designed to detect very small changes in the rate of precession of the neutron spins which correlate with the direction of a strong applied electric field with respect to a weak magnetic field in the chamber. The increase in sensitivity of the method stems partly from the relatively long time (30 seconds) for which it is possible to keep each neutron in the combined fields, and partly from the small time average of the velocity of each neutron. This should be about 10^5 times smaller than previous experiments, thereby reducing unwanted relativistic interactions between the magnetic moment and the electric field. One of the most challenging technical problems is the need to reduce magnetic field changes in the chamber to 10^{-8} gauss or less over periods of 1 minute. This requires carefully-made magnetic shielding and the use of sensitive magnetometers for monitoring purposes. Another technical problem is the need to apply high voltages while maintaining very small leakage currents in the vicinity of the chamber. Experimental tests are in progress on prototype shields and a prototype chamber.

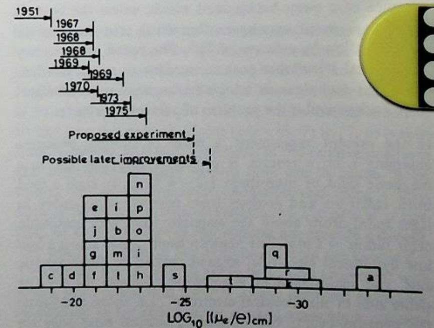

Figure 1.31 The progress of experimentally-determined upper limits for the dipole moment of the neutron. The boxes show theoretical predictions labelled alphabetically in chronological order. (Experiment 46)

EXPERIMENT 47

A Measurement of the Neutron Lifetime

Sussex University; ILL; Rutherford Laboratory

The free neutron is β-active and decays according to the scheme

$$N \rightarrow p + e^- + \tilde{\nu}_e$$

The end-point energy of the electron spectrum is 782·9 ± 0·4 keV and the maximum kinetic energy of the recoiling proton is 0·755 keV. Four independent determinations of the neutron half-life have been reported since the β-decay of the neutron was first observed in 1948 and the currently accepted value of 10·61 ± 0·16 min is in conflict with the previous best determination of 11·7 ± 0·3 min. This disagreement has yet to be satisfactorily resolved.

The motivation for establishing an accurate value of the neutron half-life is the need to determine the vector and axial vector coupling constants for nuclear β-decay by a technique whose accuracy is not significantly limited by uncertainties associated with nuclear structure effects. The most promising approach in this respect is to combine a value of the neutron half-life with a measurement either of the electron-neutron spin correlation coefficient in polarised neutron decay or the vector coupling constant determined from the ft-values of β-transitions between mirror nuclei. The neutron half-life is also an important parameter in astrophysical calculations on the production of helium by thermonuclear processes in stellar systems.

A neutron half-life determination requires making an absolute measurement of the neutron density throughout a selected volume of neutron beams which may be achieved using neutron absorbers such as ^3He or ^{10}B. This must be combined with a measurement of the rate of emission of decay particles, either electrons or protons, from the source volume, and this necessitates counting decay events in the presence of a γ-ray background which, unless the beam is specially prepared, may have a flux which is in excess of the β-particle flux by a factor of 10^8. The recoil protons may be counted if suitable post-acceleration is employed but, whichever technique is adopted, the separation of signal from background is the problem of prime importance.

In the present experiment, a beam of thermal neutrons emerging from a reactor is projected perpendicular to a magnetic field of magnitude 1·2 - 4 Tesla. In such a field both electrons and protons from neutron decay move in tight spiral orbits about the magnetic field, with maximum orbit radius ~ 3 mm. The neutron beam passes across a hollow cylindrical electrode, aligned parallel to the magnetic axis, and maintained at a potential of about 40 KV. At either side of this "central electrode", i.e. above and below the neutron beam, two coaxial cylindrical electrodes are maintained at potentials of about 41 KV. This combination of electrodes, in conjunction with the magnetic field, behaves as a potential well of depth ~ 1 keV which traps protons from neutron decay, and these may be stored for significant periods of time before being recorded. At the end of the selected trapping period, the trap is opened by applying a 1 KV negative pulse to one electrode; the proton is released and accelerated down to earth where it is detected in a silicon surface barrier detector.

This system has the following special advantages:

(a) the effective volume of neutron beam is defined by the length of beam cut off by the lines of magnetic force passing through the bounding edge of the proton detector. This volume is independent of the distribution of neutrons across the beam and is determined by the ratio of magnetic field strengths at the beam and at the detector.

(b) when the protons are stored for a period T_t and the counter output spectrum is sampled for a period T_s following the application of the trap pulse, the background is reduced by a factor of T_s/T_t and in practice reductions of the order $1{\cdot}5 \times 10^{-4}$ may be achieved.

The apparatus has been tested on the low flux (3×10^6/cm^2/sec) swimming pool reactor LIDO at AERE Harwell, where the half-life was measured as 10·92 ± 0·42 min., most of the error originating in the very high background and poor counting statistics. In the present experiment a modified version of the existing system is to be used at a high flux facility (~ 10^9/cm^2/sec) in conditions of low γ-ray background and zero flux of fast neutrons. Under these circumstances the major difficulties associated with the earlier low-precision measurement should disappear.

EXPERIMENT 48

Measurement of Triple Scattering Polarization Parameters in Nucleon-Nucleon Scattering at 500 MeV

(Basque Collaboration), Bedford College, London; AERE Harwell; Surrey University; Queen Mary College, London; British Columbia University; Victoria University

In this experiment at TRIUMF, Vancouver, the first protons onto target arrived in February and by late summer the crew of the sector-focussed H^--cyclotron had achieved simultaneous extraction of two beams of continuously variable energy at currents approaching 100 nA. The optical properties of beamline used by the BASQUE group have been studied and optimised, and are close to the calculated properties. The arrays of scintillation counters and multiwire proportional chambers (MWPCs) have been fully tested, and all of the latter now operate reliably at very nearly 100% efficiency. The first measurement was a calibration of the analysing power of the carbon scatterer in the MWPC array, and preliminary results are shown in Figure 1.32. These were obtained using a gaseous hydrogen target, instead of the liquid hydrogen target to be used in the final configuration. The superconducting solenoidal magnet, built by the Rutherford Laboratory Applied Physics Division for spin precession, performed entirely to specification and has been trouble-free. The liquid hydrogen target was installed later in the year, and final calibration data taken.

During the year a proposal to measure the Wolfenstein spin rotation parameters D, R and R′ at several energies in p-p scattering, in addition to the corresponding n-p measurements, was approved. It involves no additional apparatus and will be implemented as soon as a polarised proton beam is available at TRIUMF. The ion source and injection line for this beam have been installed and tested, and acceleration of polarised H^- ions is imminent. The second objective in early 1976 is to determine the optimum angle of the polarised neutron beam produced in the reaction $^2H(\vec{p},\vec{n})$; this is essentially a measurement of R_t and D_t in this reaction. This, and the p-p experiment just mentioned, will precede the n-p measurements and will provide the first new physics results from the BASQUE collaboration.

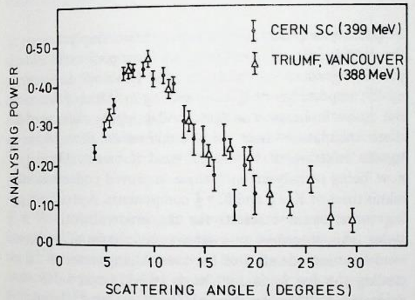

Figure 1.32 Effective analysing power in p-carbon scattering near 400 MeV as a function of lab. scattering angle. The preliminary data from TRIUMF is compared with published measurements from CERN. (Experiment 48)

EXPERIMENT 49

Experiments with K^-- Mesic Atoms

Birmingham University; Surrey University; Rutherford Laboratory

A slow negatively charged hadron (pion or kaon) travelling through matter can be captured by an atom so as to move in an atomic orbit around the target nucleus. In the capturing process the hadron expels an electron from the target atom by the Auger effect and will then occupy an atomic orbit which corresponds to a highly excited state of the hadronic or "exotic" atom. The hadron will initially cascade through the atomic energy levels by Auger transitions and then by radiative transitions in which X-rays are emitted. Finally the strong interaction between the hadron and the nucleus becomes important and the hadron will be captured. As a result of this interaction the final observable X-ray transition is frequently broadened and shifted in energy as well as being attenuated. Measurements of these parameters give information about the very low energy kaon-nucleus interaction and capture process together with the possibility of obtaining information about nuclear properties in the surface region.

So far measurements of the shift and width of the last observable transition for kaonic atoms have generally been restricted to the light and medium weight nuclei. For heavier nuclei either there are problems due to the overlapping of transitions of very similar energy or the nuclei may be deformed giving difficulties in the interpretation of the experimental data. Measurements have been made in this experiment for the $K^-(6 \rightarrow 5)$ transition for Ag and Cd where the problem is the adjacent $K^-(8 \rightarrow 6)$ transition which is very close in energy. The experimental results seem to deviate from the predictions of simple theoretical models and further calculations will be necessary. Some anomalies and disagreements in earlier experiments on S, Co and Ni have been resolved by the present work.

Attenuation of exotic atom X-ray intensities may also occur if there is a significant coupling between the atomic energy levels and those of the nucleus. A few cases exist where the energy of an E2 transition in the nucleus is very close to that of a ($\Delta n = 2, \Delta \ell = 2$) atomic transition. In these resonant conditions configuration mixing can then occur, which results in radiationless excitation of the nucleus. This manifests itself as an attenuation of the appropriate X-ray yields and a measurement of the attenuation yields additional information about the hadron-nucleus strong interaction. Two cases of E2 nuclear resonance have been observed in the present work; these are for pions on Cd^{111} and Cd^{112} and for kaons on Sn^{122}. For pionic cadmium the $5 \rightarrow 4$ and $4 \rightarrow 3$ transitions are attenuated relative to the $6 \rightarrow 5$ transition. For kaonic tin the intensity of the $6 \rightarrow 5$ transition is halved compared with the intensity of the same line for a natural isotopic mixture.

The ground state quadrupole moment of nuclei with $I > \frac{1}{2}$ can give rise to hyperfine splitting of the atomic levels. For example in the case of tantalum, where $I = \frac{7}{2}$ and the quadrupole moment is large, the kaonic levels are split sufficiently to affect the line shapes observed with a Ge(Li) detector. In this case the transition from $(n\ell) = (8, 7)$ to $(7, 6)$ is split into 21 components and predictions of the relative positions and intensities of these various lines can be made. After folding in the experimental resolution and using a least squares fit of the predicted function to the data it is possible to extract values of the electric quadrupole moment. The values obtained in this experiment from the kaonic $8 \rightarrow 7$ transition for Ho and Ta are in very good agreement with values from pionic and muonic X-rays obtained elsewhere. In addition to the effect of the electric quadrupole moment of the nucleus, it is also possible to observe transitions where the strong interaction has an effect. In this case it is hoped that information about the mass quadrupole moment might be extracted from the data.

A systematic study of the γ-rays from nuclear interactions of stopped kaons, stopped pions and in-flight pions is in progress. For an ^{27}Aℓ target and incident kaons the interaction with a single proton leaving ^{26}Mg is found to be dominant and about seven times more probable than the interaction with a single neutron (leaving ^{26}Aℓ), confirming the important role of the Y*(1405) in the absorption process. The yields of other nuclei such as ^{23}Na (an α less) and ^{24}Mg (a triton less) are found to be surprisingly high; a result obtained in earlier pion experiments.

The recent observation of the dominance of Ho^{165} (π^-,xn) reactions (where x is an odd number) when pions are stopped in holmium is not fully understood. In the present experiment with kaons stopped in holmium the pattern of residual nuclei and rotational transitions is very different. In particular the reaction with a single proton (expected because of the Y*(1405) dominance) to give ^{164}Dy is apparently absent. It is hoped that a comparison of the kaon and pion data will throw some light on the way in which hadrons interact with deformed nuclei.

EXPERIMENT 50

Measurements of the Decay Rate $\pi^0 \to e^+e^-$ with the Omicron Spectrometer

Birmingham University; Oxford University; Daresbury Laboratory; University College, London

Omicron is a large volume multi-particle magnetic spectrometer which exploits the good duty-cycle of the CERN Synchrocyclotron. The initial programme includes a mixture of nuclear and particle physics at intermediate energies with emphasis on the determination, so far unmeasured, of the $\pi^0 \to e^+e^-$ rate, this being the specific responsibility of the British members of the collaboration.

The Rutherford Laboratory has provided the former heavy-liquid bubble-chamber magnet for which new poles are being constructed using scrap steel from the old Liverpool synchrocyclotron. With drift and proportional chambers on-line to a small local computer, such spectrometers can produce data faster than the large central computer can determine particle momenta; so the new poles have been designed, using the Rutherford Laboratory's GFUN 3-D magnet design programmes, to give a magnetic field shape which allows very fast analytic methods of determining momenta.

EXPERIMENT 51

Coulomb/Nuclear Interference in Alpha Particle Scattering

King's College, London

An experimental study has been completed using the Tandem Van der Graaff at AERE Harwell, of forward angle inelastic alpha scattering from ^{52}Cr, ^{56}Fe, ^{60}Ni and ^{64}Zn to investigate the interference of Coulomb and nuclear contributions. Angular distributions have been obtained between 10 and 160° for scattering from the ground and first excited states at 15 and 18 MeV for all these four nuclei, and at 19 MeV for ^{64}Zn. Inelastic scattering excitation functions have also been measured at 25° for the first excited state from 11–19 MeV in steps of ~ 0·5 MeV. Reduction of the data is now complete and an optical model analysis of the scattering from the ground states is in progress.

In addition a preliminary analysis of two step processes in the ^{12}C(d, ^{3}He) ^{11}B reaction has been performed using a pure K = $\frac{3}{2}$ rotational model for ^{11}B. The work demonstrated the importance of K band mixing in ^{11}B and as a result the coupled channels' inelastic and stripping codes used for these calculations have been modified to allow them to handle mixtures of several different K values. The data is now being reanalysed with these improved codes assuming admixtures of K = $\frac{1}{2}$ and K = $\frac{3}{2}$ components. Apart from giving more accurate results for the predominantly K = $\frac{1}{2}$ states, this procedure now allows the calculation to be extended to include all 5 of the lowest lying states of ^{11}B including the J = $\frac{1}{2}^-$ and $\frac{3}{2}^-$ levels at 2·214 and 5·019 MeV respectively. The inelastic scattering in the ^{12}C and ^{11}B channels has been successfully completed for all the first five levels of the latter nucleus.

Theoretical studies of inelastic scattering have been pursued along two main lines. The first of these has been concerned with the development of a coupled channel's inelastic scattering code employing the random phase approximation. The programme has been used to fit inelastic scattering of deuterons from ^{12}C associated with the ^{12}C(d, ^{3}He) ^{11}B work described above. The second line of study has involved a search for a simple general method of including exchange contributions in collective model inelastic scattering calculations. An approach has been developed which covers both the real and imaginary parts of form factors and the model is being applied to analyse inelastic proton scattering from ^{12}C, ^{24}Mg and ^{40}Ca at 20, 40 and 80 MeV.

EXPERIMENT 52

Scattering of Polarized ^{3}He Beams

Birmingham University; King's College, London

For some time, scattering studies with ^{3}He beams have been hampered by the lack of information on the spin orbit interaction. Whereas upper limits to its size have been determined by double scattering and spin flip measurements, a definitive measurement is very hard to achieve with these techniques. The spin orbit interaction produces its major effect on elastic scattering cross sections at backward angles. It is exactly this region that is most sensitive to the separation of discrete optical potential ambiguities as well as a number of second order effects such as spin-spin interactions. Thus a measurement of the strength of the spin orbit force is an urgent necessity for the development of helion scattering studies.

The recent development at Birmingham University of a polarized helion ion source has enabled polarization measurements up to 33·4 MeV to be made, and a set of experiments has recently been completed on targets of ^{27}Al and ^{26}Mg. Measurements of the polarization in elastic scattering, the asymmetries in inelastic scattering and the asymmetries in the (h,α) reaction have been completed using the full energy ^{3}He beam.

This data together with the cross section measurements of Shahabuddin gives comprehensive scattering data for these nuclei. Preliminary analyses with both microscopic and conventional optical model potentials show great promise. Comparison between the ^{26}Mg (ground state 0$^+$) and ^{27}Al (ground state $\frac{5}{2}^+$) data will also provide information on target spin effects.

The inelastic scattering and neutron pickup reaction data will be analysed initially using the conventional distorted wave Born approximation and the collective model.

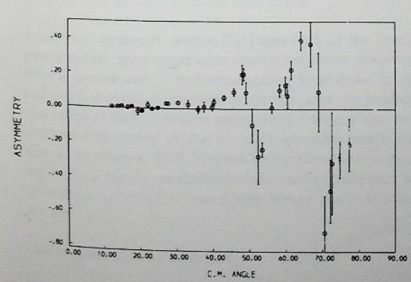

Figure 1.33 Elastic Scattering polarizations for ^{26}Mg($^3\vec{He}$, ^{3}He) at 33·4 MeV. (Experiment 52)

EXPERIMENT 53

Helium 3 Elastic and Inelastic Scattering and the (h,α) Reaction

King's College, London

It is well known that measurements of ^{3}He elastic scattering at sufficiently high energies and sufficiently large angles allows the identification of a unique optical potential. Measurements of helion elastic scattering on ^{56}Fe at 33, 53 and 83 MeV using the UKAEA Variable Energy Cyclotron (VEC) have demonstrated this effect and allowed the development of a microscopic folding model which formulates this unique potential.

The microscopic optical model referred to as the "3 parameter" model derives the imaginary potential using the "forward scattering approximation", and applying this model to the elastic scattering cross sections from the even Samarium isotopes at 53·4 MeV has shown up some of the deficiencies of the model with regard to the density dependence of the effective nucleon-nucleon interaction. In the scattering of ions it is necessary to include the effect of the density of both the target and incident particle. The improvement produced by including such double density effects is shown in Figure 1.34, where the comparisons are made for the case of ^{144}Sm (h,h), where the formulation of the folding model including the density of the projectile is referred to as the "nucleus-nucleus" model. The obvious applicability of the scattering of heavier ions has led to the measurement of elastic and inelastic scattering of helions and lithium ions on the calcium isotopes, ^{40}Ca, ^{44}Ca, ^{48}Ca. Not only are these nuclei the most commonly used ones for optical potential studies, but measurements with alpha beams have exhibited intermediate structure features which make the (h,α) reaction of further interest. The measurements with the VEC 53 MeV helion beam are complete and the ^{7}Li beam studies are scheduled.

EXPERIMENT 54

Elastic and Inelastic Scattering of 53 MeV ^{3}He from the Samarium Isotopes

King's College, London; Oak Ridge National Laboratory

An analysis has recently been completed of the scattering of ^{3}He from the 0$^+$, 2$^+$ and 3$^-$ states of $^{144, 148, 150}$Sm and from the 0$^+$ and 2$^+$ states of $^{152, 154}$Sm using both distorted-wave Born approximation (DWBA) and coupled channels calculations. The table compares the values of the quadrupole deformation parameter β_2 obtained from the current analyses. The DWBA predictions fit the 2$^+$ and 3$^-$ data fairly well except at forward angles, but the slope of the cross-sections is not quite correctly predicted. Coupled channels calculations have been performed using a vibrational model

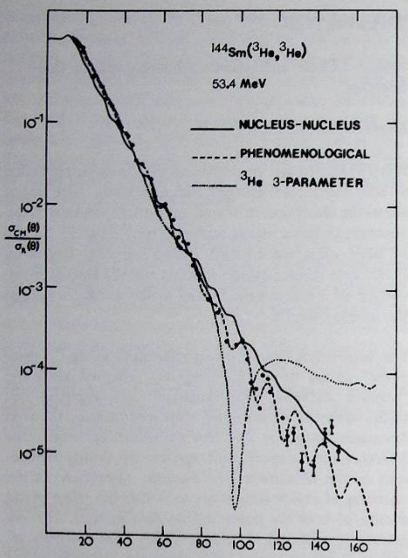

Figure 1.34 Fits to ^{144}Sm (^3He, ^3He) at 53·4 MeV using a phenomenological potential, the "3 parameter" model potential and the "nucleus-nucleus" model potential which includes the saturation in the effective interaction. (Experiment 53)

for $^{144,148,150}Sm$ and a rotational model for $^{152,154}Sm$. Two sets of searches were carried out; one where the potential depths and deformation parameters were varied, keeping the geometrical parameters constant, and another where all parameters were varied to obtain the best fit. Using fixed geometrical parameters, the fits to the data were found to deteriorate with increasing target mass (and therefore nuclear deformation). The fits of the 2^+ and 3^- states of ^{148}, ^{150}Sm were characterized by a poor prediction of the slope of the experimental cross-sections. For $^{152,154}Sm$ improved fits could be obtained by including Coulomb excitation in the calculation and by explicitly coupling higher (in this case 4^+) levels in the calculation together with deformation parameters of higher multipolarity (β_4 and β_6) in addition to β_2.

When all the parameters were varied, some interesting trends were revealed. The fits were characterized by decreasing diffuseness for the real potential and by decreasing radius and increasing diffuseness for the imaginary potential, with increasing mass of the target nucleus. For the rotational nuclei, the calculation included coulomb excitation but only the 2^+ state was coupled using only β_2, and the fits were as good as or better than those obtained using the fixed geometry. It is possible that the changing geometrical parameters are a result of the increasing collectivity of the nuclei with increasing mass and that these effects are more or less eliminated when higher order effects are correctly taken into account. The resulting optical parameters are then almost identical throughout the range of nuclei in agreement with the conclusions of Hendrie et al.

1.3 Theoretical High Energy Physics

The Theory Division pursues a range of research programmes. Much of this work is phenomenological, concerned with analyzing the theoretical implications of new data from the world's accelerators, and the experimental consequences of new ideas. During 1975 the most striking new results and ideas have centred on ψ-particle physics and the implication of new quantum numbers such as charm or colour, but progress has also continued in other areas.

Theory Division also organizes activities involving the whole British particle physics community. The Annual Theoretical Physics Meeting, that took place at the Rutherford Laboratory during January 6–8, was attended by about two hundred people. The summer visitor programmes attracted active physicists from Denmark, Israel, Japan, Poland as well as Britain. A topical meeting on the charmed current was convened at the Coseners House in November.

Charm production in strong interactions

If the new quantum number charm exists, there must be new charmed particles, and they should be produced in strong interactions at high enough energies – just like the associated production of strange particles. It is interesting and important to see what cross sections may be predicted. Taking present ideas about Regge pole exchange and duality, and generalizing SU(3) to SU(4) symmetry, the comparison with strange particle production can be made quantitative. The scale of charmed particle masses and Regge trajectories is determined by the ψ mass. It then follows that charm-exchange trajectories are displaced downward relative to strangeness-exchange trajectories, and associated charm production is strongly suppressed relative to strangeness production. The results are sensitive to the precise choice of trajectory parameters, but even the most optimistic assumptions give very small charm production cross sections, typically suppressed by factors 10^{-3} or less compared to strangeness production at the same energy.

A different approach, within the framework of the quark parton model, gives larger cross section estimates however. Several phenomena – including scaling breakdown in ep scattering, ψ photo-production properties, and μ/π production ratios at large transverse momentum – suggest that the charmed component in the proton's quark-antiquark sea may be as much as 20%. This can be translated into a specific formula for the production of charmed particle pairs in pp collisions, that gives typical high energy values of order 0·1 mb.

Charm production by neutrinos

Neutrino scattering is a promising place to search for evidence of charm or other new quantum numbers. Although all cross sections are small, the predicted charm production effects are relatively large and easy to interpret. The high energy neutrino data has been analyzed and compared with current theories, including the original charm model and recent proposals incorporating V + A currents and more new quarks, using the quark-proton framework and explicitly integrating the various experimental neutrino spectra.

In the usual $\nu N \rightarrow \mu X$ inclusive measurements, one simply looks for anomalies in the cross sections $d^2\sigma/dxdy$ that are not explained by conventional quark transitions. The most celebrated anomaly is in the $\bar{\nu}N$ y-dependence at small x, large y; it can indeed be explained by charm production in several theories, but the uncertainties in data and in the quark-parton distributions make this effect by itself unconvincing.

Much stronger candidates for charm production are the dimuon events $\nu N \rightarrow \pi^-\pi^+X$, where the second muon is supposed to come from a charmed hadron decay. This is a much clearer signal, since conventional hadronic transitions are believed to contribute little here. Analysis shows that the properties of dimuon events put strong constraints on theories of the weak charm current. They indicate that νN charm production at present energies comes largely from valence quarks, whereas $\bar{\nu}N$ production comes from the quark-antiquark sea in the nucleon target. This is consistent with several versions of charge 2/3 charm quark production, but excludes theories based on a new quark of charge $-4/3$; it indicates no appreciable excitation of the new charge $-1/3$ quark of vectorlike theories.

Relations between neutrino and antineutrino scattering

There are some general relations between the differential cross sections for the scattering of neutrinos and antineutrinos by electrons (or by partons), that follow simply from assuming a nonderivative point interaction and Born approximation. In effect, the y-dependences of the sum and difference of neutrino and antineutrino cross sections are restricted to the following forms

$$\sigma(\nu) + \sigma(\bar{\nu}) = Ay^2 + B(2-y)^2$$
$$\sigma(\nu) - \sigma(\bar{\nu}) = Cy(2-y)$$

These relations are already known in some particular cases, as results of explicit calculations, but a derivation from simple general considerations has now been given. These relations include the usual parton-model results for the y-dependence in deep inelastic neutral current interactions. There are some simple extensions to charged current interactions. The final neutrino need not be identical with the initial.

Similar results can be derived for an arbitrary target, that need not be pointlike but remains unexcited, provided locality is assumed at the neutrino vertex. The relations also hold when the target is excited, if the final neutrino differs at most by helicity flip from the incident neutrino, and if the part of the interaction that flips neutrino helicity is C- or P-invariant. On the other hand, to relate the y-distributions in any scattering from a non pointlike target, one must assume the absence of a mass-scale.

Weak neutral current effects in e^+e^- annihilation

In e^+e^- annihilation processes, the interference between the electromagnetic current and any other neutral currents present provides useful information about the structure of the latter. For example, the interference term is either independent of or quadratically dependent on $e^\pm$ transverse polarization for V or A currents, but is linearly dependent for S, P or T currents. The information in the interference term has been analyzed for inclusive and exclusive channels of the following kinds, $e^+e^- \rightarrow hX$, $e^+e^- \rightarrow h_1h_2X$, $e^+e^- \rightarrow \pi^+\pi^-$, $e^+e^- \rightarrow \pi^+\pi^-\pi^0$, including possible spin determinations for final hadron h.

With a future machine of centre-of-mass energy about 30 GeV, the inclusive channels would be sensitive to neutral weak currents of the same strength as the charged currents, but the exclusive channels would require much stronger neutral currents for measurable effects.

Large transverse momentum phenomena

This subject has great interest. Hadronic inclusive cross sections of large transverse momentum p_T are much larger than expected from an extrapolation of small p_T behaviour. This may be a consequence of the scattering of a single constituent of one hadron on a single constituent of the other; indeed, new azimuthal correlation data strongly supports this picture. However, at a more quantitative level the theoretical situation is confused. In particular, the measured particle ratios are difficult to understand, and rapidity correlation data has no simple interpretation yet. New pion beam data too is hard to reconcile with simple models.

Among other investigations, wide angle amplitudes involving a reggeon have been studied in constituent and field theory models; the usual form of scaling law is found. The large p_T exclusive photoproduction cross section has been estimated, using local duality and a quark model for the inclusive process; surprisingly good agreement with data is found. High energy photoproduction of heavy muon pairs has been calculated in the parton model, yielding a Drell-Yan type of factorization; this offers a new parton-model test, but the cross-section is very small. Inclusive baryon production at large p_T has been studied, assuming a multiple quark scattering mechanism; the results agree with the experimental scaling law, and also offer an explanation of nuclear target effects. A phenomenological study has been made of large p_T spectra and particle ratios: the significance of the away-side rapidity distributions has been discussed.

Meson resonances

A useful by-product of the new ψ-phenomena is the study of familiar hadrons in novel situations. For example, the decay $\psi' \rightarrow \psi\pi\pi$ affords an exceptionally pure sample of I = 0 S-wave dipion production: experiment shows a marked depletion of events at small dipion mass. This effect is readily explained, not only here but also in processes like $\pi N \rightarrow \pi\pi N$ near threshold, by the on-shell appearance of the Adler zero. The zero position varies from reaction to reaction, so there is no scope for inferring $\pi\pi$ phase shifts, but the appearance of the zero underlines the relevance of PCAC for low-momentum pion physics.

The apparent new extension of the meson spectrum also lends urgency to understanding the older meson families. There has been work on two problem families of the old SU(3) quark model, the 0^{++} scalars and the 1^{++} axial vector mesons. For the scalars, the main problem was the apparent superfluity of I = 0 candidates, S*, ϵ, ϵ', but the possibility of a conventional quark model interpretation has now been demonstrated. It is important to pursue further experimental checks, however, since this is a likely channel in which to look for additional exotic configurations, if they exist. For the 1^{++} family, the long-standing problem has been to determine whether the apparent candidates A_1, Q, etc. are in fact resonances. A particular resonance interpretation of A_1 in 3π production was pursued and shown to necessitate companion resonances in other partial waves, including a π'. There are indications of an analogous effect in $K\pi\pi$ production.

Geometrical scaling of the Pomeron

Geometrical scaling (GS) is a very simple property, conjectured to hold for high energy elastic scattering amplitudes, whereby changes with energy simply take the form of changes in radial scale. Experimentally it holds approximately for pp, πp and Kp scattering data, at least above 100 GeV, but its origins and implications are not yet fully understood. GS seems to be a property of the Pomeron amplitude (i.e. diffraction), not of Regge pole exchanges. This makes ϕN scattering an interesting case to study, because here Regge pole exchanges are forbidden and the Pomeron should dominate at relatively low energies. It turns out that the ϕN data obeys GS even at 4 GeV.

GS also has interesting consequences for the real part of the Pomeron amplitude, that is determined at high energy by the energy-dependence of the dominant imaginary part. GS correlates the energy-dependences at different momentum transfers t, and hence predicts the t-dependence of the real part.

Each elastic scattering channel obeys GS in a different way, with a different dependence of opacity on radius. The intriguing possibility exists that, with some suitable rescaling of opacity, all channels may be described by a single universal function. New Fermilab data gives encouraging indications that all channels may indeed be described by a universal eikonal function, with appropriate opacity and radial scales. Furthermore, the relative eikonal strengths in the different channels are roughly in accord with the quark model, suggesting that these systematics are not accidental.

Unitarity and duality in hadron physics; multiparticle phenomena

Unitarity and duality form the basis of a general framework for understanding hadron collisions which has been developed at the Rutherford Laboratory, and early successes of this approach were described in last year's report. Starting from dual amplitudes containing proper reggeons, a Pomeron singularity is automatically generated. Both the reggeon and Pomeron trajectories have to satisfy certain consistency conditions which can be formulated as integral equations. Solving these equations yields values for parameters such as the Pomeron intercept and slope and the triple-range coupling, all of which are in semi-quantitative agreement with experiment. The Pomeron couplings to external states are predicted to be proportional to those of the reggeons. The proportionality factor is also calculated and the prediction is subjected to some quite stringent phenomenological tests which find the factor close to the calculated value. The extension of similar considerations to production reactions leads to the two-component model at moderate energies. The non-diffractive component proceeds via a definite production mechanism of resonant clusters which in principle allows the calculation of all exclusive and inclusive cross-sections. A first crude attempt assuming isotropic cluster decays already yields semi-inclusive correlation functions in good agreement with experiment.

The solution of the integral equations involved in the reggeon bootstrap is generally complicated, but an important practical break-through results from invoking a one-dimensional approximation of the scattering situation. In this way the Pomeron can be examined analytically in the dual unitary scheme and one can inspect explicitly the properties of the Pomeron, e.g. SU(3) breaking, in the scheme. Despite the crudeness of the approximation, the prediction for the size of the reggeon promotion of the trajectory is correct. The approximation has proved very useful in allowing calculations of non-planar quark duality graphs. The famous but empirical Zweig-rule suppression, which supposedly explains the narrowness of the ψ and ψ' particles can be given a fundamental basis by calculating these non-planar contributions, which are topologically identical to those involved in calculating the Pomeron singularity. There turn out to be three types of Zweig-violating decay graphs whose different topologies neatly explain the systematics of different exclusive decay rates of the new particles.

Studies of particular problems, such as the analytic properties of reggeon-reggeon scattering, which have direct relevance to the dual unitarisation scheme, have continued. Semi-local duality for the reggeon-reggeon amplitude has been checked against data on quasi-three body production processes and gives a reasonable average description of the data.

In a given energy region, it may be assumed that of the many loop diagrams which build up the Pomeron singularity, just one dominates. This 'local loop dominance' gives SU(N) symmetry for couplings, Gell-Mann Okubo mass formulae and exchange degeneracy for trajectories. The crossing and factorisation properties of the Pomeron can also be studied in this one-loop approximation. The loop which involves the exchange of a baryon is found to be important at low energies and provides a natural explanation of the differences at these energies of meson-baryon and baryon-baryon processes.

The dual unitarity equation, with some approximations, can be treated as an equation involving the n-particle cross-sections. Comparing with data on multiplicities constrains the reggeon intercept close to 0·5.

Diffraction has continued to be studied from the phenomenological viewpoint; there is particular interest in double-Pomeron exchange processes and what additional information can be gleaned from experiments set up to search for this mechanism.

One highlight of the year, in the multiparticle field, was the VIth International Colloquium on Multiparticle Processes, organised by the Rutherford Laboratory and held in Oxford in July. The recent work of the group was among the topics discussed by participants who had come from about twenty countries.

Vacuum Polarisation in Strong Potentials

Studies have continued of the properties of lepton bound states and vacuum polarisation in strong short range potentials, in particular the phenomena associated with the critical potential at which bound states are drawn into the negative energy continuum. This is an area of quantum electrodynamics for which normal perturbation theory techniques cannot be used, but in which the induced charge distribution can be determined by computer summations over the perturbed continuum levels. Further work has been carried out on the replacement of this summation by a Green's function contour integral which allows more rapid convergence, and on the renormalisation of the first order quadratic divergence using a subtraction technique similar to that commonly adopted for the Coulomb potential.

Application of the results to elementary particle models has proceded along two lines. The first arises from the fact that a short range critical potential has the unique capability of producing a lepton bound state localised to sub-hadronic dimensions. The hypothesis that hadronic weak interactions involve such localised lepton states would thus necessitate the existence of critical potentials within the parton constituents, which in turn leads to a contribution to electron-hadron scattering, and hadron pair production, initially of the form $137q^2a^2$ (momentum transfer q, potential range a) and should thus be observable as a rising component of the cross section. The second topic concerns the necessity to redefine the vacuum by one unit of charge when the critical potential value is reached; computations have been initiated to determine the observable properties of the wavepacket which results when such a redefined vacuum state is re-expanded in terms of the normal zero-potential vacuum state, to test the hypothesis that such transitions might be involved in, or responsible for, the known charge-changing weak leptonic currents.

1.4 Instrumentation and Data Handling

Particle Physics research demands a continual supply of new and specially-designed equipment, apparatus and materials to satisfy the individual requirements of experiments, and the Rutherford Laboratory provides the specialist skills to answer the needs of experimental groups working both at the Laboratory itself and at other research centres.

Besides meeting the immediate requirements of Particle Physics research, these projects can also lead to important applications in other research areas and provide additional impetus for development work in industry.

Data Handling

The operating system developed in the Laboratory for data acquisition using the DDP516 computer has now been installed in the computers used for Nimrod experiments studying πN interactions (e.g. Experiment 12) and is currently being installed in a very demanding charged hyperon experiment at the CERN SPS (Experiment 39). The important contribution made by this operating system towards simplifying the adaption of these computers to new experiments has led to the development of a real-time operating system for the GEC 4080 computer. This system called RUFUS (Rutherford 4080 User System) forms the basis of the software for a nuclear physics experiment studying X-rays from K-mesic atoms (Experiment 49) on Nimrod, the proposed experiment studying parity and time reversal invariance (Experiment 45) at ILL, Grenoble, and the control computer on the new Nimrod injector (Section 6.1.3).

Additional work on small computers has included the provision of utility programs for the GEC 4080, a general study of hardware and software features needed in experimental and control application and an investigation of high level programming techniques.

The problems of track recognition and background rejection, common to all high-energy physics experiments, are being studied. Track-finding algorithms have been written for the RMS project (Experiment 20) where large volumes of data are expected, and particular emphasis has been placed on speed of execution. The elimination of unwanted backgrounds has traditionally been achieved for counter experiments by the application of mass cuts. However, extra information, such as time of flight, pulse height and vertex position, is often available. For the experiment at the CERN PS studying $\bar{p}p$ interactions (Experiment 2) background rejection has been improved by a factor of two by adopting an approach in which additional quantities are included in a constrained kinematic fit.

Detector Development for the Charged Hyperon Experiment (Experiment 39)

Transition Radiation Detectors

In preparation for the SPS Hyperon Experiment, a prototype lithium foil transition radiation detector was constructed. Techniques were developed for assembling the very soft, very reactive lithium foil (50 μm thick) into a stack of sheets each separated by 500 μm while preserving it from contact with the ambient air in which it oxidises in a matter of minutes. 1000 foils were assembled into 10 modules of 100, the spacing being obtained by corrugations pressed into the foil and the whole enclosed in an aluminium tank with a 50 m-thick beryllium window as a downstream window for transition radiation X-rays. The detector stack filled with helium gas was successfully used in a test carried out by members of the Hyperon collaboration.

Reflectors for Gas Cerenkov Counter

The gas Cerenkov counter for the Hyperon experiment requires a low-mass high-quality reflector for short wavelengths. This reflector was constructed in eight separate units, which when mounted onto a common frame can be adjusted to form the complete reflector. Each reflector unit consists of a honeycomb backing bonded together with epoxy resin, with a face of melinex which is aluminized to give the required reflectivity. This highly reflective aluminium surface is protected by a coating of magnesium fluoride. These reflectors have a mass of approximately 8 Kg/m^2 and reflectivities over the whole surface of 80%.

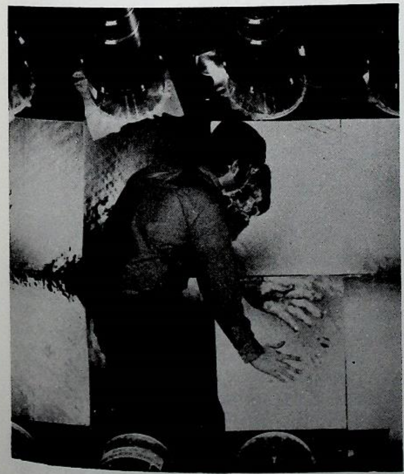

Figure 1.35 Low-mass reflecting surface (Photo: CERN)

Lead Glass Cerenkov Counter

This piece of equipment acts as an electron discriminator in the Hyperon experiment. The counter consists of three separate walls of lead glass each 1 m high, 2·55 m wide and 150 mm thick.

Thirty-four glass blocks make up each of the three modules, each block measuring 150 mm x 150 mm x 500 mm and weighing 46 Kg, giving a total weight of glass of 4692 Kg (4·7 tons). Each block has a 5″ Photomultiplier tube attached to one end and the blocks are packed together closely to achieve minimum clearance, presenting a solid wall of glass without gaps or structure to hold the blocks in place.

The three glass walls and their photomultipliers are housed in a large magnetic shield box.

The complete unit is supported at beam height by a frame which, with an associated extension trolley, will allow each module to be separately drawn out of the shield box for servicing. The modules move on stainless steel runners bearing on P.T.F.E. faced rails. This allows free movement of the units, while providing sufficient friction to inhibit unwanted movement. The shield box is maintained at a constant temperature by two air-conditioning units, and the temperatures of eighteen of the photomultipliers are monitored and recorded.

Laser Interferometer

An optical refractometer system has been developed for use on the Hyperon 300 Gas Cerenkov Counter, and provides a continuous measurement of the gas refractive index which can be fed into the data logging system.
A low power helium-neon laser is used to energise a Jamin type interferometer which is located inside the counter chamber. One light beam passes through the chamber gas, while the other one passes through an evacuated reference tube. The beams are recombined and the resulting fringe pattern is focussed onto an array of three phototransistors.

The centre phototransistor counts the number of fringes which pass while the outside pair determine the fringe shift direction. This information is continuously displayed on an 'up-down' counter.

Standardization is achieved by filling the reference tube with chamber gas such that both beams pass through similar paths, then setting the counter to zero.

As the reference tube is evacuated the fringe shift is counted, and the final value is digitally multiplied by a preset scale factor and directly displayed as a refractive index. Any subsequent fringe shift updates the fringe count so that a continuous reading is obtained.

The refractive index value is provided as an analogue signal suitable for a data logging system.

Noise pickup problems associated with the 'up-down' counter have been completely eliminated by choosing a CMOS logic system operating from an independent 15 volts supply. Optical couplers have been included in all the input and output lines to the counter, which is completely enclosed inside a copper box. Motorized needle valves control the filling and evacuation of the reference tube to enable remote controlled standardization to be carried out. This is done semi-automatically at approximately twelve hour intervals. The system uses a 900 mm reference tube, giving an overall resolution of approximately 3×10^{-7} in the value of (n - 1).

Rapid Cycling Vertex Detector Project (Experiment 19) – Wire Spark Chambers and Counters

For the Rapid Cycling Vertex Detector experiment to be mounted on Nimrod, the main trigger will consist of four low mass cylindrical spark chambers, and the pre-trigger of a scintillator array. This assembly including readout boards and thyratron pulsers will all be mounted on one support plate for easy installation and alignment. It will be positioned in the bore of a magnet having a field of about 2 Tesla, the spark chambers being concentric with the bubble chamber.

The cylindrical spark chambers which are of the capacitive readout type vary in size from 610 mm dia. x 725 mm active height to 916 mm x 1055 mm. Construction of the low mass spark chamber consists of a laminate of melinex/expanded polystyrene/"film-wire" formed into shells which are then spaced accurately apart by insulated rings to form the active gas filled gap. Both the readout wires and the H.V. cathode wires are of 70μ dia. Be/Cu with a pitch of 1·5 mm and run vertically, parallel to the chamber axis. Working voltage of the first chamber is approximately 3·4 KV.

Fourteen scintillator/lightguide assemblies constitute the pre-trigger array. The photomultipliers have to be mounted more than 1·2 metres above the top of the magnet so that they can work efficiently in the stray field of the magnet.

Multiwire Proportional Counters with one Vertical Minimum Mass Edge

Proportional counters with one vertical minimum mass edge and parallel anode and cathode wires have been built and tested in the Laboratory for an experimental team using Nimrod to study K-p elastic differential cross-sections (Experiment 9). It will operate as one of a pair used to identify forward scattered particles in the area of the main beam.

The counters have an active area of 300 mm x 300 mm with vertical sense cathode wires wound at 2 mm pitch. They are constructed by mounting the cathode wires and both planes of anode wires on 'C' shaped frames, all wires being parallel to each other. The wires were stretched between the two cantilevers formed by the frame which were prestressed to maintain wire tensions. The assembled frames were enclosed in a gas-tight polyester film hood, dry sealed to a common base which also supported the sense plane, the electronic amplifier system and carried the beam line assembly locations. Hence the only mass presented in the beam area was the anode, the cathode wires and two thicknesses of 0·05 mm polyester film. Subsequent testing has shown that these chambers have a 300 volt plateau when operating at 4·6 KV using a gas mixture of 15½% CO_2 0·3% Freon in Argon.

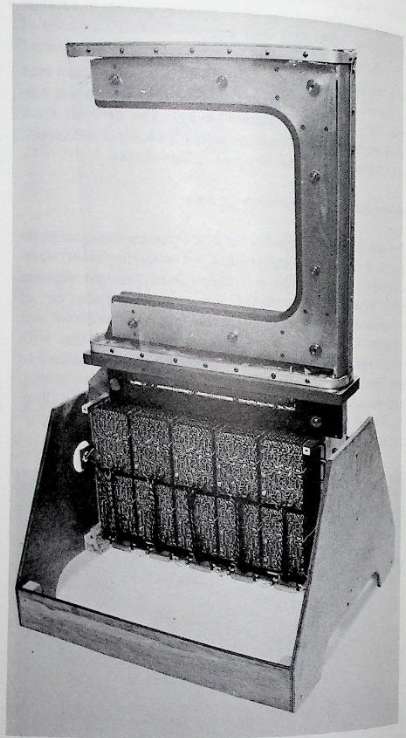

Figure 1.36 Proportional counter with one vertical minimum mass edge

Low-mass Capacitive Readout Wire Spark Chambers

The spark chambers constructed for the experiment studying polarisations in KN interactions (Experiment 13) are low-mass multigap type, on average 0·75 m square, with 50 gaps. The essential requirements in their construction were a low density active area (the density achieved per gap is 0·08 gm/cm²), wire positions known to within ± 0·25 mm and parallel gaps to ensure multispark efficiency.

The chambers consist of low mass laminates made from two layers of 5 mm thick expanded polystyrene bonded with a controlled amount of epoxy resin and with layers of film wire on the external faces which provide the H.T. or earth planes. The laminates are cured for 48 hours between flat plates to maintain flatness, which in most cases is better than 0·15 mm. The laminates are spaced apart with perspex frames which control the spark gap, and the whole stack is located by dowels to outer Al-alloy frames which form a protective cradle. From these outer frames a melinex gas-tight window allows for pressure equalisation preventing bowing of the outer laminates. The laminates and perspex frames are bonded together using silicone rubber which is applied in the form of a fillet with an embedded nylon cord. By pulling this cord, the fillet can be broken and the chamber easily dismantled.

To maintain the specified accuracies for both the construction and the alignment in the beam line, a film-wire gauge to monitor the standard of film-wire by checking straightness and pitch of wires was manufactured, together with a master jig which relates wire position and sense of beam centre and to the external datum on the chamber. All components had their datum references drilled or, in the case of film-wire, punched from this jig, resulting in a very accurate construction.

A beam line alignment jig was also made which again had its datum reference drilled from the 'masterjig' and enabled the spark chamber support structure to be accurately aligned.

X-Ray Imaging and Development Work on the X-ray Multiwire Proportional Counter (MWPC)

A study was made of the fundamental physical limits on the spatial resolution of a xenon-filled MWPC. The various interactions of the incident X-ray with the counter gas and the resulting spread in position at which the event was recorded was examined using a monte-carlo computer model. The calculations showed that in a narrow band of incident X-ray energy (40-45 keV) a xenon-filled MWPC at ambient pressure can give spatial resolution of the order of ·5mm fwhm but that at other energies the resolution deteriorates rapidly.

A specially-developed X-ray detector system has been used extensively during the past year to evaluate its potential in various fields of X-ray technology. Readout signals and picture can be displayed either in colour or black and white on a television screen, and pictures can be stored on disc and processed off-line using a variety of programs designed to extract more useful information from the raw data pictures. The equipment has been demonstrated to a wide audience and several applications have been suggested for possible evaluation. The system is currently being used to test its performance as a method of measuring bone density variation. Initial results look promising and it is hoped to carry out further clinical trials in collaboration with staff from Leeds General Infirmary.

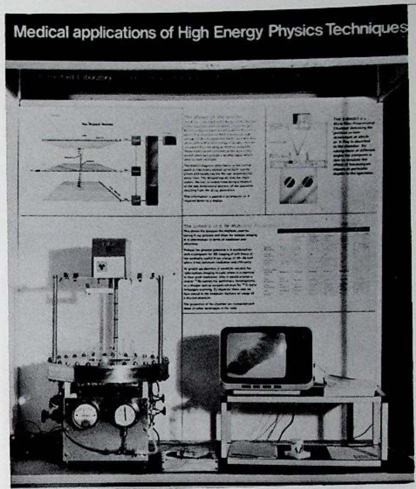

Figure 1.37 Demonstration of X-ray Multiwire Proportional Counter mounted at Royal Society

Channel Plate Electron Multipliers

Tests have recently been completed on a new photomultiplier utilising channel plate electron multipliers as the gain producing elements. With a charge gain of $\sim 10^7$ this device showed two particularly attractive features for applications in high-energy physics, namely a very short transit time (5 ns) and the ability to operate in magnetic fields as high as 1 Tesla without screening. It is only some 50 mm long and, because of the absence of magnetic screening, very light. The tube is as fast as a conventional linear focussed device, having an anode pulse rate time of the order of 2ns.

Beam Current Monitor for Nimrod 70 MeV Injector

The design and manufacture of all the equipment for this system is now complete. Tests on the operation of the various elements, current transformers, signal processing electronics, control stations, etc, have been carried out both on individual elements and on a simulated system connected up under laboratory conditions. All the performance specifications previously reported were achieved and the system has now been installed in the accelerator complex. Commissioning will continue as the new accelerator system is progressively brought into operation.

Drift Chambers

In the course of the present year drift chambers based on previous prototype designs have been built and operated successfully in the meson production experiment at the

Rutherford Laboratory (Experiment 3) and further chambers are now being assembled for an experiment at the Fermi Laboratory in the US. The first drift chamber made at Rutherford and designed to operate in magnetic fields is now being installed and tested in an M3 magnet for use in the CP-violation experiment scheduled for 1976.

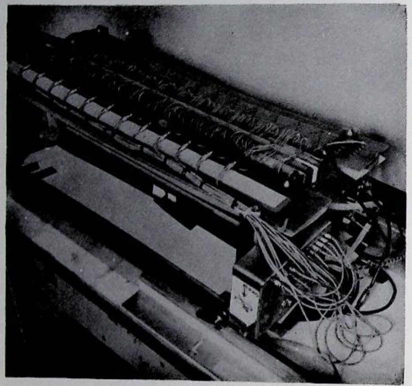

Figure 1.38 Drift chamber development

Testing Multi-wire Proportional Chambers by Glow Discharge Photographic Techniques

A method of testing multiwire proportional chambers by glow discharge and photographic techniques has been evolved principally to enable faults on large chambers to be identified quickly and positively.

The chambers are filled with high purity nitrogen and subjected to a current of about 300 μA. After dark adaptation a glow discharge can be seen. Analysis of this discharge reveals faults such as slack or open circuit wires, contamination and misalignment of planes.

Gas Monitor for Multi-Wire Proportional Chambers

A single wire proportional chamber has been constructed for use as a gas monitor to detect changes in the "magic gas" used in multiwire proportional chambers (MWPCs).

The unit has a rapid response so that it is able to detect changes in the gas long before the changes affect the MWPCs and the amplitude of the output pulse is such that it may be used to drive standard UKAEA 2000 series electronic units.

The unit is used in conjunction with a discriminator and a ratemaker to give an output which varies in count rate with changes in the gas mixture.

'Film-Wire' Technology

In order to construct spark chambers, a means has been found whereby Be/Cu wire 0·075 mm diameter can be bonded down on polyester (melinex) film at an accurate pitch of 1 mm in such a way that the top of the wire is conducting. Large areas of this 'film-wire' can be produced in sheets up to 1·5 m wide and 8 m long. Both the diameter of the wires and the pitch at which they are laid down can be varied. Some spark chambers are required to be flat with no frames to give maximum useful active area while some chambers need to be cylindrical. On both flat and cylindrical chambers some planes of wires need to be at an angle to their neighbours. This film-wire is then bonded down to low mass material of the shape required for the spark chamber.

It is now possible to make chambers with each wire running continuously to the outside and by manipulating the film-wire, remote readout is possible without the need for any soldered joint other than the last connection. It is also possible to bond a second polyester film on top of the wire so that the wires are now completely insulated.

Many thousands of wires can be connected to the spark chambers in a form where the film-wire is cut into strips about 25 mm wide and bunched together.

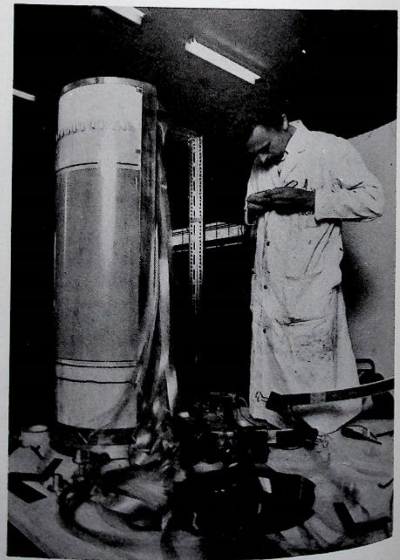

Figure 1.39 Working with Film-Wire

Low Mass Structures for Spark Chambers

The construction of spark chambers currently being designed requires that they should be built from a structural material of minimum mass and radiation length, and at the same time be dimensionally stable and accurate over a long period. It is also essential that the structures should be easily made by normal workshop processes. The best material appears to be ordinary expanded polystyrene, which can be purchased in various thicknesses enabling laminated sheets to be made up by sticking together multiple thicknesses using epoxy resin.

For flat sheets this is a simple process, resulting in flat stable sheets of low mass material more stable and rigid than the same thickness of expanded polystyrene. Cylinders can be made by wrapping the thin polystyrene round a former and sticking it with epoxy resin. This can be machined very accurately using a coarse grinding wheel running at a high speed. A number of flat and cylindrical chambers have been constructed and tested successfully.

Electronics Development

Many thousands of channels of multi-wire proportional counter (MWPC) read-out electronics have been commissioned during the year. The smooth progress of this work has been due largely to the success of a hybrid circuit amplifier-shaper developed in a collaboration between the Laboratory and an industrial firm. The read-out systems have been designed taking account of the part played by MWPC signals in forming event triggers. Two systems of particle multiplicity detectors, with different degrees of flexibility have been developed.

The system developed for data acquisition and control on the 70 MeV Nimrod Injector has been manufactured, tested and installed. It comprises over 100 instrumentation amplifiers and a CAMAC computer system including analogue to digital converters, input modules, output modules and an autonomous program controller. The CAMAC system occupies six crates.

Two NMR spectrometers have been constructed to measure both proton and deuteron polarization. Since the deuteron spectrum is relatively wide, the spectrometers have been designed to tune the coils automatically as the frequency is swept. This will improve the base line shift and simplify the measurement of the small deuteron signal. A signal enhancer will be used to improve the signal to noise ratio.

Signal enhancers of this type could be used in many applications involving the detection of repetitive signals immersed in incoherent noise or interference. These include vibration analysis in complex structures, bio-medical signal analysis, spectroscopy, oceanographic echo sounding, seismic exploration and ultrasonic flaw detection.

In addition to these completed projects, development continues in the fields of special purpose computing hardware, drift chamber electronics, precision TV camera applications, beam profile monitoring electronics and special instruments. These include a magnetic tape drive controller, a beam spill time monitor and a special display scaler.

Electronics Services

Design and Manufacture. During the year, 54 new designs of printed circuit boards were produced with a continuing trend to larger boards with greater circuit complexity. Manufacturing work was completed to the value of £250,000. Over 50% of this work was done by outside contractors and the internal effort totalled 32,000 man hours.

Electronics Servicing. The Instrument Repair Section handled over 2,800 commercial instruments for repair and calibration. After initial diagnosis about 40% of this total was handled by specialist outside firms. The high cost of replacement instruments has increased the need to make major repairs to many of the old instruments existing in the laboratory.

The large amount of electronic equipment manufactured during the year for high-energy physics experiments has sustained a heavy load of testing and commissioning. In particular considerable effort has been devoted to setting up electronic systems in the various beam lines.

Track Analysis Machine Support. Operational improvements to the 30 scanning and digitising machines has continued and a BESSY machine (a scanning and measuring table for film from the new large bubble chambers) has been commissioned successfully connected on line to an IBM 1130 computer. Design work is completed to enable other machines to be modified to handle the 70 mm film due from the Big European Bubble Chamber (BEBC) next year. This work includes a design study for a low cost, locally made scanning and digitising table to provide 17- and 30- times magnification using parts of obsolete machines.

1.5 Radiological Experiments

Negative pions offer advantages over the usual γ-ray treatment because being heavy charged particles they can penetrate deep to a target volume and deposit much of their kinetic energy in a stopping region. They are absorbed there – causing further local ionization to be deposited by fragments of atomic nuclei shattered by the liberation of the pions' rest mass.

The result is a variation of dose with depth such that an initial flat region, 'the plateau', is followed by a high dose region, 'the peak'. Beyond the peak the dose falls rapidly to a low value. The biological damage is further enhanced at the peak because the nuclei fragments are densely ionizing and more efficient than fast particles.

The inverse ratio of the required doses of two specified radiations at the same dose rate, one of which is a reference radiation, usually γ-rays, to produce equal damage is known as their Relative Biological Effectiveness (RBE). Further, the absence of oxygen, as occurs in tumours with a poor blood supply, produces less radioresistance to the fragments than to γ-rays. The ratio of doses required to produce the same level of damage without and with oxygen is known as the Oxygen Enhancement Ratio (OER).

These RBE and OER parameters have been measured in bean roots and a programme is continuing to study effects on very sensitive *in vivo* systems of normal tissues in mice, on single cells, namely chromosome aberrations in white blood cells (lymphocytes) and on the reproductive capacity of cancer cells in culture.

The results show the expected behaviour in the bean roots and single cell systems but in the sensitive *in vivo* systems of normal tissues, little difference in response to pion radiation at peak or plateau has been detected, other than that due to an additional dose at the peak. The sensitive nature of those normal tissues studied at present may make the results not generally applicable to other normal tissues.

The study of other *in vivo* systems, including normal tissues as well as tumours will become possible when the new Nimrod injector enables a higher dose rate to be obtained. It is essential in this work to study the effectiveness of pions on tumour regression in relation to normal tissue damage.

EXPERIMENT 55

Chromosome Aberrations in White Blood Cells

National Radiological Protection Board; Rutherford Laboratory

A beam with a broadly-peaked dose region will be required for the irradiation of solid tumours. This may be achieved by combining pions of different energies and an experiment is under way to investigate the profile of biological damage in such a beam. Human blood samples have been irradiated in a water phantom along the axis of the beam generated by pions of 50, 64 and 80 MeV. A dose of 150 rads measured in the peak was delivered in 3 cycles of 3 energies and the blood samples are being analysed for chromosome damage to lymphocytes. The incomplete analysis has yielded aberration levels in the peak close to those expected from previous dose-response work and the levels are approximately constant over about 10 cm.

EXPERIMENT 56

Irradiation of Frozen Cancer Cells

Glasgow Institute of Radiotherapeutics; Rutherford Laboratory

The cells were frozen at liquid nitrogen temperatures to reduce biological and chemical activity, for in such a state there is little dose rate dependence. Following earlier work which determined the RBE for the pion beam at the peak position and for 14 MeV neutrons, further experiments have investigated the response of frozen Hela cells at other absorber depths at a number of beam positions. A specially-designed cell holder of much smaller volume was used to improve the resolution of this 'biological dosimetry' technique.

Preliminary results from this experiment indicate that the value of the RBE is 1·9 at the peak dose region falling to near unity elsewhere, except for an intermediate value near the surface.

EXPERIMENT 57

Irradiation of Cancer Cells at Room Temperature

Medical College of St. Bartholomew's Hospital

No irradiations were made during the year as a system of cultured cancer cells held in a gelatine matrix was being developed which will enable very detailed depth-damage and OER profiles to be obtained.

EXPERIMENT 58

π^- Irradiation of the Testis

Medical College of St. Bartholomew's Hospital

The survival of spermatogonial cells and the loss of testis weight are two further radiosensitive *in vivo* endpoints that have been measured using the π^- meson beam in the Barts programme. Mice were irradiated in the testes area whilst breathing either air or 10% oxygen in nitrogen.

Testis Weight. Groups of six mice were irradiated for each dose, gas and position, with one mouse in the peak dose area simultaneously with one in the plateau area. 28 days later their testes were removed, weighed and compared to those of control animals. Figure 1.40 shows the air and 10% oxygen points for peak and plateau π^- doses at about 100 rad h^{-1}; the dashed lines are fitted to similar weight loss data following doses of 14 MeV electrons at 400 rad sec^{-1}.

The oxygen enhancement ratio (OER) for the electron data is ~ 1·6 and that for π^- mesons is ~ 1·0. For π^- mesons there is no difference in effectiveness of peak compared to plateau doses which is in agreement with the previous *in vivo* data. There appears to be a dose rate effect in that all the π^- points are displaced to the right of the air high dose rate electron points. This dose rate effect would mask any RBE effect between pions and electrons and it will therefore be necessary to obtain comparable low dose rate γ or X-ray curves for testis weight loss before more can be said about the RBE of π^- mesons compared with more conventional radiations.

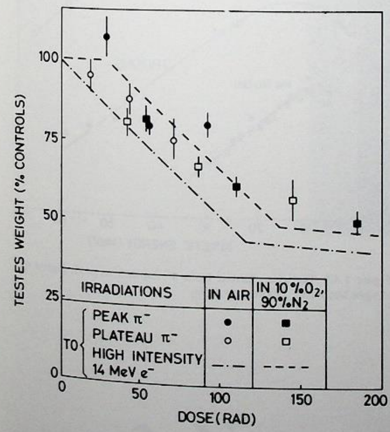

Figure 1.40 Response of mice testes weight. (Experiment 58)

Spermatogonial Survival. Groups of four mice were irradiated as for the testis weight experiment, and ninety hours later their testes were removed, fixed, sectioned and stained. Stage VIII tubules were examined for resting primary and pre-leptotene spermatocytes in both irradiated and sham irradiated mice. At the time of irradiation the primary spermatocytes counted were present as late type A or early intermediate spermatogonia. The experiment therefore examines the ability of irradiated spermatogonia to divide twice and produce in ninety hours primary spermatocytes, assuming there is no radiation induced prolongation of the cell cycle.

Figure 1.41 shows the peak and plateau spermatogonial survival data plotted for a range of π^- meson doses together with data for mice given external Cobalt-60 γ-rays at 6 rad min^{-1}. The OER for π^- mesons is ~ 1 and there is no difference in the effectiveness of peak compared to plateau doses and the RBE for π^- mesons relative to ^{60}Co γ-rays at a comparable dose rate is also ~ 1.

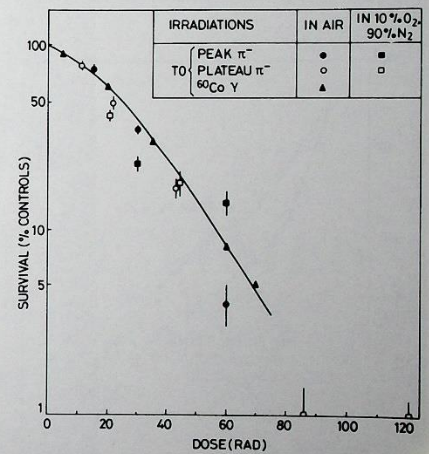

Figure 1.41 Spermatogonial survival. (Experiment 58)

EXPERIMENT 59

Study of the Physical Nature of π^- Induced Radiation

Medical College of St. Bartholomew's Hospital; Leeds University; Rutherford Laboratory

Though it has been known for a long time that negative pions produce nuclear disintegrations, the nature of the reaction and the products are not all well known. In these experiments the products and resultant ionization are being studied as a function of absorber composition and depth using ion chambers, proportional chambers, photographic emulsions, silicon detectors and counter telescopes. This will enable models of biological action to be compared to our data.

Ionization Event Size Spectra

A spherical Rossi proportional counter has been used to obtain ionization event size spectra in different positions over the pion depth-dose profile. This chamber has a sensitive volume of diameter 1·27 cm, however, when filled with a tissue equivalent gas mixture at reduced pressure, ~ 50 torr, it produces an effective sphere diamater of 1μ m, which is of the order of cell dimensions. The instrument is calibrated in terms of event size by means of an internal α-emitter, ^{244}Cm.

Some initial experimental data for peak and plateau positions with the chamber immersed in a water phantom is shown in Figure 1.42. This data indicates that the number of strongly ionizing events (>10 keV/μm) in the peak dose area is greater, by a factor of about 5, than the number in the plateau.

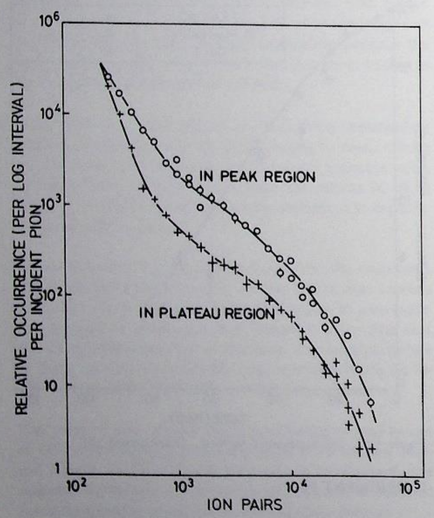

Figure 1.42 Ionisation observed in equivalent of ~1μm sphere of tissue. (Experiment 59)

Pending the development of a constant pressure flow gas rig it is hoped to obtain further event size data with a small parallel plate proportional chamber. This chamber offers the advantage of being able to observe the radiation field over much smaller actual volumes than the spherical chamber.

Charged Particle Spectra

Particles emitted following π^- capture at the ionization peak in oxygen, Tissue Equivalent Liquid and Simulated Bone, and from carbon at peak and plateau, were identified and measured by a counter telescope in a vacuum. This comprised one of several totally depleted Si specific ionization detectors of various thicknesses, and a thick Si detector or CsI (Tl) scintillation counter measuring residual energy.

Preliminary spectra for protons, deuterons, tritons and He nuclei are given in Figure 1.43 for stopping pions in Oxygen (thick water absorber in a 12·5 μm mylar walled container). This data will be normalised to and compared with carbon data and that of the other materials. Li nuclei spectra will also be derived from existing data.

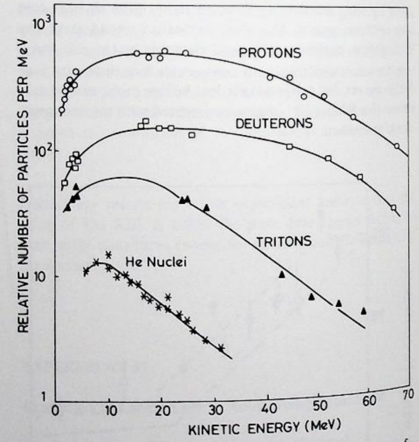

Figure 1.43 Particles emitted from π^- capture in peak region of oxygen absorber. (Experiment 59)

2. Neutron Beam Research

View of a neutron collimator

2. Neutron Beam Research

The Neutron Beam Research Unit (NBRU) has responsibility for neutron beam activities in the Laboratory, and the year's work has covered three main areas: neutron source and instrumentation studies and development; support for the large UK community of neutron beam users, both at home and abroad; and participation and collaboration in neutron beam science projects.

On the instrumentation development front, a highlight in the Rutherford Laboratory context has been the successful adaptation for neutron beam purposes of foil-stretching techniques which were perfected some years ago in the Laboratory for the construction of lightweight mirrors and spark chamber electrodes. Neutron collimators some 10% more efficient than the best previously-reported devices (and much better than many collimators actually in service at the present time) are now being routinely produced for a number of reactor centres. Related thin film techniques are also being used for the production of efficient neutron polarizing devices.

Another area in which the resources and expertise of the Rutherford Laboratory have proved invaluable is future source studies. It is now widely accepted that pulsed accelerator systems will provide the most realistic route to meeting scientific needs in the 1980s, and the NBRU in its ongoing programme of work on future sources has concentrated its attention on various accelerator options. It has become apparent that a potentially world leading source could be provided using some of the resources available at the Laboratory, a feasible design for a new proton synchrotron which could be used for neutron production has been drawn up by a Laboratory accelerator team. The proposal is described in detail in Section 6.2.

As in previous years, a significant proportion of the NBRU effort has been devoted to support of the UK neutron beam programme, in which over 270 university staff, research associates and research students are involved in projects on reactors in the UK, at the Institut Laue-Langevin (ILL), Grenoble and occasionally at Risö in Denmark and Chalk River in Canada; over 170 visits have been arranged to ILL alone. In addition the NBRU has continued in collaboration with the Atomic Energy Research Establishment (AERE), Harwell and with university staff in the development of improved neutron scattering methods, both at reactors and at the Harwell linac.

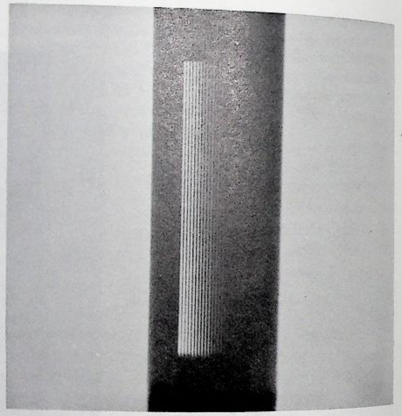

Figure 2.1 An example of the excellent collimation of thermal neutron beams which can be achieved using the stretched film technique. The extreme left-hand slot of the collimator was lined with the centre of a 2·5 cm diameter neutron beam at a distance of 4m. Blades in direct line with the neutron beam at the left-hand side of the collimator are seen in sharp focus but, with the increasing angular divergence of the beam as successive blades become further off-centre, increasing absorption is seen until no neutrons at all are transmitted through the right-hand side.

2.1 Neutron Beam Instrumentation

Neutron Collimators

A method for the construction of neutron collimators from stretched plastic film has been developed, and has already been used for production of nearly twenty collimators, with further orders in hand. The technique derives from experience at the Rutherford Laboratory in stretching aluminised Melinex films to make lightweight mirrors and spark chamber electrodes for High Energy Physics experiments.

The basic principle for neutron work is that of the Soller collimator which consists of a set of equidistant and parallel plates which absorbs neutrons, thereby restricting the divergence of the transmitted neutron beam to a fraction of a degree. Excellent results have been achieved using stretched Melinex film coated on each side with a paint loaded with gadolinium oxide to form an efficient absorber for neutrons incident at glancing angles. The gaps between films can be as small as ½ mm yielding a short compact collimator. Beam divergences down to 10 arc minutes are easily attained, with beam obscuration no more than about 5%. Figure 2.1 shows details of construction and performance. By the end of the year, 18 collimators had been supplied to ILL and several more were on order, including a set for use on the AERE Harwell reactors. Others are being designed for use at reactors in Denmark and Sweden.

Neutron Guides

The prototype neutron beam "bender" was successfully tested at DIDO, Harwell, in December 1974. A transmission efficiency of 0·4 at a wavelength of 12 Å was measured which compares to a theoretical value of 0·56 obtained from a computer model of the system. The measurement was repeated seven months later and the same result, within experimental error (± 10%) was obtained, showing that the properties of the device had not changed in a normal laboratory environment. The prototype device consists of 11 Melinex foils, 0·025 mm thick, coated with copper on both sides, spaced by 0·25 mm and curved to a radius of 1880 mm. This produces a deflection of 5° in a length of 160 cm. Methods of assembling more films at a faster rate are now being developed.

Because of the special problems and techniques required to deposit metal films on thin plastic substrates, both for the bender work and for the work on polarizers for long wavelength neutrons to be described later, a vacuum deposition facility has been assembled and is now in operation.

Some tests have been carried out on stretched Melinex films to see how the surface wavyness might change at elevated or reduced temperatures. The conclusion was that the films for benders or collimators will not be adversely affected at temperatures below − 10°C and 35°C.

Work on the development of position sensitive detectors (PSDs) has continued through the year. The manufacture of PSDs based on channel electron multiplier plates is being carried out by an external firm, and a 90-channel linear PSD with a very compact ceramic vacuum envelope is in the final stages of manufacture. Work is continuing on the manufacture of a 60 x 60 channel area PSD with a positional resolution (in the detector itself) of 0·75 mm. Methods of optically coupling the lithium loaded glass scintillator to the channel plate detector are being studied — especially methods of "demagnification", ie coupling a scintillator assembly with moderate spatial resolution (say 3–5 mm) to the detector which has an inherently high resolution (a fraction of a mm). For the linear detector, a stack of tapered light guides has been made to couple a stack of scintillators, each one 3 mm wide, to the detector module which has a resolution of 1 mm. Aluminised Melinex is used to form the reflecting walls of 92 tapered light guides of rectangular cross-section. Measurements of the transmission efficiency have been made of light from a scintillator irradiated at the wide end and detected at the narrow end by a photomultiplier.

A common feature of all the detectors under study is the use of lithium loaded glass scintillator. This material has excellent properties but is sensitive to γ-radiation. A study has been made of an old idea for γ rejection which makes use of the fact that the output pulses due to γ-rays are smaller and shorter than those from neutrons — the so called "pulse shape discrimination" technique. Using modern fast electronics, this has proved to be a quite satisfactory technique and will be utilised for PSDs.

Another development has been the demonstration of coincidence techniques in neutron counting to reduce detector noise. The use of the glass scintillator, which is transparent to its own output light, means that a scintillation event can be used to stimulate a channel in a PSD and a separate photomultiplier, the latter being common to all channels. Only pulses from a PSD channel which are coincident with one from the photomultiplier are accepted, thus greatly reducing the output pulse rate due to detector noise. In addition, the γ discrimination technique previously described can be applied to the photomultiplier only and is not needed on each PSD channel, thus reducing the quantity of electronic hardware required. These techniques are applicable to both linear and area PSDs.

Arising out of the study of optical coupling methods is an alternative way of using scintillators in large size PSDs of moderate resolution. It has been found that the light output from a small piece of scintillator can be transmitted down a flexible light guide with adequate efficiency to "drive" a photomultiplier. Furthermore it is possible to operate two photomultipliers from the same scintillation event by using two separate light guides coupled to the same piece of scintillator. This enables a coding system to be arranged. As a simple example consider three photomultipliers appropriately coupled by light guides to seven pieces of scintillator (either in a linear or area array). A scintillation event in one piece will trigger a unique combination of photomultipliers – a "signature" which can be decoded easily using modern electronics. Preliminary measurements have been encouraging and a 100 channel linear array with 3 mm resolution is being assembled as a prototype detector. Combined with the γ discrimination and coincidence techniques described above, this promises to be a very effective PSD.

Polarizing Filters

The polarizing filter containing polarized ^{149}Sm nuclei is undergoing the final stages of its commissioning. $^{149}Sm^{3+}$ ions are introduced as the dope into a deuterated cerous magnesium nitrate single crystal (CSMN), and following an extensive theoretical analysis of the heat transfer problem in the crystal, it has now been decided to place this filter in the ^3He dilute phase of the dilution unit mixing chamber. The dilution refrigerator has now operated at a stable temperature of 17 mK (measured by nuclear orientation of ^{60}Co), and the main outstanding problem is to correlate the nuclear orientation temperature with that given by the magnetic susceptibility of CMN, which will be the standard thermometer used on the dilution refrigerator. The current plans are to test the polarizing property of the CSMN filter during the first part of 1976, and to examine the performance of a metallic ferromagnetic material, $Sm_{.04}Pr_{.96}Al_2$. The eventual aim is to use the polarizing filter as the spin analyser of scattered beams at neutron wavelengths $\lambda \sim 1$ Å in polarization analysis experiments. Figure 2.2 shows a view of the filter container attached to the dilution unit.

Polarizing Mirrors

Further investigations have been made of the method of polarizing long wavelength neutron beams ($\lambda \gtrsim 5$ Å) by total reflection from magnetized thin films of cobalt:iron evaporated onto various plastic substrates. In the initial measurements, carried out at ILL, specular reflection of the unwanted spin-down neutrons was observed from the substrate surfaces at (glancing angle (θ)/wavelength (λ)) values ~ 1 mrad Å^{-1}. To reduce these reflections the use of (CH_2) substrates such as polypropylene and polymethylpentene (TPX), which should be non-reflecting for the spin-down neutrons, has been investigated and a decrease in polarization (indicative of spin-down reflection) was observed at lower (θ/λ) values ($(\theta/\lambda) \gtrsim 0{\cdot}5$ mrad Å^{-1}). An analysis of the results suggested that the spin-down reflections which occur at these small (θ/λ) values are due to the magnetic film being only 80% saturated in the applied magnetic fields used ($\sim 0{\cdot}14$ Tesla). A theoretical calculation showed that it should be possible to achieve nearly 100% polarization at (θ/λ) down to 0·1 mrad Å^{-1} by increasing the cobalt content of the magnetic film. Tests of this hypothesis have now been made and the results are being analysed. The objective of the work is to produce a multiple film polarizing device similar to the neutron beam bender previously described.

Figure 2.2. Polarizing filter attached to dilution unit mixing chamber.

Spin Flippers and Polarimeters for Long Wavelength Neutrons

Methods are being investigated for accurately measuring the polarization of long wavelength polarized beams, and on non-adiabatic spin-flippers for such beams where there is an appreciable wavelength spread. Design studies on a Stern-Gerlach polarimeter have been completed, and work on its construction is now commencing; it is hoped to carry out the first neutron experiments early in 1976. Flipping efficiency measurements on a Drabkin "two-coil" flipper and a Dabbs "current sheet" flipper have been performed at a wavelength of 1 Å. The Drabkin flipper gave flipping ratios greater than 120 for both Co:Fe and Heusler alloy spin analysers, which indicated that the flipping efficiency was 100% along the axis of the coils. The Dabbs foil also gave high flipping efficiencies (> 99%) in an optimized arrangement of the magnetic guide fields; however its performance depends critically on the interaction between the guide fields and the flipper fields.

Pressure Cells for Scattering Samples

Following considerable user interest in the possibilities of working with samples at high pressure, a survey has been made of the techniques used in the construction of pressure cells and the requirements of the users. The survey has been published as a Rutherford Laboratory Report RL-75-096. As a result of this work a proposal is to be presented to the Neutron Beam Research Committee (NBRC) of the Science Research Council for the construction of a "standard" cell which would satisfy the majority of the users' requirements and provide a useful start in a UK high pressure programme.

Pulsed Source Instrumentation

A cold moderator for the present AERE Harwell linac has been constructed. The moderator material is polythene maintained at a temperature of 77K inside an aluminium can which is itself inside an aluminium vacuum envelope. A transfer line is used to supply liquid nitrogen to the moderator from a dewar positioned outside the target cell. Thermal tests of the cooling capacity of the system are under way with an electrical heat input of 400 W, to simulate heating by the beam.

Close collaboration has been maintained throughout the year with AERE staff, both in the development of new instruments for the existing linac and in planning the target cell for the new linac. For example, NBRU staff have collaborated closely with AERE staff in the construction of the inelastic scattering test experiment (mentioned in the last report) which is now being commissioned. In this set-up the incident neutron energy is defined by a standard AERE mechanical chopper, appropriately phased with the linac pulses to yield a maximum transmission at a wavelength of 0·538 Å. With a distance of 5 m between the moderator and rotor an energy resolution of about 2·3% is obtained. The energy of the scattered neutrons is determined by time-of-flight of banks at ^3He detectors at mean angles of 5, 10 and 15° on an arc in the vertical plane. Consequently the elastic peaks will occur around momentum transfers of Q = 1, 2 and 3 Å^{-1} for this incident energy. In addition, a backward angle ($2\theta = 150°$) counter bank has been installed for measurements at large energy and momentum transfers.

Design Study for a Cold Source for the PLUTO Reactor

During the year, a feasibility study has been carried out for a new cold source for the PLUTO reactor at AERE, Harwell, following the recommendation of a number of NBRC working groups in 1974. A joint Rutherford Laboratory/AERE working group has prepared a costed proposal for a design using a supercritical hydrogen gas, at a temperature of approximately 25K, as the moderator fluid cooled by circulation through a "cold box" situated close to the reactor face. The cold box operates by expansion of high pressure gaseous helium through an expansion machine, helium compressors being situated outside the reactor shell. The source would be viewed from two sides. The total estimated cost is £800K at October 1975 prices.

Equipment for ILL

The polarized beam diffractometer, D3, (delivered to ILL in July 1974) was successfully commissioned and has been in routine service since March 1975. It has already collected data on ferric borate, ferrous phosphate $4H_2O$, cobalt fluoride under uniaxial pressure, uranium carbide, a series of Fe-V solid solutions in the composition range 5–22% vanadium and the intermetallic component Au_4V. In collaboration with ILL staff, some extensions have been made to the instrument software package and a set of programs have been written to enable further data processing and physics calculations to be carried out on the ILL PDP-10 central computer.

The split coil superconducting magnet for use on the D3 and D5 instruments was delivered and successfully commissioned at ILL. First tests on D5 will begin in January 1976 and the first experiment on D3 is scheduled for later that month. The NBRU has provided a fourth circle for D3 which will control the specimen rotation angle within the asymmetric Helmholtz magnet.

The diffuse scattering apparatus, D11B, which is being supplied to ILL was described in last year's report. The inbeam sections were delivered to ILL earlier in the year, and were installed during the October reactor shutdown. A view of the installed components is shown in Figure 2.3. The rotary table and five position cryo-sample changer are under test at the Rutherford Laboratory and are due to be delivered early in 1976, together with the safety alarm system developed at the Laboratory.

The NBRU is collaborating with ILL in the design and manufacture of an ultra-cold neutron (UCN) facility to be installed on an inclined beam hole. Preliminary designs and cost estimates have been prepared. The facility consists of a room temperature water convertor for neutrons which are

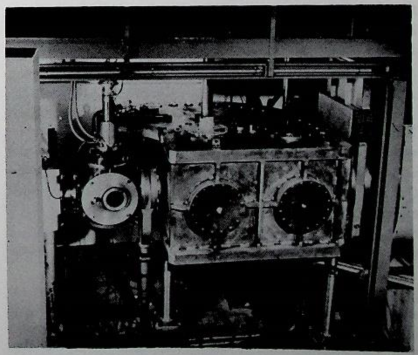

Figure 2.3 Diffuse scattering apparatus D11B after installation at ILL. Long wavelength neutrons enter from a neutron guide on the left, and the small angle scattering apparatus D11A carries on to the right.

transported up an inclined hole through a polished stainless steel guide tube. Outside the reactor the beam is brought into the horizontal plane by a curved glass guide tube (length 6 m radius of curvature 10 m). The latter is immersed, for shielding purposes, in a large tank containing 25 tons of water. The NBRU is investigating the manufacture of the in-pile part and vacuum equipment while ILL will probably make the curved guide tube, shield tank and support structure.

2.2 Future Source Studies

In its continuing study of future neutron sources the NBRU has concentrated its attention on pulsed accelerator-based systems as offering the most realistic route to meeting the scientific needs in the 1980s. A significant event during the year has been the approval for AERE Harwell to construct a new electron linac some ten times more powerful than the present facility. The NBRU are collaborating with University and AERE staff in specifying the scientific requirements for a viable thermal neutron scattering programme to be mounted at the new facility. In addition, attention has been given to the possibility of carrying out a feasibility study for a neutron booster which would increase the neutron output by a factor of about 20, enabling the source to be competitive with the highest flux reactors for many applications requiring epithermal neutrons.

It has also been recognized that a high repetition rate proton accelerator giving an even higher intensity could be built using state of the art technology (indeed such a project has been proposed at the Argonne National Laboratory). Preliminary designs have been prepared by the Rutherford Laboratory General Studies Division for a suitable synchrotron, and are described in detail in Section 6.2. The design would utilize various resources (buildings, accelerator components) which could be made available at the Laboratory. Since neutron intensities should be two orders of magnitude greater than the AERE linac, it is believed that this represents the most cost effective source that has been considered.

2.3 Data Analysis Studies

The advent of higher flux facilities has emphasised the necessity for careful evaluation of data collection, analysis and correction in carrying out high accuracy experiments. Under the wide title of data correction several directions, both experimental and theoretical, are being followed. In many cases the work has been carried out in close collaboration with University teams.

(a) Monte Carlo techniques for simulation of elastic and inelastic scattering experiments are being used for investigating problems associated with multiple scattering and absorption. Programs are now in routine operation for both elastic and inelastic scattering. The work on elastic scattering involves applications both to constant wavelength experiments and to time-of-flight diffractometry.

(b) Analytic techniques for data reduction and analysis have been applied to data from instruments in the UK and at ILL. Also analytic techniques have been used to obtain resolution functions for inelastic instruments.

(c) An experimental programme to investigate the standards used in polarization analysis has been mounted. The precision of the separation of spin-flip and non-spin-flip scattering depends strongly on the errors involved in the calibration of the polarizer, analyser and spin flipper. Preliminary measurements have been made at the ILL to obtain these errors. Further measurements are planned in collaboration with the University of Kent.

(d) An experimental programme to measure the multiple scattering from vanadium is being carried out using polarization analysis on the D5 spectrometer at ILL. Experimental results are being combined with Monte Carlo techniques.

(e) The generally used standard for calibration is vanadium. However at very long wavelengths this has a high absorption giving a scattering which is very anisotropic. Measurements have been made on other alternative materials such as zirconium which has a much more favourable ratio of scattering to absorption at longer wavelengths.

(f) The advent of high flux instruments raises the problem of the ultimate limitation in counting errors. In collaboration with Reading University and the ILL, calculations and measurements have been made on the limiting effects of dead time errors and dead time jitter in standard counting chains.

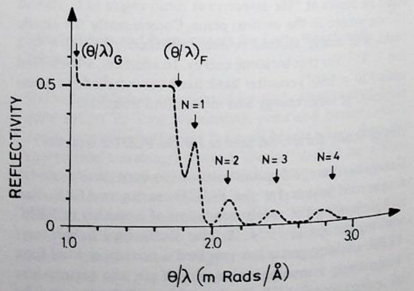

Figure 2.4 Fresnel interference fringes have been seen in neutron beam experiments using polarizing mirrors. This shows a typical set of fringes measured on a film of magnetised iron:cobalt; the arrows show positions calculated from elementary optics theory. (see 'Polarizing Mirrors', p 60).

2.4 Participation in Neutron Beam Science

Members of the NBRU have continued with a variety of scientific programmes using neutron beams, frequently in collaboration with University groups. A selection of current projects is described.

Dynamics of Molecular Systems

A series of neutron scattering experiments on molecules intercalated into layered transition-metal chalcongenides has been carried out as part of a continuing joint programme with Oxford University and ILL. Experiments, both elastic and inelastic, have been carried out on the compounds $MS_2.NH_3$ (M = Ti, Nb, Ta) in which the NH_3 molecules are sandwiched between the disulphide sheets. In these materials there is considerable interest in the behaviour of the intercalated NH_3s because of their modifying effect on the superconducting properties of the material. In order to determine the diffusional behaviour of the NH_3 molecules, in particular to separate and define the nature of rotational and translational modes, high resolution inelastic measurements have been made on single crystal samples of $TaS_2.NH_3$ using different spectrometers at ILL. This work is continuing in parallel with a related programme concerning diffusion dynamics in superionic compounds.

Work has commenced on the dynamics and structure of the anomalous liquid, vanadium pentaflouride. A polymeric structure has been conjectured to account for the properties of this material, but to date there has been little direct evidence to confirm this. Prior to undertaking a full measurement of the structure factor S(Q), S(Q,ω) data has been collected out to momentum transfers of $Q \sim 10$ Å^{-1} on the short wavelength time-of-flight spectrometer at ILL, and these measurements have provided a sound base for carrying out the structure experiments. A surprising side result is the absence in the neutron data of strong molecular modes which are known from infra-red and Raman spectroscopy to occur around 40 MeV. It is proposed to investigate this aspect in more detail.

Liquid Crystals

Previous measurements of the quasi-elastic line broadening caused by random diffusive motions in both a smectic-A liquid crystal and a nematic liquid crystal have shown that the characteristic period of these random motions remains constant with temperature for the nematic material but is strongly temperature dependent for the smectic-A material. Further measurements have therefore been carried out on a material, di-heptoxyazoxybenzene, which exhibits both a smectic-A phase and, at a higher temperature, a nematic phase. Analysis of the results, which is now under way, should enable one to conclude whether or not the temperature dependence observed in the smectic-A phase is due to distinct differences between the random microscopic molecular motions in the two phases. The work on smectic phase of liquid crystals is being continued in collaboration with Exeter University.

Local Atomic Arrangements in Titanium-Zirconium

The titanium-zirconium system is completely α-β isomorphous having a β (b.c.c) high temperature phase and a α (h.c.p) low temperature phase. As in a large number of titanium alloys, a proportion of β phase is retained on quenching down to the α phase. Titanium alloys are particularly attractive to study using neutrons, as null matrix systems can be produced, and this leads to a simplification of expressions used to relate the local atomic arrangements to the observed scattering. Due to the retention of some β phase, low temperature measurements are difficult to interpret and hence a better understanding is obtained by measurements at elevated temperatures. Measurements have been made in collaboration with ILL staff on null matrix Ti-Zr at a range of temperatures from 700°C to 450°C covering a range from β, through α + β, to α phase. A large |Q| range was measured on the D4 diffractometer at ILL and intensity oscillations observed out to high |Q| values. Preliminary analysis indicates that although measurements crossed two structural changes, the local clustering arrangement is not greatly affected. Work in the near future to measure the small angle scattering will enable any changes in cluster sizes to be measured.

Structure Refinement of Silica and Aluminium Phosphate Tridymite

Measurements have been made, in collaboration with Oxford University, of the structure of the tridymite phases of silica and aluminium phosphate. Powder neutron diffraction combined with a profile analysis technique enables accurate structure refinements to be made. Data has been taken on the D2 diffractometer at ILL and preliminary refinements have been made. Further higher resolution measurements will be needed to complete the refinement.

Magnetic Studies

The magnetic structure determination of dysprosium manganate $DyMn_2O_5$ has been continued in collaboration with Queen Elizabeth College, London at ILL. The large unit cell dimensions make a precise determination of the magnetic structure difficult from powder measurements alone and the data has now been augmented by the (hkO) reflection intensities collected from a single crystal sample. This data is now being analysed using the spin-density Patterson technique but preliminary evaluation confirms the doubling of the a-axis in the magnetic cell, and indicates that both dysprosium and manganese atoms carry an ordered moment below 8K.

Polarized neutron studies of the weak ferromagnets $FeBO_3$ and $Fe_3(PO_4)_2\ 4H_2O$ have both been started in collaboration with ILL staff using the D3 diffractometer. $FeBO_3$ has the calcite rhombohedral structure, which is common to the weakly ferromagnetic carbonates of Mn, Co and Ni. The trivalent ferric ions order at 348K and a weak basal plane ferromagnetism is established. The experiment should determine the covalency parameters of the borate anion and measure the degree of exchange polarization of the boron atoms.

Ferrous phosphate tetrahydrate has a monoclinic structure a = 10·541, b = 4·638, c = 9·285, β = 100° 43·7′ at 4·2K. There are two crystallographically inequivalent iron sites and their moments lie approximately parallel with an average orientation perpendicular to the a axis. The moments are arranged antiferromagnetically in the a-c plane but there is a small degree of canting which results in a weak ferromagnetic moment parallel to b and of average value 0·84 $\mu B/Fe^{++}$. A set of (hOℓ) flipping ratios for 150 independent reflections out to sin θ/λ = 0·75 Å^{-1} were measured on D3 at ILL. The sample was held in a field of 1·6T and at 4·2K. This data was augmented by data for the strongest reflections at a wavelength of 0·7 Å, so that extinction and multiple scattering corrections could be estimated more accurately. Even without these corrections it is clear that the canting on the Fe_I atoms is much larger than that on the Fe_{II} atoms, the ferromagnetic moments being approximately in the ratio 2:1. The fully corrected data will be used to investigate the orbital states of the two ferrous atoms and may also lead to an estimate of the covalency parameters for the phosphate anion.

2.5 Support of the UK Neutron Beam Programme

The NBRU's role in the Science Research Council's support of United Kingdom University teams in the field of neutron beam scattering has continued throughout the year. Using reactors in the UK, at ILL Grenoble and occasionally at Risö in Denmark and Chalk River in Canada, over 270 university staff, research associates and research students are involed in the SRC's programme.

Proposals for SRC-supported experiments on reactors at home or abroad are made bi-annually through the NBRU. A total of 298 proposals were submitted during the year, 2 for the Risö reactor, 112 for UK reactors and 184 for Grenoble. The use of ILL facilities has continued to increase, and at the end of the year the ILL programme included 105 experiments involving UK groups. Funds for all approved experiments, ie travel/subsistence and materials/equipment, are made available to University teams through the NBRU. Over 500 claims for travel and subsistence were processed during the period. Three new Rutherford Laboratory/University agreements were set up making a total of 21 in operation for this method of funding of materials and equipment purchases. Members of the NBRU maintain close contact with ILL staff and provide a liaison service for UK users. Over 170 visits to ILL were arranged during the period under review, and transport of equipment and samples for experiments has been provided on over 70 occasions.

3. Laser Research

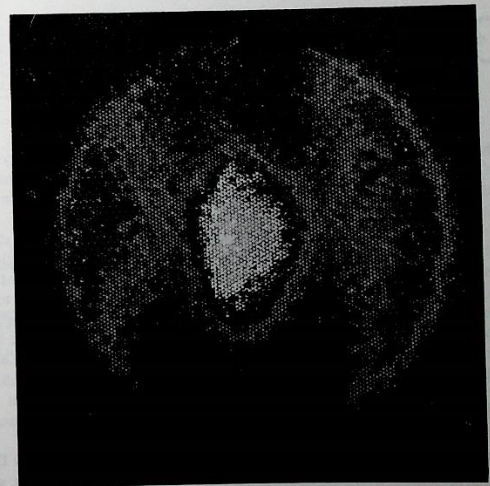

Laser Compression

3. Laser Research

During the early part of the year, development continued of the plans to establish Central Laser Facilities at the Rutherford Laboratory in collaboration with the Atomic Energy Authority, but the joint proposal was not approved by the Government. In July, therefore, the Science Research Council decided to seek approval for facilities of its own at the Rutherford Laboratory. Although more modest in scale than the joint project, the plans for the New Laser Centre met the requirements of a reduced but still challenging university research programme. Government approval to proceed in setting up the Laser Centre was obtained in October.

The Laser Centre will initially be provided with a high power neodymium:glass laser capable of delivering a peak power of 800 Gigawatts (8×10^{11} watts) in two beams, together with a range of diagnostic and experimental equipment for monitoring the laser and supporting the experimental programme. When these first installations are operating satisfactorily it is proposed to start a programme on the development of new high power lasers.

The first experiments will study the interaction of single beams from the laser with plane targets at powers up to ~ 100 Gigawatts. A wide range of topics in plasma physics and non-linear optics is accessible for study using the single beam/plane target interaction. Later, when the full two-beam system is operational, irradiation of spherical targets will allow the study of dense states of matter produced by laser compression.

In the closing weeks of the year the suppliers of the high power glass laser and of the first batch of diagnostic and experimental equipment were chosen and contracts are expected to be placed in early 1976. The first stages of the laser are planned to be operational by September 1976 with the full 800 GW system coming into operation in the first quarter of 1977. To realise these target dates the laser must be installed initially in existing laboratory space, but eventually it is intended to provide appropriate purpose-built accommodation for the lasers and support activities.

A Laser Division was established at the Rutherford Laboratory to undertake the setting up, operation and further development of this work. The direct staff of the Division is expected to reach approximately 40 in 2–3 years' time. 6 of these were in post at the end of the year.

Throughout the year the Director of the Rutherford Laboratory was advised on policy for the Laser Centre by a Steering Committee chaired by Professor D. J. Bradley, and there is a Users' Advisory Committee chaired by Professor Gibson which contains some 20 representatives of potential user groups.

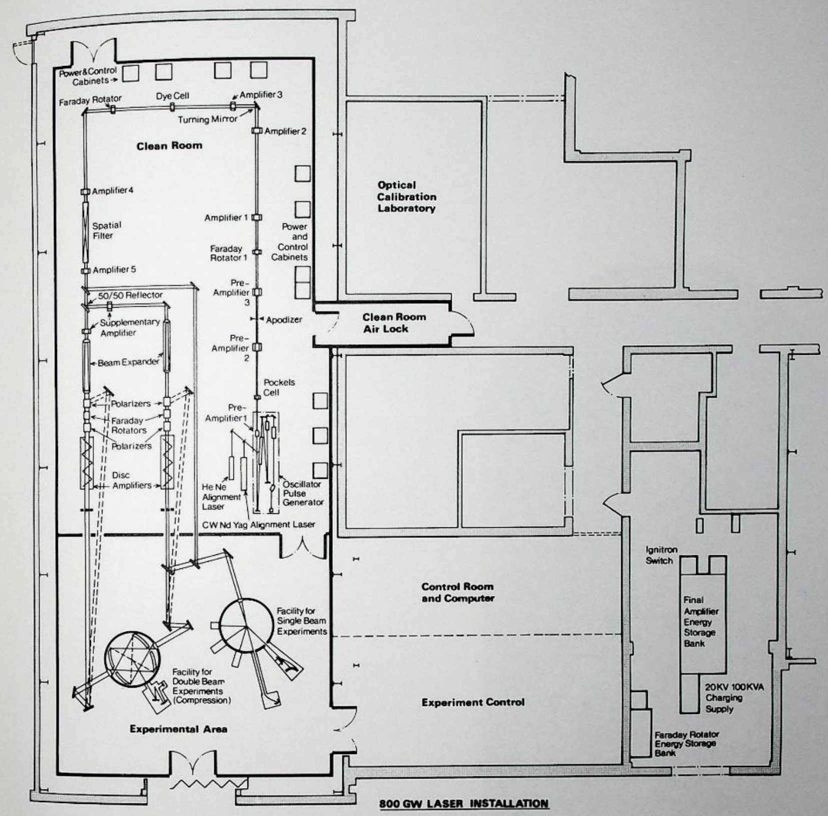

Figure 3. Proposed layout of Central Laser Facilities at the Rutherford Laboratory

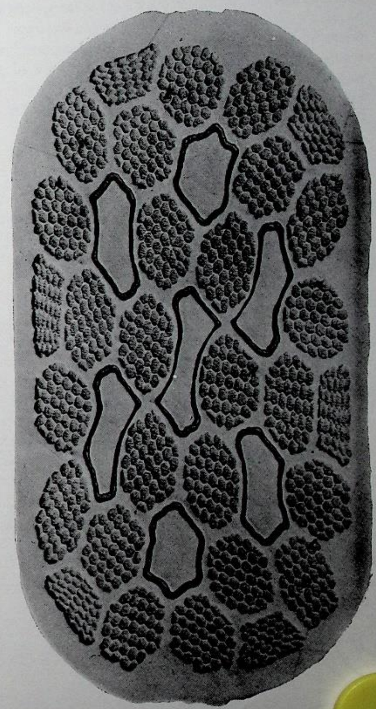

4. Forward Technology

Filamentary Niobium-Tin composite

4. Forward Technology

Physics research requires a continual supply of sophisticated apparatus, which in turn demands a wide range of technical and engineering expertise. A major proportion of the Rutherford Laboratory's resources have therefore always been geared to the design, development and production of experimental apparatus.

Forward Technology – the support of ongoing research over a wide field – involves specific projects which are technically complex and require the attention of a dedicated multi-disciplined project team (examples are polarised targets and a rapid-cycling vertex detector for special particle physics experiments and instrumentation for upper atmosphere research), together with fairly long-term research studies of technical importance to the future of particle physics and to other areas of science and engineering (for example superconductivity, computing facilities for magnet design, etc).

To support such a wide spectrum of activities, the Laboratory has available the following resources:

1 Personnel: specialists in applied physics, mechanical and electrical engineering, computing and computer-aided design, metallurgy, electronics, mathematics, cryogenics, vacuum technology, superconductivity and optics.

2 Hardware: as well as the apparatus constructed for particular applications, a number of test facilities are available for more general use, for example: a superconductor sample test rig, apparatus for measuring the mechanical properties of materials at low temperature, a number of magnets and cryostats, a helium-3 refrigerator and a helium-3/helium-4 dilution refrigerator. Computer programs have been developed for special requirements, particularly for magnet design using interactive techniques and for the design of cryostats.

3 Organisation: because of the varying requirements which have to be met, a rather flexible organisation exists, with a broad division between advanced apparatus projects and the superconducting magnet programme. To provide additional skills, personnel from outside the Laboratory's Applied Physics Division or Department of Engineering Science can be seconded to the project teams as and when required.

In the future the Rutherford Laboratory expects to become involved in several new areas representing projected national needs outside the field of particle physics. Several of these will call upon expertise of the groups involved in forward technology, particularly in the superconductor field, where already several of the magnets currently under development are for non-particle physics applications. Reflecting this change in direction, the Engineering Board of the Science Research Council now provides the financial support for the research into niobium-tin superconductors.

The GESSS – Group for European Superconducting Systems Studies – Collaboration involving the Rutherford, Karlsruhe and Saclay Laboratories, originally set up to study superconducting synchroton magnet designs, has now taken responsibility for aspects of the Euratom Tokamak design. This covers the requirements of a new generation of plasma containment equipment for fusion studies and the Rutherford Laboratory has contracts for superconductor development and for computer-aided magnet design.

In the field of superconducting ac generators, the Laboratory has a responsibility to provide liaison between Universities working in this area. Superconductor test facilities, previously at the Royal Radar Establishment Malvern, are now transferred to Rutherford Laboratory.

However new particle physics projects, particularly associated with the CERN II programme, will continue to provide important instigation for technological development.

4.1 Polarised Targets

A necessary requirement for the full understanding of a large class of particle scattering processes is a study of the spin dependence of the reactions. One way to accomplish this is by providing proton or neutron targets whose spin axes are preferentially aligned along a given direction. This can be effectively achieved by a process known as "dynamic polarisation" for which the necessary requirements are: the target material (usually an organic compound containing free protons), a high magnetic field, a very cold environment (0·5K) and microwave power.

The three polarised targets currently under construction are of widely differing types, each providing a unique facility. The aim has been nevertheless to retain standard components wherever possible so as to reduce design and construction costs, maintain flexibility in terms of spares, and allowing permutation of the components to provide new facilities in the future.

Axially Polarised Target PT–55 (Experiment 12)

All major sub-systems have been assembled and tested individually. In particular, the helium-3 liquefaction system and the superconducting magnet with the helium-4 liquefaction system have been successfully operated.

The target cryostat has been cooled to 0·48K by the helium-3 system and held at this temperature with an electrical heater providing a load of 80 milliwatts. This is in good agreement with the design calculations. Under these conditions the consumption of liquid helium-4 was measured to be less than 4 litres/hour.

The coils of the superconducting magnet were first tested in an open cryostat early in the year. In these tests a homogeneity close to the specified ±1 part in 10^4 at 2·5 Tesla over the target volume of 5 cm long by 3 cm diameter was achieved.

The complete magnet was then assembled and tested under the specified conditions of 2·5 Tesla and 4·3K. An improved homogeneity of ±0·5 parts in 10^4 over the target volume was achieved by retrimming the coil currents with a pair of cylindrical soft iron shims in position. The vertical section of the field plot is shown in Figure 4.2. The stability of the field was measured over 24 hours using a nuclear magnet resonance system. Over the first 8 hours the field was stable within the specified 0·5 parts in 10^4 and over the last 16 hours this improved to be within ±0·05 parts in 10^4. Although the magnet quenched at 2·26 Tesla during its first charging it subsequently reached the required test field of 2·62 Tesla at 4·4K. The current decay in each coil during a quench was measured and the results were in good agreement with the values computed using the QUENCH programme.

During the tests of the complete magnet liquid helium was supplied automatically by the liquid helium-4 system, the main component of which is a CTI-1400 helium liquefier. The consumption of the magnet and transfer lines was 13 litres/hour corresponding to a magnet heat leak of 6 watts. The excess liquefaction capacity of the system was measured at 8 litres/hour of which 4 litres/hour will be used to supply the helium-3 system.

The NMR polarisation measurement system and the 70 GHz microwave power system have been checked in the laboratory and the complete polarised target is being assembled for the commissioning programme.

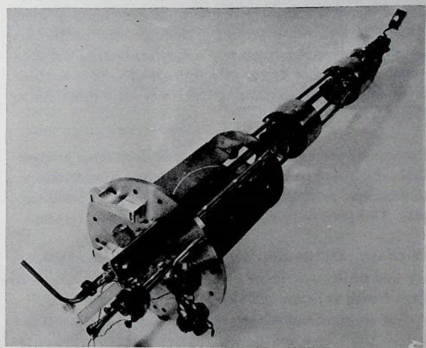

Figure 4.1 The internal part of the PT55 target cryostat. This assembly is withdrawn during loading of the cavity, which can be seen on the extreme right.

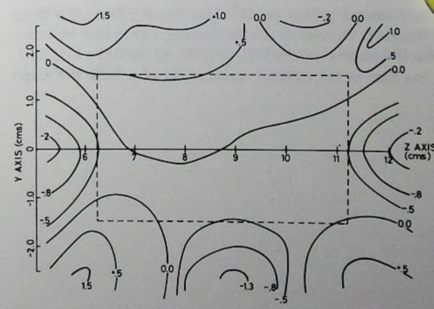

Figure 4.2 A contour map showing the field homogeneity in a vertical plane through the PT55 magnet axis. The contours are numbered in parts in 10000. The dotted line indicates the position of the target.

Polarised Deuteron Target (Experiment 13)

During the first test of the complete apparatus in December, protons in a propanediol sample were dynamically polarised. This test completed a year in which almost all components of the target were assembled and brought together for final commissioning.

All major components were first individually studied. The magnet was re-shimmed to improve the field homogeneity over the target volume to ± 0·8 parts in 10^4. The oil booster pump performance was measured. The cryostats and pumping systems were first installed in the laboratory for full cryogenic tests, in which, for example, a temperature of 0·43K at 80 milliwatts load was achieved. The NMR system was tested by making measurements both at room temperature in the target magnet, and using a small proton sample in the laboratory helium-3 refrigerator; the value of the analogue signal enhancer was amply demonstrated in these tests. The microwave system, including a new carcinotron power supply and a frequency measuring system, was commissioned. Studies of the effectiveness of various methods of coupling the waveguide to the cavity were made during the year.

Because of the expense of the 30 cc of deuterated propanediol which will be used as target material, considerable attention has been given to its preparation using small samples. This involves the addition of paramagnetic centres.

Particular care has also been taken in the design of the cavity and in the way in which the material (which has to be kept frozen at below 180K) is loaded in the cryostat.
A few short commissioning runs remain to be carried out before the target will be available for particle physics research.

Frozen Spin Polarised Target for RMS (Experiment 20)

A polarised proton target of the frozen spin type is being designed for use in the Rutherford Laboratory Multiparticle Spectrometer (RMS). In order to provide a long holding time in the ambient magnet field of 1 Tesla the target will use the helium-3/helium-4 dilution cycle to allow holding temperatures of less than 0·1K. The cryostat is based on that at present in use at CERN. On the basis of this experience at CERN it is expected that a proton polarisation in excess of 90% will be achieved and that the relaxation time will be more than 1000 hours.

The uniform polarising field of 2·5 Tesla will be provided by specially designed supplementary pole pieces which will be added to the RMS magnet. This will be offset from the axis of the spectrometer to minimise the interference with the particle beams.

Polarised Target Research and Development

Research has continued into the production of the target material, propanediol doped with Chromium-V. This has included studies of the factors affecting the chemical reaction, such as light and the addition of water, and also further examination of the dilution process for the production of deuterated material.

Since for the propanediol it is essential to form a glass, the effect on the freezing process of additional chemicals has been studied. Melting points of mixtures have been determined in the search for a material which is solid at room temperature.

The coupling between nuclear and electronic spin which is responsible for dynamic polarisation and nuclear relaxation has been studied in the doped propanediol and in other dilute paramagnets. Measurements have been made of the separate relaxation rates of the two components of the spin energy – their interaction with an applied magnetic field and with each other – and of the decay of polarisation in the presence of a weak radiofrequency field, distant from the nuclear resonance by many linewidths. The experiments have given some insight into how nuclear polarisation diffuses in the field gradient surrounding each paramagnetic centre, and have demonstrated the existence of a coupling between the nuclear and electronic spins which is induced by the radiofrequency field itself.

4.2 Rapid Cycling Vertex Detector

This project is in the final construction phase and is scheduled for commissioning and its first experiment early in 1976 (Experiment 19).

During the year, several difficult problems had to be overcome. The most serious of these was the failure of the chamber-body aluminium alloy to withstand the arduous fatigue pressure-cycling duty demanded by the physics programme. Very little design data was available initially for the alloy which was best able to meet the strength and transparency-to-nuclear-particles requirements. A comprehensive testing programme was therefore undertaken the results of which indicated a need to thicken up the chamber walls and to reduce the working stresses. The chamber body for the first cooldown will be 3 mm thick. This is likely to lead to problems of high background when triggering the device but will allow commissioning tests to continue without fear of premature failure of the chamber walls. An additional chamber body is also being prepared which will have a thinner wall but the final machined thickness will not be specified until operational experience is obtained.

After a long test programme a satisfactory glass to glass-reinforced plastic seal using a silicon rubber compound has been developed and incorporated into the optics cartridge.

Considerable experience has been gained in operating the electromagnetic expansion vibrator and this item is now mounted in its final position in the trench under the magnet. Noise levels will be monitored carefully during commissioning.

The fast cycling cameras have been commissioned and will be capable of taking pictures at the rate of 10 per second during the accelerator flat top using the telecentric camera lenses specially designed and mounted by the lens design group at Imperial College. The first lens has been tested and is diffraction limited at its full field angle using the restricted wavelength band provided by the flash tubes and associated filters.

The chamber will be monitored and logged by a PDP8I computer without which operations at the cycling rates envisaged (up to 60 Hz) would not be feasible.

4.3 Low Temperature Research Facility

A commercial dilution refrigerator is available at the laboratory for low temperature experiments down to about 30 mK. Experiments are planned using the refrigerator for research into dynamic polarisation for which the use of a superconducting solenoid and designs for a fluorinated plastic mixing chamber have been investigated.

During the year, and in collaboration with Bristol University, measurements have been made on the superconducting transition in polysulphur nitride. The crystals were grown at Bristol and the experiments carried out on the dilution refrigerator. Preliminary experiments observed the transition at zero field and in transverse applied fields.

Measurements made at the laboratory by a group from Nottingham University showed that an organic complex of TCNQ behaved as a metal, showing increasing electrical conductivity from room temperature down to about 30 mK (Nature, 259).

4.4 Superconducting Magnets and General Superconductor Research

In the past decade, the Laboratory has played a leading role in research and development work for the applications of superconductivity. The initial impetus arose from the requirements of particle physics research for magnetic fields larger in magnitude and volume than were possible using conventional iron-cored magnets; significant advances in this field have already been made possible by the availability of much larger bubble chamber and spectrometer magnets, as well as many other special purpose high-field devices. Pulsed superconducting magnets for accelerators have now been developed so that their feasibility is established. The continuing support at the Laboratory for particle and neutron-beam research is represented by several magnets under construction, while an extensive programme of on-going research into new conductors and into constructional techniques is under way.

Progress in superconducting magnets in connection with particle physics has made it possible to pursue new applications for superconductors, and as a major research group in this field, advice and assistance has been sought from the Laboratory on these new uses. Examples are magnetic levitation for high speed transport applications, AC generators and toroidal magnets (Tokamaks) for fusion research, the latter relying for their next advance on the use of superconducting magnets.

Pulsed Dipole Magnet AC5

This prototype synchrotron magnet was completed according to plan early in the year and has since been extensively tested under a.c. and d.c. excitation.

Measurements of the complete integral of the field taken through the magnet showed it to be particularly uniform in the useful aperture. The data was Fourier analysed in the usual way to characterise the field distribution and showed that within 80% of the bore, no angular harmonic contributed an error of more than 0·08%. The magnet behaved well on pulsing to the design field of 4·5T and the total losses, measured electrically, were as expected.

Despite the special construction some 'training' was still observed, though in this magnet the range appears to be rate dependent and the full short sample performance of the conductor, corresponding to a peak field of 5·9T, can only be reached by very slow excitation. This unexpected electromagnetic instability in the conductor is the subject of continuing investigation. Experiments so far suggest that there is no deleterious effect on the conductor due to the high clamping pressures arising from the two stage shrink fit method of construction.

DC Dipole Mk1

This large dipole magnet is expected to produce a transverse field of $\sim$ 5·5T over a volume 130 mm diameter and 1·1 m long. Construction of the magnet suffered a set-back early in the year when faulty insulation on the superconductor caused a series of severe insulation failures during the winding of the second pole. In spite of repeated attempts to rectify these faults, the insulation on this pole, consistently fell below the standards required and it finally became necessary to abandon the pole. A new length of superconductor has been obtained and insulated to a higher standard. Using this conductor, a replacement second pole has been wound without difficulty.

The magnet is now virtually complete and ready for pressure impregnation. Because the use of epoxy resin at high pressure has produced training in small magnets, paraffin wax will be used instead of resin to impregnate the magnet. The use of a wax impregnant rather than resin will also allow the magnet to be tested at different impregnation pressures.

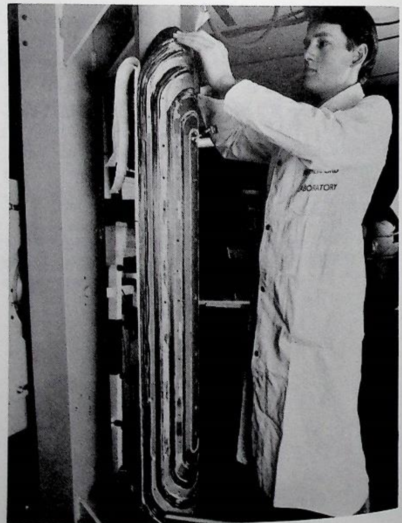

Figure 4.3. Winding the DC Dipole Mk 1.

A detailed experimental programme is planned in which the performance of the magnet will be measured at different temperatures in the range 4·2K - 3·0K and different impregnation pressures up to a maximum of 20 MNm^{-2}. For this work the magnet will be cooled in a simple 'tub' cryostat. When the experimental programme is complete, the magnet will be sealed into a fully operational cryostat allowing room temperature access to the high field volume. It will then be used by a group at Imperial College for optical spectroscopy work on the diamagnetic Zeeman effect.

DC Dipole Mk 2

Work has started on the construction of a second DC dipole magnet, similar in size and general specification to the first. The purpose of this magnet is to provide more information about training and to develop and improve the techniques first tried out in the Mk 1 dipole so that a design of this type might be offered for use as a beam transport magnet or a similar application.

Although the magnet will use much of the tooling and equipment produced for the first dipole, notable advances have been made in the fabrication of very accurate metal spacers, using numerically controlled machining techniques for the end spacers and special extrusion techniques for the side spacers. Some test winding has been carried out.

In order to avoid the unfortunate experience of poor insulation encountered in the first magnet, considerable attention has been paid to the insulation of the conductor. A small experimental insulating machine has been set up in the laboratory for this investigation. By careful attention to detail it has proved possible to insulate the superconductor to much higher standards than the usual commercial product. The occurrence of pinholes has been reduced, the breakdown voltage increased and the dimensional tolerance improved.

Hexapole Magnet for Neutron Beam Research

There has been steady progress in research and development work to establish the winding procedure and coil construction for this magnet. The full quantity of insulated conductor will be delivered soon and manufacture of the final windings is scheduled to start early in 1976. Work to verify the behaviour of the assembly on cool-down is currently in progress. Engineering methods used in the construction of this magnet have been used to facilitate the design and construction of the niobium-tin prototype hexapole.

Niobium Tin Hexapole

This will be the first transverse field 'saddle' magnet to be made in the laboratory using filamentary niobium tin. It is being built to develop the necessary technology and to provide a prototype for similar neutron beam handling elements. The design is very similar to that of the niobium-titanium hexapole except that the iron yoke has been omitted and the length reduced to 0·3 metres, this being a convenient size to demonstrate the principle of the design. It is expected that this magnet will produce a higher peak field (~7T) and a higher second derivative of field in the aperture (~ 1·8T m^{-2}) than the niobium titanium version. This increase reflects the higher critical current densities and critical fields which may be obtained from niobium tin.

As with previous filamentary niobium tin magnets made at the laboratory, each pole of the hexapole will be heated to react the niobium tin after winding is complete. To facilitate the use of this technique in complex winding shapes, a new insulation technique has been developed. As before, the insulation used is a glass fibre braid but glass fibre alone has been found to be very fragile and easily damaged when the conductor is bent round tight corners. To protect the glass from damage during winding a thin coating of perspex has been applied to the outside of the braided conductor. This coating may also be used to bond adjacent turns together during winding; at the completion of each layer gentle heat is applied and the turns are squeezed together. In this way a very dense and compact winding may be produced. When the winding is complete, it is first heated to $\sim$ 350°C in vacuum, at which temperature the perspex distils off. The temperature may then be raised to $\sim$ 650°C for several days to react the niobium tin. After cooling to room temperature, the winding may be impregnated with epoxy resin.

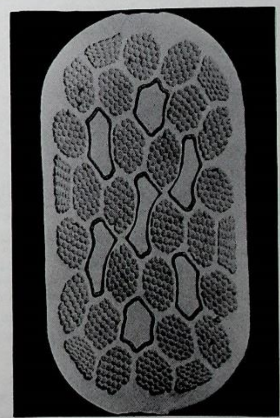

Figure 4.4 Filamentary Niobium-Tin Composite for the Hexapole: 41070 filaments of Nb_3Sn in a bronze matrix with seven large copper filaments each surrounded by a diffusion barrier. Overall dimensions 1·1mm x 2·2mm (Photo AERE Harwell).

A test winding, using plain copper conductor insulated with glass and perspex is complete and will be reacted and impregnated. The conductor, shown in cross section in Figure 4.4 has been delivered by AERE, Harwell. It has been tested to check that the critical current density after reaction is satisfactory and that the purity of the large filaments of copper is not contaminated by tin after reaction, ie that the diffusion barrier surrounding the copper is intact. Tests have also been carried out to ensure that these properties are not degraded when the conductor is bent around the tight radii involved in winding the hexapole.

High Field Insert for NMR Magnet

At the request of the SRC Science Board, the laboratory is supervising the development of a high field niobium-tin insert magnet by the Oxford Instrument Company Ltd. The insert will form part of the 460 MHz high resolution NMR system being developed for use by a biochemistry group at Oxford University.

Several tests have been carried out into constructional techniques and as a result, it is planned to adopt the react-after-winding technique described above using a 0·6 mm diameter conductor insulated with glass braid and perspex. No particular difficulties are anticipated in the winding of this magnet but some problems have been experienced in releasing the impregnated magnet from its winding former because it is not possible to apply any of the usual release agents to a former which must be heated to 650°C.

A good persistent current joint will be needed in this magnet to ensure an adequate stability of field with time and this has not so far been achieved with filamentary niobium tin. Joints have been tested with resistances of $\sim 10^{-9}$ but a resistance of $\sim 5 \times 10^{-12}$ ohm will be needed if the finished magnet is to meet the required decay rate of < 1 part in 10^7 per hour without the need for continuous correction. Development of several promising ideas is continuing.

Solenoid for a Large Polarised Target

Work was started on the design of a superconducting solenoid for a polarised target, as part of the European muon collaboration programme, to be carried out on the CERN SPS.

The solenoid is 1·6 m long by 200 mm internal diameter and is required to produce a 2·5T magnetic field, with a homogeneity of ± 1 part in 10^4 within the target volume of 1m long by 5 cm diameter.

Preliminary optimisation of the coil geometry has been completed, using the interactive graphics technique to obtain the required field and homogeneity. The problems which arise with the 200 KJ of stored energy during a quench have also been investigated.

Split Pair Solenoid for a Rapid Cycling Bubble Chamber

A proposed multi hadron experiment for the CERN SPS involves a rapid cycling bubble chamber, which requires a superconducting split-pair solenoid.

A design study was carried out on the optimisation of the parameters and overall costs. The most limiting parameter was the large gap between the coils, to provide a ± 16° emittance angle in the dip plane and ± 30° in the magnet bending plane.

A series of coils with varying diameter and coil gap were examined and costed, to enable the overall experiment parameters to be re-optimised.

Magnet for a Large Aperture Spectrometer

A programme of hadron physics proposed for the CERN ISR requires a superconducting spectrometer magnet. A collaboration between the Lawrence Berkeley Laboratory in the USA and the Rutherford Laboratory has been set up to carry out a design study on the magnet.

The magnet is required to produce a 1·5T magnetic field in the plane of the ISR particle beams and yet provide maximum free exit for secondary particles. The field inside the magnet must be reasonably homogeneous to assist with identification of the particles.

A design has been proposed which consists of five thin solenoid coils 1·6 m diameter and spaced at 0·8 m. The peak field on the inside edge of the coils is 4T. The total number of ampere turns is 4·25 x 10^6 and the stored energy is 10MJ. An iron yoke weighing 100 tonnes and consisting of two end poles and eight side limbs is proposed. The design of this complex magnet has been pursued in some detail, to enable a realistic cost estimate to be prepared.

Superconducting Magnets – Training Research

Superconducting magnets impregnated with epoxy resin frequently suffer from premature quenching owing to localised release of energy, thought to arise principally from intermittent local cracking on a microscopic scale within the coil. If the coil is instead impregnated with a low yield strength material, all such cracking occurs at low current and stress levels, and no quenching of the coil results. A full scale demonstration of this idea, using a 4 Tesla quadrupole coil assembly filled with paraffin wax, showed that the system could be operated reliably at above 95% of critical current with negligible training. Measurements of the change in inductance with increasing field showed that the bulk coil movement was less than 1 in 10^3, confirming that the impregnant will adequately transmit the coil forces to the containing structure.

A computer simulation of the training effect was developed which successfully correlated a variety of types of training behaviour; this could be used to extrapolate to other field levels, stress levels, and temperatures, in particular the expected behaviour of high field niobium-tin coils using different types of impregnant.

A possible way to reduce the incidence of cracking in epoxy resin impregnated coils would be to maintain the resin under a strong compressive stress. Experience has shown that precompression can often reduce training effects in resin impregnated coils. In an attempt to produce a very uniform precompression, a series of small superconducting coils has been constructed in which the winding has been impregnated with resin at high pressure. The windings are enclosed in a pressure vessel so that the precompression may be retained on curing the resin and also on cooling the magnet to low temperature. It has been found however that these magnets exhibit severe training. Although this is a disappointing result, it is also a very interesting one because the effect is so marked and it merits further study.

Superconducting Composites

The laboratory's development contract with Imperial Metals Industries (IMI) Limited for the production of filamentary niobium titanium composites has been concluded during the year. This very successful collaboration, which started in 1968 was initially responsible for the production of the filamentary superconductors, now in almost universal use. It then proceeded to the development of a wide range of very sophisticated pulsed magnet conductors containing up to 150,000 filaments with an array of resistive barriers to reduce inter-filament coupling. Collaboration with IMI will continue in the future in the development of niobium tin composites and large conductors for Tokamak experiments.

Figure 4.5 shows the most recent niobium titanium composite; it has been made by hydrostatic extrusion and contains 8500 filaments, each separated from its neighbours by a resistive cupro-nickel barrier. The hydrostatic extrusion process has two important advantages over conventional extrusion: it produces much less distortion of the composite, allowing complex arrays of resistive barriers to be extruded without damage, and it allows very thin walled extrusion canisters to be used, minimising the proportion of wasted space in the finished composite. So far composites of this type have only been made on a small scale using the hydrostatic extrusion press at the National Engineering Laboratory (East Kilbride) but full scale production could be achieved using for example the very large hydrostatic extrusion press at the National Standards Laboratory (Perth).

Development of the bronze process for the production of filamentary niobium tin has continued and during the year work in collaboration with AERE Harwell has concentrated on two main problems: the optimization of current density at high fields and the improvement of diffusion barriers. It has been found that the high field critical current depends most strongly on the upper critical field of the Nb_3Sn which is a function of the stoichiometry of the compound. Good stoichiometry is therefore the most important single parameter in the achievement of high currents at high fields; grain boundary effects appear to only be important at low fields. A collaboration has been established with a group in the Department of Metallurgy at Imperial College with a view to correlating current density in Nb_3Sn with microstructure; this promises to be very fruitful. The technology of diffusion barriers has advanced to the point where composites can be heat treated for many hundreds of hours to react the niobium tin with no contamination of the pure copper. It is of course essential to have pure copper in the composite to provide dynamic stability and protection.

New geometrical arrangements within the composite have also been tried out. Figure 4.6 shows a composite, currently under production at IMI, in which the islands of Nb_3Sn filaments in bronze are enclosed by a diffusion barrier in a pure

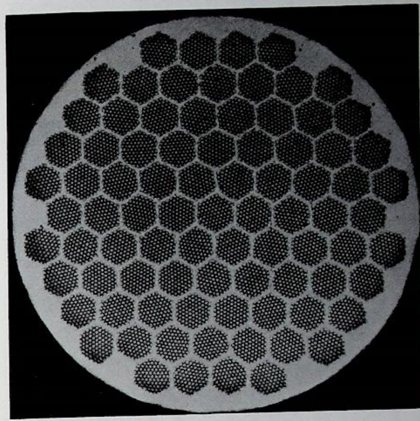

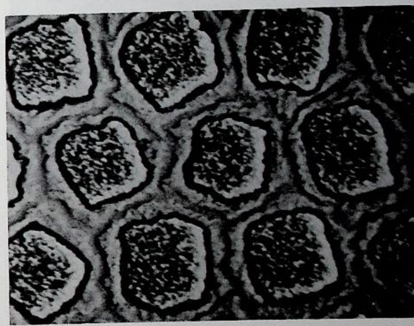

Figure 4.5 (Top) Hydrostatically extruded Niobium-Titanium composite with 7225 filaments. (Bottom) Individual filaments surrounded by pure copper and a cupro-nickel diffusion barrier. Overall diameter of composite 0·6mm (Photos IMI Ltd).

copper matrix. This has the advantage of allowing a much greater proportion of copper in the composite but is not so suitable for pulsed use. If successful, this conductor will be used in the hexapole programme to make a spare experimental pole. Similar conductors are also in process at AERE, Harwell.

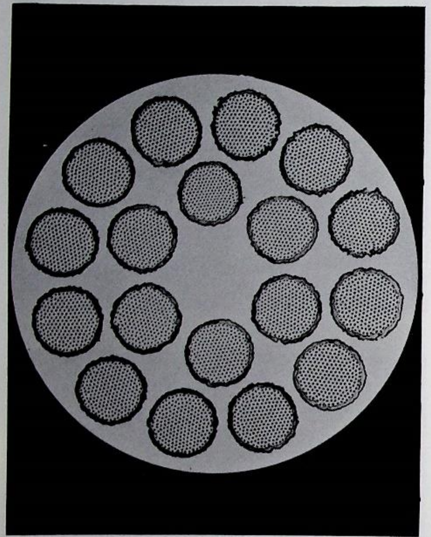

Figure 4.6 Filamentary Niobium-Tin composite with copper matrix; eighteen islands of bronze each containing some 125 filaments with each island surrounded by a diffusion barrier and immersed in a pure copper matrix. Overall diameter 1mm (Photo IMI Ltd).

Superconductor Testing Facilities

During the year, the superconductor testing service provided by the Royal Radar Establishment, Malvern has been closed down and the Rutherford Laboratory has been asked to continue this service to industry. The laboratory has agreed to undertake this and the service is now operating. It is available to all UK users and details may be obtained from Mr M N Wilson, ext. 6134.

In order to accommodate the extra demands imposed by the testing service, the Tokamak conductor work and university collaboration, the superconductor testing facilities have been extended and reorganized. The new test area has been designed to allow three experiments to be run simultaneously and to allow routine measurement to be completed quickly and economically. Four cryostats are now in operation allowing the following types of measurement:

1 Large samples (85 mm dia magnet bore available) in DC fields up to 8·5T at sample currents of up to 10,000A
2 Large samples (85 mm dia magnet bore available) in AC fields up to 6T and 1·3T sec^{-1} at sample currents of up to 10,000A
3 Small samples (50 mm magnet bore available) in DC fields up to 10·5T at sample currents up to 2000A
4 Straight wire samples under a tensile load of up to 50Kg in a DC field of up to 3T at sample currents of up to 2000A

A collaboration with Warwick University, started during the year, will use the large AC test rig to measure AC loss in fluctuating fields of the type expected in superconducting AC generators or a magnetically levitated vehicle.

Tokamak Conductor

As a member of the GESSS collaboration, the Laboratory has been asked to participate in the Euratom thermonuclear fusion programme by developing, in collaboration with IMI Limited, a large conductor suitable for a tokamak fusion reactor. Such a conductor must be large and robust (tokamak coils are typically 10 metres in diameter), it must be capable of being produced economically on a large scale and yet it must only suffer small AC losses in pulsed fields. Basic experimental and theoretical work is under way on losses in pulsed fields aligned parallel to the conductor (a relatively unexplored area) and plans are in hand for the small scale production of two different types of conductor at IMI.

Magnetic Levitation

Magnetic Levitation is currently arousing some interest as the possible basis of a future high speed transport system. Several different systems are under investigation at Warwick, Sussex and Aberdeen universities, at Imperial College and at many other research establishments in Japan, Germany, USA, and Canada.

A new idea for obtaining stable levitation of iron by means of a superconducting magnet has recently come from the Theory Division of UKAEA Culham Laboratory, and the idea has been verified experimentally at the Rutherford Laboratory; stable levitation has been obtained, indicating that the theoretical ideas are basically correct. The new system appears to offer several advantages over other systems currently under investigation and to be adaptable to a wide range of iron/superconductor topologies. For these two reasons, it is proposed to initiate a small programme of basic work on the new system.

Materials Development

The selection and testing of plastics materials, rubbers and resins for use in superconducting equipment is an important part of the support work for high energy physics experiments and finds particular application in superconducting magnets.

Plastics materials are notoriously intractable at low temperatures and the strains set up by differential contraction or temperature differentials within the material are sufficient to cause failure. The incorporation of reinforcing fillers such as mineral fibres or fabrics is particularly beneficial.

A wide range of epoxide resin systems has been characterised for toughness, thermal contraction and mechanical properties at ambient and low temperatures; this extends from low viscosity pure resins suitable for impregnating tightly wound solenoids to heavily filled resins of putty-like consistency suitable for moulding component parts having low thermal contraction coefficients. From this range a selection may be made to meet the requirements of most applications. Epoxide resin systems have been formulated to withstand radiation doses of 10^{10} rad with little deterioration in mechanical properties. The current research programme includes an investigation into the influence of the properties of resins on material behaviour when incorporated as impregnants into tightly packed structures.

4.5 Computing Applications

Magnet Design Computer Programs

The applications software for the numerical solution of magnetic field and magnet design problems has been significantly improved and extended in scope. The GFUN 3D package for computing three-dimensional magnetic fields has been successfully applied to a wide variety of problems. In particular, many external organisations have made use of this facility under contract, including Culham Laboratory for Tokamak Fusion Magnet design, University of Sussex and British Rail for levitated transport magnet design and International Research and Development Co. for superconducting ac generators.

The recent introduction of the GEC 4080 as a front end processor for the Laboratory's main IBM 360/195 computer has enabled a fresh approach to be made in the ergonomics of magnet design programs. The GFUN interactive graphics magnet design program has three distinct stages of operation:

1 Data entry
2 Analysis
3 Interpretation of results.

GFUN consists of an on-line program at present running in the central computer which services stages 1 and 3, and a batch program which services stage 2. If the magnet geometry is simple some analysis can also be done in the on-line program.

Work is in progress to transfer the on-line GFUN program from the IBM to the GEC 4080 minicomputer. The advantages from this will be:

1 More efficient usage of the 360
2 Several simultaneous on-line users
3 Virtually unlimited scheduling for magnet design
4 Improved graphics facilities using GINO-F package from the Computer-Aided Design Centre (CADC).
5 Improved program facilities resulting from the need to redesign the program.

The two computers will communicate via a high speed link. Figure 4.7 shows a typical magnet geometry defined using the new on-line program and displayed using the Hidden Lines program from CADC.

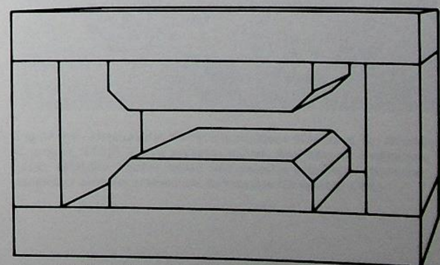

Figure 4.7 Type I Nimrod bending magnet geometry defined using the GFUN program.

Fusion Magnet Design

A contract was set up with Culham Laboratory to develop a suite of computer programs for Tokamak magnet design work to facilitate the stress analysis of a large toroidal system. Figure 4.8 shows a diagram of one such design using 40 separate short coils of 'D' shape to form the torus. The special 'D' shape is introduced to minimise the shear stresses. Small differences in the shape of the 'D' have a considerable effect on the shear stress. Figure 4.8 shows the variation of shear stress ($R\theta$ component), along the central filament of the coil, for three slightly different shapes.

The GFUN 3D program has also been used to explain the first field measurements on the Culham DITE Tokamak and to predict the behaviour of the plasma. The Tokamak has now been operated and the containment time was very close to the computed value.

Other Engineering Applications

The new data input and graphics package developed for use with the GEC 4080 has been designed as a general program capable for use with any applications program requiring the three-dimensional modelling of problem geometries as data. These new facilities can be used to model geometries for programs for stress analysis and diffusion problems. Also it is hoped to implement computational facilities for the solution of time-dependent problems associated with engineering design.

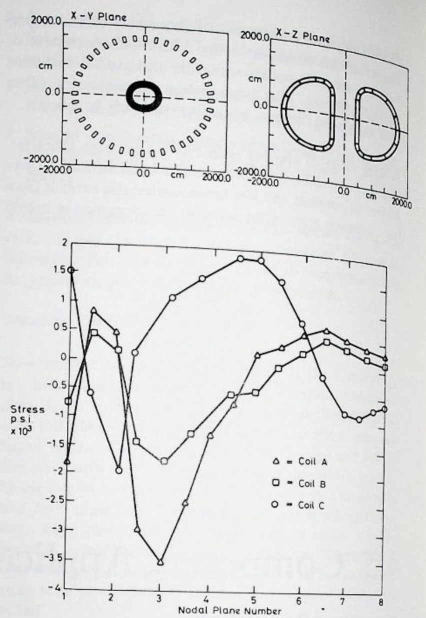

Figure 4.8 (Top) Layout of D coils in a 40-coil Tokamak. (Bottom) $R\theta$ shear stress variation along central filament of coil for three slightly different D shapes.

4.6 Infra-Red Radiometers for Atmospheric Research

Oxford University Rutherford Laboratory collaboration

Pressure Modulated Radiometer (PMR) Nimbus 'F'

This two-channel radiometer was launched from NASA's Western Test Range in June 1975 and is performing well providing synoptic data of the atmosphere's temperature profile up to 90 Km in height. Excellent comparisons were obtained from the selective chopper radiometer on Nimbus 'E' up to its ceiling height of 45 Km after 3 years in orbit. This experiment is still providing excellent data after well exceeding its designed capability.

Stratospheric And Mesospheric Sounder (SAMS) Nimbus 'G'

This complex radiometer for temperature and composition atmospheric sounding is to be launched in 1978 with the engineering model to be delivered in October 1976. Work is well advanced on sub-assemblies for this model which have been vibration tested.

PMR for Venus Orbiter – Pioneer Spacecraft

The engineering model of the PMR which is very similar to the SAMS pressure modulators is complete and has been despatched to Jet Propulsion Laboratory of Caltech for incorporation in the rest of the Vortex experiment.

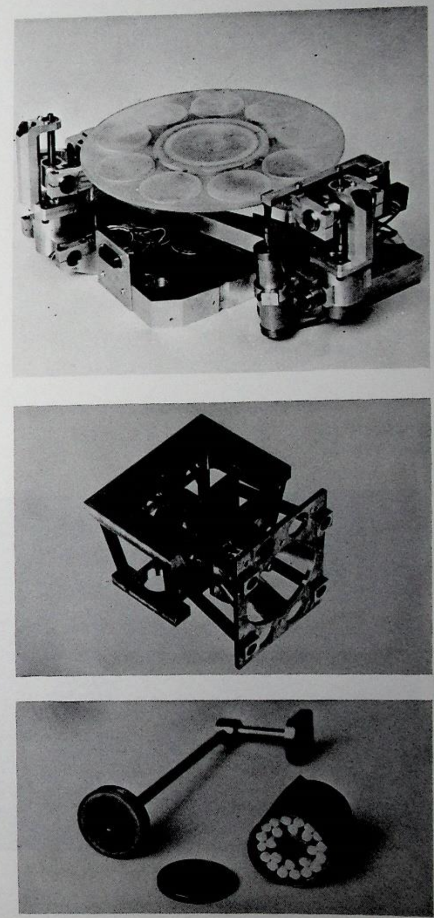

Figure 4.9 Atmospheric research equipment developed for Nimbus G project. (Top) 2 Axis scanning mirror, seen here on a vibration plate. (Middle) Passive cooled cold detector assembly. (Bottom) Molecular sieve for connection to Pressure Modulated Cells.

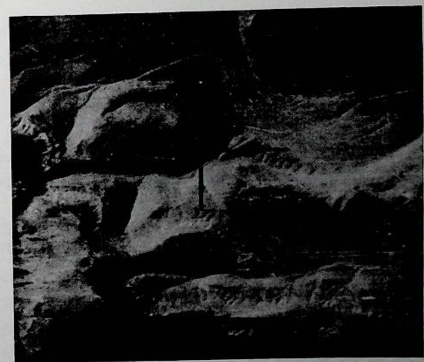

5. Laboratory Computing

Reconstructed digital picture of part of the earth's surface

5. Laboratory Computing

Computing at Rutherford Laboratory has two main functions: to carry out the extensive data handling and analysis required for the High Energy Physics and other research programmes with which the Laboratory is directly involved, and to provide computing services for university engineers and scientists supported by specialist Science Research Council committees. This broad split of activities is reflected in the organisation of the Laboratory's computer resources into the Atlas Computing Division, catering mainly for outside users, and the Computing and Automation Division, supporting the Laboratory's experimental research programme. The two divisions work in close cooperation in areas of common interest to all users, especially in data communications and networks.

5.1 Atlas Computing Division

At the end of August 1975, the Director of the Atlas Computer Laboratory, Dr J Howlett CBE, retired. The responsibility for the Laboratory was transferred to the Director of the Rutherford Laboratory at the beginning of September 1975 when it became the Atlas Computing Division of the Rutherford Laboratory.

This Division provides computing facilities to university-based research workers who obtain approval from the specialist subject committees of the Science Research Council for the computational aspects of their work. The committees which make the awards of computer time deliberate on applications for research grants for which funds are allocated by the Science Research Council through its Science, Engineering, and Astronomy Space and Radio Boards. The Atlas division provides computing facilities to the National Environmental Research Council (NERC) in consequence of the central agreement concluded between the two Councils concerning computing for NERC Institutes, and to other Government funded bodies.

The Atlas computing facilities are based on an ICL 1906A computer and on a 20% share of the Rutherford Laboratory's central IBM 360/195 computer. There is a complex system of connections for data communication to both computers from a large number of British Universities. The usage of the facilities is summarised in Tables 1 and 2.

Microfilm Recording

The Stromberg DatagraphiX 4020 microfilm recorder installed in 1968 has given users access to a specialised output device which records graphical and other information on microfilm or photosensitive paper. An application of the device is the production of cinefilm showing the time-dependent features of a model of a physical phenomenon being studied on the computer.

A decision was reached by SRC to replace the SD4020 machine by a more modern and sophisticated microfilm recorder, an FR80 manufactured by Information International Incorporated of Los Angeles, USA. The equipment was delivered in March and passed its acceptance trial in May. Three cameras arrived as ordered, a hard copy camera, a 16 mm precision camera, and a 35 mm camera. In addition, a microfiche camera was loaned by the manufacturer for a year, and the Atlas Computer Committee agreed to a proposal for its purchase in December.

The software available on the IBM 360/195 and ICL 1906A computers has been adapted or enhanced to permit the use of the FR80 in place of the SD4020. The ICL 1906A software was brought into service in June and that on the IBM 360/195 in November. In both cases the change was brought about smoothly and the very few cases of difficulty were quickly investigated and resolved.

The FR80 has improved features in addressibility and resolution. The quality and the registration of its output is much superior to that of the SD4020, and users have already remarked on the fact.

TABLE 1

Summary of use of Atlas share of IBM 360/195 computer during 1975

	Jan-March			April-June			July-Sept			Oct-Dec		
	Hrs	Mins	Sec	Hrs	Mins	Sec	Hrs	Mins	Sec	Hrs	Mins	Sec
Science Board												
Chemistry	151	23	26	126	26	33	107	42	32	105	43	18
Physics	70	25	28	82	24	0	54	41	58	28	59	45
Biological Sciences and EC & T	1	35	44	2	34	48	3	4	50	4	5	38
Mathematics	1	1	50	1	21	59	2	54	22		15	48
Neutron Beam Research	2	44	0	3	37	32	2	56	27	2	43	5
Meeting House		5	21	3	58	34	10	38	43	6	42	54
Total Science Board	227	15	49	220	23	26	181	58	52	148	30	28
ASR Board	61	39	15	63	40	11	45	25	16	42	25	38
Engineering Board	30	46	7	22	23	37	46	23	3	79	6	39
NERC	13	47	17	14	17	50	21	22	37	16	31	50
Atlas	30	40	8	24	48	5	20	34	16	25	51	49
Miscellaneous	7	14	58	5	27	0	6	0	41	3	56	48
Total	371	23	34	351	0	9	321	44	45	316	23	12

Atlas usage includes development of internal software projects, X-ray, package usage, graphics and other university use

Miscellaneous includes use by the International Seismological Centre, the British Museum and AWRE

TABLE 2

Summary of use of ICL 1906A computer during 1975

	Jan-March			April-June			July-Sept			Oct-Dec		
	Hrs	Mins	Sec	Hrs	Mins	Sec	Hrs	Mins	Sec	Hrs	Mins	Sec
Science Board												
Chemistry	111	31	57	131	29	33	168	22	46	188	12	55
Other subjects	317	18	11	292	18	8	244	52	45	233	6	25
Total Science Board	428	50	8	423	47	41	413	15	31	421	19	20
ASR Board	50	30	33	70	28	6	46	22	9	47	9	20
Engineering Board	105	10	11	140	54	11	190	31	12	155	35	44
NERC	19	47	35	42	56	23	32	11	54	13	15	2
SSRC	4	19	48	7	57	44	3	9	35	6	28	45
MRC	1	43	7	3	1	32	1	13	40	0	29	57
London Office	18	15	20	26	33	48	26	59	8	31	27	24
Atlas	238	40	42	291	41	20	278	29	43	309	25	8
Total	867	17	24	1007	20	45	992	13	12	985	10	40

The Atlas usage includes development work on graphical and other generally applicable software, usage by other bodies for which payment is made, and university use of graphical software

The 'Meeting House'

The objectives of the Atlas Computing Division Meeting House in Theoretical and Computational Physics and Chemistry are to provide a natural focus for activities in the general area of theoretical physics and chemistry for sponsoring projects and providing facilities for collaboration and information exchange among scientists from the universities and other research establishments. Project 1 – Electronic Correlation in Molecular Wavefunctions – has now been established. The Hartree-Fock approximation was a limiting factor in the computation of energy surfaces for use in studies of chemical reactions, and the work of the project will help alleviate this difficulty.

It was decided that the MUNICH-CI (Configuration Interaction) program, due to Professor Dr G M F Diercksen of the Max Planck Institut für Astrophysik at Munich and Dr B T Sutcliffe of the University of York, should be mounted and interfaced with the ATMOL program on the IBM 360/195 computer. The particular interests of the Atlas group in quantum chemistry resulted in the work being done at Chilton. Many improvements and other programs were incorporated during the year so that by September work was substantially complete and the program was capable of working on general open shell systems. Particular attention had been paid to providing a tool for the study of excited states. Interest in the new program system is growing and could lead to substantial demands for time especially on the IBM 360/195 computer.

The working group for Project 1 met in October and December, when a programme of further work was discussed. The 'Meeting House' was deemed to have been successful especially in highlighting the value of implementing and interfacing complex packages as a precursor to more extensive collaborative ventures.

Microdensitometer Operations

The microdensitometer installed on the Atlas premises was purchased by the SRC Chemistry Committee to provide a service to university-based crystallographers. The machine consists of an Optronics P-1000 Photoscan interfaced to a Computer Automation Alpha-16 minicomputer with 16K of 16-bit word storage together with a 7-track magnetic tape drive. The photoscan system converts photometric data on film negatives or transparencies to digital form. The optical densities in the range 0-3D are converted to a range of 256 grey levels, and the intervals of raster for measurement are 25, 50 or 100 microns.

During 1975 nearly 50 chemical structures from 27 different crystallographic groups in the UK have been analysed with the aid of the microdensitometer. Each structure entails the digitisation of an average of 10 film packs each with an average of 5 films. The Weissenberg program has been designed to enable the digitisation and subsequent indexing of the spot data to be done almost automatically and has aroused worldwide interest. The results derived from the completed analysis of the crystal structures show that within the limitations imposed by the film method of recording X-ray data, the machine and the programming method are highly accurate.

During the year the service was extended by the successful introduction of a program to deal with precession films from both small molecules and proteins. At first the indexing program was run separately on the ICL 1906A but this has now been moved to the Alpha-16 where it reduces the delay in determining the success of the scan.

The microdensitometer has applications in areas other than crystallography, although its availability for these users is limited by the priority imposed by the crystallographic service. One such application is in pneumoconiosis screening. Here the objective is to determine which, if any, of a series of lung X-ray plates contain evidence of spots. Trial runs in digitising films for the Medical Research Council (MRC) indicate that a machine of this type could be used routinely to provide this valuable health service of particular importance to the mining industry. The machine also has potential in the optical character recognition field, particularly with reference to films of the printed page, and could enable manuscripts of early texts to be digitised.

An application during the year involved digitising 16 mm and 35 mm film strips which displayed the diffraction patterns of frog muscle fibre exposed to the light of a ruby laser. The experiment aimed to measure the differences in the diffraction pattern caused by muscular contraction and relaxation. The results of the experiment were reported by Dr L Nwoye of Hull University at a conference in Copenhagen, and aroused a great deal of interest.

Other Applications

Much of the work of the Atlas Computing Division lies in sustaining and developing the computing facilities used by university research workers. Many of the projects have considerable scientific importance.

The orbit of the Ariel 5 satellite is the concern of the control centre at Appleton Laboratory. The ICL 1906A computer provides a standby service for Appleton including a test run each day to check the data communications system. In addition, the Mullard Space Science Laboratory at Holmbury uses the IBM 360/195 to analyse the data collected by the satellite. The discovery of stellar X-Ray sources with rapidly varying intensity has provoked great interest in the data, and has stimulated a demand for rapid turnround when the computing facilities are used to investigate a suspected new source.

The work of the primary processing of the Ariel 4 satellite data was concluded early in the year. The Universities of Sheffield and Manchester have continued to analyse the scientific content of the data and the FR80 microfilm recorder plays a significant part in this work.

The data collected in the S2/68 experiment carried on the ESRO TDIA satellite had been almost completely scanned to form a base of information about stars and their positions, when the S2/68 Data Committee decided that much fainter objects should also be included in the base. A rescan of the whole set of magnetic tapes is now in progress, and will continue during 1976.

Other large scale projects being undertaken by university users on the Chilton computers include:

Numerical study of the pulsar magnetosphere by Dr M Petravic of Oxford University;

Study of liquids by computer simulation by Professor K Singer of Royal Holloway College, University of London;

Research in atomic and molecular physics by the group led by Professor P G Burke of the Queen's University of Belfast;

Various studies in quantum chemistry by Professor R N Dixon and others at the University of Bristol.

Molecular orbital calculations on small and large molecules by Dr W G Richards of Oxford University;

Neutron, optical, and X-ray studies of amorphous materials by Dr M J L Sangster of the University of Reading;

Computer simulation of crystalline interfaces by Dr A G Crocker of the University of Surrey;

Computational studies of galactic evolution, fused salts, and semiconductor design where particle simulation methods are applicable by Professor R W Hockney of the University of Reading.

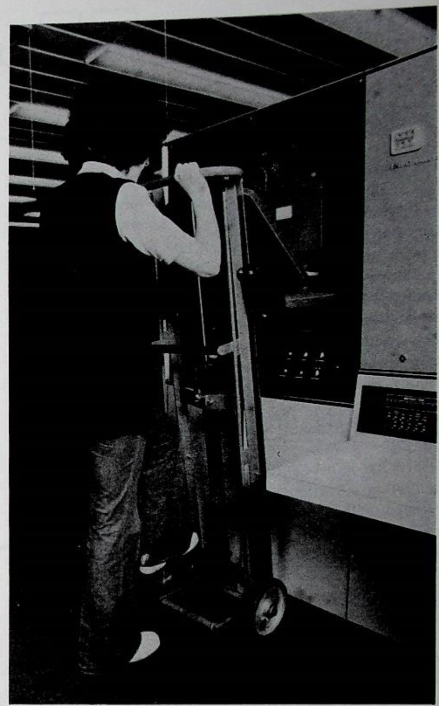

Figure 5.1 Mounting a camera in the FR80 Microfilm Recorder (see p 84).

5.2 Computing and Automation Division

5.2.1 Services

The central Rutherford Laboratory IBM 360/195 computer is a 3 Mbyte machine with an extensive range of peripherals and remote links (see Figure 5.2). The main enhancements to this system were upgrades to tape drives and discs. Four 9-track tape drives were upgraded to quadruple density (6,250 bpi) during the first quarter and the remaining four during the last quarter. Six of the sixteen IBM 3330 disc drives were upgraded from 100 Megabytes to 200 Megabytes, and eight new 200-Mbyte Memorex drives were delivered for installation during the first quarter of 1976. A second Block Multiplexor is on order.

The system remained under saturated conditions throughout 1975, with central processor utilization averaging 89%. Over 8200 hours of good time were available to users. After deducting operational overheads, this provided 5892 hours of accountable central processor time. Despite this extreme pressure, allocations to projects and job turnround have been effectively côntrolled by means of COPPER, a priority system designed to hold back long production runs to off-peak periods and allow several levels of fast turnround during prime shift.

A dominant feature of the installation is the large "star" network giving access from many remote sites. These remote "workstations" provide almost the full range of facilities available to local users, in particular card input, line printer output and on-line keyboard terminal access. The terminals provide file handling facilities (mainly via the Rutherford Laboratory's ELECTRIC system), job entry, output retrieval and graphical output, and can access any of the other facilities provided, including the connections to the US ARPA network. The number of remote workstations has increased by 10 to over 30, and over 50% of all jobs now enter the central computer this way. Printing capacity and line speed have been upgraded for the most heavily used workstations, and some have had an extra 8K of core and more terminals added. Remote computing is now an established and reliable service.

Progress has been made on a number of projects to allow intercommunication between sub-networks. ARPANET in the United States is the best-known linked-computer network, and a link to ARPANET from the IBM 360/195 via the UK node (directed by Professor Kirstein) at University College, London, has been in operation for some time. Any terminal connected to the 360/195 can now submit authorised jobs to computers on ARPANET, and jobs can be submitted from terminals on ARPANET to the IBM 360/195. This latter service is used mainly by collaborators in the United States working with UK groups on high energy physics experiments.

In the UK, the Post Office is well advanced in setting up an Experimental Packet Switching Service (EPSS) with aims similar to ARPANET. Transmission should begin during 1976 and plans are well developed for the Rutherford Laboratory to test this system in collaboration with Daresbury, Edinburgh Regional Computing Centre, Glasgow and other EPSS centres. In parallel with this work and using the same communications protocols, a less ambitious project is in progress to link the 360/195 directly to the Atlas ICL 1906A and the IBM 370/165 at Daresbury.

The Honeywell DDP224 satellite computer was taken out of service towards the end of the year. It was bought in 1965, originally as a front end to the ORION central computer, and at one time served two automatic measuring machines, an interactive display, twelve terminals of various types, and a fast link to the experimental area. Recently it was used mainly as an interface for interactive graphics terminals based on the 360/195, an activity now taken over by a new GEC 4080 computer, which has a processor power of approximately one Atlas unit and is therefore a substantial computer in its own right. It is linked to the central computer, and software has been written to allow job submission, output retrieval and file transfer. Several applications are now using the GEC 4080 for interactive graphics computing. The GEC 4080 is regarded as a natural development of a conventional workstation, giving local processing power backed by a remote job entry service to the 360/195.

Operations

A statistical summary of computer operations appears in the following tables while

$$\text{machine efficiency} \quad \left(\frac{\text{scheduled time - down time}}{\text{scheduled time}}\right)$$

$$\text{and CPU utilisation} \quad \left(\frac{\text{CPU time used}}{\text{scheduled time - down time}}\right)$$

are shown in Figure 5.3. Machine availability remained high, averaging 97·8% (98% in 1974) and CPU utilisation increased to 89% (83% in 1974), representing an extra 601 hours CPU time this year, of which 480 were taken by user programs. This was achieved by system improvements and a full year's use of the third megabyte of core. User jobs rose by 75,000 to over 600,000.

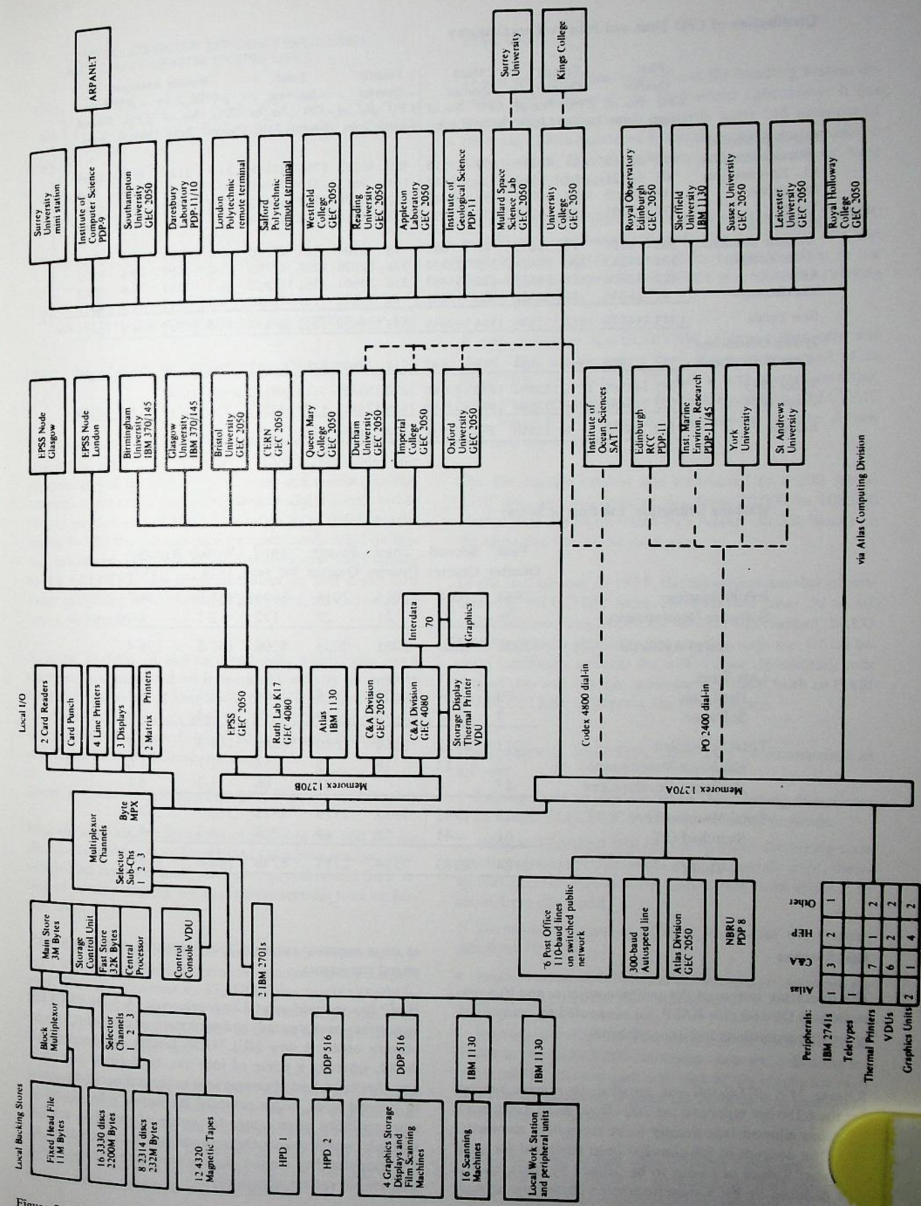

Figure 5.2 The central Rutherford Laboratory IBM 360/195 with its peripherals and remote links.

Distribution of CPU Time and Jobs by User Category

	First Quarter CPU (hours)	First Quarter No. of Jobs	Second Quarter CPU (hours)	Second Quarter No. of Jobs	Third Quarter CPU (hours)	Third Quarter No. of Jobs	Fourth Quarter CPU (hours)	Fourth Quarter No. of Jobs	Total for Year CPU (hours)	Total for Year No. of Jobs	Weekly Averages 1975 CPU (hours)	Weekly Averages 1975 No. of Jobs	Weekly Averages 1974 CPU (hours)	Weekly Averages 1974 No. of Jobs
HEP Counters and Nuclear Structure	427	40916	424	40249	454	41058	459	40273	1764	162496	33·9	3125	26·2	2568
RL–Film Analysis	65	10721	160	9702	125	8310	193	9815	543	38548	10·4	741	10·4	704
RL–Others	77	15662	115	17007	94	17442	92	15376	378	65487	7·3	1259	6·3	1352
Theory	52	5101	24	4277	30	3812	33	4119	139	17309	2·7	333	4·6	541
Universities														
Nuclear Structure	105	5724	72	5830	68	7082	90	8104	335	26740	6·4	514	6·4	402
Film Analysis	204	16312	300	22423	382	22322	321	22098	1207	83155	23·2	1599	20·5	1505
Atlas	372	30306	351	34672	322	31893	316	35961	1361	132832	26·2	2554	27·4	1905
Miscellaneous	41	19836	36	18768	39	17099	49	23183	165	78886	3·2	1517	2·3	1213
User Totals	1343	144578	1482	152928	1514	149018	1553	158929	5892	605453	113·3	11642	104·1	10190
System Control and General Overheads	342	984	390	554	369	642	317	697	1418	2877	27·3	55	25·0	60
Totals 1975	1685	145562	1872	153482	1883	149660	1870	159626	7310	608330	140·6	11697		
Totals 1974	1523	126460	1866	135584	1664	132689	1656	138217	6709	532950	129·0	10249	129·0	10249
Increase	162	19102	6	17898	219	16971	214	21409	601	75380	11·6	1448		

Machine Utilisation (all time in hours)

	First Quarter	Second Quarter	Third Quarter	Fourth Quarter	Total for Year	Weekly Averages 1975	Weekly Averages 1974
Job Processing	1964	2060	2054	2016	8094	155·6	154·7
Software Development	36	23	31	22	112	2·2	1·7
Total Available	2000	2083	2085	2038	8206	157·8	156·4
Lost Time							
Hardware	70	34	22	38	164	3·1	3·1
Software	3	5	7	4	19	0·4	0·3
Total Scheduled	2073	2122	2114	2080	8389	161·3	159·8
Hardware Maintenance	13	12	18	15	58	1·1	1·6
Hardware Development	37	8	–	21	66	1·3	2·1
Total Machine Time	2123	2142	2132	2116	8513	163·7	163·5
Switched Off	61	41	52	69	223	4·3	4·5
Totals	2184	2183	2184	2185	8736	168·0	168·0

IBM Systems

The operating system of the central computer and its workstations is OS-360 plus HASP, supplemented by many locally written extensions and improvements.

Release 21·8 of OS-360 was installed, to provide support for the 6250 bpi tapes and the 200 Mbyte discs. Local modifications allowed tape density to be recognised automatically. The concept of job-class has been abolished for most purposes: instead of having to be defined by users, class is now deduced by the system from other characteristics such as main memory requests, time estimates, and set-up peripheral statements.

HASP has received several improvements. A NORESTART option has been created, and workstations can print jobs in priority order. A new MULTIJOB facility has been introduced, whereby a string of jobs can be defined in such a way that execution of certain jobs in the string can be made to depend upon codes returned by earlier jobs. Another new capability helps a user (or group of users) to ensure that jobs which could otherwise conflict with each other in the resources they require, such as writing to common data sets, are not run simultaneously.

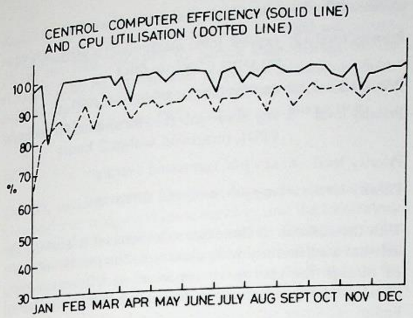

Figure 5.3 Central computer efficiency and CPU utilisation.

The maximum HASP job-number has been increased to 999, which has entailed an increase in HASP's checkpoint area on disc. It will be difficult to increase this number further because a maximum of three decimal digits seems rather deeply written into HASP by its originators. Before the increase to 999 the job queues were temporarily filled on several occasions. The state of the queues is now made known to the ELECTRIC file handling system, so that it can turn away jobs being submitted to a full system, instead of going into a waiting state.

A close analysis of system overheads, which rose more sharply than expected with increased activity at remote workstations, revealed that much of the HASP activity was concentrated in a single area (£GETUNIT). Modifications were made which saved about 10 hours of CPU time per week, and ELECTRIC response improved.

Local Systems – MAST/DAEDALUS

Message switching facilities are provided in the 360/195 by the locally-written MAST/DAEDALUS software subsystem, which also controls local satellite computers and their attached devices. During the year this subsystem took on further work.

1 The IBM STAIRS package (an information retrieval system) has had DAEDALUS terminal handling code incorporated. This allows access to STAIRS from any MAST/DAEDALUS terminal, but only one at a time at present. The main application for STAIRS is the SLAC High Energy Physics preprint database.

2 Routines were written for a PDP 11/45 so that, if attached to the IBM 1130 workstation in the main experimental area, it will behave like a standard device on a standard satellite. This development will allow the PDP 11/45 on an experimental beam line to access the 360/195 for data transfer capabilities, and tests will start shortly.

ELECTRIC

This is an interactive multi-access file handling system designed and written at the Rutherford Laboratory. It has proved very popular, with currently some 615 users out of the total of 866 registered to use the system. In response to user requests, several additions and modifications were made during the year.

A scheme to allow transference of files between ELECTRIC and OS data-sets was introduced. This mechanism was also built into the PRINT command for outputting files to the line printer, and into the ELSEND procedure for entering ELECTRIC files from cards.

A new version of the ELECTRIC reference data card was issued. This was produced from line printer output of an ELECTRIC file using ELECTRIC's text layout facilities. Work began on typing the User's Manual into ELECTRIC files, where it can more easily be kept up to date. A new version is due in 1976.

The file storage data-set was transferred to a 200 Mbyte 3330 disc, and increased in size from 70,000 to 108,000 blocks. This can be increased by a further 30,000 blocks on the same disc should the need arise.

In the first quarter of 1975, the maximum number of simultaneous ELECTRIC users was increased from 30 to 40, and it was not long before the 40 limit was reached. ELECTRIC suffered a gradually deteriorating response, which became intolerable towards the end of June. Monitoring code was written and changes subsequently made, both to HASP and ELECTRIC, to improve the performance.

The changes in ELECTRIC itself may be summarised as follows:

1 Improvement in the algorithm for routing lineprinter output to ELECTRIC in order to reduce overheads;

2 Using an additional 18K of core to avoid overlaying code which processes the commands most frequently used, thereby reducing the number of overlay swaps from about 2 to about 1 per command;

3 Increasing the number of input buffers for users' messages from 32 to 64;

4 Implementing asynchronous job submission to minimise delays caused by HASP's internal reader;

5 Running a utility program once a week to re-order the blocks in the ELECTRIC file storage data-set, collecting together all the files for each user and all the blocks for each file. This considerably reduces the physical arm movement when accessing the disc.

These and other system improvements combined to bring the response time down to an acceptable level before the end of the year, even with 35-40 users logged-in.

The MUGWUMP graphics filing system has filled up on a number of occasions, despite automatic deletion of unused files. Work is beginning on a major change to the filing structure in order to increase the available space and make it more compatible with ELECTRIC's filing system.

Time Control and Turnround

The COPPER facility was designed at the Rutherford Laboratory to share out CPU time according to agreed limits, and to control turnround. As demand has increased, COPPER criteria have been adjusted to provide an effective means of sharing out the available CPU time.

Two further levels of turnround control were added (priorities 6 and 10) during the year. The general user now has a choice of five levels at which to submit his work:

Priority level 12: express jobs, maximum 10 seconds CPU, no tapes or set-up discs

Priority level 10: express tape or set-up disc jobs

Priority level 8: any short job (i.e. maximum 90 seconds CPU), turnround within 2 hours

Priority level 6: any job, turnround overnight

Priority level 4: any job, weekend turnround

With the addition of these two extra levels it is believed the user has a sufficiently wide choice. As the pressure increased through the year the times issued at different priority levels were adjusted to keep turnround within the agreed limits.

5.2.2 Computer Networks

The Laboratory has continued to take an active interest in computer networks with their potential advantages in providing very flexible remote access to computing facilities. During the year work has progressed on three main projects; operational use of the ARPA network, network connection of the Daresbury Laboratory's 370/165 and the Atlas Computer Division's 1906A with the Laboratory's 360/195, and the design of protocols for use with the Post Office's Experimental Packet-Switched Service (EPSS). The Laboratory has also collaborated with CERN, DESY, ESA (European Space Agency) and EIN (European Informatics Network) to make a proposal to the EEC Commission for support of experiments in high-speed data transmission between CERN and Rutherford using the EIN network and the Orbital Test Satellite (to be launched by ESA in 1977).

ARPANET

ARPANET is a telecommunications network connecting some 65 sites in the USA, mostly University and Government research laboratories. An experimental link to the Department of Statistics & Computer Science at University College, London, has been created by the Advanced Research Project Agency (ARPA) to investigate all aspects of such an international link. This Department has had a line to the 360/195 for some time, and as part of the above experiment this line has been connected to the ARPANET via a PDP 9 "gateway".

During the year traffic has been growing between the USA and the 360/195 via ARPANET. By the end of the year some five groups of users, all from collaborating teams involving US members, were accessing the 360/195 from across the Atlantic. The collaborations are involved in High-Energy Physics, Nuclear Structure and Seismology, and nearly 700 jobs were submitted to the 360/195 via ARPANET during the year, taking 2½ hours CPU time.

There is also a growing traffic in the reverse direction, with five UK groups accessing US computers via terminals on the 360/195 connected through ARPANET. Again they are mostly parts of collaborating teams, in High-Energy Physics (accessing machines at Harvard, Illinois and Carnegie-Mellon Universities and at Lawrence Berkeley Laboratory), Atmospheric Physics (accessing the University of California, San Diego) and in Computer Science (using ILLIAC IV at NASA-AMES, and accessing MIT, Boston).

During the year facilities have been arranged to permit Professor F Walkden of Salford University to undertake three dimensional supersonic fluid flow calculations on the AMES Research Centre ILLIAC 4 computer through the ARPA network. The CFD compiler has been obtained and mounted on the IBM 360/195 to permit code written for the ILLIAC 4 to be written and tested by simulation. Some backing store transfer routines have been written with the interface defined by the CFD compiler documentation.

EPSS

The UK national EPSS computer network experiment has been under development for some time, and the Laboratory has continued its active role in the Study Groups set up by the Post Office to design common high-level protocols for use in communications across the network. Protocols for file transfer (FTP) and the use of interactive terminals (ITP) have been agreed and published during the year.

The first test facilities have recently been made available by the Post Office on the London Exchange, and full service is scheduled for the London, Manchester and Glasgow Exchanges by mid-1976. The Laboratory has a 48K bits/sec line to the London Exchange, and work has started on programming a GEC 2050 to act as gateway for this line to be connected to the 360/195. This gateway will be ready for the start of regular service on the network. Work has also started on converting the GEC 2050 Remote Job Entry (RJE) software to allow direct connection of these workstations to EPSS. A slow-speed line (4·8K bits/sec) to the Glasgow Exchange has been installed for testing the new station software, which will also be ready for the start of EPSS service.

Atlas–Daresbury–Rutherford private network

In parallel with the design work for EPSS, work has proceeded on a private network to join the IBM 370/165 at the Daresbury Laboratory, the ICL 1906A at Atlas and IBM 360/195 at Rutherford Laboratory. A joint working party has agreed EPSS-compatible protocols for this network, and testing of the first phase of the development will start at the beginning of 1976. The general plan is for a phased implementation of full networking with protocols compatible with EPSS, allowing the system to function either on the Post Office network or on the existing private lines linking the sites. This will allow the Laboratories to take full advantage of national computer network facilities without excessive dependence on the public network, which at this stage is still experimental.

By end-1976 the connections to the Rutherford Laboratory will be as shown in Figure 5.4.

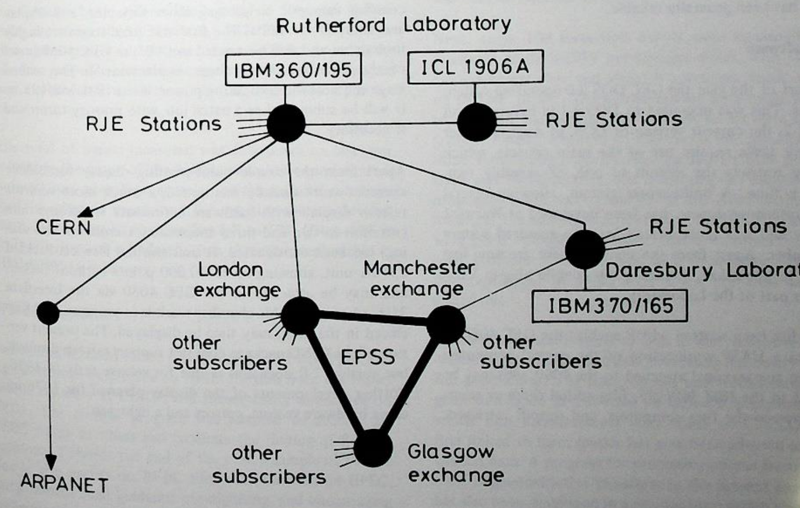

Figure 5.4 Proposed network for Rutherford Laboratory computers.

5.2.3 GEC 4080 Computer

The GEC 4080 was bought in 1974 to replace the old DDP 224 computer (installed ten years ago and the only one of its type still working in Europe). The 4080 is a powerful 'minicomputer' with processing power of approximately one 'Atlas unit' for FORTRAN programs, and will enable interactive graphics programs to be removed from the central computer. This is important because two standard graphics programs (for magnet design and 'rescue' of bubble chamber events) occupy valuable main memory space during their operation.

Hardware

The GEC 4080 configuration at the end of 1975 included 128K of core, a card reader, 200 lines/min Tally printer and a Tektronix 4014 storage display all added during the year, and one magnetic tape unit temporarily attached. A high-speed refresh display with light pen driven by an Interdata 7/16 minicomputer is being used for 'rescue' of failed bubble chamber events, initially as a direct replacement for the old IDI display driven by the DDP224.

There have been some problems with power supplies, magnetic tape drives and disc units, including one severe head crash necessitating replacement of an entire unit, but the hardware has been generally reliable.

System Software

At the start of the year the GEC DOS 2·0 operating system was in use. This was upgraded to DOS 2·1 in February and to DOS 2·2, the current version of DOS, in August. Under DOS many tasks require use of the main console, which effectively restricts the system to one, or possibly two, users at a time. A multi-access system, allowing several users simultaneous access, has been developed at Warwick University and was incorporated into the standard system in September. Apart from the console there are now five terminals in operation, including one mobile plug-in VDU in another part of the Laboratory.

Software has been written which enables the GEC 4080 to be used as a HASP workstation of the central computer. Thus from any terminal attached to the 4080, jobs may be submitted to the IBM 360/195, files edited there or transferred between the two computers, and output retrieved. For example, source files of a program may be held on the central computer and, on instructions from a 4080 terminal, transferred to the GEC machine for compilation and execution. Conversely, work is in progress to give access to the 4080 from any terminal attached to the central computer.

Applications

The new bubble chamber 'rescue' system based on the Hewlett-Packard 1301A was put into operation in November and 2000 events have already been processed. Slight improvements have been introduced but the system, as seen by the operators, is very similar to that which it replaced and the results are very similar. The input data arrives on magnetic tape, and the output, comprising new 'master point' coordinates, is collected on disc and transferred to tape in large blocks for subsequent processing on the central computer.

The standard graphics program package GINO-F (Version 1·8), developed at the Computer-Aided Design Centre in Cambridge, was installed on the GEC 4080 in the summer and is being used in the magnet design program GFUN. The design process falls into three stages: setting up magnet parameters and making preliminary small calculations; calculating magnetic fields and other variables; and display and analysis of results. The first and third stages are highly interactive and will be carried out on the GEC 4080 (most of the first has already been implemented). The second stage requires the computing power of the IBM 360/195, so it will be submitted as a batch job, with priority turnround if necessary.

Apart from the simple point-plotting display for bubble chamber work already mentioned, a much more versatile refresh display with hardware coordinate transformations (rotation in two and three dimensions, translation and scaling) has been constructed. It uses another Hewlett-Packard 1310A unit, showing up to 40,000 points without flicker, and may be attached to the GEC 4080 via the Interdata 7/16 when no bubble chamber work is in progress, and files stored in the 4080 may then be displayed. The present version of the GINO package does not support refresh displays, but version 2·0 does and is due for release early in 1976. Further developments of the display planned for 1976 include hardware vectors, cursors and a light pen.

5.2.4 Film Measuring and Data Analysis

HPD (Hough-Powell Device) Operations

Measuring has been concentrated this year on film from the CERN 2-metre chamber and the older Saclay 81cm chamber. The numbers of three-view events (including remeasures of GEOMETRY/KINEMATICS failures) were

K^-p (14 GeV/c) (Experiment 8)	5,000
π^+d (4 GeV/c) (Experiment 6)	6,000
K^0p (< 1 GeV/c) (Experiment 16)	40,000
K^-p (~1 GeV/c) (Experiment 14)	
in 2m chamber	57,000
in 81 cm chamber	82,000
	190,000

Measuring for the 14 GeV/c K^-p and 4 GeV/c π^+d experiments is now finished. A total of 302,000 events was measured over five years for the K^-p experiment from film taken in 1969-1972, and 276,000 (including 46,000 for Durham) on π^+d film exposed during 1970-1972.

The K^0p events included all those remaining on film exposed in 1972, and 34,000 on 1974 film. The low energy K^-p events in the 2m chamber included 11,000 to complete the second run of this long experiment in 1970, and 27,000 pre-digitised by a collaborating group at Imperial College using film from the third run in 1972. The 81cm chamber film was exposed in 1970 and was originally intended for another purpose, but it contains many events for the present experiment, of which nearly half were measured in the year.

The total of events measured was 45% down on last year, reflecting the state of the bubble chamber experiments in progress, and advantage was taken of the reduced measuring load to schedule more time for machine system development. There was an encouraging fall to 12% (from 16% in 1974) in loss of scheduled time directly attributable to HPD-DDP516 hardware.

HPD Development

Some modifications to the film transport and signal processing electronics were made on HPD2 for film from the BEBC bubble chamber at CERN, and subsequently duplicated on HPD1. The control program was adapted to decode the BEBC frame numbers and facilitate the finding of fiducial positions. Towards the end of the year, a sample of 100 22 GeV/c π^-p events on BEBC film was measured on HPD2, using normal road guidance pre-digitising, and encouraging preliminary results were obtained. Film from the CERN 2-metre chamber was measured on HPD1, with results generally similar to HPD2. The main control console was modified to allow operation of both HPDs, and an engineer's mobile auxiliary console provided. Nearly all of the hardware changes were completed by the end of the year, and DDP516 software to support the new consoles and tandem HPD operation is well advanced. It was decided to amend the HPD control program in the central computer so that it should communicate directly with the DDP516 satellite computer, instead of using the MAST message-handling software, and this work was well under way by the end of the year.

Software

Software developments have been concentrated on BEBC film and data from the π^-p spark chamber experiment at Nimrod (experiment 12). The latest version (3·22) of the CERN HYDRA programming system was made available on the central computer, and provides additional features required by the large bubble chamber geometry (LBCG) processors now current. Tests were made on 22 GeV/c π^-p events from BEBC (experiment 27), starting with 12 four-view events measured on a Vanguard semi-automatic machine. All visible fiducial marks were measured, for determining optical constants, together with a maximum of 28 points on each track, spread over an arc length up to 360°. Reconstruction in LBCG showed track errors equivalent to less than 10 microns on film.

Next, some 200 three-view events were measured on the relatively crude BESSY pre-digitiser tables, with four fiducial marks per view and about 8 points per track, covering up to 180° of arc. The measurements were made primarily to establish the system, and helix fit errors were naturally greater. Finally, a sample of 100 events was pre-digitised on three views using ordinary road guidance (three points per track and two fiducials), but restricting the length of track measured to not more than 90° of arc. After setting-up the machine, the sample was measured on HPD2. The results were good enough to indicate that a modified version of road guidance could be used as a production system for this experiment in BEBC after a few problems have been sorted out.

Vidicons are used instead of film in the Nimrod π^-p spark chamber experiment, and data processing has nearly reached full production. The track finding and reconstruction program developed in 1974 for an earlier π^-p experiment, in which film measurements were made on CYCLOPS, and first linked to form sparks, has now been adapted to handle vidicon data. A program for processing output from the low mass magnetostrictive chambers in the present experiment has also been developed in a general form which should find other applications. Finally, a system was established for generating optical constants automatically from grid information. This will simplify an awkward first stage of production data processing.

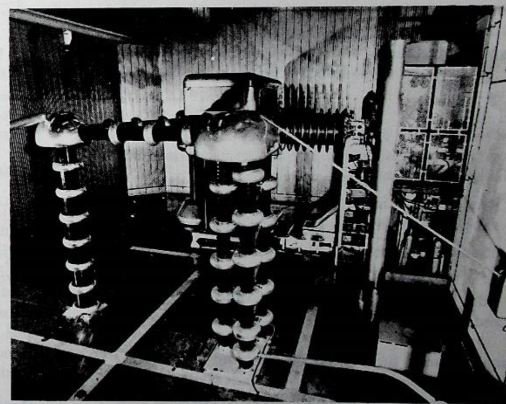

6. Accelerator Operations and Development

High-voltage area for accelerator injector

6. Accelerator Operations and Development

Accelerator operations at the Rutherford Laboratory are centred on Nimrod, the 8 GeV/c proton synchrotron, which is an integral part of the UK High Energy Physics research programme and forms a central facility for use by many collaborations of scientists at both national and international level. The new 70 MeV injector, now being commissioned, will considerably enhance the capabilities and resources available for a wide range of research activities.

Preliminary studies have indicated that an 800 MeV high intensity proton synchrotron for producing intense fluxes of neutrons and pions can be built very economically at the Rutherford Laboratory.

6.1 Nimrod

6.1.1 Operation of Nimrod

Nimrod has continued to operate on a 3-weekly cycle. Usually about 17½ days of each cycle were allocated to High Energy Physics, with the remainder being accounted for by start-up, accelerator development and minor maintenance.

Nimrod was shut down from February to June, for a large programme of installation and major maintenance work. This included amongst other items:-

1 Rebuilding of the Hall 1/Magnet Room main shield wall, associated with the new Hall 1 beam complex.

2 Installation of the new X1 extracted proton beamline in the magnet room.

3 Work in connection with the new 70 MeV beam transfer and inflector system.

Running during the year was mainly into Hall 3, where a total of six experiments could be provided with beams simultaneously. Two of the newly installed beams in Hall 1, K18 for the Rapid Cycling Vertex Detector (see Experiment 19), and K20, started preliminary beam tuning in November. Simultaneous sharing of the beam between the Hall 1 and Hall 3 users was realised by using the "peeling off" technique (see Section 6.1.2).

The operations record is:

High Energy Physics Research	Hours
Scheduled time	3700·3
Realised beam time	3208·1
i.e. "beam on" for 86·7% of scheduled physics research time	

The remainder of the year is accounted for as follows:–

	Hours
Machine Physics and start-up	1039·0
Routine maintenance and minor modifications at 21-day intervals	212·3
Shutdown periods for major modifications and maintenance, including Christmas holiday	3808·4

Total number of protons accelerated to full energy was about $13{\cdot}6 \times 10^{18}$

Machine pulses, with beam, totalled $4{\cdot}17 \times 10^{6}$

Circulating beams in excess of 4×10^{12} protons per pulse and extracted proton beams of typically 2×10^{12} protons per pulse were readily and reliably achieved. A peak extracted intensity of $2{\cdot}3 \times 10^{12}$ protons per pulse was recorded for a short period of running. Machine repetition rates varied between 15 and 22 pulses per minute, with flat-tops of 550-900 milliseconds, according to user requirements.

Analysis of Nimrod Off Time

Total Scheduled Operating Time 4739·34 hours
Total Off Time 832·91 hours

	Beam Time Lost Hours	% of Scheduled Op Time	% of Nimrod Off Time
1. Faults and Routine Inspections			
Vacuum Systems	173·72	3·67	20·86
Extraction Systems	(130·08)	(2·74)	(15·62)
(a) Power Supplies	56·63	1·19	6·80
(b) Plunging Mechanisms	50·72	1·07	6·09
(c) Magnets	22·73	0·48	2·73
Coolant Systems	103·33	2·18	12·41
Synchrotron RF/Beam Control/ TV/Diagnostics	90·97	1·92	10·92
Beam Line Magnets (in machine areas)	80·87	1·71	9·71
Injector	70·29	1·48	8·44
Nimrod Magnet Power Supply	(55·65)	(1·17)	(6·68)
(a) Converter Plant	27·52	0·58	3·30
(b) Rotating Plant	22·73	0·48	2·73
(c) Ripple Filter Plant	5·40	0·11	0·65
Inflector System	27·63	0·58	3·32
Nimrod Magnet	5·37	0·11	0·64
Targets and Target Mechanisms	3·18	0·07	0·38
Pole Face Winding Systems	2·14	0·05	0·26
Miscellaneous	28·86	0·61	3·46
2. Other Reasons			
Start up	50·83	1·07	6·10
Public Electricity Supply	9·99	0·21	1·20
	832·91	17·57	100·00

Figures for Vacuum and Extraction Systems include routine inspection time.

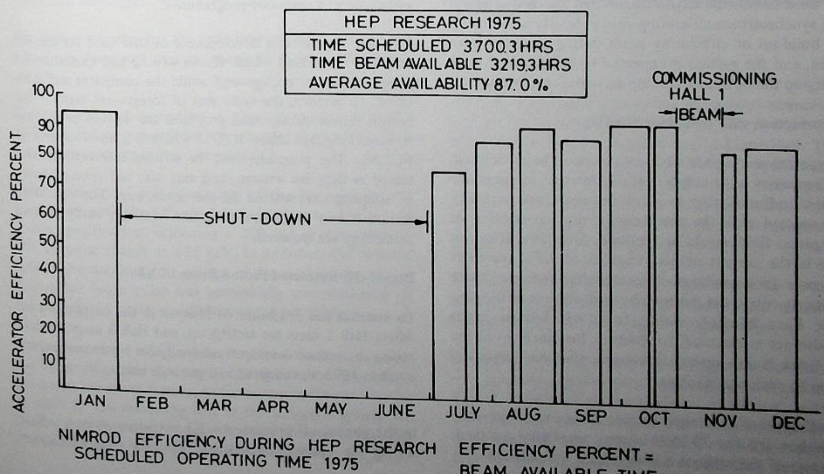

Figure 6.1 Nimrod operation record during 1975

Magnet Power Supplies

The magnet was pulsed during the year using both motor alternator flywheel sets and the complete converter plant with good overall performance. The arc back rate continued at a very low level.

Operating statistics for the year are as follows:–

Machine running time	4645 hrs
Machine pulsing time	4446 hrs
Total pulses	4,957,160

Nimrod has now completed over 75 x 10^6 pulses.

Drive Motor

Because the fault in No 1 drive motor stator (reported last year) was rather unusual with an inherent risk to the insulation, it was decided to carry out a Dielectric Loss Analysis on the stator windings after repair in addition to the conventional tests, in order to prove its integrity.

All the tests proved satisfactory and the repaired motor was re-installed and commissioned in April 1975. The bi-directional motor thus reverts to its status as a spare.

6.1.2 Nimrod Development

Beam Measurement at Injection

To do measurements on full intensity, unstructured circulating beams, a full aperture ferrite beam transformer was installed in a straight section of the machine. The transformer used one of the ferrite frames that are held as spares for the synchrotron accelerating cavity. Satisfactory signals of the build-up of circulating beam during injection were obtained, and the system is expected to be of special value in setting-up the optimum conditions with the new injector.

Field Correction with Pole Face Windings

Measurements were made of the variation in betatron oscillation frequency with radius over the aperture of the machine. These indicated that to accelerate the higher intensity beam expected with the new injector more correction of the magnetic field would be required. This necessitates an increase in the current-carrying capacity of the connections to the pole face windings. The upgrading is taking place progressively round the machine by replacement of the plastic Pole Face Winding cooling tubes with copper pipes which also act as electrical conductors. Replacement of the plastic tubes is also necessary because they have deteriorated due to radiation damage.

The cooling tubes at Straight Section 2 were replaced while the new box for the 70 MeV injector was being installed. Only 3 sets of the original 8 now remain unmodified.

Control Room Computer

During the Nimrod shutdown the operating system of the main control room PDP-8 computer was changed in such a way that the insertion of a new task no longer required the assistance of a specialist programmer.

The new system is a development of that used on the K9 and K19 beamlines which allows writing and execution of programs in the background while the computer still continues to perform the same sort of foreground tasks it did before. These background programs are written in an easy to learn language called RTI-75 which is a development of FOCAL. The programs may be written interactively and tested as they are written, and may also call upon a library of subprograms written in the same way. The operating staff can now write new programs relatively easily, as and when they are required.

Peeled Off Extracted Proton Beam to X1

To increase the flexibility of Nimrod in the particular case where Hall 1 users are setting up, and Hall 3 users are data taking, a method developed originally for a previous experiment in 1973 was adapted and put into use.

In the peeling-off process, the X3 extraction system is first set up for optimum efficiency. The X1 plunged extract magnet is then positioned radially so as to divert some of the X3 protons on their way to the X3 exit port into the X1 exit port on Nimrod. This method permits a full energy, low intensity beam of a few 10^{10} protons per pulse being sent to Hall 1 users and about 1·8 x 10^{12} protons per pulse to Hall 3 users every machine burst.

Measurement of Extracted Beam

A system of strip secondary emission chambers was built for the Hall 1 extracted beamline, which allows the beam position and profile to be measured in the horizontal and vertical planes at up to 16 positions. The system is controlled via the main control room computer and data from any three chambers can be displayed on each beam pulse. The system was first used during the commissioning of the new X1 extracted beam complex.

6.1.3 70 MeV Injector for Nimrod

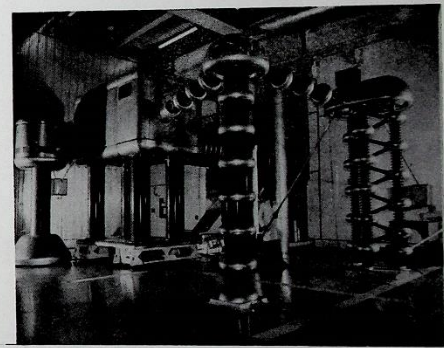

Installation of the major components of the new injector was completed during the year and the commissioning of individual items of equipment proceeded.

The fourth and final accelerating tank was delivered in June and installed in its final position in the Linac Hall. Problems with brazing and electron beam welding processes in the manufacture of the drift tubes for this tank and for tank 1, which had delayed manufacture, were finally solved and delivery of the drift tubes was completed in September. An extensive programme of drift tube vacuum testing, and of insulation and magnetic testing of the associated quadrupole focussing magnets was carried out by Laboratory staff, covering all stages of manufacture and concluding with acceptance tests once the drift tubes had been finally closed by electron beam welding. All drift tubes have now been assembled and aligned within the tanks.

The power supplies for the drift tube quadrupoles and for the beam transport system magnets were installed and tested.

Measurement and correction of the accelerating field distribution at low power level was completed on tanks 2 and 3 and is proceeding in the case of tank 1.

Final operational commissioning of the pre-injector was completed with the DC accelerating column achieving its design specification, delivering a 200 mA proton beam of 500 μs pulse length at 665 keV. In addition, the bouncer system, for stabilising the voltage of the accelerating column during the beam pulse was successfully commissioned on the pre-injector under conditions of full beam loading.

Measurements on the pre-injector beam were made using the beam diagnostic equipment installed in the first half of the beam transport system, which connects the pre-injector to tank 1. The remaining half of the transport system, including two focussing magnets and the bouncer cavity, will be installed when work on tank 1 is completed.

Another important stage in the equipment commissioning was achieved with the operation of the first of the four identical RF systems installed in the Linac Hall. This system was successfully operated at its full specification, delivering a power of 4·25 MW to a dummy load with 800 μs pulses at a repetition rate of 1 pulse per second. RF power of 1·7 MW has also been fed into tank 2 to achieve the required field level for proton acceleration.

The RF field level stabilisation system and the servo tuning system for tank 2 were both satisfactorily tested during high power operation of tank 2 without beam.

During the Nimrod shutdown Straight Section Box No. 2 was removed together with its plunging mechanism. A new Box 2, which sits at the junction of Nimrod and the 70 MeV injector, was installed and the inflector mounted within it. Also the main components of the beam transport system between the linac and the synchrotron were installed.

The system comprises 21 quadrupole magnets arranged as triplets, four steering magnets, two bending magnets and an electrostatic deflector, as well as a de-buncher cavity and an extensive system of beam monitoring equipment.

The de-buncher will be fed with RF power via a fast acting ferrite phase shifter. This device will allow the energy of the injector beam to be changed by up to 1 MeV during the 500 μs pulse to optimise the injection into the synchrotron.

The Nimrod GEC 4080 computer was delivered and installed during the year. Programs to assist in the commissioning stages of the injector were written, and some of the interfacing to the diagnostics and control system was developed.

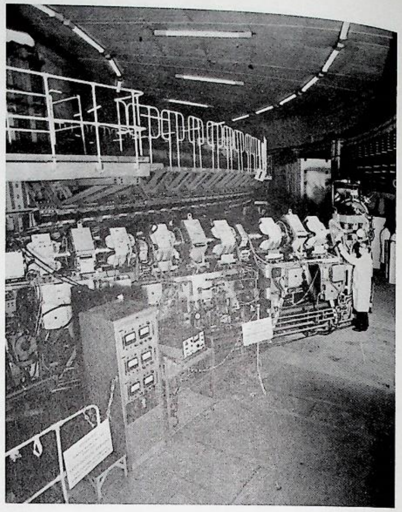

Figure 6.3 Part of the beam transfer system from the 70 MeV injector into Nimrod.

6.1.4 Experimental Areas and External Beams

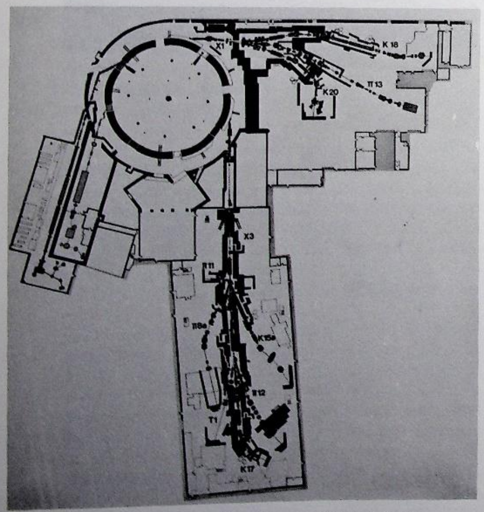

Figure 6.4 Nimrod experimental areas and external beams.

Hall 1

The year commenced with the removal of the P81 beamline. Later in the year equipment was installed in the new blockhouse in Hall 1. The blockhouse is of spacious design to reduce handling times for component removal. Control equipment for water, electrical services and vacuum pumping equipment are located outside the blockhouse where personnel are shielded from areas of high induced activity.

The X1 beam emerges from Octant 3 and is split into three branches each feeding one secondary beam. In Phase 1 the beam is shared between them on a pulse by pulse basis with a pair of switching magnets located in the Magnet Hall.

Preliminary commissioning of the extraction system yielded fluxes of up to 2×10^{12} protons per pulse using the conventional thin-septum Piccioni method. The alternative "peeling off" X1 extraction system referred to earlier gave a flux of $\sim 5 \times 10^{10}$ ppp for a 10% reduction of X3 intensity. This is sufficient to allow the three Hall 1 secondary beams to do much of their setting up work and also one of them ($\pi 13$) to take a significant fraction of its data in parallel with Hall 3 data taking, which significantly improves the scheduling of the overall Nimrod experimental programme.

Hall 1 – Phase II Sharing Scheme

Design work for the Phase II sharing magnets, described in last year's Report, has been completed and a prototype 10 mm septum magnet has been built.

Hall 2

It has been decided to discontinue the role of Hall 2 as an experimental area for experiments taking secondary beams from targets internal to Nimrod. The area was cleared of equipment and a store for the mounting number of radioactive components was established there.

Hall 3

On completion of the $\pi 9$ experiment a test facility called T1 was set up in its place to permit the checking of experimental equipment prior to its installation in its final location. Four teams of physicists had used the facility by the end of the year.

N5 Beam for Experiment 41

Design work was carried out for the installation of a neutral Kaon beam to replace the present $\pi 8a$ beam at the X3 target station in Hall 3 during 1976. The beam consists of a series of collimators and magnetic fields to sweep clear the charged particles from the target and those produced by secondary interactions down the beam. A production angle of 16° is used to take advantage of the faster fall-off neutron production over that for Kaons. The beam acceptance is 10·4 μsr and is limited by the small dimensions of the experimental apparatus and the beam length required to clear out the charged particles.

Predicted fluxes for the beam are $1{\cdot}9 \times 10^4$ Kaons and $7{\cdot}2 \times 10^5$ neutrons for 10^{12} protons incident at the X3 target. The variation in relative particle flux with production angle is shown in Figure 6.5.

Electrostatic Separators

The two separators installed in Hall 3, a single tank unit in K17, and a three tank unit in K15a, have operated satisfactorily during the year. The single tank unit has had its performance improved and is operating with an 80 mm gap and an electric field strength of 7·5 kV/mm.

Three separators have been installed in the new Hall 1 beam complex: a single tank unit for K20 and a two tank unit for K18.

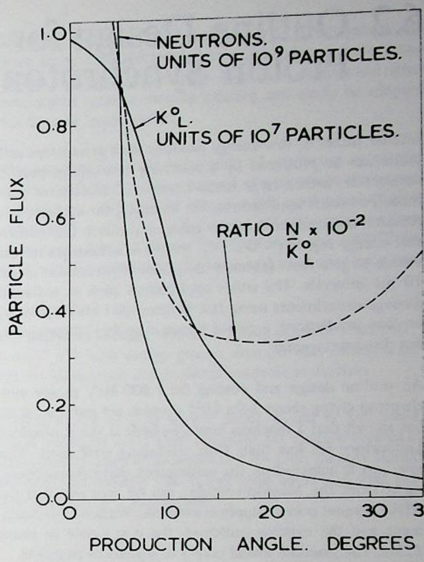

Figure 6.5 Variation in particle flux with production angle for proposed N5 beam.

6.2 Outline Design for a High Intensity 800 MeV Proton Synchroton

Intense fluxes of low energy particles such as neutrons and pions can be produced by a relatively low energy proton accelerator with a large mean current of accelerated protons. For some applications, for example, for carrying out research on condensed matter using neutrons in the epithermal energy region ($\sim$ 0·1 eV), there are advantages for the source to give short (about 1 μs) pulses of particles at about 10 ms intervals. For other applications such as radiation damage experiments using fast neutron (0·1 MeV upwards) or pion irradiations, a pulsed source is neither advantageous nor disadvantageous.

An outline design and costing for a 800 MeV proton synchrotron giving about 2·5 x 10^{13} protons per pulse at 50 Hz has shown that a machine could be built at the Rutherford Laboratory for less than £7m, excluding staff costs. This low cost is achieved on the assumption that existing equipment from the Nimrod complex can be used and that the NINA magnet power supply is available. Without this equipment and the existing buildings, the cost would be about £25m. The machine would take 3 to 4 years to complete.

The basic specification of the machine is:

Energy	800 MeV
Protons/pulse	2 x 10^{13}
Protons/sec	1 x 10^{15}
Injection energy	70 MeV
Peak magnetic field	0·7 Tesla
Beam size vertical	140 mm
horizontal	280 mm
Bending radius	7 m
Mean radius	26 m

Although the peak energy is low, the fast cycling nature (50 Hz) of the machine, which requires long straight sections for the accelerating RF cavities, leads to the relatively large mean radius. The machine fits conveniently into the Nimrod magnet hall (see Figure 6.6). To reach the space charge limit of 2·5 x 10^{13} protons per pulse, 20 mA of H^- ions are accelerated in the Nimrod 70 MeV injector and stripped in the accelerator to give the required number of protons. A new magnet system is required made from thin laminations to cut down eddy current effects. It is anticipated that initially the NINA magnet power supply will be used (at a saving of about £1·3m); further optimisation is required to determine whether the full energy will be reached with it. The vacuum requirements are not onerous – about 5 x 10^{-7} Torr – and will be achieved by using the magnet structure to form the vacuum vessel as in the Fermi Laboratory booster. The peak RF accelerating voltage is 140 kV. There is a frequency swing from 0·7 MHz to 1·6 MHz requiring cavities tuned by biassed ferrite. The total length of RF cavity is 12 m distributed in two of the five straight sections. Two of the other straight sections contain the equipment for extracting the protons into Experimental Halls 1 and 3. The pulsed nature of the accelerator giving 0·5 μs pulses of protons every 20 ms is well matched to time of flight techniques with neutrons. The existing Halls appear to be well suited to contain the experimental equipment. Control of the accelerator is carried out using a computer control system of which the central computer is the Nimrod GEC 4080 control computer.

The Nimrod magnet hall provides sufficient shielding for the accelerator. 'Hot-spots' can be covered by the use of existing shielding. Care will have to be taken to control beam losses to reduce induced activity levels. Components will have to be designed bearing in mind induced activity and radiation damage in materials. Electrical, cooling and other mechanical services already existing can easily be adapted for the new requirement.

The accelerator would be capable of producing an average of 3 x 10^{16} neutrons per second at a target in the experimental area. This would give a peak epithermal flux of about 10^{16} n cm^{-2} s^{-1} eV^{-1} at 0·5 eV which may be compared with 2 x 10^{14} n cm^{-2} s^{-1} eV^{-1} in the 2000°C hot source at the reactor at the Institut Laue-Langevin, Grenoble.

For radiation damage studies it would produce about 10^{14} n cm^{-2} s^{-1} with energy greater than 0·1 MeV, about a factor ten higher than usable fluxes available at reactors.

Intense beams of 150 MeV/c pions would be produced. These would be more than adequate for medical studies of the effect of pions on tumours and for pion therapy should clinical trials indicate that it has some advantage over present radio-therapy techniques.

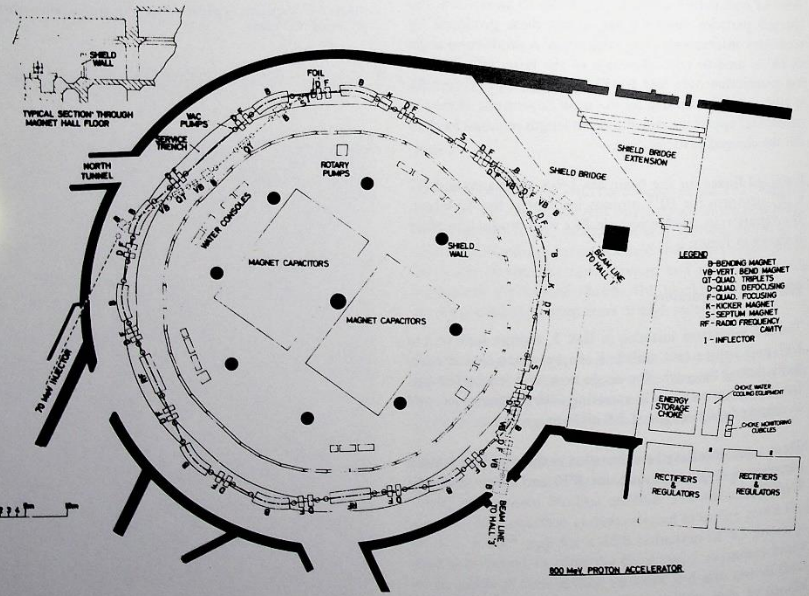

Figure 6.6 Proposed design of high intensity synchrotron.

6.3 EPIC

Plans for EPIC, which would have given the United Kingdom a chance to provide a facility unrivalled in the world, foundered during 1975.

As indicated in the 1974 Report, a proposal to build EPIC, a 14 GeV electron-positron storage ring, was presented to the Science Research Council in November 1974. The Council endorsed the strong scientific case for EPIC but in view of the uncertainty of financial resources deferred giving final approval but invited exploration of possible international participation in the project. During the year work continued on improvements to the design of the machine and on experimental work which had relevance to the general technology of accelerators and storage rings as well as to EPIC. The work specifically for EPIC was terminated in September when the German government approved PETRA, a machine similar to EPIC but without the development potential to go to electron-proton physics, at the DESY laboratory at Hamburg. With the approval of PETRA, financed on a national scale, EPIC will clearly not be built since discussions at, for instance, ECFA (European Committee on Future Accelerators) indicated that one high energy electron-positron storage ring in Europe is sufficient to support the physics need. Discussions are under way to investigate arrangements for British physicists to use PETRA.

Development of the design

Developments of the design for EPIC were reported in an Addendum to the Proposal (Rutherford Laboratory Report RL-75-146). One of the main improvements to the design was in the method of filling the main storage ring with positrons.

The filling time of a storage ring is limited mainly by the rate of production of positrons in the injection system, and by the need for a slow cycling rate determined by the beam size damping time in the main ring. The first limitation can be overcome by pulse modulating the beam into fewer bunches of higher intensity as described in the EPIC Proposal; the second by the use of a fast cycling booster and an intermediate storage ring, or, as developed for EPIC during this year, by letting the main ring act as its own intermediate storage ring. This accretion scheme for filling the main ring follows a proposal for the Cornell Storage Ring (1975).

The main ring accumulates the charge in many bunches injected in bunch trains from the fast cycling booster. When the required total charge is obtained, the bunches are collected into the two bunches required for the collision mode (the 'accretion' bunches). Each bunch is in turn transferred to the booster which acts as a delay path to return it to the main ring with appropriate phase so that it coincides with one of the accretion bunches. The main ring and booster remain at fixed energy, 5 GeV, during the accretion process. To achieve correct phasing between the main ring and booster there must be precise relationships between their circumferences; their respective RF frequencies; and the length of the transfer lines which must be related to the bunch spacing. For the EPIC system there were 10 bunches in the booster and 91 in the main ring prior to accretion, and their circumferences were in the ratio 10/91.

The components of the EPIC injection were as before, ie. a 100 MeV electron linac, a 200 MeV positron linac, a 5 GeV booster synchrotron (NINA, suitably modified), which now cycles at 53 Hz. Thus the original resonant combination of NINA magnets and power supply could be used unmodified, with a considerable saving in cost.

Further study indicated that there was a somewhat conservative estimate for the RF power requirement. Using the same amount of RF power as in the proposal, viz. 4 MW, the centre-of-mass energy at which maximum luminosity could be achieved was raised from 28 GeV to 29·5. Finer control of the beam size and characteristics, with a view to achieving the best possible luminosity-energy relationship, was achieved by the introduction of a variable triplet of combined function (bending and focusing) magnets in place of the singlet combined function magnets in the proposal and by the addition of dipole 'wiggler' magnets at the end of the curved part of the magnet lattice. Space was also allocated at the end of the insertions for magnets with reduced magnetic field. These were introduced to lower the energy of X-rays from local synchrotron radiation, resulting in a reduced background problem at the experimental apparatus.

More detailed investigation allowed the vertical space for the beam in the vacuum vessel to be increased without changing the magnet gap. This was necessary following experience on the lower energy storage ring SPEAR at SLAC.

Modifications to the design of the main ring vacuum vessel were also made to make the inside shape of the vessels the same through the dipoles and quadrupoles in the curved part of the machine. This was to minimise the RF power losses resulting from higher order mode excitation in cavity-like structures in the vacuum vessel.

The operating currents for the magnets were generally increased with a resultant simplification in the magnet coils. A simplified form of RF cavity structure was proposed in which the cavities are constructed from oxygen-free copper by brazing or electron beam welding.

The control system proposed for EPIC made use of a distributed computer system employing 19 computers linked together via serial data links. Primary interfacing between the computers and the storage ring equipment was via both serial and parallel CAMAC systems. The software was based on a control language real-time interpreter with direct access to the computer operating systems. Enquiries indicated that suitable computers, complete with adequate software systems could be obtained from several manufacturers.

Experimental work

A 2-cell aluminium RF cavity was obtained to study the longitudinal and transverse higher modes in cavities for high energy storage rings and to evaluate different cell-coupling schemes. It is planned to continue this work. A single-cell copper model was used to study the relative merits of electron beam welding and hydrogen furnace brazing for fabricating multi-cell cavities. This work is being done in conjunction with the Welding Institute.

Two 30-foot-long SPEAR vacuum chambers were obtained from SLAC to aid in the development of pumping and cleaning techniques for aluminium vessels. A small chamber capable of achieving 10^{-10} Torr has been commissioned. This is useful for outgassing tests on small samples and has already found application in tests on materials in scientific experiments in rockets. In order to investigate cheap methods of manufacture, two 4·5 m long magnet dipoles have been assembled. One is made from mild steel, the other from special magnet steel. Measurements are in progress to enable valuations of the different types to be made.

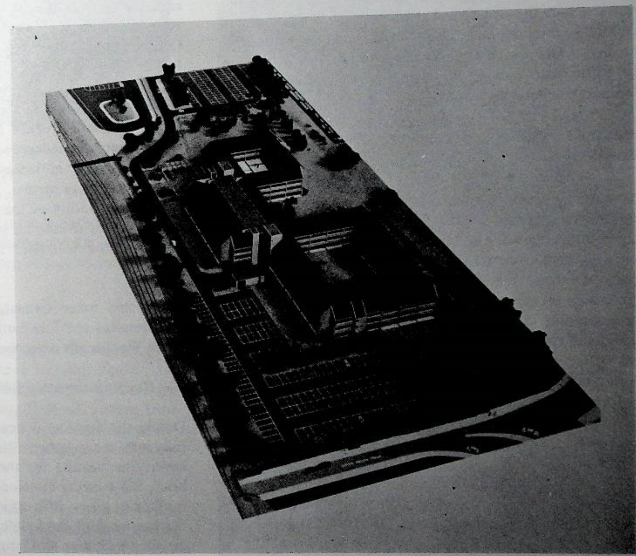

7. Design and Construction of Buildings for the Science Research Council

Proposed development for SRC and NERC at Swindon

7. Design and Construction of Buildings for the Science Research Council

In April 1972 the Science Research Council Works Unit was set up at the Rutherford Laboratory with the following terms of reference: "To provide to all Council establishments and other nominated participants a consulting engineering service; to undertake new works of a specified magnitude and the maintenance of plant and buildings; and to provide advice as required by Operating Divisions on construction work financed from research grants."

During 1975 the Council Works Unit has again had another active year carrying out a wide range of work at the SRC establishments which call upon its services. These establishments include the Appleton Laboratory, the Chilbolton and Winkfield Observatories, the Royal Observatory Edinburgh, the Royal Greenwich Observatory, the London Office and the Rutherford Laboratory, which now includes the Atlas Computer Laboratory.

Appleton Laboratory, the Chilbolton and Winkfield Observatories

The construction of the new Computer Building with its Integrated Environmental Design Concept continued, progressing throughout the year according to schedule. The building will be completed and commissioned in early 1976 ready to receive the ICL 1904A computer in the Spring. The design incorporates heat-recovery techniques and with the computer in operation, sufficient heat is recovered to provide all requirements for re-heat on the air conditioning and office heating under all weather conditions. Special consideration was given in the design to the good thermal performance of the building envelope and to the particular noise problem at Appleton Laboratory with the flight path from Heathrow overhead.

In conjunction with the Computer Building new electrical supplies have been installed and extensive modifications made to the 11KV and 415v supplies at the Laboratory to allow for the increased loads and improve the security of the supply.

A considerable amount of work was done during the year on the design for a major development at the Appleton Laboratory site. The design included for office accommodation, laboratories, balloon test facilities, a conference room and plant room. The design covered some 2500 square metres. Several alternative schemes were considered again using traditional construction similar to the new Computer Building with energy conservation very much in mind. An Industrial Development Certificate was obtained and estimates submitted.

A new building extension to house a balloon test facility was completed and handed over.

The UK5 control centre has been extended to cater for the UK6 satellite project. This had to be carried out with the minimum of down-time of the existing area with in-flight control of the Ariel V satellite taking place from the existing control centre.

Various other works have also taken place at Appleton, eg the design of a new Gatehouse, upgrading of the Spur road and modifications in the Main Building, including the provision of a new staircase to comply with the Fire Prevention Officer's requirements. Optimum Start Controls were added to the boilers to give better fuel economy.

A building extension at the Chilbolton Observatory, consisting of laboratory, office and storage accommodation, was completed and handed over. This work also included a new boiler and air conditioning plant, together with the renewal of the fire alarm system. An interesting maintenance item was the repainting of the main aerial dish on the site. A large diesel generator for standby electrical supplies was installed at the Winkfield Field Station (a NASA tracking station).

Preliminary token estimates have been prepared for buildings, services and foundation systems for a proposed Millimetre Wavelength Astronomy Facility.

The Royal Observatory Edinburgh

During the Summer a new boiler installation was successfully installed together with a new gas main. The installation covers the heating for the main building. As part of the brief, the existing electrode boilers were retained and this resulted in a very difficult installation in a confined space in the basement of the building. The very latest controls were installed including an Optimum Start facility. A diesel generator set was also installed for standby supplies to the existing computer and other essential supplies on the site.

Some major design work was carried out for the provision of a new workshop, welding bay, storage facilities, plant room offices and associated areas, and assistance was also given in the planning of two additional temporary buildings.

Several other minor schemes were worked on which included a covered way, modifications to the reception area and to existing temporary buildings. Assistance was also given for the Mauna Kea observatory project in Hawaii.

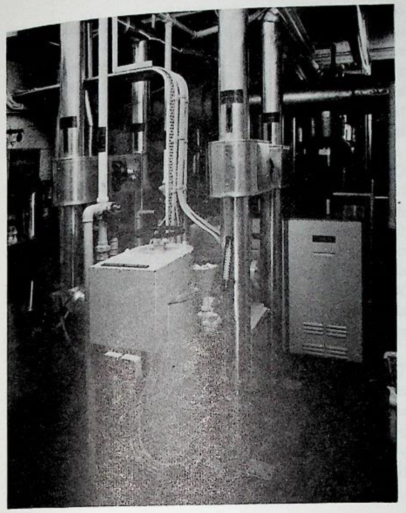

Figure 7.1. Boiler installation for Royal Observatory, Edinburgh.

Maintenance assistance was also provided which included repairs to the domes, roof and windows of the Main Building which is listed as being a building of architectural merit.

The Royal Greenwich Observatory

To commemorate the Tercentenary of the founding of the Observatory at Greenwich in 1675, a reclining equiangular sundial was erected at Herstmonceux Castle. This sundial was designed to be capable of giving Greenwich Mean Time correct to a minute, to be easily read and to be of novel design, so serving as a fitting memorial to 300 years of distinguished work.

Schemes were produced and costed for extensions to the Time & Nautical Almanac building and the conversion of the archives store for office accommodation, while the Galaxy fire detection system was renewed with a new detection system using a battery supply. Further design work was done on the thermal insulation for the Isaac Newton telescope.

Schemes were also prepared for modifications and additions to the Castle to comply with the Fire Prevention Officer's requirements, special attention being paid to the architectural qualities of the fabric, particularly some of the fine handcarved and moulded staircases and doors. Other Fire Prevention Officer's requirements involved some work to the Physics Building.

London Office

The largest project being managed by the Council Works Unit at present is a new Office Building at Swindon, which will be occupied by the Science Research Council and the Natural Environment Research Council. Design work has been progressing this year and tenders will be invited ready to start construction on site in the Spring of 1976. Completion and occupation is planned for the Spring of 1978. The building is traditional in construction, accommodation being arranged on three floors, having an area of some 15000 square metres. When occupied the development will accommodate some 700 staff. The challenge of the project is in the development within a tight budget and timescale of an aesthetically satisfying scheme despite the depressing site, the adjacent railway and the noise levels.

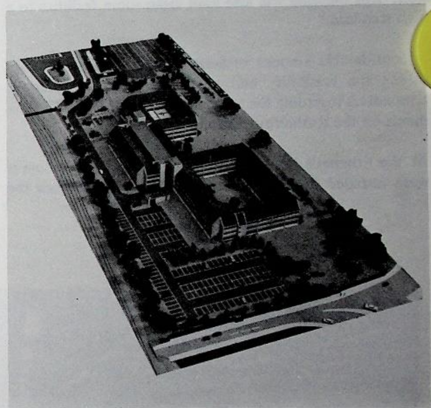

Figure 7.2 Design of new office building for the Science Research Council and the Natural Environment Research Council.

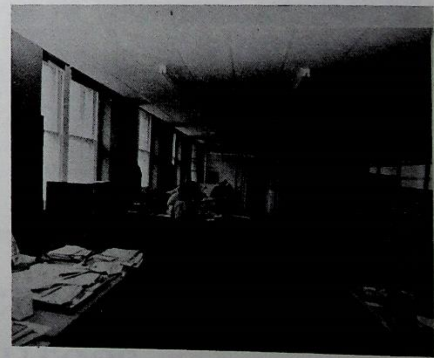

Figure 7.3 New office accommodation at Swindon for the Science Research Council, converted from old British Rail workshops.

Work was completed this year increasing office accommodation at Swindon for London Office staff. This consisted of converting obsolescent British Rail workshops in Suites I, II and III. The work was successfully completed to a short timescale with a fixed completion date.

Rutherford Laboratory

Design work was carried out on temporary accommodation for the new Laser Centre (see Section 3) inside an existing building. The requirements called for a high degree of clean room conditions.

Schemes were also prepared for a new permanent laser building consisting of a laser hall, target areas, capacitor banks with associated laboratory and office accommodation. This building will also have clean room facilities to a high standard.

A considerable amount of design work was done in establishing the feasibility and approximate costs of various alternatives regarding the siting of future computer developments on the Rutherford Laboratory site.

At the Cosener's House in Abingdon, new gas-fired boilers were installed during the Summer. The year also saw the completion of the design for extensive alterations to Cosener's House. This scheme involves the addition of Conference Room facilities, the conversion of the old stables into study bedrooms and the conversion of the existing boathouse into staff accommodation. The alterations are of particular interest as all the buildings on the site are listed buildings due to their historical and architectural character.

Other works on the Rutherford Laboratory site this year have included alteration and modification of staircases and doorways for fire prevention purposes, landscaping schemes for courtyards and a coldstore for the Restaurant. A wide range of minor schemes were also designed and installed including a 'clean room' for EPIC development work, an EPIC RF laboratory and a new RMS magnet control room. Designs have also been completed for work in the main staircase and reception areas to the Main Building R1.

The Council Works Unit also has other functions which include maintenance advice and inspections for the various establishments within SRC and giving advice for grant aid purposes for research projects. One project investigated this year was for the construction of blasting pits for investigation into implosive welding techniques at Leeds University.

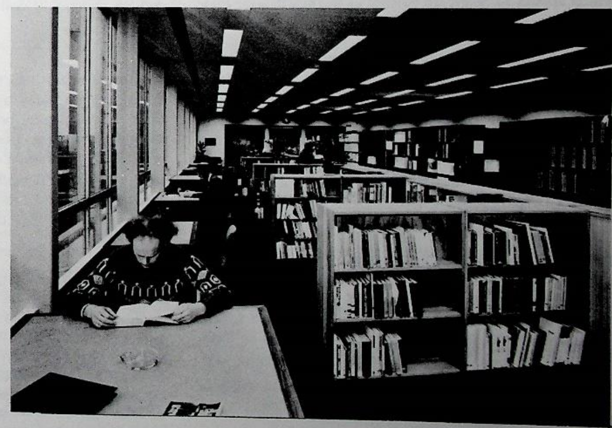

8. General Laboratory Resources

8. General Laboratory Resources

The range of scientific activities supported by the Laboratory on-site and at other research centres together with the requirements of its ever-widening circle of users demands a high level of support services and an efficient and flexible administration.

As well as the services and functions described in this Section, the Laboratory provides comprehensive backup in many other areas, including communications, housing, transport and office services and library, printing and photographic facilities, all having a direct bearing on the efficient day-to-day running of the Laboratory's activities, the quality of its output and the well-being of employees and visiting scientists, and which are none the less important for not being explicitly described in an annual summary of the Laboratory's work.

8.1 Health and Safety Group

The Robens Report of 1972 reviewed the complex system of safety legislation which had grown up piecemeal over the years and made recommendations which formed the basis of the Health and Safety at Work Act 1974. This important piece of safety legislation has unified the various safety inspectorates into one body – the Health and Safety Executive – which is now responsible for enforcing the Act, which applies to nearly all persons at work, whatever they do.

It has always been the policy of the Rutherford Laboratory to maintain high standards of safety which do more than simply satisfy legal requirements, and the Laboratory's established safety procedures already went a considerable way towards meeting the stringent requirements of the 1974 Act. However it was decided to reconstitute the Safety Group and the Radiation Protection Group, and to institute a two-tier safety committee structure consisting of a Safety Policy Committee and Divisional Safety Committees.

The Policy Committee aims to set safety standards and to review safety records. It is an advisory committee, including membership qualified to give expert advice in particular fields. The Divisional Committees' main objectives are to monitor safety performance and to bring to bear on local problems the best available experience to promote safe working and the good health of employees.

Safety

The former Safety Group and the Radiation Protection Group have been reconstituted as the Health and Safety Group. It is responsible to the Head of the Engineering Division and is required to advise on general safety, fire prevention, radiological protection, site emergency procedures, etc. It has executive responsibilities for the statutory examination and certification of certain plant and installations.

Prior to the reorganisation, bi-annual safety tours of the Laboratory were carried out by members of the Safety Committee, Safety Group and the AERE Fire Brigade. Divisional Safety Committees now tour their own areas, and are required to deal with safety problems as and when they arise.

A series of safety induction training courses has been continued using a video-tape and colour monitor to present films on radiological protection, fire prevention, first aid and safety handling. The course includes participation in a practical demonstration of fire fighting and artificial respiration. The film "It shall be the Duty" was shown to well over half the staff of the Laboratory, and a lecture on the Health and Safety Executive by a senior inspector was well attended.

Registered items of equipment are required to be inspected on a regular basis by the safety group staff or insurance inspectors. They include (1974 figures in brackets):– lifting machines 351 (375), lifting tackle 2542 (2535), pressure vessels 908 (939), safety valves 335 (309), fire prevention devices 52 (52), breathing apparatus, etc. 145 (148), and experimental high voltage apparatus 400 (381).

90 accidents were reported during the year. Investigation of the causes of these accidents showed that, as in the previous year, a high proportion of these could have been avoided by greater awareness and individual care by the persons injured or involved. The accident statistics of the past ten years are shown in Figure 8.1.

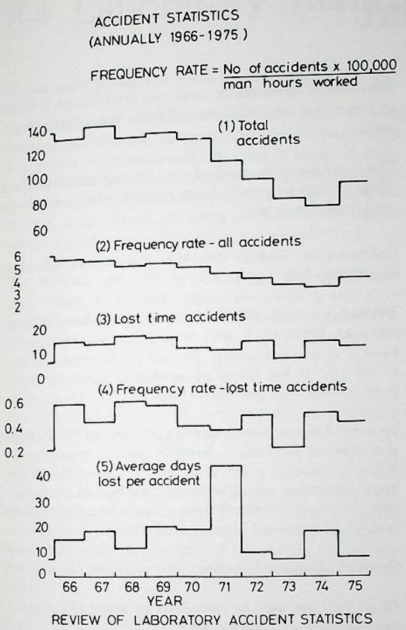

Figure 8.1 Accumulation of accident statistics.

Radiation Protection and Research

During the year the Laboratory continued to maintain standards of radiological safety well within the limits laid down by national and international bodies. In particular the results of personal dosimetry show that no one working in the Laboratory exceeded the permitted external radiation levels. The distribution of radiation dose was very similar to that of previous years, namely for every ten workers exposed to N Rem/year only one received (N + 1) Rem/year. There were no accidents of note during the year.

The former Radiation Protection Group (now merged into the Health and Safety Group) has continued to give advice and to carry out investigations related to accelerator shielding, induced radioactivity and some aspects of radiation damage. This included studies for the new Nimrod injector and the EPIC projects (see Section 6).

The feasibility of developing a camera for detecting the distribution of radiation leakage from shielding is being studied. This is based on a multi-wire proportional chamber operating in coincidence with a small detector (in a manner rather analogous to a pin-hole camera).

The Group has continued its interest in and active support for the work of the radiobiological group (Section 1.5).

8.2 Chemical Services

General chemical services are provided in the fields of water treatment, chemical analysis, corrosion prevention and control, safety matters and waste disposal. The section is also required to assist with many other matters relating to chemical aspects of the work of the Laboratory, such as the production of nuclear physics target materials, electroplating, and site effluent control.

Chemical analysis is used as a method of quality control on the performance of the water treatment plants and to investigate any serious incidents of corrosion. Maloperation of the treatment plants can quickly prove to be expensive in terms of time and materials, and corrosion in cooling water circuits operating continuously for much of the year could have serious consequences.

Use is made of corrosion inhibitors but the addition of such materials is frequently precluded by consideration of water purity or volume throughput and corrosion rates can only be controlled by attention to quality and by careful selection of constructional materials.

A diverse range of chemical matters are routinely tackled by the chemical services section, from the gold plating of the internal surfaces of fine tubes 2 - 3 metres long to the collection and disposal of toxic and other waste chemicals arising within the Laboratory.

8.3 Manufacturing Support

Manufacturing support is provided by mechanical and electrical workshops, with an outside manufacturing and estimating section.

A very wide range of equipment is manufactured in the workshops often with only sketchy instructions and information. During the year approximately 700 separate jobs were undertaken. Assistance was also given outside the workshop to Nimrod Division during machine shutdowns and also on the construction of the 70MeV Injector.

Over 1,000 jobs were placed by the Outside Manufacturing Section, ranging from simple flanges to the reclining equiangular sundial for the Royal Greenwich Observatory (Section 7).

Some of the more interesting items supplied by the Group include:

Magnet Measuring Survey Device

This device is a general purpose tool which is used to position probes between magnet poles to determine the characteristics of the field. Its range is 3½ metres longitudinally and laterally and 2 metres vertically, all monitored by digital readout.

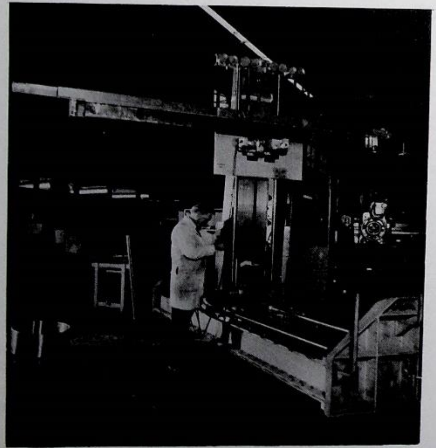

Figure 8.2 Magnet survey measuring device.

Considerable development work was involved, particularly in connection with alignment of slides and rigidity of columns.

The first item to be surveyed with this equipment will be a 300ton magnet currently being constructed at the Laboratory (Experiment 20).

Collimator for Medical Multi-Wire Proportional Chamber (see Section 1.4)

The basic requirement was for a disc approximately 200mm diameter, 50mm thick, with a maximum number of apertures of equal cross section, through the thickness, parallel to the axis. It was also required that the thickness of the walls between apertures should be an absolute minimum.

To meet these requirements, strips of brass foil 50mm wide and 0·05mm thick were passed through a special set of rollers to produce corrugations of 60° across the width. These strips were coated with resin, and layered alternately with flat pieces of foil to form a matrix of small equilateral triangles of side length approximately 1mm.

Secondary Emission Chambers

These units are used in beam lines to detect the position and magnitude of a particle beam.

Each assembly houses fifteen detector plates, ·005mm thick, stretched taut and adhered with resin to aluminium alloy rings. These plates are set at specified positions in a vacuum vessel and connected electrically to counting devices outside the chamber.

With such thin foil, extreme care was required at all stages of manufacture. In addition many interstage vacuum testing, cleaning, potting and wiring operations were involved calling for close co-operation between a number of sections.

2,000 Amp Power Supply

The requirement was for a portable power supply to be used for testing superconducting coils.

The equipment was built into a castor mounted frame. The main electrical source is from a series of linked alkaline cells. The output which can be varied from 0-2,000Amp is controlled by banks of transistors powered by a separate battery system with its own charging unit built-in.

8.4 Laboratory Maintenance and Supplies

Maintenance; Mechanical, Electrical and Building

During the year the Mechanical and Electrical Services Maintenance Sections continued their work of planned and breakdown maintenance on a wide range of plant and equipment which includes large computer air conditioning plants, site electrical supplies and distribution, building lighting and heating, water, steam, gas, compressed air, cranes, helium recovery plant, cooling water plant, mobile trucks, etc.

The Building and Civil Section carried out maintenance work which ranged from major roof repairs to door locks and included the maintenance of Rutherford Laboratory housing and Cosener's House.

Electricity Supply and Consumption

The electricity supply at Rutherford Laboratory is taken from the 132K grid and distributed at 11Kv. It is metered at entry points to the site and also individual substations and building switchrooms are monitored to keep in touch with changing demand requirements. Cost and consumption estimates are provided by M&E Services Group and actual consumption is costed at monthly intervals. Figure 8.3 shows the pattern of consumption over the last five years at Rutherford Laboratory with the estimated consumption for 1975/76.

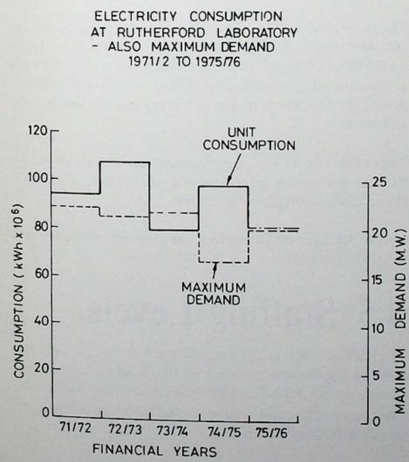

Figure 8.3 Use of electricity over the last five years.

Fuel Economy

Over the past year considerable progress has been maintained with regard to reducing steam consumption at Rutherford Laboratory. Incoming steam supplies are metered at the points of entry to the site, all steam supplies being bought from AERE, Harwell. Individual buildings are also metered and this provides the detailed knowledge of consumption patterns which is essential in assessing possible improvements and final results. Figure 8.4 shows the annual consumption pattern for the Rutherford Laboratory over the last few years and indicates the reductions achieved so far despite the addition of several new buildings.

Apart from the reduction of office, workshop and experimental area temperatures generally over the past year, efforts to reduce steam consumption have been concentrated in two main areas.

1 To provide suitable temperatures at the place of work during occupied hours only (normally approximately 45hrs out of a total 168hrs per week).

2 To reduce site mains losses during the summer months by shutting off steam supplies wherever possible.

A major advance has been the installation of Optimum Start Controls and 8 buildings at Rutherford Laboratory now have this form of control. Heating is mainly provided during normal working hours with a pre-heating period which is automatically determined, depending on internal and external ambient conditions, to give satisfactory room temperatures for the start of the occupied period. The following table gives an indication of the effect of installing Optimum Start Controls in several buildings with a comparison of steam consumption for the most recent Period available (mid-October to mid-November) before and after fitting Optimum Start Controls.

Steam Consumption (lbs) mid-October to mid-November period

Building	1972	1973	1974	1975
R1 Link	515,570	495,570	636,480	*253,150
R1 West	555,260	417,970	*108,930	*118,930
R12	727,260	499,160	774,550	*418,540
R18	150,110	121,121	128,083	*77,738
R20	191,750	137,840	238,830	*144,220
R34	546,380	699,960	427,840	*241,400

* with Optimum Start Controls.

The effect of the summer shut-down of some steam mains is shown in Figure 8.5, a graph giving 1974/75 steam consumption and 1975 consumption to date.

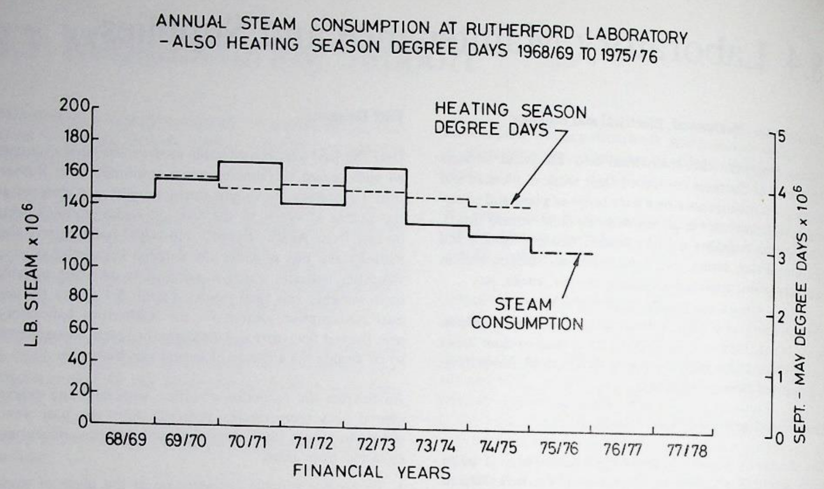

Figure 8.4 Annual steam consumption pattern.

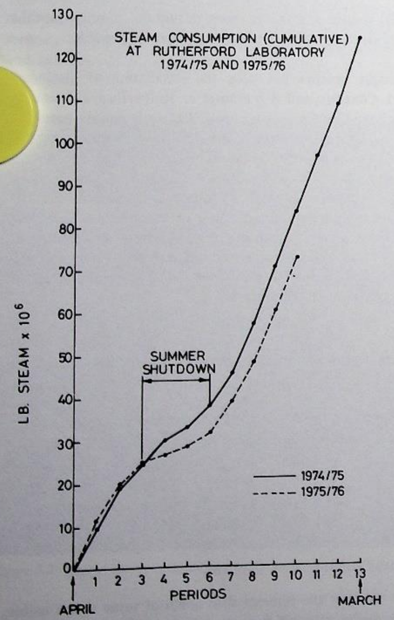

Figure 8.5 Economies in steam usage.

Helium Supply and Recovery

On completion of the $\pi 9$ experiment, consumption of liquid helium at Rutherford Laboratory fell from an average of 6,000 litres per week to an average of 1,500 litres a week, the year's total being a little over 62,000 litres.

The recovered gas high pressure static store capacity was increased to nearly 4,200m^3, being the equivalent of well over 5,000 litres of liquid. In addition an articulated trailer with a capacity of approximately 370m^3 of gas was commissioned for the return of gas to the supplies for purification and resale.

Approximately 17% of the recovered gas was reliquified on the site during the commissioning of the BOC Turbocool closed circuit refrigerator/liquefier.

Overall Rutherford Laboratory gas recovery efficiency was approximately 80%.

8.5 Staffing Levels

The staff position at the beginning and end of the year was affected by the incorporation of the Atlas Computer Laboratory as the Atlas Computing Division of the Rutherford Laboratory. The third column in the table shows the numbers of Atlas staff transferred.

Changes during 1975

	Opening Strength 1.1.75	Gains: Non-Atlas	Gains: Atlas	Losses	Closing Strength 31.12.75
NON INDUSTRIAL					
Senior and Banded Staff	31	1	3	2	33
Science Group	254	44·5	68	23·5	343
Professional and Technology Group	330	12	4	14·5	331·5
Administration Group	75·5	6	8	9	80·5
Research Associates	45	23	5	21	52
Non-Techs and Stores	36	1	1	2	36
Librarian	1	1	1	1	2
Secretarial and Typing	30	9	10	12·5	36·5
Photographers	3	0	0	0	3
Photoprinters	5	2	1	2	6
Machine Operators	53·5	7·5	21	15·5	66·5
Hostel Manageresses	2	2	0	1	3
Telephone Operators	2	0	0	0	2
Total Non Industrial	868	110	122	106	994
INDUSTRIAL					
Craft	155	32	1	20	168
Non-Craft	114	31·5	12	25·5	132
Apprentices	20	12	0	6	26
Total Industrial	289	75·5	13	51·5	326
GRAND TOTALS	1157	185·5	135	157·5	1320

The figures listed under "changes" include new entrants, resignations and promotions. Staff on sandwich courses, and those working part-time are counted as half.

8.6 Staff Relations

Quarterly meetings of the local Whitley Committee, including the Annual Meeting chaired by the Director, maintained regular communication between the local Staff Side and Management. Additional meetings with management were convened to discuss various matters, the most important of which was the use of contract staff, where a local agreement was concluded concerning contract design staff working at the laboratory. Staff Side members continued to monitor the placing of design work with outside contractors and expressed concern at the use of self-employed staff on this work.

Staff Side were greatly disappointed by the announcement of the discontinuance of the EPIC project. They welcomed the confirmation of the proposal to set up the Laser facility on the Chilton site, although regretting the withdrawal from the project of the UKAEA.

Staff Side members were involved in discussions following the Council's decision to incorporate the former Atlas Computer Laboratory as the Atlas Computing Division of the Rutherford Laboratory and continued to watch the interests of the staff involved.

Regular three-monthly meetings of the Local Joint Consultative Committee (including the annual meeting chaired by the Director) continued to provide fruitful communication between management and industrial employees. A recurring item of discussion has been the phased reduction in contract labour, which continued during the year.

Shop Stewards representing the various Trades Unions recognised at the Laboratory continued to serve on the Safety, local Staff Suggestions Awards Committee and on the various divisional productivity sub-committees, thus providing further opportunities for exchange of ideas and expressions of opinion between management and employees. Industrial employees ceased to be represented on the Restaurant Committee, but the Trade Union side expressed their disappointment at the loss made by the Restaurant, despite increased charges.

The Trades Union side welcomed the approval by the Government to establish a Laser Facility on the Chilton site. They also welcomed the arrangement whereby employees of the Rutherford Laboratory may now participate fully in the operation of the UKAEA Research Group Welfare Fund.

8.7 Finance

The Laboratory's expenditure for the financial year 1975/76 was £14·83 million, of which £1·45 million was for capital (including £0·36 million on the initial stage of setting up the Laser Centre) and £13·38 million was recurrent. Corresponding figures for 1974/75 were £10·87 million, £1·37 million and £9·50 million. The upward trend in Laboratory expenditure reflects the significant diversification of work during 1975/76, including responsibility for the Atlas Computer Laboratory and the inception of the Laser Centre.

A brief analysis of the net expenditure is given below.

	£ million
Staff expenditure (salaries and wages, insurance, superannuation, etc)	6·84
Research and development (see below)	6·54
Plant and equipment	1·30
Building works	0·15
Total	14·83

A proportional representation of the breakdown of the research and development expenditure into divisional and other main components is shown in the pie chart.

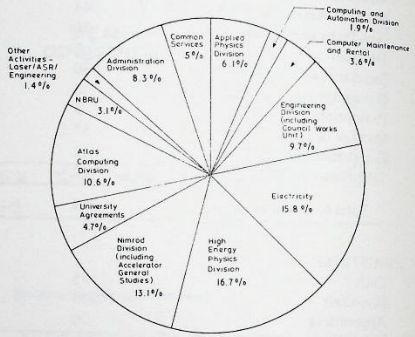

Figure 8.6 Breakdown of research and development expenditure.

Appendix 1 Rutherford Laboratory Reports and Publications

RL-75-001
The $\Lambda\Lambda$ mass spectrum produced by 2·2 Gev/c K^- Interactions on nuclei.
J G Guy, S N Tovey

RL-75-002
Helicity structure of the Triple-Regge formula.
N Sakai, J Uschersohn

RL-75-003
Contribution of the Δ to radiative muon capture.
D Beder

RL-75-004
Hydrogen removal from neon-hydrogen gas mixtures.
E W Fitzharris

RL-75-005
A general technique for the analysis of two-amplitude processes.
A A Carter

RL-75-006
Computing and Automation Division quarterly report Sept-Dec 1974.
W Walkinshaw, A T Lea

RL-75-007
A gas monitoring unit for multiwire proportional chambers.
J B Marsh, J E Boon, K H Souten, B O'Hagan.

RL-75-008
A report on the Basque superconducting magnet project.
G Gallagher-Daggitt

RL-75-009
Proceedings of the 1974 school for young high energy physicists.
H Muirhead

RL-75-010
Q factor measurements on Tank 1.
E G Sandels, J E Ellis

RL-75-011
The budding Pomeron in the free approximation to $\pi\pi$ inelastic channels.
M R Pennington

RL-75-012
On the real part of a geometrical pomeron.
J Dias de Deus

RL-75-013
Shims for the EPIC prototype dipole magnet.
A G Armstrong, J Simkin, C W Trowbridge

RL-75-014
K^-p elastic scattering between 1094 MeV/c and 1377 MeV/c.
P C Barber

RL-75-015
12 ft argonne bubble chamber TST project – first operational test (guidelines).
E W Fitzharris, J H Foster

RL-75-016
The kinetics of electron cooling.
G I Budker, Ya S Derbenyov, H S Dikanski, V V Parkhomchuk, D V Pestrikov, A N Sikrinsky

RL-75-019 (revised)
Polarised targets for thermal neutron beams; a review.
S F J Cox

RL-75-020
Fine slit neutron collimators using stretched film.
P D Hey, B Mack, C Carlile

RL-75-021
Longitudinal head-tail in EPIC.
H G Hereward

RL-75-022
RF losses due to ripple in the beam induced voltage.
M H R Donald

RL-75-023
Proceedings of the HPD collaboration meeting at the Rutherford Laboratory, October 1974.
A J Oxley

RL-75-024
The meson and baryon loop to make the pomeron.
M R Pennington, A Gula

RL-75-025
Phenomenological tests of f-dominated pomeron in inclusive reactions.
R G Roberts

RL-75-026
A contention system for CCITT/U24 synchronous modems/device to gain access to multiplexors/computers.
K W Taylor

RL-75-027
Nimrod operation and development – quarterly report Oct-Dec 1974
D E Gray

RL-75-028
Computers for the EPIC control system.
R Rosner

RL-75-029
Computer programs used in the UK for the analysis of neutron scattering data.
G C Stirling

RL-75-030
Is the absence of semi-inclusive correlations compatible with the cluster model?
A Gula

RL-75-031
Notes on a Cornell-type injection scheme for use in EPIC.
A Carne, G Rees

RL-75-032
CIGAR (Computer Introduction Guide and Reference). User Support Section, C & A Division.
R Taylor

RL-75-033
Radiation response to mammalian cells after irradiation with a beam of π^- mesons.
A J Mills, J D Lewis, W S Hall

RL-75-034
Some in vivo effects of π^- mesons in mice.
J E Coggle, M V Gordon, P J Lindop, J Shewell

RL-75-035
Engineering note. 70 MeV injector alignment proposals – Part 4 HEDS alignment.
R Lascelles

RL-75-036
High energy fixed angle scattering involving a reggeon.
D Scott

RL-75-037
Some effects of the synchrotron radiation from EPIC.
J R J Bennett

RL-75-038
Power supply for EPIC booster.
J Riedel

RL-75-039
On phase shift analysis of one dimensional scattering.
J Formanek

RL-75-040
Status of EPIC.
D A Gray

Rl-75-041
Multiplicity bootstrap and the dual unitarity equation.
J Dias de Deus

RL-75-042
Local loop dominance in the dual unitarity scheme.
J Dias de Deus, I Uschersohn

RL-75-044
Observations and measurements with drift chambers at the Rutherford Laboratory
J E Bateman, J F Connolly

RL-75-045
Partial wave analysis of the Q region in the reactions $K^-p \rightarrow K^-\pi^+\pi^-p$ and $K^-p \rightarrow \bar{K}^o\pi^-\pi^o p$ at 14·3 GeV/c.
S N Tovey, J D Hansen, K Paler, T P Shah, S Borenstein, B Drevillon, B Chaurand, R A Salmeron, A Borg, D Denegri, Y Pons, M Spiro

RL-75-046
Possible Tigner-type filling schemes for EPIC.
N M King

RL-75-047
Suppression factors in charmed particle production.
R J N Phillips, V Barger

RL-75-049
A new range of adaptable equipment for multiwire proportional chamber readout.
D J White

RL-75-050
Emission of Auger electrons in μ-mesic atoms and escape of charged particles when μ-mesons are captured by light (C.N.O.) and heavy (Ag, Br) nuclei.
Yu A Batusov

RL-75-054
Kinematical constraint on density matrix.
J Formanke

RL-75-055
Kaon-Nucleon partial wave amplitudes below 1·5 GeV/c for I = 0 and 1
B R Martin

RL-75-056
Modification to the injection scheme for EPIC.
D A Gray

RL-75-057
A simple method of constructing various shaped moulds for casting resin sheet.
R W Roberts

RL-75-058
Computing and Automation Division quarterly report. Dec 1974-March 1975
W Walkinshaw, A T Lea

RL-75-059
Measurement of K^-p elastic differential cross sections between 610 and 943 MeV/c.
R Homer et al

RL-75-060
Superconducting materials; some recent developments.
M N Wilson

RL-75-061
A pressure impregnated superconducting dipole.
M N Wilson, R B Hopes, R L Roberts

RL-75-062
The $\psi' \rightarrow \psi\pi\pi$ decay as a test of PCAC.
D Morgan, M R Pennington

RL-75-063
A stacked film bender for cold neutron beams.
J C Sutherland, H Wroe

RL-75-064
On the analytic properties of the reggeon-reggeon amplitude.
J Kwiecinski

RL-75-065
A preliminary design of a superconducting wiggler magnet for the Daresbury laboratory SPS.
P Clee et al

RL-75-066
New developments in the magnet design computer program GFUN.
A G A M Armstrong, C J Collie, N J Diserens, M J Newman, J Simkin

RL-75-067
The production of the ω^o-meson in the reaction $\pi^+d \rightarrow p_o p\omega^o$ at 4 GeV/c.
I G Bell, M Dale, D Evans, J V Major, J A Charlesworth, D J Crennell, M J Emms, J B Kinson, B J Tracey, M P Votruba, P L Woodworth, R L Sekulin

RL-75-068
Cornell-type injection scheme for EPIC – notes on longitudinal phase space matching.
M Donald

RL-75-069
Nimrod operation and development: Jan-March 1975.
D E Gray

RL-75-070
High energy photoproduction of heavy muon pairs.
D M Scott

RL-75-071
Nucleon exchange: a simple description.
A Gula, M Pennington

RL-75-072
A_2^o production by charge exchange in π^+n Interactions at 4 GeV/c.
I G Bell, M Dale, D Evans, J V Major, J A Charlesworth, D J Crennell, R L Sekulin, M J Emms, G T Jones, J B Kinson, B T Tracey, M P Votruba, P L Woodworth

RL-75-073
Quantum electrodynamics: translations of papers by Heisenberg, Dirac and Weisskopf.
J B Sykes (translator), P F Smith (editor)

RL-75-074
The pulsed superconducting magnet AC5.
J H Coupland

RL-75-075
Report on the organisation of the XVII International Conference on High Energy Physics.
J R Smith

RL-75-076
The hot cathode ionization gauge.
P E Gear

RL-75-077
Outgassing of vacuum materials, Part 1.
R J Elsey

RL-75-078
Outgassing of vacuum materials.
R J Elsey

RL-75-079
Inclusive K^{*-} (890) and $\bar{K}^{*o}$ (890) production in 14·3 GeV/c K^-p interactions.
K Paler, S N Tovey, T P Shah, J J Phelan, R J Miller, M Spiro, R Barloutard, M Bardadin-Otwinowska, A Borg, B Chaurand, B Drevillon, J M Gago, R A Salmeron

RL-75-080
Some consequences of an attempt to identify clusters with resonances.
A Gula

RL-75-081
Branching ratios of the f^o meson.
M J Emms, J B Kinson, B J Stacey, M F Votruba, P L Woodworth, I G Bell, M Dale, J A Charlesworth, D J Crennell, R L Sekulin

RL-75-082
A spin-parity analysis of the 3π system produced in the reaction $\pi^+d \rightarrow \pi^-\pi^+\pi^+d$ at 4 GeV/c.
M J Emms, G T Jones, J B Kinson, B J Stacey, M F Votruba, P L Woodworth, I G Bell, M Dale, J V Major, J A Charlesworth, D J Crennell

RL-75-084
Building a general framework for hadron collisions.
Aurenche, Ng, Paton, Tsou, Chan, Gula, Irami, Roberts

RL-75-085
Long-range correlations as phenomenological probe of non-scaling behaviour.
J Kwiecinski, R G Roberts

RL-75-086
The meson and the baryon in the one loop dual model of the pomeron.
M R Pennington, A Gula

RL-75-087
K^+n elastic and change exchange scattering between 430 – 940 MeV/c.
R J Homer

RL-75-088
An interferometer with an automatic throughput of information for the measurement of the refractive index of a gas in a wide range.
G A Shelkov, J Schueler

RL-75-089
New data and partial wave analysis for the reaction $\pi^-p \rightarrow K^oN^o$,
K W Abbott

RL-75-090
A multi-programmed computer system for the interactive examination of experimental data.
R P Hand, J S Hutton, D Maden, R A Rosner

RL-75-091
How high are higher symmetries?
F E Close

RL-75-092
An alternative scheme for variable damping in EPIC.
G H Rees

RL-75-094
A one-dimensional approximation for the pomeron in the dual unitarity scheme.
N Sakai

RL-75-095
Condensed matter research using pulsed neutron sources: a bibliography.
D F R Mildner, G C Stirling

RL-75-096
High pressure techniques for thermal neutron scattering.
C J Carlile, D C Salter

RL-75-097
An initial survey of EPIC lattice configurations using triplet damping.
J Maidment

RL-75-098
K^-p reactions from 0·960 to 1·355 GeV/c involving two-body final states.
Rutherford Laboratory, Imperial College collaboration

RL-75-099
A high performance circulating system of gas damping for spark chambers.
L K Bogandova et al

RL-75-100
Is the A_1 a resonance?
D Morgan

RL-75-101
Geometrical Scaling in ϕN Scattering.
R J N Phillips, V Barger

RL-75-102
Control on the Rutherford Laboratory central computer.
M M Curtis

RL-75-103
Difficulties for SU(N) quark models of the new particles.
E Colglazier, K J Barnes, A J G Hey, R K P Zia

RL-75-104
Programming Standards and Documentation.
J S Hutton

RL-75-105
A new Upper Limit for the branching ratio of the decay $\eta \rightarrow \pi^o e^+e^-$.
M R Jane et al

RL-75-106
A measurement of the electromagnetic form factor of the eta meson and of the branching ratio for the eta Dalitz decay.
M R Jane et al

RL-75-107
K^-p elastic scattering between 1·73 GeV/c and 2·47 GeV/c.
P C Barber et al

RL-75-108
Vacuum polarisation for finite range potentials, using Green's functions
P F Smith, J D Lewin

RL-75-109
Geometrical scaling and the Pomeron.
J Dias de Deus

RL-75-110
MAGIC: a computer code for design studies of insertions and storage rings.
A S King, M J Lee, W W Lee

RL-75-111
TOK users' guide.
N J Diserens

RL-75-112
Preliminary results of the polarisation of cold neutron beams produced by total reflection from magnetised cobalt:iron thin films.
J Penfold, J C Sutherland, W G Williams, J B Hayter

RL-75-113
Building up Reggeons and the Pomeron from duality and unitarity.
N Sakai

RL-75-114
Computing and Automation Division quarterly report, March–June 1975.
W Walkinshaw, A T Lea

RL-75-115
New results on strangeness ±1 baryons presented at Palermo conference.
R T Ross

RL-75-116
Intersection of two quadrilaterals in a plane.
D Bryan, A G Armstrong

RL-75-117
Stress analysis studies in Tokamak magnet devices.
N J Diserens

RL-75-119
A direct method of measuring polarisation of a slow neutron beam.
B G Erozolimski

RL-75-121
Mk II plunging magnet mechanism lubrication.
K G Potter

RL-75-122
Relating inclusive and exclusive meson photoproduction at large transverse momentum.
D Scott

RL-75-123
Regge phenomenology of inclusive processes.
D P Roy

RL-75-124
Leptonic coupling types and the question of strangeness-changing semileptonic neutral currents.
D S Beder, G V Dass

RL-75-125
Scaling laws and quark model in strong interactions.
J Dias de Deus

RL-75-128
Polarised neutron diffraction from single crystal Tungsten-186 in a magnetic field.
Y A Alexandrov et al

RL-75-129
The choice and optimisation of a moderator for a pulsed slow neutron source and neutron moderation in ice and polyethylene at low temperatures.
S N Ishmaev, I P Sadikov

RL-75-130
An iterative method for solving the non-linear magnetic field integral equation.
J Simkin, C W Trowbridge

RL-75-133
Status of the O^+ nonet.
D Morgan

RL-75-134
Deviant closed orbits caused by some systematic errors.
N M King

RL-75-135
First observation of the relativistic rise in bubble density in a neon-hydrogen bubble chamber.
C M Fisher, J G Guy, W A Venus

RL-75-136
Post irradiation mechanical properties of radiation resistant case epoxy resin systems.
J T Morgan, G B Stapleton

RL-75-137
A Nimrod magnet correction system.
I S K Gardiner

RL-75-138
The DRIO package users guide.
C S Cooper

RL-75-142
Strong interaction effects in Kaonic atoms.
C J Batty et al

RL-75-143
Proceedings of international colloquim on multiparticle reactions.
H M Chan, R J N Phillips, R G Roberts

RL-75-144
Finesse – Rutherford Laboratory users' guide.
N J Diserens

RL-75-145
Measurement of Lorentzian linewidths.
B L Roberts et al

RL-75-146
Addendum to a proposal to build a 14 GeV electron-positron colliding beam facility, EPIC.

RL-75-147
Models for the production of new particles in photon and hadron collisions.
D Sivers

RL-75-148
Duality for the Reggeon-Reggeon amplitude – a study through quasi three body reactions.
R G Roberts

RL-75-149
The development of a graphite to copper joint for injector diagnostics.
D Baker

RL-75-150
Relaxation and cooperative behaviour of higher polarised nuclei.
S F J Cox

RL-75-151
Neutrino and antineutrino scattering by electrons and partons.
G V Dass, J S Bell

RL-75-154
System software for experimental applications on a GEC 4080.
B J Charles and D Maden

RL-75-157
Computing and Automation Division quarterly report, June-Sept 1975.
W Walkinshaw, A T Lea

RL-75-158
Charm production by partons in neutrino scattering.
R J N Phillips, V Barger, T Weiler

RL-75-159
A partial wave analysis of the $(3\pi)^o$ system from the charge exchange reaction $\eta^+ n \rightarrow \pi^+\pi^-\pi^o p$ at 4 GeV/c.
M J Emms et al

RL-75-160
A new photomultiplier tube utilising channel plate electron multipliers as the gain producing elements.
J E Bateman, R J Apsimon

RL-75-162
Extended ENPLOT (FAPLOT) and FASUMX.
I J Bloodworth

RL-75-163
FAGEOM and FAGRIND.
I J Bloodworth

RL-75-164
Regge phenomenology of inelastic diffraction.
R G Roberts

RL-75-165
General relations between neutrino and antineutrino scattering.
G V Dass

RL-75-166
Report of the Rutherford Laboratory VDU committee.
J S Hutton

RL-75-167
Revised version of RL-75-158

RL-75-169
Distribution of neutrons in heavy nuclei.
A O Aganyants, G A Vartapetyan

RL-75-170
The Reggeon bootstrap.
J Kwiecinski, N Sakai

RL-75-171
Estimating the cross sections for the production of new particles.
D Sivers

RL-75-172
A simple geometrical approach to particle production in collisions with nuclei.
J Dias de Deus

RL-75-173
Magnetic design of the AC5 dipole magnet.
T C Randle

RL-75-174
Tests of the universality of the impact parameter distributions in high energy hadron collisions.
J Dias de Deus

RL-75-176
Geometrical aspects of high energy elastic scattering.
R J N Phillips, V Barger

RL-75-177
Zweig rule and violations as consequences of dual unitarisation.
Chang Hong Mo, R G Roberts, J Kwiecinski

RL-75-179
Dimuon data test weak current models.
R J N Phillips

RL-75-180
Nimrod operation and development quarterly reports, April-June, July-Sept 1975
D E Gray

RL-75-183
Recovery in mammalian cells irradiated with π^- mesons.
A J Mill, J D Lewis, W S Hall

RL-75-185
PDP-8 Computer systems.
J T Hyman

RL-75-186
Extraction from lattice 'A' of the 800MeV, 50Hz synchrotron.
A Carbe, B W Jones

RL-75-187
Lattice parameters in CG machines, with particular reference to Nimrod.
N M King

RL-75-188
Intense neutron sources based on accelerators.
A Carne

RL-75-190
The design of a graphics processor.
M Holmes, A R Thorne

RL-75-191
Strength of aluminium vacuum chamber extrusions.
J R J Bennett

RL-75-192
J/ψ, ψ' and related decays from dual unitarisation.
Chang Hong-Mo, K Konishi, J Kwiecinski, R G Roberts

RL-75-194
Median plane dynamics in 'straight' combined function magnets.
N M King

Appendix 2 Publications and Other Accounts of Laboratory Work

Publications and accounts of Laboratory work, including Rutherford Laboratory Reports (Appendix 1) are listed here under the Section of the Annual Report to which they correspond.

Section 1 Particle Physics

1.1.1 Meson Spectroscopy

J B Lister
Production of a neutral dipion system using a 12 GeV/c negative pion beam in the Omega spectrometer.
Thesis, Westfield College, London

J Mawson
Study of neutral non-strange bosons produced in π^-p interactions at 8 GeV/c
Thesis, Birmingham University

J D Dowell et al
Study of neutral bosons
Paper submitted to International Conference on High Energy Physics, Palermo

E Eisenhandler et al
Measurement of differential cross-sections for proton-antiproton annihilation into charged pion and kaon pairs between 0·79 and 2·43 GeV/c
Nuclear Physics B 96 p109-154

E Eisenhandler et al
Evidence for structure in the proton-antiproton elastic cross-section
Paper submitted to International Conference on High Energy Physics, Palermo

P I P Kalmus
Antiproton-proton annihilation into charged pion and kaon pairs.
Structure in the Antiproton-proton elastic cross-section
Papers presented at International Symposium on $\bar{N}N$ interactions, Syracuse

E Eisenhandler et al
Antiproton-proton elastic differential cross sections between 0·69 and 2·43 GeV/c
Contributed paper to Washington meeting of American Physical Society

M J Emms et al
A_2^0 production by charge exchange in π^+n interactions at 4 GeV/c
Physics Letters 58B, 117

M J Emms et al
Production of the ω^0 meson in the reaction $\pi^+d \to p_s p\, \omega^0$
Nuclear Physics B98,1

M J Emms et al
Spin-Parity analysis of the 3π system produced in the reaction $\pi^+d \to \pi^-\pi^+\pi^+d$ at 4GeV/c
Nuclear Physics B93, 1

M J Emms et al
Branching ratios of the f^0 meson
Nuclear Physics B96, 155

M J Emms et al
A spin-parity analysis of the $\pi^-\pi^+\pi^+$ system produced coherently in 4 GeV/c π^+d interactions
Proceedings of the Daresbury Study Weekend on 3-particle phase shift analysis and meson resonance production

M J Emms et al
Partial-wave analysis of the 3π system in the reaction $\pi^+d \to \pi^+\pi^-\pi^0 pp_s$
Proceedings of the Daresbury Study Weekend on 3-particle phase shift analysis and meson resonance production

P L Woodworth
Dipion production in a 4 GeV/c π^+d experiment
Thesis, Birmingham University

B J Stacey
Studies of deuteron collisions with positive ions at a beam momentum of 4 GeV/c
Thesis, Birmingham University

I Bell
Production of resonance particles in pion deuteron reactions at 4 GeV/c
Thesis, Durham University

Janet Thomas
Analysis of positive pion neutron reactions at 4 GeV/c using a deuteron bubble chamber
Thesis, Durham University

C M Fisher, J G Guy, W A Venus
First observation of the relativistic rise in bubble density in a neon-hydrogen bubble chamber
To be published in Nuclear Instruments and Methods

M Bardadin-Otwinowska et al
Inclusive production of charged and neutral sigma hyperons in K^-p interactions at 14·3 GeV/c
Nuclear Physics B90, 397

D Denegri et al
Evidence for double dissociation in K^-p interactions at 14·3 GeV/c
Nuclear Physics B91, 54

S N Tovey et al
Partial wave analysis of the Q region in the reactions $K^-p \to K^-\pi^+\pi^-p$ and $K^-p \to \bar{K}^0\pi^-\pi^+p$
Nuclear Physics B 95, 109

K Paler et al
Inclusive $K^{*-}(890)$ and $\bar{K}^{*0}(890)$ production in 14·3 GeV/c K^-p interactions
Nuclear Physics B96, 1

B Drevillon et al
K^-p elastic scattering at 14·3 GeV/c
Nuclear Physics B97, 392

M Bardadin-Otwinowska et al
Inclusive anti-lambda production in K^-p interactions at 14·3 GeV/c
Nuovo Cimento Letters 13, 597

M Bardadin-Otwinowska et al
Inclusive production of Y^* resonances in K^-p interactions at 14·3 GeV/c
Nuclear Physics B98, 418

D Denegri et al
Double dissociation in the reaction $K^-p \to K^-\pi^+\pi^-n\pi^+$ at 14·3 GeV/c and Pomeron factorisation
Saclay preprint DPhPE 75-06

M Spiro et al
New evidence for K*(1780) production
Saclay preprint DPhPE 75-12

H Abramowicz et al
Lambda polarisation in the reaction $K^-p \to \Lambda$+ anything at 14·3 GeV/c
Submitted to Nuclear Physics B

B Drevillon et al
Partial-wave analysis of the low-mass $\bar{K}^0\pi^+\pi^-$ system produced in the reaction $K^-p \to \bar{K}^0\pi^+\pi^-n$ at 3·95 and 14·3 GeV/c
Ecole Polytechnique preprint LPNHE/X/75

Inclusive production of Δ^{++} and Δ^0 in K^-p interactions at 14·3 GeV/c
Paper presented at International Conference on High Energy Physics, Palermo 1975

Inclusive analysis of Ξ^- production in K^-p interactions at 14·3 GeV/c
Paper presented at International Conference on High Energy Physics, Palermo

Study of low-mass $\bar{K}^0\pi^+\pi^-$ systems in the reactions $K^-p \to \bar{K}^0\pi^-p$ and $K^-p \to K^-\pi^+n$ at 14·3 GeV/c
Paper presented at International Conference on High Energy Physics, Palermo

Inclusive charged pion production in K^-p interactions at 14·3 GeV/c
Paper presented at International Conference on High Energy Physics, Palermo

Rutherford Laboratory reports (see Appendix 1) RL–75–067, 072, 081, 082, 089, 135, 159, 162, 163

1.1.2 Baryon Spectroscopy

K W Abbott et al
New data and partial wave analysis for the reaction $\pi^-p \to K^0\Lambda^0$
Paper presented at International Conference on High Energy Physics, Palermo

G Conforto et al
Mass spectrum in the Q-region of strange mesons produced in π^-p collisions at 6·15 GeV/c
Nuovo Cimento Letters 13, 265

G P Gopal et al
K^-p reactions from 0·960 to 1·355 GeV/c involving two-body final states
To be published in Nuclear Physics B

Partial wave analysis of $\bar{K}N$ two-body reactions between 1500 and 2200 MeV
Paper presented at International Conference on High Energy Physics, Palermo

R A Stevens
Study of π^-p interactions in the 1 GeV/c region
Thesis, Imperial College, London

Study of K_L^0 interactions in the range 300–800 MeV/c
Submitted to International Conference on High Energy Physics, Palermo

W Cameron
Study of K_L^0 interactions in the range 300–800 MeV/c
Thesis, Glasgow University

Rutherford Laboratory reports (see Appendix 1) RL–75–001, 014, 059, 087, 098, 107, 115

1.1.3 Intermediate Energy Production Mechanisms

C J S Damerell et al
K^+n elastic and charge exchange scattering between 430 and 940 GeV/c
Nuclear Physics B94, 374

A Berglund et al
Study of the reactions $\pi^+p \to K^+\Sigma^+$ and $K^-p \to \pi^-\Sigma^+$ at 10 GeV/c
Physics Letters 57B, 100

A Berglund et al
Study of the line reversed hypercharge exchange reactions $\pi^+p \to K^+\Sigma^+(1385)$ and $K^-p \to \pi^-\Sigma^-(1385)$ at 10 GeV/c
To be published in Physics Letters

C J S Damerell et al
SU(3) comparison of line charge exchange and hypercharge exchange reactions
To be published in Physics Letters

C J Adams et al
Measurement of K^-p elastic differential cross sections between 610 and 943 MeV/c
Nuclear Physics B96, 54

1.1.4 Higher Energy Experiments

Data from inclusive particle production at low transverse momenta and large angles at the CERN ISR
Presented at International Conference on High Energy Physics, Palermo, and International Colloquium on multiparticle reactions, Oxford

R P Mount et al
Λp interactions below 24 GeV/c
Physics Letters 58B, 228

R E Ansorge et al
Charged particle multiplicities in 100 GeV/c pp interactions
To be published in Physics Letters B

R E Ansorge et al
Measurement of the inclusive forward neutron spectrum produced in proton-copper interactions at 24 GeV/c
Nuclear Physics B97, 439

J R Carter et al
Measurement of the inclusive forward γ, Λ^0 and K_s^0 spectra produced in proton-copper interactions at 24 GeV/c
Submitted to Nuclear Physics B

J G Rushbrooke et al
The difference between $\bar{p}p$ and pp topological cross-sections up to 100 GeV/c
To be published in Physics Letters B

J G Rushbrooke et al
Spin-parity analysis of diffraction np $(p\pi^-)$p and the question of parity-change rule
Submitted to Physical Review D

B Alper et al
Production spectra of $\pi^\pm$, $K^\pm$, $p^\pm$ at large angles in proton-proton collisions at the ISR
Nuclear Physics B100, 237

1.1.5 Weak and Electromagnetic Interactions

M R Jane et al
A new upper limit for the branching ratio of the decay $\eta \to \pi^0e^+e^-$
Physics Letters 59B, 99

M R Jane et al
Measurement of the electromagnetic form factor of the eta meson and the branching ratio for the eta Dalitz decay
Physics Letters 59B, 103

Rutherford Laboratory Reports (see Appendix 1) RL–75–105, 106

1.2 Nuclear Physics

V J Howard et al
Differential cross sections for np and nd elastic scattering near 130 MeV
Nuclear Physics A218, 140

J A Edgington et al
Measurement of neutron-proton bremstrahlung near 130 MeV
Nuclear Physics A218, 151

M W McNaughton et al
The ^{2}H(n, np)n reaction at 130 MeV
Nuclear Physics A239, 29

Bikash Sinha, Feroze Duggan, R J Griffiths
Microscopic optical model for ^{3}He
Nuclear Physics A241, 229

R Eagle et al
53 MeV scattering from Samarium isotopes
Journal of Physics G 1, 358

S A Weinrose
The unambiguous helion optical potential at 83 MeV
Journal of Physics G 1, L1

S A Weinrose, R J Griffiths, N M Clarke
Interaction of helium ions with ^{56}Fe at 83 MeV
Journal of Physics G 1, 334

Bikash Sinha
Nucleus-Nucleus optical potential
Physical Review C11, 1546

R Eagle, R J Griffiths, B C Sinha
Microscopic optical model analysis of helium 3 scattering from Samarium isotopes
Physics Letters 57B, 31

C J Batty
Total cross-sections for pions on light nuclei
Czech. Jour. Phys. B25, 286

C J Batty, S F Biagi, R A J Riddle, B L Roberts, G J Pyle, G T A Squier, R E Hawkins
Strong interaction effects in kaonic atoms
Submitted for publication in Physics Letters

B L Roberts, R A J Riddle, G T A Squier
Measurement of Lorentzian Linewidths
Accepted for publication in Nuclear Instruments and Methods

V J Rajaratnam
Pion reaction cross-sections and nuclear sizes
Thesis, Surrey University

C J Webb
Studies of Inelastic Scattering and of Two Step Processes in Single Nucleon Transfer Reactions
Thesis, Queens University, Belfast

R Eagle
The Interaction of ^{3}He ions with Samarium Isotopes
Thesis, Bedford College, London

M Brown, R Golub, J M Pendlebury
Monte Carlo calculation of Ultra Cold Neutron Flow through long tubes with a realistic angular distribution of reflected neutrons
Nuclear Instruments and Methods 25, 61

R Golub, J M Pendlebury
Super-thermal sources of ultra-cold neutrons
Physics Letters 53A, 133

R Golub
Neutrons in Bottles
McGraw-Hill Yearbook of Science and Technology, 1976

J A Edgington et al
Elastic scattering of polarized neutrons from deuterium
AERE Report PR/NP20 (1974) 14

N M Clarke et al
Scattering of O^{16} ions from ^{28}Si, ^{59}Co and ^{60}Ni at 142 MeV
Proceedings of Pittsburg Conference, Bull. APS, Nov. (1974)

B C Sinha
The Ion-ion interaction potential and effective interactions
International Conference on Nuclear Clusters, University of Maryland

The following papers were submitted to the Europhysics Conference on Nuclear Interactions at Medium and Low Energies at Harwell, March 1975:

a) T B Robinson, V R W Edwards
A experimental study of Coulomb-nuclear interference in the inelastic scattering of 15–18 MeV alpha particles

b) B C Sinha, F Duggan, R J Griffiths
The microscopic helium potential

c) R Eagle
Inelastic scattering of ^{3}He from Samarium isotopes at 53 MeV

d) P W Tedder, V R W Edwards, B C Sinha
Exchange contributions to proton inelastic scattering from collective nuclei

e) B C Sinha
The Nucleus-nucleus optical potential

f) B C Sinha
The Ion-ion interaction energy and the critical angular momentum of fusion

Rutherford Laboratory Reports (see Appendix 1) RL–75–142, 145

1.3 Theoretical High Energy Physics

V Barger, J Luthe, R J N Phillips
Tests of geometrical scaling and generalizations
Nucl. Phys. B88, 237

V Barger, R J N Phillips
The derivative rule for helicity-flip amplitudes
Nucl. Phys. B87, 221

V Barger, R J N Phillips
Elastic scattering slope and total cross section relations
Nucl. Phys. B97, 452

V Barger, R J N Phillips
Geometrical scaling in ϕN scattering
Phys. Letters 58B, 197

V Barger, R J N Phillips
Properties of ψN scattering
Phys. Letters 58B, 433

V Barger, R J N Phillips, T Weiler
Dimuon production by neutrinos: tests of weak current models
SLAC preprint December 1975

V Barger, T Weiler, R J N Phillips
Vector meson dominance calculations for the antineutrino anomaly and dimuon production
Wisconsin preprint May 1975

V Barger, T Weiler, R J N Phillips
New charm current effects in neutrino scattering
Phys. Rev. Letters 35, 692

V Barger, T Weiler, R J N Phillips
Right-handed weak currents in neutrino scattering
Phys. Letters 59B, 56

V Barger, T Weiler, R J N Phillips
Charge-symmetry tests in neutrino scattering
Wisconsin preprint August 1975

V Barger, T Weiler, R J N Phillips
Parton distributions from neutrino data
Wisconsin preprint August 1975

D S Beder, G V Dass
Leptonic coupling types in $K^+ \to \pi^+ \ell^+ \ell^-$ decays and the question of strangeness-changing semileptonic neutral currents
Phys. Letters 59B, 444

J S Bell, G V Dass
On neutrino and antineutrino scattering by electrons and by partons
Phys. Letters 59B, 343

H M Chan, J E Paton, S T Tsou
Diffractive scattering in the dual model
Nucl. Phys. B86, 479

H M Chan, J E Paton, S T Tsou, S W Ng
Regge parameters from duality and unitarity
Nucl. Phys. B92, 13

F E Close
Current quarks and constituent-classification quarks: some questions and ideas
Workshop on quarks and hadronic structure, Erice

A K Common, M R Pennington
Sum rules for inverse $\pi\pi$ scattering amplitudes
Nuovo Cim. 25A, 219

G V Dass
Nondiagonal neutral currents and the scattering of neutrinos and antineutrinos by electrons
Nucl. Phys. B101, 125

G V Dass, H Fraas
Pomeron factorization and the reaction $\gamma N \to \phi N$
Annals of Phys. 92, 315

G V Dass, G G Ross
Tests of the space-time properties of neutral currents in e^+e^- collisions
Phys. Letters 57B, 173

G V Dass, G G Ross
Neutral weak currents in e^+e^- annihilation to hadrons
CERN report (1975)

J Dias de Deus
Geometrical scaling, quarks and the Pomeron
Acta Phys. Polon. B6, 613

J Dias de Deus
Real part of the geometrical Pomeron
Nuovo Cim. 28A, 114

J Dias de Deus
Multiplicity bootstrap and the dual unitarity equation
Nucl. Phys. B92, 469

J Formanek, B Franek
Do extensive air shower data provide reliable information on the proton-proton total cross section?
Nucl. Phys. B92, 427

A Gula
Is the absence of semi-inclusive correlations compatible with the cluster model?
Lett. Nuovo Cim. 13, 432

A Gula, M R Pennington
Nucleon exchange: a simple description
Nucl. Phys. B97, 461

T Inami, R G Roberts
Phenomenological tests of f-dominated Pomeron in inclusive reactions
Nucl. Phys. B93, 497

J Kwiecinski
On the analytic properties of the reggeon-reggeon amplitude
Nucl. Phys. B97, 475

J Kwiecinski, R G Roberts
Long-range correlations as a phenomenological probe of non-scaling behaviour
Phys. Lett. 57B, 349

P V Landshoff, J C Polkinghorne, D M Scott
Production of baryons with large transverse momentum
Cambridge preprint DAMTP 75/13

D Morgan
Rearrangement effects in three-body final states
Proceedings of Daresbury Study Weekend, February 1975

D Morgan
Status of the O^+ nonet
Proceedings of the ZGS Summer Symposium, Argonne National Laboratory

D Morgan, M R Pennington
The $\psi' \to \psi\pi\pi$ decay as a test of PCAC
Phys. Rev. D12, 1283

M R Pennington
What a dominating ρ and weak exotics can do for $\pi\pi$ scattering near threshold
Nuovo Cim. 25A, 149

M R Pennington
The budding Pomeron in the tree approximation to $\pi\pi$ inelastic channels
Nucl. Phys. B90. 131

M R Pennington, A Gula
The meson and the baryon in the one loop dual model of the Pomeron
Nucl. Phys. B96, 535

G A Ringland, R O Raitio
Phenomenological analysis of high p_T spectra and the angular multiplicity correlations in high p_T collisions
Stanford preprint SLAC-PUB 1620 T/E

R G Roberts
Regge phenomenology of inelastic diffraction
Invited talk at Gordon Conference 1975

D P Roy
Regge phenomenology of inclusive processes
Invited talk at Oxford Conference 1975

N Sakai
Building up Reggeons and the Pomeron from duality and unitarity
Invited talk at Palermo Conference 1975

N Sakai
A one-dimensional approximation for the Pomeron in the dual unitarity scheme
Nucl. Phys. B99, 167

N Sakai, J Uschersohn
Helicity structure of the triple-Regge formula
Nucl. Phys. B92, 507

D M Scott
High energy fixed-angle scattering involving a Reggeon
Nucl. Phys. B93, 345

D M Scott
Relating inclusive and exclusive meson photoproduction at large transverse momentum
Phys. Letters 59B, 171

Rutherford Laboratory Reports (see Appendix 1)
RL–75–002, 003, 011, 012, 024, 025, 030, 036, 039, 041, 042, 047, 054, 055, 062, 064, 070, 071, 073, 080, 084, 085, 086, 094, 100, 101, 103, 108, 109, 113, 122, 123, 124, 125, 133, 143, 147, 148, 151, 158, 161, 164, 165, 167, 170, 171, 172, 174, 176, 177, 179, 192

1.4 Instrumentation and Data Handling

Rutherford Laboratory Reports (see Appendix 1)
RL–75–004, 007, 015, 044, 049, 057, 160

1.5 Radiological Experiments

D C Lloyd, R J Purrott, G W Dolphin, D H Reading
An investigation of the characteristics of a negative pion beam by means of induced chromosome aberrations in human peripheral blood lymphocytes
International Journal of Radiation Biology 27, 223

R J Purrott
Chromosome aberration yields in human lymphocytes exposed to fractionated doses of negative π^- mesons
To be published in International Journal of Radiation Biology

A J Mill, J D Lewis, W S Hall
Radiation response of mammalian cells irradiated with a beam of π^- mesons
To be published in British Journal of Radiobiology

A J Mill, J D Lewis, W S Hall
Recovery in mammalian cells irradiated with a beam of π^- mesons
To be published in British Journal of Radiobiology

J E Coggle et al
Some *in vivo* effects of π^- mesons on mice
To be published in British Journal of Radiobiology

N F Kember, F A Smith, A G Perris
An approach to microdosimetry in a π^- meson beam using nuclear emulsions
Phys. Med. Biol. 20, 918

A H W Nias, D Green, D Major, D R Perry, D H Reading
Determination of RBE values for fast neutrons and negative pions using frozen HeLa cells
British Journal of Radiobiology 47, 800

Rutherford Laboratory Reports (see Appendix 1) RL-75-033, 034, 183

Section 2 Neutron Beam Research

W G Williams
Errors and Corrections in the Separation of Spin-Flip and Non-Spin-Flip Thermal Neutron Scattering Using the Polarization Analysis Technique
Presented at Neutron Diffraction Conference, Petten

W G Williams
A Review of the Polarization Analysis Technique in Thermal Neutron Scattering
Presented at Neutron Diffraction Conference, Petten

P L Davidson
Position Sensitive Slow Neutron Detectors Using Channel Electron Multipliers
Presented at Neutron Diffraction Conference, Petten

J C Sutherland, H Wroe
A Cold Neutron Beam Bender Using Multiple Thin Plastic Films as Curved Guide
Presented at Neutron Diffraction Conference, Petten

D F R Mildner, J M Carpenter
An Optimised Monte Carlo Simulation for Neutron Time-of-Flight Diffraction
Presented at Neutron Diffraction Conference, Petten

C J Carlile, K Krebs
Quasi-elastic Neutron Scattering and Orientational Motions in Liquid Crystals
Mol Cryst Liq Cryst 29, 43

C J Carlile, D K Ross
An Experimental Verification of the Churley - Elliott Model for the Diffusion of Hydrogen in α-phase Pd/H
Sol State Comms. 15, 1923

M J Cooper et al
Development of computing facilities for the neutron beam experiments at Harwell
AERE Harwell report AERE-R8098

Rutherford Laboratory Reports:

J B Forsyth, C P Jackson
Andromache Data Processing on the Rutherford Laboratory IBM 360/195
RL-74-115

J B Forsyth, C P Jackson
Curran Data Processing on the Rutherford Laboratory IBM 360/195
RL-74-116

J B Forsyth, C P Jackson
Amendment to the Rietveld Computer Program for the Profile Refinement of Neutron Diffraction Powder Patterns Modified for Anisotropic Thermal Vibrations by A W Hewat RRL 73/897
RL-74-122

B H Meardon
Efficiencies of Long Thermal Neutron Detectors
RL-74-144

J B Forsyth, K M Knight, P E Smith
Input Display Unit
RL-74-163

and RL-75-020. 029, 063, 095, 096, 112 (see Appendix 1)

Section 4 Forward Technology

4.1 Polarised Targets

M Ball, P Clee, N Cunliffe, J Simkin
Superconducting magnet for a polarised target nuclear physics experiment
Presented at International Conference on Magnet Technology, Frascati

Rutherford Laboratory Report RL-75-150 (see Appendix 1)

4.4 Superconducting Applications

M N Wilson, R B Hopes, R L Roberts
A pressure impregnated superconducting dipole
Presented at International Conference on Magnet Technology, Frascati

C A Scott, D C Larbalestier
Superconducting magnets
Physics Bulletin, May 1975, p213

J A Lee, C F Old, D C Larbalestier
Some aspects of multifilamentary Nb_3Sn production
Presented at CNRS international colloquium

D C Larbalestier
Filamentary superconducting wires
Presented at symposium on non-ferrous metal wire drawing, Brussels to be published in Revue ATB Metallurgie

M N Wilson
Superconducting materials: some recent developments
Presented at International Conference on Magnet Technology, Frascati

J H Coupland
The pulsed superconducting magnet AC5
Presented at International Conference on Magnet Technology, Frascati

D Evans, G B Stapleton
Cryogenic applications of epoxide resins
Presented at the RPG symposium, Bristol

D B Thomas
Magnets and cryogenics
Contribution to Isabelle summer study, Brookhaven

D A Baynham
Magnet protection
Contribution to Isabelle summer study, Brookhaven

D B Thomas
The work of the GESSS collaboration
Presented at International Conference on Magnet Technology, Frascati

P F Smith, B Colyer
A solution to the training problem in superconducting magnets
Cryogenics 1975, 201

Rutherford Laboratory Reports (see Appendix 1) RL-75-008, 060, 061, 074, 136, 173

4.5 Computer Applications

A G A M Armstrong et al
New developments in the magnet design program GFUN
Presented at International Conference on Magnet Technology, Frascati

Rutherford Laboratory Reports (see Appendix 1) RL-75-066, 111, 117

Section 5 Laboratory Computing

M J Holmes, A R Thorne
The design of a graphics processor
Proceedings of the Electronic Displays Conference 1975, Vol 2

C J Adams et al
File transfer protocol
Post Office Experimental Packet Switching Service, Study Group 2

C J Adams et al
An interactive terminal protocol
Post Office Experimental Packet Switching Service, Study Group 2

A D Bryden
Implementation of programs from other computers on a GEC 4080
Elliott Computer Users' Association Annual Meeting

A S Dunn
HASP multi-leaving and file transfer to and from a GEC 4080
Elliott Computer Users' Association Annual Meeting

P C Thompson
Utilities – a plea for action
Presented at SEAS 75 anniversary meeting, Dublin

R Taylor
SEAS looks at future data processing requirements
Presented at SHARE XLIV, Los Angeles

R Taylor
Future requirements for productive programming
Presented at SEAS spring technical meeting, Aalborg

M W Johnson et al
Wave-number dependent concentration fluctuations in liquid mixtures
J Phys C 8, 751

M W Johnson et al
Crystal structure of deuterium fluoride
Acta Cryst B31, 1998

Rutherford Laboratory Reports:

J F McEwan
Line printer throughput rates for RJE stations attached to the 360/195
RL-74-005

D S Greenaway
2DTRAX: a computer program for spark chamber track finding in two dimensions with zero guidance
RL-74-010

RL-75-006, 026, 058, 102, 114, 138, 023, 032, 139, 157, 190, 105, 106 (see Appendix 1)

Section 6 Accelerator Operations and Development

6.1 Nimrod

Rutherford Laboratory Reports (see Appendix 1) RL-75-027, 069, 180

6.3 EPIC

Rutherford Laboratory Reports RL-75-013, 021, 028, 031, 037, 0.38, 040, 046, 056, 068, 092, 093, 097, 146

Appendix 3 Lectures, Seminars and Meetings

Seminars in High Energy Physics

A Gula (Krakow and RL, 15 Jan)
Multiparticle production in a cluster model.

C Hamar (Cambridge, 22 Jan)
Statistical bootstrap and multiparticle processes.

R Campbell (Imperial College, 29 Jan)
Extraction of $K\pi$ phase shifts for the reaction $K^+n \rightarrow K^+\pi^-p$ at 2–3 GeV/c.

B Webber (Cambridge, 5 Feb)
Impact parameter structure of multiparticle production.

R Baker (RL, 12 Feb)
Partial wave analysis of $\pi^-p \rightarrow \Lambda K$ using the Barrelet zeros method.

N Sakai (RL, 19 Feb)
Spin of leading clusters and the slope of the overlay function.

M Corden (Birmingham, 26 Feb)
Isobar model analysis of K^-n giving $K^-\pi^-p$, $K^o\pi^on$.

C Froggatt (Glasgow 5 March)
Recent developments in $\pi\pi$ scattering.

D Crennell (RL, 12 March)
Analysis of the $(3\pi)^o$ system from $\pi^+d \rightarrow \pi^+\pi^-\pi^o\, pp_s$

L Jones (Cambridge and Illinois, 19 March)
Parity of Regge cuts.

R Savit (CERN and NAL, 9 April)
Reggeon theory on a lattice.

R Gibson (Queen Mary College, 16 April)
$p\bar{p}$ scattering between 0·69 and 2·43 GeV/c.

R. Phillips (RL, 23 April)
Charmed particle production.

J Davies (RL, 30 April)
π^-p charge exchange polarisation.

F Elvekjaer (CERN, 7 May)
Geometrical framework for 2-body reaction and large p_T phenomena.

S D Ellis (NAL and Cambridge, 14 May)
Chival confinement.

A Clark (RL, 20 May)
Report on the Washington APS meeting.

D Morgan (RL, 21 May)
$\pi\pi$ interactions in ψ' and A_1 decays

I Corbett (RL, 3 June)
News from the labs.

E Squires (Durham, 4 June)
Bags and nuclear forces.

G V Dass (RL, 10 June)
Nondiagonal neutral currents.

K Green (Oxford, 12 June)
Elastic and inelastic polarised target measurements at 8 GeV/c.

G Kalmus (RL, 18 June)
Results from a low energy $K_L^o p$ scattering experiment.

K Paler (RL, 2 July)
Topics presented at Palermo.

P Hoyer (Stony Brook, 9 July)
t-channel view of s-channel resonances.

R T Ross (RL, 16 July)
Palermo review of Y* spectroscopy.

A Bialas (Krakow and RL, 23 July)
Particle production from nuclei.

M Kugler (Weizmann Inst. and RL, 30 July)
Current quarks, constituent quarks and resonances.

D Horn (Tel Aviv, 20 August)
Photoproduction of ψ.

P Kroll (Wuppertal, 17 Sept)
Geometrical scaling.

R Kelly (LBL and RL, 24 Sept)
Pion-nucleon partial wave analysis.

R J N Phillips (RL, 1 Oct)
New particles and neutrino interactions.

P Thornton (Imperial College, 8 Oct)
Partial wave analysis of diffractively produced $p\pi^+\pi^-$ states.

M Kawaguchi (KEK, 14 Oct)
Quark model and large angle scattering.

C J S Damerell (RL, 22 Oct)
New results on hypercharge exchange reactions.

K Choudhury (Daresbury, 29 Oct)
Study of current fragmentation in deep inelastic scattering.

E Barrelet (Ecole Polytechnique, 12 Nov)
Developments in the method of zeros.

K Barnham (Imperial College, 19 Nov)
Partial wave analysis of $\pi^+p \rightarrow \pi\pi N$.

G Shaw (Manchester, 26 Nov)
Photo-absorption, vector dominance and shadowing.

H Osborn (Cambridge, 10 Dec)
Some models of quark confinement.

D Atkinson (Groningen, 17 Dec)
Continuum ambiguities in π^+p phase shift analysis.

NIMROD Lectures on Particle Physics

G Wolf (DESY, 13 Jan)
Results on electroproduction in exclusive channels.

L Caneschi (CERN, 20 Jan)
Theories with interacting Pomerons.

K Paler (RL, 27 Jan)
K^-p interactions at 14·3 GeV/c.

E W Colglazier (RL and Princeton, 3 Feb)
Threshold pion production by weak neutral currents.

J Steinberger (CERN, 10 Feb)
Results of the CERN-Heidelberg K^o experiment and the status of the superweak model of CP violation.

R Sekulin (RL, 17 Feb)
π^+d interactions at 4 GeV/c and the production of vector and tensor mesons.

J S Ball (CERN, 24 Feb)
Diffraction scattering at infinite energies.

M Breidenbach (SLAC, 6 March)
Latest results from SPEAR.

C J S Damerell (RL, 10 March)
Study of the reaction $\pi^+p \rightarrow K^+\Sigma^+$ and $K^-p \rightarrow \pi^-\Sigma^+$ at 10 GeV/c.

C A Heusch (SLAC–CERN, 17 March)
Hadron production in muon-nucleon collisions.

F E Close (CERN, 24–26 March)
Series of 4 lectures.

M Albrow (RL, 7 April)
Recent results and future programmes at the ISR.

P D B Collins (Durham, 14 April)
The Pomeron, Regge cuts and scaling.

F J M Farley (Shrivenham, 21 April)
First results of the CERN (G-2) experiment.

H P Nielsen (Niels Bohr Inst., 28 April)
Dual string.

K Berkelman (Cornell and DESY, 5 May)
Latest ψ results from DORIS.

C Michael (Liverpool 12 May)
Resonance production at high energy.

S C C Ting (MIT and DESY, 16 May)
New results on J particles from Brookhaven.

P V Landshoff (Cambridge, 19 May)
Large p_T and the quark structure of the nucleon.

B R Martin (Univ. College, London, 2 June)
I = o KN amplitudes.

B Alper (RL, 9 June)
Summary of British-Scandinavian ISR experiments.

J G Taylor (King's College, London, 23 June)
Metal bending and all that.

D Faiman (Weizmann Inst. and RL, 30 June)
Is there ideal mixing amongst the baryons?

H R Rubinstein (Weizmann Inst & RL, 7 July)
Two photon physics in the resonance region.

Vera Lüth (SLAC, 14 July)
Quantum numbers and decay modes of ψ resonances.

C Quizg (FNAL, 21 July)
Structure of multiparticle production.

A Masaike (KEK, 22 Sept)
Experiments planned in Japan.

R Delbourgo (Imperial College, 29 Sept)
Supersymmetry.

J Dias de Deus (RL, 13 Oct)
Geometrical scaling.

R Marshall (Daresbury, 20 Oct)
Backward photoproduction of ρ and f mesons.

R Tucker (Lancaster, 27 Oct)
Dual string dynamics and the baryon problem.

F Vannucci (3 Nov)
SPEAR studies on ψ and ψ' decays.

W Jentschke (CERN, 10 Nov)
The CERN experimental programme.

D Sivers (RL, 17 Nov)
Production of new particles in a boorish world.

R L Kingsley (RL, 24 Nov)
Right-handed currents for the weak interactions.

N Booth (Oxford, 1 Dec)
Deep inelastic muon-nucleon scattering at high energies.

B Shen (CERN, 8 Dec)
Study of double Pomeron exchange processes at the ISR.

R Cashmere (Oxford, 15 Dec)
There are two Q meson resonances.

Rutherford Laboratory Lectures

E H Cooke-Yarborough (AERE, 9 Jan)
Thermo-mechanical oscillators.

M F Land (Sussex, 30 Jan)
Visual guidance and pursuit mechanisms of insects in flight.

E H Kass (US Nat. Academy of Sciences, 20 March)
Medical aspects of space flight.

P F Chester (CEGB, 10 April)
Power problems and possibilities.

D C Phillips (Oxford, 8 May)
Macromolecular architecture.

Margaret Gowing (Oxford, 5 June)
Science and politics.

E T Hall (Oxford, 11 Sept)
Archaeometry: the physical sciences applied to the arts.

G A Nowacki, N Hayes and J E Denney (23 Oct)
Vegetable protein.

J Davoll (Conservation Society, 6 Nov)
How much energy do we need?

I Glendenning (CEGB, 4 Dec)
Non-nuclear power: the potential of nature.

Seminars in Computing

C Maclean, G Macpherson, S Sharrock, P Wilde (RL, 17 Jan)
Experience using a special-purpose hardware processor in an experiment at the ISR.

C Adams (RL, 31 Jan)
The GEC 4080 interactive graphics computer.

R Taylor (RL, 14 Feb)
Report of the SEAS future requirements project.

D B Scott (Glasgow, 28 Feb)
Computer-assisted learning projects in medicine and mathematics.

A R Mayhook (RL, 25 April)
STAIRS.

P Kirstein (UCL, 9 May)
Current experience of the UCL node into ARPA

D Haworth (Manchester, 23 May)
Review of the UMRCC 1906A/7600 joint system.

B R Martin (Appleton Lab, 6 June)
Satellite control and data processing at the Appleton Laboratory.

J T Hyman (RL, 11 June)
CERN SPS computer control system.

A R Mayhook and A Storner (RL, 20 June)
Mini discs and volume protection.

J MacEwan (IBM, 9 July)
The IBM international SWITCH network.

C S Cooper, C D Osland, P C Thompson (RL, 18 July)
Three current projects.

3 October
SEAS 1975.

17 October
General meeting.

M J Newman (RL, 31 Oct)
3D modelling.

P Kritzinger (Imperial College, 13 Nov)
Computer installation management methodology and techniques.

T G Pett, C S Cooper (RL, 28 Nov)
ELECTRIC – past, present and future.

R M Payne (SRC, 9 Dec)
Administration of SRC grants on the ICL 1906A computer.

K C T O Sumorok (RL, 12 Dec)
Acquisition and processing of data from an experiment in Omega.

Meetings and Special Events

Informal Theoretical Physics Meeting (6–8 Jan)

V Suller and N Marks (Daresbury, 13 June)
The Daresbury Synchrotron Radiation Facility.

R Billinge (CERN, 1 July)
The SPS Magnet System.

Institute of Physics meeting (16 July).

Laser Meeting (17–19 Dec).

Summer School for High Energy Experimentalists
Oxford (7–26 Sept).

VI International Colloquium on Multiparticle Processes
(Oxford, 14–19 July)